<u>**İSTANBUL TECHNICAL UNIVERSITY ★ INSTITUTE OF SCIENCE AND TECHNOLOGY**</u>

DETERMINATION OF LATERAL SWELLING PRESSURE

Ph.D. Thesis by
Hüsnü Korhan ÖZALP

Department : **Civil Engineering**

Programme : **Soil Mechanics and Geotechnical Engineering**

MARCH 2011

İSTANBUL TECHNICAL UNIVERSITY ★ INSTITUTE OF SCIENCE AND TECHNOLOGY

DETERMINATION OF LATERAL SWELLING PRESSURE

Ph.D. Thesis by
Hüsnü Korhan ÖZALP
(501032302)

Date of submission :	**15 October 2010**
Date of defence examination:	**23 March 2011**

Supervisor (Chairman) :	**Prof. Dr. Ahmet SAĞLAMER (ITU)**
Members of the Examining Committee :	**Prof. Dr. Mete İNCECİK (ITU)**
	Prof. Dr. Feyza CİNİCİOĞLU (IU)
	Prof. Dr. Orhan EROL (METU)
	Assoc. Prof. Dr. Recep İYİSAN (ITU)

MARCH 2011

İSTANBUL TEKNİK ÜNİVERSİTESİ ★ FEN BİLİMLERİ ENSTİTÜSÜ

YANAL ŞİŞME BASINCININ
BELİRLENMESİ

DOKTORA TEZİ
Hüsnü Korhan ÖZALP
(501032302)

Tezin Enstitüye Verildiği Tarih :   15 Ekim 2010
Tezin Savunulduğu Tarih :   23 Mart 2011

Tez Danışmanı :   Prof. Dr. Ahmet SAĞLAMER (İTU)
Diğer Jüri Üyeleri :   Prof. Dr. Mete İNCECİK (İTU)
Prof. Dr. Feyza CİNİCİOĞLU (İU)
Prof. Dr. Orhan EROL (ODTÜ)
Doç. Dr. Recep İYİSAN (İTÜ)

MART 2011

FOREWORD

TABLE OF CONTENTS

viii

ABBREVIATIONS

C	: Percent of clay size finer than 0.002mm
C_C	: Compression Index
CEC	: Cation Exchange Capacity
COLE	: Colloid Contend and Linear Extensibility Value
CS	: Constant Surcharge
CVS	: Constant Volume Swell Test
e	: void ratio
Ei	: Expansion Index
I_p	: Plasticity Index
Kr	: Ring Stiffness
KS	: Swell Presure Ratio
LFST	: Lateral Free Swell Test
LR	: Laterally Restrained
LSPR	: Lateral Swelling Pressure Ring
OSO	: Oedometer Swell Overburden Test
PVC	: Percent Volume Change
S	: Swell Potential
SO	: Swell Overburden Test
TSO	: Triaxial Swell Overburden Test
VR	: Vertically Restrained
w_f	: Final Water Content
w_i	: Initial Water Content
w_L or LL	: Liquid Limit
w_n	: Natural Water Content
w_{opt}	: Optimum Water Content
w_p or PL	: Plastic Limit
ZLST	: Zero Lateral Strain
ε	: strain
γ	: Unit Weight of Soil
$\gamma_{dry,max}$	: Maximum Dry Unit Weight
σ_{sL}	: Lateral Swelling Pressure
σ_{sV}	: Vertical Swelling Pressure
σ_V	: Overburden Pressure (Surcharge value in the triaxial swelling tests)

x

LIST OF TABLES

LIST OF FIGURES

DETERMINATION OF LATERAL SWELLING PRESSURE

SUMMARY

Expansive soils can be defined as soils that under some conditions are capable of increasing its volume when getting wet. It is well known that structures placed over or in expansive soils face problems due to soil heave upon the change of the soil moisture.

The primary aspect of research on swelling has always been to predict the swelling behavior of the expansive soils in the vertical direction. Nevertheless, expansive soils change their volumes in lateral direction as well as in the vertical direction. The mandatory to predict lateral swelling pressure has forced the establishment of triaxial swelling pressure tests.

One of the well known methods for measuring the lateral swelling pressure is the use of thin wall oedometer which was first introduced by Komornik & Zeitlen, (1965) and then also developed by several investigators.

The objective of this study was to investigate the rate of lateral swelling pressures expected to act on retaining systems of deep excavations and tunnels in expansive soils. The variation of swelling pressures dependent on depth and the rigidity of the facing element were investigated.

The Lateral Swell Pressure Ring has been redesigned for this study. The ring height has been increased and a pressure cell has been added to the device. Different than the similar device of Ofer (1981), the cell pressure restaining the specimen to swell in lateral direction was hydraulic pressure rather than air pressure. The pressure cell, surrounding the thin walled ring gave the ability to predict the lateral swelling pressures under zero lateral strain conditions. Moreover, three strain gauges have been mounted on the ring, each configured as a quarter bridge, to monitor the non-homogenous behavior of the specimen in the horizontal plane.

Several swelling tests have been performed on compacted clay specimens. Various test types have been utilized in order to obtain comprehensive lateral swelling pressures. The results are compared with swell pressures obtained in these tests in vertical direction as well as with the triaxial swelling pressure test results of previous studies.

First, a series of tests have been made in accordance with the methodology of the previous studies using the thin walled lateral swelling pressure ring. So, by comparing the results obtained from these tests with the results of the tests of other researchers, the reliability of the test set up has been validated. Then, the contribution of the pressure cell, added to the recently manufactured testing device has been investigated.

The test results have revealed that a strain induced automatic cell pressure triggering is necessary for greater accuracy for lateral swelling pressure prediction under zero lateral strain conditions. If, automatic cell pressure triggering is not present, which is the case in this study, the adjustment of a testing technique like "The Method of Equilibrium (Fourie, 1989)", will avoid side effects of possible failures of lateral stress adjustment by the cell pressure increase.

YANAL ŞİŞME BASINCININ BELİRLENMESİ

ÖZET

Şişen zeminler, ıslandıkları zaman hacimlerini arttıran zeminler olarak tanımlanırlar. Şişen zemin tabakaları üzerine veya içerisine inşa edilen yapılarda, zemin tabakalarının su muhtevasındaki değişime bağlı olarak gelişen şişme davranışı etkisinde büyük problemler ile karşılaşıldığı bilinmektedir.

Şişme basıncına yönelik araştırmalarda genel olarak şişme potansiyeline sahip zemin tabaklarından düşey yönde etkiyen şişme basıncı araştırılmıştır. Oysaki şişen zeminler, hacimlerini düşey ve yatay yönde şişerek genişletirler. Yanal şişme basıncının belirlenmesinin kaçınılmaz hale gelmesi, üç eksenli şişme basıncı deneylerinin gelişimini beraberinde getirmiştir.

En çok bilinen yanal şişme basıncı ölçme yöntemlerinden bir tanesi, ilk olarak Komornik ve Zeitlen (1965) tarafından geliştirilen ince cidarlı ödometre halkası kullanılarak yapılan üç eksenli şişme basıncı deneyleridir. Bu yöntemde kullanılan test cihazı çeşitli araştırmacılar tarafından geliştirilerek günümüze kadar gelmiştir.

Bu çalışmanın çıkış noktası, derin temel kazılarının yapılabilmesi için inşa edilen iksa sistemlerine veya tünellere etkiyen şişme basıncının araştırılmasıdır. Çalışma kapsamında, şişme basıncının derinlikle değişimi ve kaplama rijitliği ile değişimi araştırılmıştır.

Bu çalışma için, şişme basıncı ölçen, inceltilmiş ödometre halkasına sahip cihaz geliştirilmiş ve yeniden üretilmiştir. Ofer (1981) tarafından geliştirilen cihazdan farklı basınç hücresinde hava basıncı yerine hidrolik basınç kullanılmıştır. Ödometre halkasının etrafına eklenen basınç hücresi sayesinde, numunenin yanal şişmesi engellenerek, sabit hacimde şişme basıncının ölçülmesi mümkün hale gelmiştir. Buna ilave olarak, inceltilmiş çelik halkaya yerleştirilen üç adet srain gauge çeyrek köprü devresi ile bağlanmış ve her bir strain gauge bağımsız ölçü alabilir duruma getirilmiştir. Böylelikle numunenin yatay eksende anizotropik şişme davranışı incelenebilmiştir.

Geliştirilen ekipman ile kompakte edilmiş kil numuneleri üzerinde çok sayıda deney yapılmıştır. Çalışmanın sırasında, karşılaştırılabilir sonuçlara ulaşmak amacıyla, birden fazla test yöntemi izlenmiştir. Böylelikle, çalışma kapsamında yapılan testlerden elde edilen sonuçlar, hem kendi içinde hem de önceki çalışmalardan elde edilmiş sonuçlar ile karşılaştırılarak değerlendirilmiştir.

İlk olarak, önceki çalışmalarda izlenen yöntem takip edilmiş ve yapılan testlerden elde edilen şişme basıncı dağılımları, diğer araştırmacıların elde ettiği sonuçlar ile birlikte ele alınarak, geliştirilen ve bu çalışma için üretilen aletin güvenirliliği doğrulanmıştır. Devamında yapılan şişme basıncı deneyleri ile inceltilmiş ödometre ringine eklenen basınç hücresinin katkısı incelenmiştir.

Çeşitli yöntemler takip edilerek yapılan şişme basıncı deneylerinin sonucunda, hücre basıncını otomatik olarak tetikleyen bir ekipmanın gerçek anlamda sabit hacimli şişme basıncı deneyi yapmak için kaçınılmaz bir zorunluluk olduğu görülmüştür. Otomatik tetiklemeye sahip bir test cihazı olmadığı, bu çalışma kapsamında kullanılana benzer ekipmanlarla yapılan şişme basıncı deneylerinde, numunenin yanal şişme basıncını belirlemek üzere, Fourie (1989) tarafından tavsiye edilen "Denge Yöntemi" ile şişme basıncı deneyleri yapılmasının, genleşmeye bağlı ferahlama etkisinden dolayı yapılacak ölçüm hatalarının önlenmesi açısından faydalı olacağı görülmüştür.

1. INTRODUCTION

1.1 Expansive Soils in General

Expansive soils can be defined as soils that under some conditions are capable of increasing its volume when getting wet. Expansive soils expand to a significant degree upon wetting and shrinks upon drying. It is well known that structures placed over expansive soils and tunnels in expansive soils face problems due to soil heave upon the change of the soil moisture. "Types of structures most often damaged from swelling soil include building foundations and walls of residential and light buildings, highways, canal and reservoir linings, and retaining walls" (US Army, TM 5–818–7, 1983).

The description in the strategy report of the Transportation Research Laboratory of UK on expansive soils, the complexity of understanding the behavior of expansive soils has been made as follows: "Expansiveness is a property of the soil. There is no direct measure of this property and therefore it is necessary to make use of comparative values of swell, measured under known conditions, in order to derive a method for assessing expansiveness. Consideration of the mechanisms of interaction between water and clay soils show that the three most important components are the clay minerals, the change in moisture content or suction and the applied stresses. The type of clay mineral is largely responsible for determining the soil property referred to as the intrinsic expansiveness. It is the change in moisture content or suction that controls the actual amount of swell which a particular soil will exhibit under a particular applied stress" (Gourley et. al., 1983).

Regarding to Fu Hua Chen, the potentially expansive soils are confined to the semi arid regions of the tropical and temperate climate zones. Potentially expansive soils can be found everywhere in the world. The reason why they are still not recognized in the underdeveloped nations is the small amount of construction (Chen, 1988).

"In semi – arid climates, overlying structures often induce heave in swelling soils because the natural transpiration of moisture by vegetation and evaporation from the ground surface is inhibited. In arid climates, the heave of structures arises from the alteration of the moisture regime of the subsoil's as a result of land utilization and development (Dhowian et. al., 1990)."

1.2 Lateral Swelling Pressure and the Aim of the Study

The primary aspect of research on swelling has always been to predict the swelling behavior of the expansive soils in the vertical direction. Related to this, the uplift failure caused by this behavior and remedial measures have been studied extensively. Nevertheless, expansive soils change their volumes in lateral direction as well as in the vertical direction. By restraining the lateral volume change tendency of soils with the construction of a retaining wall or a tunnel lining, the restraining element is being employed with responding the large swell pressures. This additional lateral pressure caused by swelling is being missed in most of the cases during the lateral earth pressure calculations. Furthermore, it has been noted in some of the investigations, which will be studied in the following paragraphs of this thesis, that lateral swelling pressures may be much greater than swelling pressures to be exerted in the vertical direction.

Adequate and correct prediction of lateral swelling pressure is important in that the lateral restrainment elements like a retaining wall or tunnel facing can be designed to withstand the earth pressures to act on them in the reality. Besides, the mandatory to predict lateral swelling pressure has forced the establishment of triaxial swelling pressure tests. Triaxial swelling pressure tests have proven that one dimensional swelling tests result with overestimation of swelling pressures.

Several methods have been developed in the past to measure the three dimensional swelling behavior of expansive clays. One of the well known methods for measuring the lateral swelling pressure is the use of thin wall oedometer which was first introduced by Komornik & Zeitlen, (1965) and then also developed by several investigators. Ofer (1981), has made one of the major developments on this device by adding an air tight chamber around the ring of Komornik & Zeitlin in order to counterbalance any lateral strain swell with air pressure.

The objective of this study is to investigate the rate of lateral swelling pressures expected to act on retaining systems of deep excavations and tunnels that are constructed in expansive soils. Furthermore, the variation of swelling pressures dependent on depth and the rigidity of the facing element were investigated. For this purpose, the Lateral Swell Pressure Ring of Ofer has been redesigned, by applying water pressure instead of air pressure for the restrainment of lateral swell strains. Moreover, three strain gauges have been mounted on the ring, each configured as a quarter bridge, to monitor the non homogenous behavior of the specimen in the horizontal plane.

Several swelling tests have been performed on compacted clay specimens. Various test types have been utilized in order to obtain comprehensive lateral swelling pressures and they were compared with swell pressures obtained in these tests in vertical direction as well as with the results of one dimensional swelling pressure tests obtained from conventional methods described in ASTM D 4546-03.

2. REVIEW OF THE RELATED LITERATURE

2.1 Type and Origin of Expansive Soils

As mentioned before, expansive soils are encountered all over semi arid and arid regions of the world. As well described by Rao (2006), the occurrence of swelling is only possible if the soil is unsaturated. If the unsaturated soil increases its water content it swells.

Countries and regions familiar with problems caused by expansive soils can be listed as; The United States, India, Countries of the Arabian Gulf, South Africa and West European Countries etc. Turkey also has areas covered with expansive clays. Several problems had been faced in the past, starting from Istanbul in the West of Turkey passing through Ankara, and spreading to eastern cities like Adana and Diyarbakir.

Soils which can be associated with expansive clays belong to two main groups. The first group comprises the basic igneous rocks, such as the basalts of the Deccan Plateau in India, the dolerite sills and dykes in the central region of South Africa and the gabbros and the parent rocks have decomposed to form montmorillonite and other secondary minerals. The second group comprises the sedimentary rocks that contain montmorillonite mineral as a constituent which breaks down physically to form expansive soils (Chen, 1988).

The montmorillonite is probably formed from two separate origins. The products of weathering and erosion of the rocks in the highlands are carried by streams to the coastal plains. The fine grained soils eventually become shale accumulating in the ocean basin. Meanwhile, volcanic eruptions sending up clouds of ash, fall on the plains and the seas. These ashes are altered to montmorillonite. (Chen, 1988)

The swelling clay samples, which were employed in the tests of this thesis, were volcanic origin including weathered montmorillonite. These samples were recovered from the Catalca Region of Istanbul City. According to the investigation made on

that area, the thickness of this Oligosen aged clay layers are around 150m (Sağlamer, 1991). Properties of the test samples will be explained detailed in the related paragraphs.

2.2 Clay Mineralogy

Regarding to Holtz and Kovacs; in civil engineering, clay often means a clay soil – a soil which contains some clay minerals as well as other mineral constituents, has plasticity and is cohesive. But clay is also the name of specific minerals such as kaolinite, illite and montmorillonite. Clay minerals are very tiny crystalline substances evolved primarily from chemical weathering of certain rock forming minerals (Holtz and Kovacs, 1981). Most soil classification systems arbitrarily define clay particles as having an effective diameter of two microns (0.002mm) or less. For small size particles, the electrical forces acting on the surface of the particle are much greater in contrast to gravitational forces, so therefore these particles are in a colloidal state (Chen, 1988).

Clay minerals in soils belong to the phyllosilicates mineral family and contain other silicates such as serpentine, pyrophyllite, talc, mica and chlorite. Due to their small sizes, their unit cells have a residual negative charge that is balanced by the adsorbtion of cations from solution (Mitchell, 1992). This is the chief property of clays controlling their volume change capacity. Therefore, clay soils differ from granular soils in that their water content do affect their engineering behavior to a great extend, where for granular soils the grain size distribution is playing major role over their engineering behavior.

The reaction of water with fine grained soils cannot be fully appreciated without an understanding of the architecture of both the clay particles and the water on an atomic scale. For a grain of quartz with roughly spherical/cubic shape there is no important change in the soil/water relationship as the particle size decreases. As the particle sizes reduce to less than one micrometer there are few quartz particles and the dominant particles are clay minerals. These clay minerals may be of various types, but all have a platy or flake shape, being very thin in one direction. This follows from the chemical make-up of the minerals. Besides this shape, the clay minerals have electrical properties which affect their movement towards one another as well as their reaction to water (Raymond, 1997).

2.2.1 Physiochemical concepts

Atoms are the smallest particles possessing definite chemical characteristics. Molecules are formed from chemically combined (bonded) atoms. Molecules represent the smallest indivisible particle of a compound. The atoms of the molecule are firmly held together by the electrochemical bonds formed through the exchange or the sharing of electrons. Interatomic bonds are of three principal types: covalent, ionic and metallic (Raymond, 1997).

A covalent bond results from the sharing of pairs of valence electrons by two or more atoms. In the ionic bond atoms of different elements, transfer electrons one to the other so both have stable outer shells and at the same time become ions, one positive, and one negative. In the metallic bond atoms of the same or different elements give up their valence electrons to form an electron cloud (electron gas) throughout the space occupied by the atoms (Raymond, 1997).

Investigations of the chemical composition and crystal structure of soils show that individual ions of different minerals may be attached (adsorbed) to the surface of a soil crystal. Water, although electrically neutral has a positive and negative centre of charge. These electrostatic charges result in an attraction to a clay crystal and the water is held to the clay crystal by hydrogen bonding. Thus minerals in the presence of water are surrounded by (fixed) adsorbed water (Raymond, 1997).

"The surface area per mass (often volume is used in place of mass) is known as "specific surface" and is a good indication of the relative influence of electrical forces on the behavior of the particle (Raymond, 1997)." "The amount of water adsorption capacity, which is related to the specific surface, is a factor which designates the magnitude of expansion. Other factors influencing soil expansion are the exchangeable ions present, electrolyte content of the clay minerals and their internal structure (Chen, 1988)."

2.2.2 Clay minerals

"Clay minerals are formed through a complicated process from an assortment of parent materials. The parent materials include feldspars, micas, and limestone. The alteration process includes disintegration, oxidation, hydration and leaching (Chen, 1988)."

As mentioned before, Clay minerals form part of a subclass of the silicate class of minerals known as the phyllosilicates. The silicates are the largest and most complex group of minerals. Approximately 30% of all minerals are silicates. The basic chemical unit of silicates is the SiO_4 tetrahedron. The structural arrangement of the tetrahedrons is what classifies the six silicate subclasses and what distinguishes their properties (Woodward et. al., 2002).

In the phyllosilicate subclass, rings of tetrahedrons are linked by shared oxygen's to other rings in a two dimensional plane that produces a sheet-like structure. The typical crystal of this subclass is therefore flat, plate, book-like and displays good basal cleavage. The sheets of tetrahedrons are connected to each other by weakly bonded cations and often have water molecules trapped between the sheets. The clay minerals are distinct from other phyllosilicates by having large percentages (often 70-90%) of water trapped between the silicate sheets (Woodward et. al., 2002). Much of the water within clays is not free pore-water but contained in the lattice of the clay minerals and adsorbed on to their surface. To expel this water, temperatures of greater than 100C° are required.

The structures of the common layer silicates are made up of combinations of two simple structural units, the tetrahedral or silica, and the octahedral or alumina, sheets. The way two fundamental crystal sheets silica and alumina sheets are stacked together, the bonding between them and the metallic ions in the crystal lattice constitute the different clay minerals (Holtz and Kovacs, 1981), (Mitchell, 1992).

The tetrahedral sheet is basically a combination of silica tetrahedral units which consist of four oxygen atoms at the corners, surrounding a single atom. Figure 2.1 shows a single silica tetrahedron.
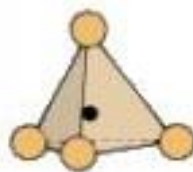
Figure 2.1: Silica Tetrahedron (Mitchell, 1992)

Figure 2.2 shows how the oxygen atom at the base of each tetrahedron is combined to form a sheet structure. The oxygens at the base of each tetrahedron are in one plane, and the un-joined oxygen corners all point in the same direction. The typical schematic representation of the silica tetrahedron which is widely used in soil

mechanics is shown in Figure 2.3. The plain view of a silica sheet has hexagonal holes.
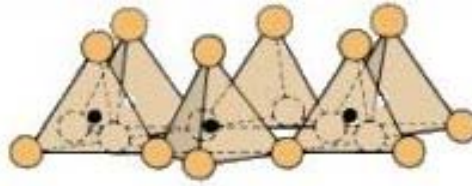
Figure 2.2: Tetrahedral Sheet (Mitchell, 1992)
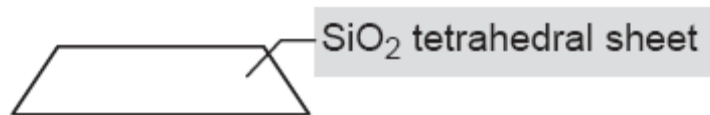
Figure 2.3: Silica Sheet (Mitchell, 1992).

The second known sheet in clay mineralogy is the octahedral sheet. The octahedral sheet is basically a combination of octahedral units consisting of six oxygen or hydroxyls enclosing aluminum, magnesium, iron or other single atom. A single octahedron is shown in Figure 2.4.
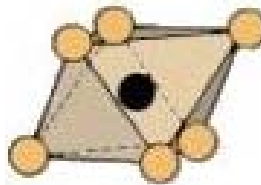
Figure 2.4: Single Octahedron (Mitchell, 1992)

In Figure 2.5 the octahedrons are shown combining a sheet structure.
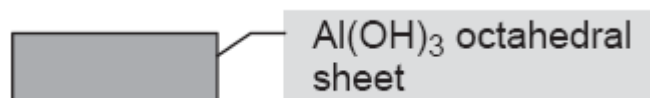
Figure 2.5: Alumina Sheet (Mitchell, 1992)

In the octahedral sheet, substitutions of different minerals can take place, which leads to different clay minerals. These ions subjected to these substitutions have approximately the same size and the process is therefore isomorphous. "If all the anions of the octahedral sheet are hydroxyls and two thirds of the cation positions are filled with aluminum, then the mineral is called gibbsite. If magnesium is substituted for the aluminum in the sheet and it fills all the cation positions, then the mineral is called brucite (Holtz and Kovacs, 1981)."

Four main groups of clay minerals are well known by geotechnical engineers:

1. ***The Kaolinite Group*** – The general structure of the kaolinite group is composed of silicate sheets bonded to aluminum oxide/hydroxide layers referred to as gibbsite layers. The silicate and gibbsite layers are tightly bonded together with only weak bonding. Kaolinite is a 1:1 phyllosilicate. Low charge afforded by low substitution is enhanced by hydrogen bonding between the tetrahedral and octahedral layers. This bonding holds 1:1 layers tightly together leaving little to no interlayer space for adsorption of cations or water. Thus kalolinite is a non expansive mineral. A typical kaolin crystal can be 70 to 100 layers thick. Figure 2.6 is a schematic diagram of the structure of kaolinite (Woodward et. al., 2002), (Holtz and Kovacs, 1981), (Thomas, 1998).
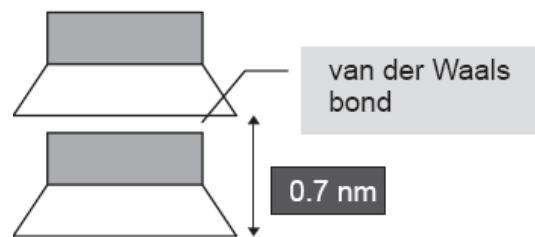
Figure 2.6: Schematic Diagram of Kaolinite Structure (Mitchell, 1992)

2. ***The Montmorillonite/Smectite Group*** – This group has several members which differ mostly in chemical content and the amount of water they contain. The structure of the group is composed of silicate layers sandwiching a gibbsite layer in a silica-gibbsite-silica stacking sequence. Thus montmorillonite is called a 2:1 mineral. The thickness of each 2:1 layer is 0.96nm, and like kaolinite the layers extend indefinitely in the other two directions. Because the bonding by van der Waals forces between the tops of the silica sheets is weak and there is a net negative charge deficiency in the octahedral sheet, water and exchangeable ions can enter and separate the layers. Thus montmorillonite crystals can be very small, but at the same time have a very strong attraction for water (Holtz and Kovacs, 1981), (Woodward et. al., 2002).

The specific surface area of interlayer zones of the smectites ranges from 50 to 120m²/g. The secondary specific surface that is exposed by expanding the lattice so that polar molecules can penetrate between layers can be up to 840m²/g. Moreover, the large amount of unbalanced substitution in the smectite minerals is the cause of their high cation exchange capacities, generally in the range of 80 to 150meq/100gm. All these are evidences of the huge susceptibility to swelling of

soils containing montmorillonite or other members of the smectites. In Figure 2.7 is the schematic diagram of a montmorillonite structure (Mitchell, 1992).

"The montmorillonitic minerals are mostly formed by restricted leaching, so that magnesium, calcium, sodium, and iron cations may accumulate in the system. The formation of montmorillonitic minerals is aided by an alkaline environment, presence of magnesium ions, and a lack of leaching. Such conditions are favorable in semi arid regions with relatively low rainfall or highly seasonal moderate rainfall particularly where evaporation exceeds precipitation (Chen, 1988)."
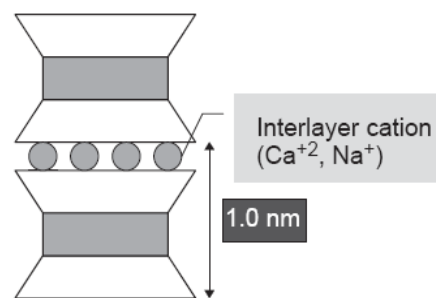
Figure 2.7: Schematic Diagram of Montmorillonite Structure (Mitchell, 1992)

3. *The Illite Group* – This group is basically hydrated microscopic muscovite mica. The structure is composed of silicate layers sandwiching a gibbsite layer in a s-g-s stacking sequence. It has the same 2:1 structure as the montmorillonite, but the interlayers are bonded together with a potassium atom. The potassium atom that bonds the sandwich layers together is much stronger than the weak van der Waals forces which bond the same layers by montmorillonitic clay minerals. Also some isomorphous substitution of aluminum for silicon in the silica is by this mineral group. Figure 2.8 is the schematic diagram of illites (Woodward et. al., 2002), (Holtz and Kovacs, 1981).
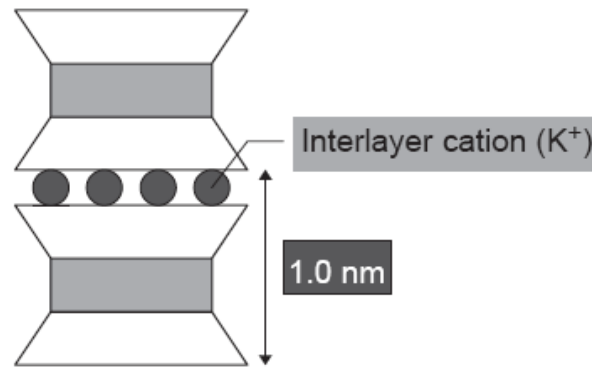
Figure 2.8: Schematic Diagram of Illite Structure (Mitchell, 1992)

4. ***The Chlorite Group*** – This group is relatively common in clay soils. It is made of repeating layers of a silica sheet, an alumina sheet, another silica, and then either a gibbsite (Al) or brucite (Mg) sheet (Figure 2.9). It could be called a 2:1:1 mineral. Chlorite can also have considerable isomorphous substitution and be missing an occasional brucite or gibbsite layer; thus it may be susceptible to swelling because water can enter between the sheets. Generally, it is significantly less active than montmorillonite (Holtz and Kovacs, 1981).
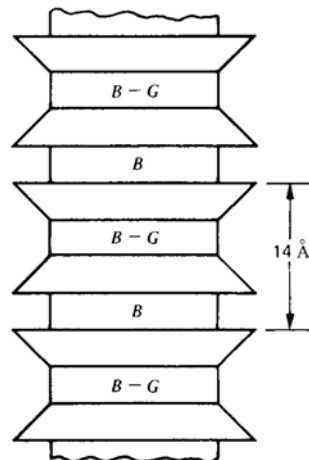
Figure 2.9: Schematic Diagram of Chlorite Structure (Holtz and Kovacs, 1981)

2.2.3 Microstructure

Clay particles are very small, often less than 1μm. The actual size depends on the specific composition and nanostructure. Kaolin particles are about 1 μm in diameter and 0.1μm thick. For such small particle sizes, surface forces are very important, and clay particles often flocculate. Common microstructures in clay–water suspensions are shown in Figure 2.10. Engineering properties of clays are affected by flocculation and aggregation. Particles that are dispersed would obviously allow the

maximum permeability. Flocculation reduces permeability, although aggregation by itself has little effect. Flocculation also affects shear strength and compressibility.
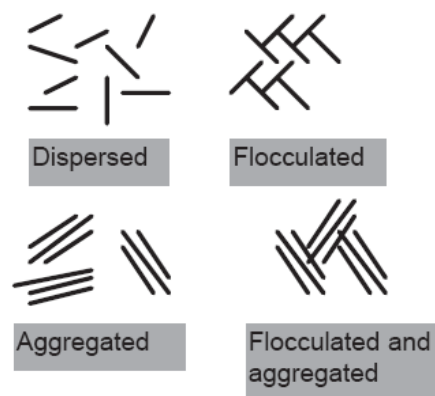
Figure 2.10: Clay microstructures showing dispersed, flocculated (edge–to–face), and aggregated (face–to–face) suspensions. (Mitchell, 1992)

2.3 Mechanism of Swelling; Diffuse Double Layer and Osmosis, Cation Exchange Capacity (CEC)

2.3.1 Mechanism of swelling based on the Double Layer Theory

The clay particles are in very small sizes and therefore their behavior is dominated by surface forces. These surface forces cause clays to adsorb water and consequently cause swelling. The explanation of this swelling is osmosis (US ARMY, TM 5 – 818 – 7, 1983).

Osmosis is defined as the movement of water molecules from an area of high concentration to an area of low concentration. It is the net movement of solvent through a semi permeable membrane from the region where the solution is more dilute to the region where the solution is more concentrated (Figure 2.11) (Chen, 1988). The pressure that must be applied to the solution in order to prevent the flow of water into the solution through the semipermeable membrane is called the osmotic pressure.

13
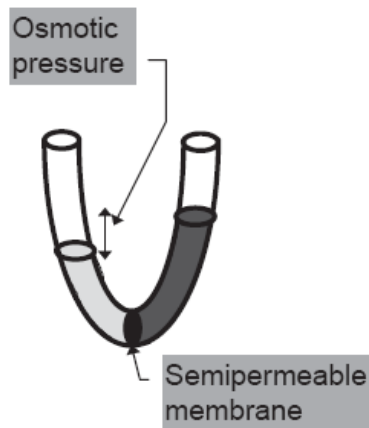
Figure 2.11: Osmosis through a Semipermeable Membrane

Before describing the mechanism of swelling, a short explanation of the double layer theory will be useful for the fully understanding of the swelling behavior of clays.

The adsorbed cations, because of their high concentration near the surfaces of particles, try to diffuse away in order to equalize concentrations throughout the pore fluid. Their freedom to do so, however, is restricted by both the negative electrical field originating in the particle surfaces and ion–surface interactions that are unique to specific cations. The escaping tendency due to diffusion and the opposing electrostatic attraction lead to ion distributions adjacent to a single clay particle in suspension that are often idealized as shown in Figure 2.12 and Figure 2.13. This distribution of cations is analogous to that of air molecules in the atmosphere, where the escaping tendency of the gas is countered by the gravitational attraction of Earth. Anions are excluded from the negative force fields of the particles, with the distribution shown in Figure 2.12. The charged surface and the distributed charge in the adjacent phase are together termed the "diffuse double layer (Mitchell, 1992)". Among several theories, proposed for the description of ion distributions adjacent to charged surfaces, the Gouy - Chapman Theory is the most famous one.

Besides Mitchell (1992), Aytekin (1992) has also referred in his study to authors mentioning the well matching results of the Gouy – Chapman Theory based calculations with the compression and swelling behavior of clays.
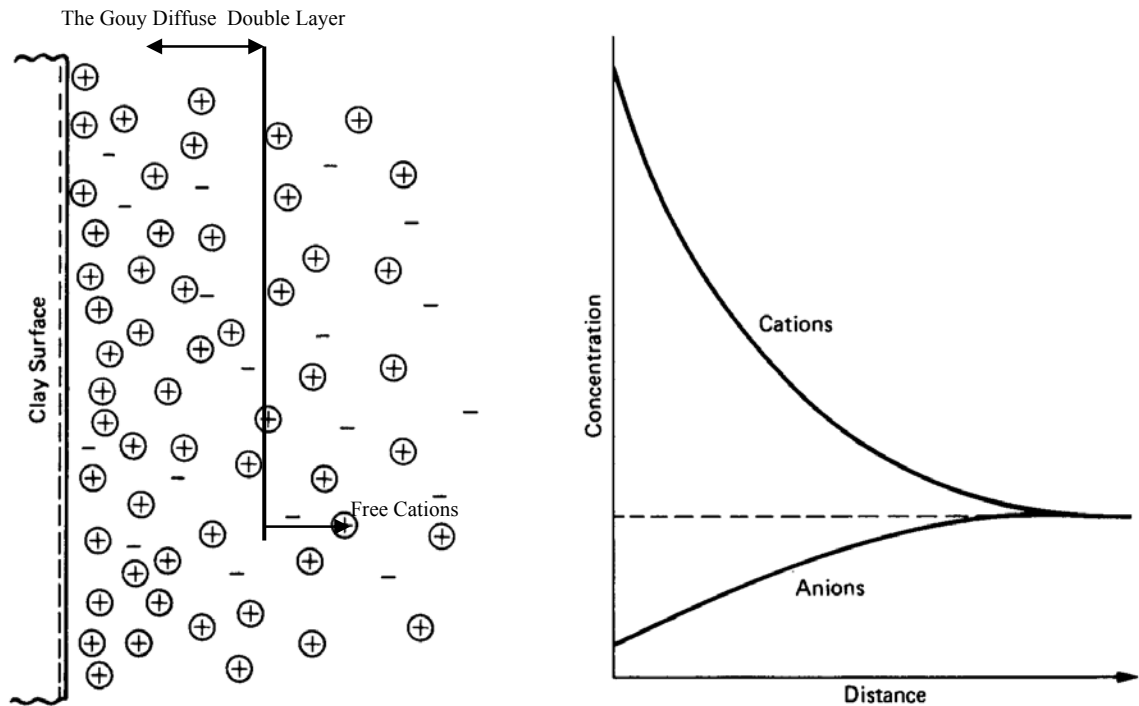
Figure 2.12: Double Layer on Clay Surface (Mitchell, 1992)

The plate shaped clay particles have negative electrical charges on their surfaces and positive charges on their edges. In order to balance these charges, cations from the pore-water solution and water molecules are attracted to the particle surface because of the polar nature of the water molecule. The positive side of the water molecule is, therefore, attracted to the negative clay surface. The positive charged sides of the water molecules cause repulsive forces between the double layers of adjacent clay particles. The negative charges on the surface of the clay particle in combination with attracted cations and water molecules are called diffuse double layer. Water molecules in diffuse double layers behave differently from water that is beyond the double layer in pore spaces. The electrical interparticle force field is a function of both the negative surface charges and the electrochemistry of the soil water. Van der Waals surface forces and adsorptive forces between the clay crystals and water molecules also influence the interparticle force field. The internal electrochemical system must be in equilibrium with the externally applied stresses and the capillary tension in the soil water. The cations attracted to the clay surfaces provide another factor in swelling behavior. Because of the attraction of the negatively charged clay particle surfaces for cations, small spaces within or between clay particles may contain a higher concentration of cations than larger pores within the soil. These conditions create an osmotic potential between the pore fluids and the clay mineral

15

surfaces. Normally, cations diffuse from a higher concentration to a lower concentration in order to evenly distribute the ions throughout the solution. In expansive soils, because ions are held by the clay particles, water moves from areas of low ionic concentration (high concentration of water) to the areas of high ionic concentration (low concentration of water) within the clay particles or aggregates. This influx of water exerts pressure, which causes clay to swell (Erzin and Erol, 2007). The electric field around clay particle acts as a semi-permeable membrane (Figure 2.13). This membrane allows water to enter the double layer but does not allow the exchangeable cations to leave. The rest of the mechanism that affect the swelling phenomenon are cation hydration capillary imbibitions and elastic relaxation. When cations hydrate, their ionic radii increase resulting in a change on the volume mass (Aytekin, 1992).

The thickness of the double layer is perhaps 30 nm. For clays that are 500 nm thick, the double layer has little effect. But for clays that are only a few nm thick, this double layer has a tremendous effect. One effect of the double layer is to cause two clay particles to repel each other when they approach so closely that the double layer of each particle begins to overlap. In this way the double layer controls flocculation, dispersion and swelling. Again, this effect is greatest for clays with a very small grain size, such that their double layer interaction dominates their behavior. Therefore, the greatest swell potential is shown by sodium montmorillonite, which has the smallest grain size. Another explanation for the effect of the interlayer cation on swelling is to consider the effect of the cation on the double layer. Calcium ions in the interlayer region compress the double layer, so the sheets are closer together and do not adsorb water and swell as easily. With sodium ions, the clay swells more easily. Thus the clay mineralogy has a direct effect on its surface chemistry. Through its effect on surface chemistry, clay mineralogy controls microstructure. The result is the engineering behavior of soil, its cohesive strength, flow behavior, permeability, and swelling potential (US ARMY, TM 5 − 818 − 7, 1983), (Chen, 1988).

Double layers overlap

Imaginary semi – permeable membrane surrounding clay particles

Higher ion concentration in the double water

Lower ion concentration in the free water
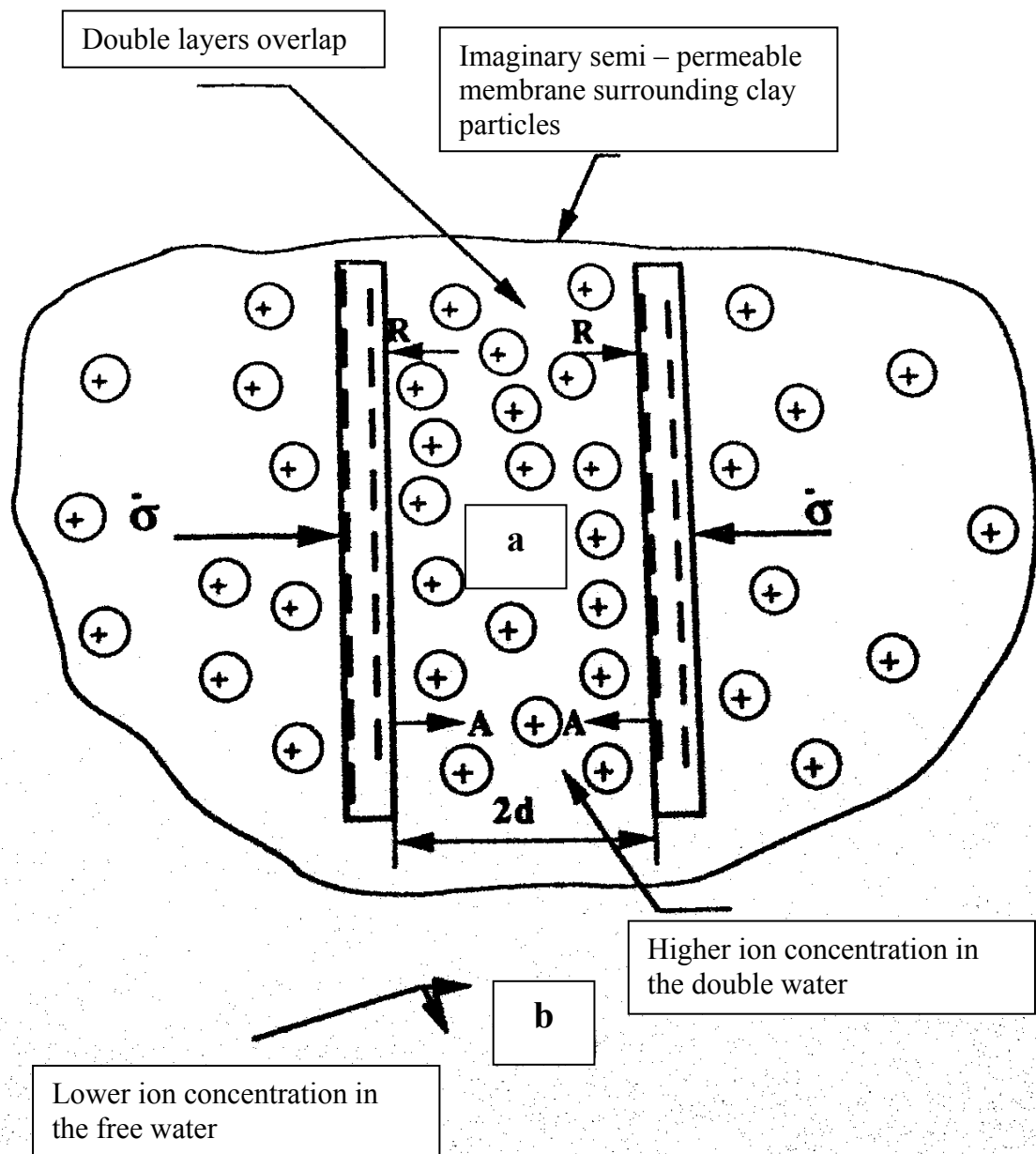
Figure 2.13: Double Layers Around Clay Particles After Ladd (1960), (Aytekin, 1992)

2.3.2 Cation exchange capacity (CEC)

Clay minerals have the property of absorbing certain anions and cations and retaining them in an exchangeable state. The exchangeable state ions are held around the outside of the silica alumina clay – mineral structural unit, and the exchange reaction does not effect the structure of the silica alumina pocket. In clay minerals the most exchangeable cations are Ca^{++}, Mg^{++}, H^+, K^+, $NH4^+$, Na^+, frequently in about that order of general relative abundance. Cations (positive ions) are more readily absorbed than anions (negative ions); hence, negative charges must be predominant on the clay surface. A cation is never permanently attached to the mineral from

which it is absorbed; it can be replaced by an excess cation, like absorbed Na+ ion can be replaced by a K+ ion if the clay is placed in a potassium chloride. The process of replacement by excess cations is called cation exchange (Figure 2.14) (Chen, 1988). The degree of isomorphic substitution in the clay particle surface is different; therefore, the layer charge density of clay minerals shows high variety. This excess of negative lattice charge is compensated by the exchangeable cations (Tombacz and Szekeres, 2006).
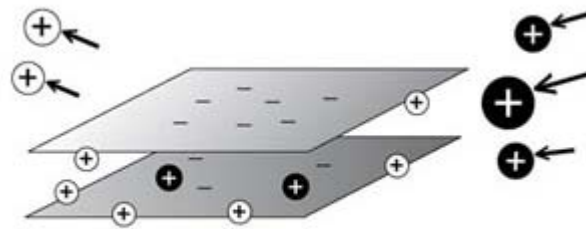
Figure 2.14: Shematic Visualization of the Cation Exchange Process

The cation exchange capacity (CEC) of soils is the maximum number of moles of proton charge dissociable from unit mass of soil (100g) under given conditions of temperature, pressure and aqueous solution composition (Sposito, 2008). Cation exchange capacity is the total of the exchangeable cations that a soil can hold at a specified pH. Soil components known to contribute CEC are clay and organic matter. The exchange sites can be permanent or pH dependent. Mineral soils have an exchange capacity that is a combination of permanent and pH dependent charge sites, while organic soils is predominantly pH dependent (Seybold et. al., 2005).

Swelling potential of soils has been related to many factors by researchers. In 1957, Gill and Reaves were the first who had reported the relationship between cation exchange capacity and swelling potential (Kariuki and Van der Meer, 2004). The dependence of percent swell on the cation exchange capacity has been shown on Figure 2.15 (Yılmaz, 2006).
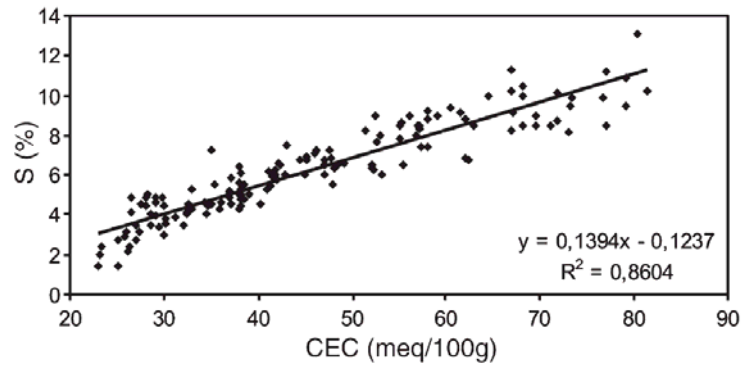
Figure 2.15: Swell Percent vs. Cation Exchange Capacity (Yılmaz, 2006)

As well known in the literautre, the kaolinite minerals are found in the nature positioned as face to edge (Figure 2.16), where the montmorillonite minerals are positioned as face to face (Figure 2.16). The difference in their positioning leads to the differences in CEC of kaolinites and montmorillonites (smectites) and therefore affects the strength of the bonds holding the minerals together (Tombacz and Szekeres, 2006).

Table 2.1 shows the ranges of cation exchange capacities of various clay minerals (Chen, 1988). Regarding to Table 2.1, montmorillonites are 10 times as active as kaolinites in absorbing cations. Table 2.1 also shows that the degrees of particle size results with the increase of the cation exchange capacity. In other words, it can be revealed that the cation exchange capacity is a factor which is controlled by the diffuse double layer around the clay particles.

Kaolinite   Montmorillonite
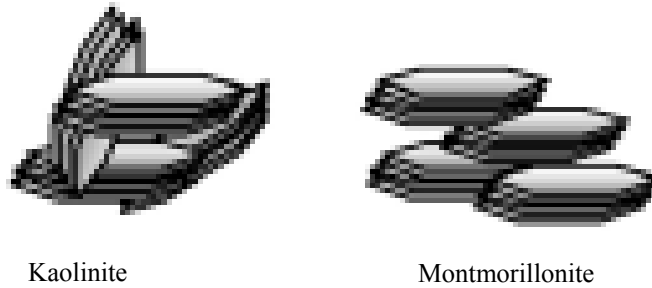
Figure 2.16: Kaolinite and Montmorillonite Structure
(Tombacz and Szekeres, 2006)

Table 2.1: Cation Exchange Capacities of Clay Minerals (Chen, 1988)

	Kaolinite	Illite	Montmorillonite
Particle Thickness (micron)	0.5 - 2	0.003 – 0.1	9.5 A
Particle Diameter (micron)	0.5 – 4	0.5 – 10	0.05 – 10
Specific Surface (m²/g)	10 – 20	65 – 180	50 – 840
CEC (milliequivalents per 100g)	3 – 15	10 – 40	70 – 80

In CEC measuring procedures, the negative charge of a material is balanced with an index-cation. Then, CEC is determined by measuring the difference between the initial and the remaining content of the index-cation. A further possibility is to re-exchange the index-cation chosen with an appropriate salt and to determine the amount of the released index-cations by radioactive counting, visible spectroscopy or by a measurement using atomic absorption. (Dohrmann, 2006)

2.4 Methods Used to Identify and Classify Expansive Soils

Many methods have been developed to measure or estimate the shrink – swell potential of soils. Some sources distinguish these methods into two groups called as; direct measuring methods and indirect estimation methods. The indirect methods can also be separated into two as mineralogical identification methods of swelling clays and as a group of correlations between the index properties and activity method results. Moreover, remote sensing methods such as hyperspectral imaging have been a tool for expansive soil detection in recent years (Ben – Door et. al., 2009), (Chabrillat et.al. 2002). Hence, these are the recent developed methods extending the scope of this thesis and therefore, they will not be mentioned within the methodologies to be described in the paragraphs below.

2.4.1 Mineralogical identification

The negative electric charges on the surface of the clay minerals, the strength of the interlayer bonding, and the cation exchange capacity all contribute to the swelling potential of clays. So, it is possible to evaluate the swelling potential of clay minerals by identifying its mineralogical constitution. The most used five mineralogical identification techniques are; X – Ray diffraction test, differential thermal analysis (DTA), dye adsorption, chemical analysis and electron microscope resolution (Chen, 1988).

The tests listed above are time consuming and require expensive equipments. Although they can be very useful for geologists or soil experts to do their research, they are not suitable in most of the cases for geotechnical engineering purposes. Most of the civil engineering projects do not require such extended tests.

The clay samples employed in the tests of this study have been subjected to X-Ray diffraction tests and their mineralogical structure has been determined. X-ray scattering technique is a non-destructive and an analytical technique which reveal information about the crystallographic structure, chemical composition, and physical properties of materials and thin films. This technique is based on observing the scattered intensity of an X-ray beam hitting a sample as a function of incident and scattered angle, polarization, and wavelength or energy (URL-1).

The results of the X – Ray diffraction tests about the mineralogical content of the test specimens will be given in the related paragraphs.

2.5 Indirect Measurement Techniques

Many investigators have studied to improve the indirect measurement techniques, because some of them are very fast to run and also cheap to conduct. The indirect measurement methods involve the use of soil properties and classification schemes to predict the shrink – swell behavior. But all these methods are based on correlations and are expected to be preliminary indicators of swelling. They are useful for the comparison of the swelling potential of different soil types. Some of the indirect methods used for the evaluation of swelling potential can be listed as Atterberg limits, free swell test, colloid content investigation and determination of linear extensibility (COLE value). Holtz and Gibbs (1956), Gill and Reaves (1957), Seed,

Woodward and Lundgreen (1962), Snethen et.al. (1977), Sridharan and Rao (1988), Kariuki and Frank van Der Meer (2003), Yılmaz (2006), Muntohar (2006), Erzin and Erol (2007) and several others have examined the classification of expansive soils and have developed charts and tables based on index properties, clay content, colloid content and etc.

2.5.1 Atterberg limits

Holtz and Gibbs in 1956 and Seed, Woodward and Lundgreen in 1962 have revealed the fundamental studies for evaluating the swelling characteristics of expansive clays regarding to Atterberg limits, especially to the plasticity index. Johnson and Snethen (1978) and O'Neil and Ghazally (2007) have proposed models outputting free swelling by inputting the liquid limit and natural moisture content of the soil. Regarding the definition of the swell potential (S): "The swell potential is defined as the percentage swell of a laterally confined sample which has soaked under a surcharge of 6,89kPa (1pounds/inch²) after being compacted to maximum density at optimum moisture content (Chen, 1988)." The models mentioned above have been listed in Table 2.2. The relationships given in Table 2.2 are only a few examples indicating the relationships between consistency limits and swelling potential.

Table 2.2: Some Relationship Between Swell Index and Consistency Limits

Model	Remarks	Reference
$S = 60K(PI)^{2.44}$ **(2.1)**	K: constant ($3.6*10^{-5}$)	Seed, Woodward and Lundgreen (1962)
$S = 0.2558e^{0.0838(PI)}$ **(2.2)**	-	Chen (1988)
$S = 2.77 + 0.131LL - 0.27\omega_n$ **(2..3)**	-	O'Neil and Ghazzally (1977)
$\log s = 0.036LL - 0.0833\omega_n + 0.458$ **(2.4)**	-	Johnson and Snethen (1978)

Bowles (2006) has summarized the values of index properties in evaluating swelling potential and classification as in Table 2.3. The table is a summary of the investigations utilized over several types of soils from different parts of the world.

A brief review of the results of the study of Kariuki and Van der Meer (2004) and the study of Sridharan and Rao (1988) are presented as follows, in order to gain a fully understanding about the relationship between consistency limits and swelling potential.

Table 2.3: Potential Soil Volume Change Classification Chart (Bowles, 2006)

Potential for Volume Change	Plasticity Index I_p	Shrinkage Limit w_s, %	Liquid Limit w_L, %	Expansion Index E_I
Low	<18	> 15	20 – 35	21 – 50
Medium	15 – 28	10 – 15	35 – 50	51 – 90
High	25 – 41	7 – 12	50 – 70	91 – 130
Very High	> 35	< 11	> 70	> 130

Kariuki and Van der Meer (2004) have shown in their study that the dependence of percent volume swell (PVC) to consistency limits is in the following order; Liquid Limit (LL), Plasticity Index (PI) and Plastic Limit (PL). According to the results of their study, Liquid Limit is accepted as the most important sign of swelling.

Sridharan and Rao (1988) has concluded in their study that; while the index properties of the smectits are controlled by the diffuse double layer which also controls the swelling, the index properties of the kaolinites are not controlled by the diffuse double layer. Sridharan and Rao exposes that the index properties shall only be used for the prediction of swelling potential of smectites.

2.5.2 Free swell test

"Free swell test consist of placing a known volume of dry soil in water and noting the swelled volume after the material settles, without any surcharge, to the bottom of a graduated cylinder. The difference between the final and the initial volume, expressed as a percentage of initial volume, is the free swell value. The swell test is very crude and was used instead of today's refined testing methods. It can be noticed that soils having free swell values over 100 percent must be considered as soils with medium swelling potentials causing damages on light structures (Chen, 1988)."

2.5.3 The effect of clay and colloid content

The effect of grain size, particularly the colloid content, on the swelling behavior of clayey soils is evident. As stated before, the swelling behavior is controlled by the diffuse double layer which increases its efficiency on the soil mass with the decreasing grain sizes. Therefore, the montmorillonite particles are the most vulnerable clay particles to swelling. The study of Sridharan and Rao (1988), which has been mentioned above, reflects this matter from a specific point of view.

For any given clay type, the relationship between the swelling potential and percentage of clay size can be expressed by the following equation:

$$S = KC^X$$ **(2.5),** (Chen, 1988)

Where;

S: Swelling potential

C: Percentage of clay size finer than 0.002mm

X: An exponent depending on the type of clay

K: Coefficient depending on the type of clay

"Where the quantity of the clay size particles is determined by a hydrometer test, quality or kind of colloid, which is reflected by X and K in Equation 2.5, controls the amount of swell. (Chen, 1988)"

It should also be noted that the prediction of swelling potential based on colloid content is not a reliable way. Yule and Ritchie (1980), Thomas et. al. (2000), Grey and Allbrook (2002) have examined the relationship between clay percentage and have found that the relationship given above is not a reliable one for swelling potential estimation.

Thomas (2000) has studied soil samples with different clay contents. At the end of the study Thomas came out with the swelling potentials vs. clay contents as shown in Figure 2.17. The study by Thomas (2000) represents that the clay content is more important for the prediction of the swelling potential of clayey soils, rather than the clay mineral type.
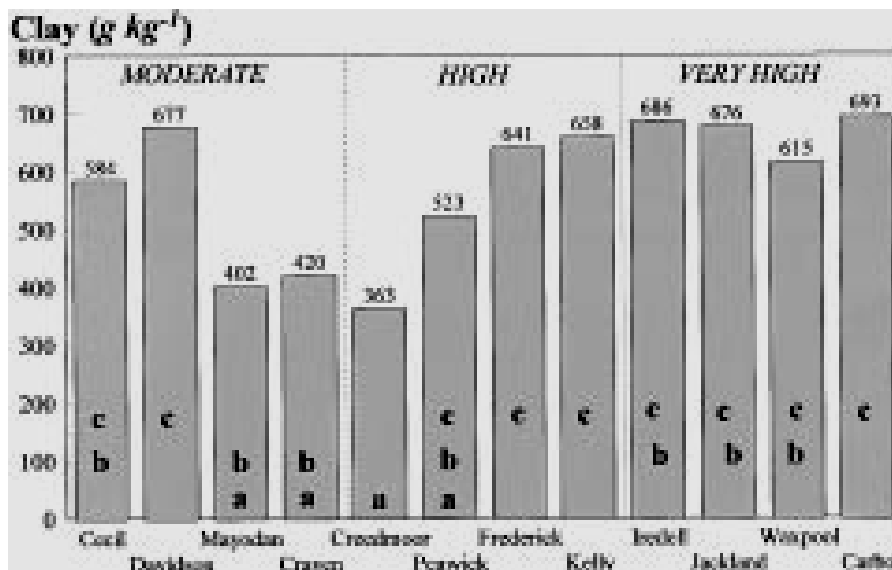
Figure 2.17: Classification Chart for Swelling Potential, (Thomas, 2000)

The activity method proposed by Seed, Woodward and Lundgreen (1962) was based on remolded, artificially prepared soils composed of 23 mixtures of bentonite, illite, kaolinite, and fine sand. The expansion was measured as percent swell on soaking from 100 percent maximum density and optimum moisture content in standard AASHTO compaction test under surcharge of 6.89kPa. The activity for the artificially prepared sample is defined as:

$$Activity = \frac{PI}{C-10} \qquad\qquad (2.6)$$

In the above given equation, where C denotes the percentage clay size finer than 0.002mm, PI denotes the plasticity index. The proposed classification regarding the activity of the sample is given in Figure 2.18. Although this method is related with the clay content, it is also related to the consistency limits of the clay mass, which is controlled by the clay type and diffuse double layer. The evaluation of swelling on both concerns together brings the dependability of the activity method.
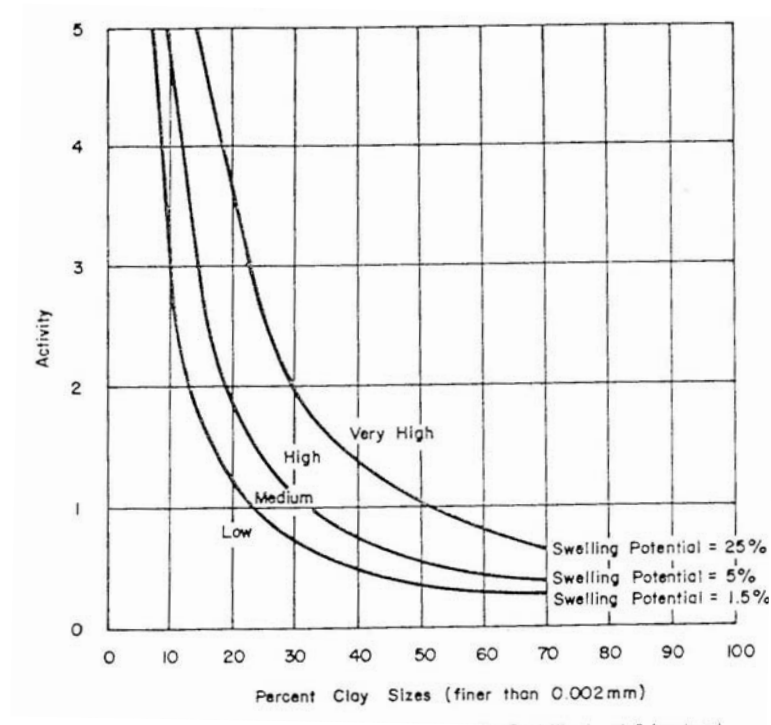
Figure 2.18: Classification Chart for Swelling Potential (Chen, 1988)

2.5.4 Measurement of suction pressure

One of the most unfailing indirect measurement technique is the measurement of soil suction stress and the volume change due to suction. Soil suction, or negative pore pressure, is significant for the observation of the mechanical properties of partially

saturated soils. Delage et. al., 1998 has visualized the effect of suction on swelling, based on their test results as in Figure 2.19.
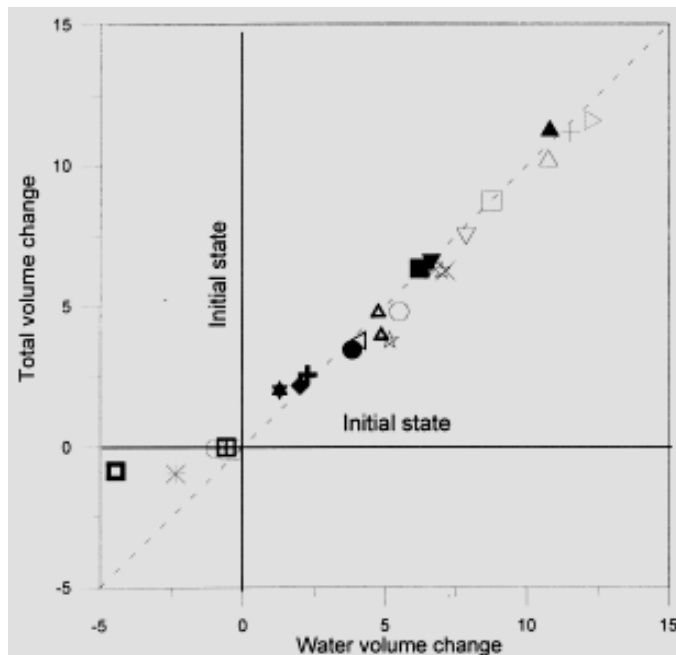
Figure 2.19: Total Volume Change vs. Change on Water Volume
(Delage et. al., 1998)

"Based on Figure 2.19, all swelling points are aligned along the biscentrix. This demonstrates that total volume changes coincide exactly with the volume of absorbed water (Delage et. al., 1998)." This clearly demonstrates the role of suction in the swelling behavior.

Richards (1941) has developed the axis translation technique which was able to control suction in the limited range of several hundred kPa. As an alternative Kassif and Ben Shalom (1971) have introduced the osmotic technique, which gave the ability to measure suction pressures up to 1.5MPa – 2.0MPa. The development of various devices made the measurement of soil suction via humidity control possible. Suction measurements up to hundreds MPa's are nowadays routine procedures (Delage et. al., 1998), (Erzin and Erol, 1992).

In swell prediction methods based on suction, swell is related to the change in the swell suction through a volume change parameter. This parameter is analogous to the compression Index (Cc) for the consolidation process, and is a property of soil (Chen, 1988), (Bowles, 2006). "The ultimate goal of the measurement of soil suction is the prediction of moisture movement and moisture equilibrium rather than the direct measurement of the swell potential (Chen, 1988)."

2.5.5 Percent Volume Change (PVC) methods

A well known indirect measurement technique is the determination of the potential volume change (PVC) of soil and was developed by T. W. Lambe (1951) under the auspices of the Federal Housing Administration. In this method, a sample is artificially compacted and placed in a fixed ring consolidometer. An overburden pressure is adapted to the sample and its vertical expansion is partially restrained by a proving ring over which a scala is placed. After adding water and waiting for two hours, the reading of the proving ring is converted to swelling pressure and to swelling index (Chen, 1988).

Another version of the same test was suggested by Anderson and Lade in 1981, which is called "Volume Change Related to the Expansion Index" (Bowles, 2006). This method is classified as a indirect method since it only intends to measure the expansion potential of the sample.

2.6 Direct Measurement Technique

The widely used method to determine the swelling pressure of an expansive soil is the direct measurement. For the direct measurement of swelling pressure conventional one dimensional consolidometer (odometer) is used.

Testing procedures for four alternative methods are standardized by ASTM with a designation number ASTM D 4546 – 86. All testing methods require that a soil specimen be restrained laterally and loaded axially in a consolidometer with access to free water.

The most accepted and common methods, which are standardized by ASTM are as follows (Dhowian et. al., 1990):

- *Free Swell:* The sample is allowed to swell freely under a seating load, and then loaded to overburden pressure plus the simulated foundation stress.

- *Swell under Low Confining Stress:* In this method, the sample is soaked in the oedometer at a low confining pressure, and the amount of swell is determined. The sample is then loaded to a stress level which is also referred to as the swell pressure, σ_s, to attain the original void ratio.

- ***Saturating the Sample Under Vertical Stress:*** The sample is loaded to vertical stress, σ_o, in one increment and then water is added to saturate the sample under the stress σ_o. The amount of volume change is related to swelling pressure.

- ***Saturation at a Constant Volume:*** The sample is saturated at a constant volume in the odometer, followed by a reduction of vertical stress, σo. Constant volume tests often terminate within 24 to 48 hours (Ofer 1981).

In the performance of a typical swell test, the more important variables involved are; state of sample, moisture content, the applied stress and the time allowed for swelling.

The free swell test gives generally the largest swelling pressure values. According to Thomas (2008), this is because that the specimen going from drier to wetter state during the first part of the test, the matric suction of the sample decreases. Then in the second part of the test, as water is forced out of the soil mass and void spaces try to return to the original void ratio upon this applied force, the original high level of matric suction is restored. Thomas (2008) states, that a part of the added force in the second part of the test shall be accepted as a type of friction as the water molecules are forced to pass between many clay particles trying to electrochemically retain them. This condition is only limited in an unswelled specimen and therefore unable to take place in a constant volume test.

As well as uniaxial direct measuring techniques, triaxial direct measuring techniques have also been developed. Since the main subject of this thesis is the lateral swelling pressure, triaxial direct measuring techniques and uniaxial techniques with limited restrainment are represented in details in the following chapters.

2.7 The Importance of Soil Sampling on Swelling Pressure Prediction

Undisturbed soil samples are needed to conduct an oedometer test and it is essential that the natural water content of soil samples must be preserved. Moreover, special sampling methods must be used to minimize the sampling disturbance, since most of the standard samplers are suitable for sampling relatively soft clays, whereas the consistencies of expansive soils vary from medium to firm (Dhowian et. al., 1990).

For remolded and artificially compacted samples it is obvious that the initial moisture content of the sample will affect the swelling pressure (Chen, 1988). Gürtuğ (2004) has investigated the effect of compaction energy on the behavior of expansive clays and has clearly shown the increase in swelling due to the increase in compaction energy. So, it shall be notified that, the variation in compaction ratio or state of the artificially prepared soil sample against its in situ state will lead to erroneous prediction of swelling pressure.

The samples subjected to swelling tests within this thesis have been artificially prepared by means of the standard proctor test. Since this study is based on the evaluation of the test results instead of reflecting an in − situ state, the use of undisturbed soil samples was not necessary. Furthermore, for a valuable comparison between the test results, all samples have been prepared under similar conditions.

2.8 Lateral Restrainment Effect on Expansion Pressure

As it is well known, most of the studies on expansive soils considered vertical expansion and with testing equipment confining the expansive clay sample laterally. Considering the volume change capacity of soils to be constant it is obvious that the tests conducted restraining the lateral expansion behavior of soil samples will lead to exaggerated expansion pressures or vertical heave.

Many engineers have recognized the three dimensional phenomenon of swelling in their early studies. Researchers like Mc Dowell (1956) and Erol et. al. (1987) have assumed in their studies that only one-third of the total volume change occurs vertically. On the contrary, Crilly et. al. (1992) indicates that the use of a single swell reduction factor would tend to overestimated heave near surface and underestimated swelling pressure at depth (Thomas 2008).

Due to Mosleh A. Al Shamrani et. Al. (2003), "A large discrepancy is usually found between heaves predicted using parameters obtained from oedometer swelling tests and those actually measured in the field. This is simply because the oedometer provides a rigid lateral confinement to the expanding soil; hence all volumetric swells are measured as vertical swells, while the vertical swell measured in the field is only part of the total volume change".

Mosleh A. Al Shamrani et. Al. (2003) have tried to minimize the restrain effect of the testing devices by measuring the swelling pressure with a modified triaxial testing device instead of an oedometer. The use of a triaxial device gave the ability to represent the loading conditions more accurately than the oedometer ring. They have experimentally evaluated the effect of lateral restraint conditions on the predicted heave of expansive soils. They have conducted a series of tests and measurements by using the triaxial and oedometer device and have compared the results with in – situ measurements. The measured swell parameters and indices were utilized to predict field heave measured in an expansive shale formation in Saudi Arabia. The soil formation in the region represents typical expansive shale 8m to 10m thick with relatively high - swell parameters. The experimental station to take the in situ measurements covered an area of 20m x 20m. Approximately 1.5m of overburden was removed before the installation of the instruments in order to expose the expansive material. A saturation system was provided to facilitate water entry to the shale formation. Six instrumented units were installed at 1m intervals. Each unit consisted of a thermocouple psychrometer stack, moisture access tube, surface heave plate, and five deep heave plates. A schematic representation of the field instruments is given in Figure 2.20. Heave, suction and moisture content have been taken regularly over a period of 54 weeks. The profile of cumulative heave down the soil profile, the initial and final moisture content and related initial and final suction values are shown in Figure 2.21.
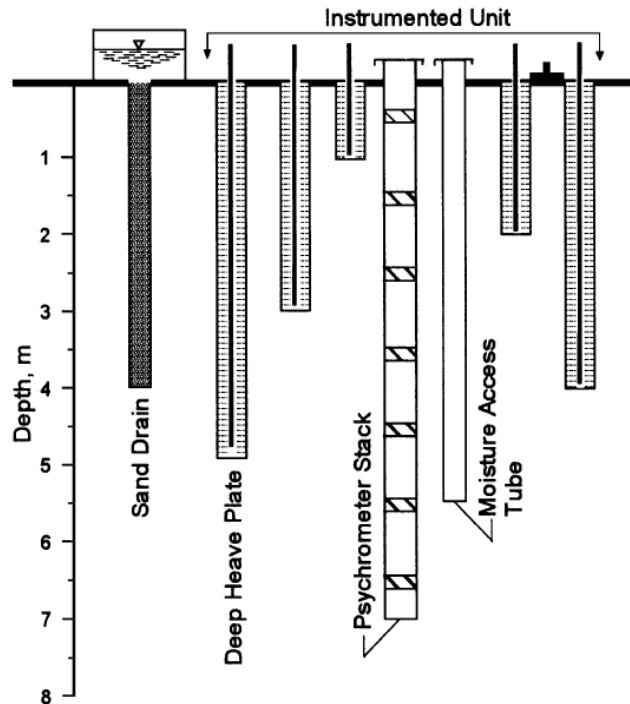
Figure 2.20: Schema of Al - Shamrani and Dhowian's Field Instrumentation
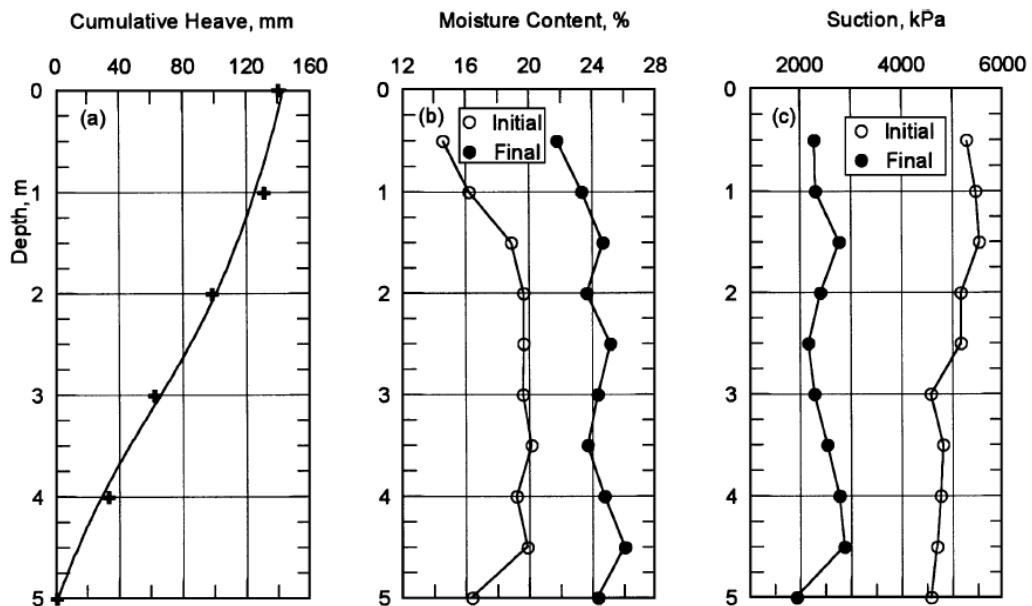
Figure 2.21: In situ Data Recorded by the Field Measurements. (Al - Shamrani and Dhowian, 2003)

As mentioned before, the laboratory swell behavior of the shale was evaluated using various oedometer testing procedures and triaxial swell tests. The aim of the study was to find out the best testing procedure and testing device which will match with results observed from field measurements.

"For laboratory tests, undisturbed samples for the oedometer were recovered from boreholes of depths ranging from 2m to 10m. Due to the highly fissured and laminated structure of the shale, it was difficult to extract intact undisturbed samples for the triaxial tests. Triaxial swell tests were, therefore, limited to compacted specimens prepared at a unit weight and moisture content comparable to the field values. In order to be able to compare the results, a series of oedometer tests were also conducted on compacted samples" (Al - Shamrani and Dhowian, 2003).

By the swell tests carried out with the oedometer, tree different procedures have been used. They were; free swell tests (ISO), constant volume test (CVS) and swell overburden test (SO).

"The triaxial swell tests were carried out in a hydraulic triaxial stress path cell of the type reported by Bishop and Wesley (1975). A schematic diagram of the layout of the testing system is shown in Figure 2.22. The axial load is applied to the sample by pressurizing the lower chamber at the bottom of the cell. The piston pushes up a loading ram, at the top end of which is the pedestal on which the soil sample is mounted. The sample is pushed upward against a stationary submersible load cell. This is a salient feature of the stress path cell that makes it possible to measure the vertical swell" (Al - Shamrani and Dhowian, 2003).
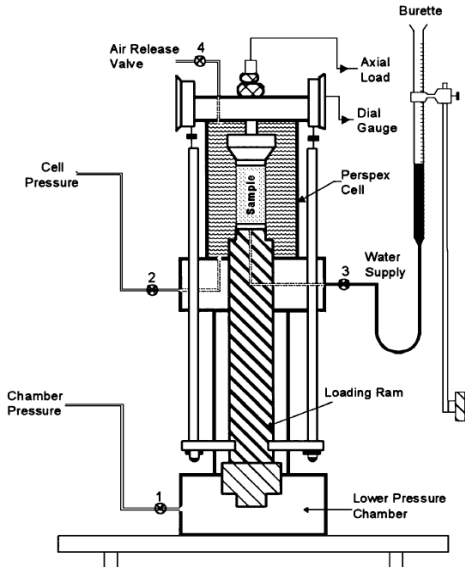
Figure 2.22: Bishop–Wesley Stress Path Triaxial and Experimental Set-up

In order to represent the stress and moisture conditions as likely as the field, the swell overburden test procedure has been applied by the triaxial tests and symbolized as TSO.

The average magnitudes of swell pressure, P_s, and swell index, C_s, for the shale, obtained in oedometer and triaxial tests, are given in Table 2.4.

Table 2.4: Shale Swell Parameters obtained from Oedometer and Triaxial Swell Tests (Al - Shamrani and Dhowian, 2003)

Swell Test	Test Equipment	Swell Pressure (kPa)	Swell Index C_s
Free Swell (ISO)	Oedometer	829	0.069
Constant Volume Test (CVS)		586	0.054
Swell Overburden Test (SO) – Undisturbed Sample		390	0.156
Swell Overburden Test (SO) – Compacted Sample		860	0.145
Triaxial Swell Test	Triaxial	1070	0.041

Subsequent to the performance of laboratory tests, heave predictions have been made based on the pressure approach. The heave values calculated based on the OSO (Oedometer Swell overburden Test) and TSO (Triaxial Swell overburden Test) test results and the in situ measured field heave values are shown in Figure 2.23. (Al - Shamrani and Dhowian, 2003)
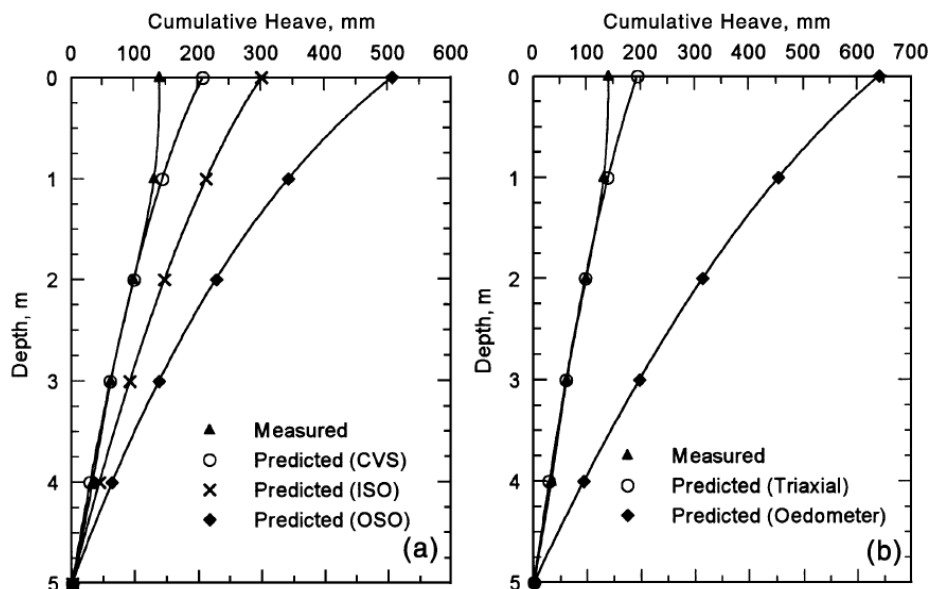
Figure 2.23: Measured and predicted heave based on pressure technique: (a) using oedometer swell parameters, and (b) comparison of heave predictions based on oedometer and triaxial data. (Al - Shamrani and Dhowian, 2003)

As it can be seen from Figure 2.23., where predicted heave values based on the triaxial test results match with the data obtained from field measurements, the oedometer test results lead to overestimated heave prediction due to lateral restraint.

A second study, pointing out the importance of the lateral restrain in swelling pressure testing was made by T. Windal, and I. Shahrour (2002). This study was based on making axial swelling deformation measurements in means of permitting the sample to deform laterally during swelling.

Windal and Shahrour have performed several free swell tests with flexible oedometer rings having different stiffnesses. The results of this study are shown in Table 2.5. Lateral swell pressures and axial swell strains recorded on free swell tests using oedometer rings with different stiffness as $K_r = 850$MPa and $K_r = 3075$MPa ended up with completely different results. Under a surcharge load of 732kPa, axial strain recorded with the stiff ring was $\varepsilon_a = 1.8\%$, where for the ring with 850MPa stiffness the axial strain value was only $\varepsilon_a = 0.2\%$ (Windal and Sharour, 2002).

Table 2.5: Influence of the Oedometer Ring Stiffness on Compacted Clay Samples Subjected to Swell Test (Windal and Sharour, 2002)

Surcharge (kPa)	Oedometer Ring Stiffness Kr (MPa)	Axial Strain ε_a(%)	Lateral Swelling Pressure (kPa)
732	850	0.2	566
732	3075	1.8	1187

Together with the development and use of testing equipment not restraining the swelling clay specimens in lateral direction, the ability to measure the lateral swelling pressure was gained. Subsequently, the importance of lateral swelling pressure has been understood. Especially for deep excavations in areas having soil profiles consisting of soils with high swelling capacities the earth retaining systems should be designed as to be able to overcome the lateral swelling pressures. Concerning the anisotropic behavior of clay type soils, lateral swelling pressures may exceed the vertical swelling pressures. Richards and Kurzene (1973) have measured on a 7.5m high retaining system in stiff clay that lateral pressures have stabilized at 1.3 to 5.0 times the overburden pressure (Fourie, 1989).

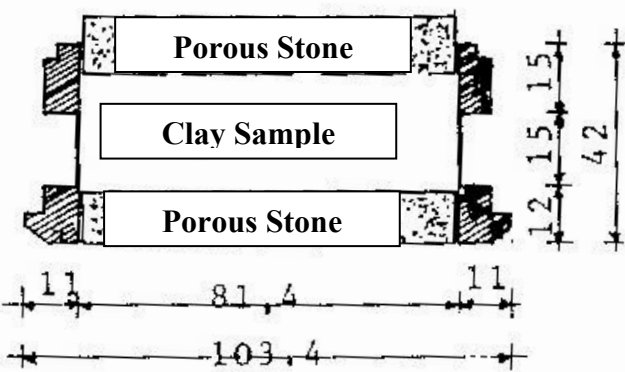## 2.9 Lateral Swelling Pressure and Measurement Techniques

The development of lateral swelling pressure has been described by Aytekin (1992) in his Ph. D. thesis "Finite Element Modelling of Lateral Swelling Pressure Distribution Behind Earth Retaining Structures". Aytekin (1992) has described the development of lateral swelling pressure as follows: "Boundaries of an expansive soil must not be restrained if the soil is to increase its volume. The ground surface increases in elevation as expansive soils swell vertically. If the ground surface is cracked and fissured, the lateral increase in volume accommodated by cracks or fissures closing as the soil mass expands into the voids of the cracks. However, when there are no cracks or fissures or when they are very small, the soil becomes restrained in the lateral directions. Thus, no volume change occurs and a lateral swelling pressure develops." It is very easy to assume the restrain of adjacent soil body's to be alike the restrain of a rigid earth retaining system. So, it wont be wrong if it is said that an improper designed earth retaining system holding back a swelling type of soil will be the cause of the development of significant lateral swelling pressures. For this reason, understanding of lateral swelling behavior of soils and the employment of the determined facts into the design has major importance. As well as earth retaining structures, buried structures, such as pipelines or tunnels are also subjected to triaxial swelling pressure. Einstein (1989) has reported a number of swelling cases about invert heave and crown displacements of tunnels in Europe. In some sections of the Kappelesberg Tunnel with a length of 415m in Germany an invert heave of 4.7m has been recorded (Hawlader et. al.)

Some examples of laboratory studies performed in order to specify the three dimensional swelling behavior including lateral swelling pressure as well as vertical swelling pressure, are summarized in the following paragraphs.

2.9.1 Thin walled lateral swelling pressure ring

Lateral swelling pressure measurements have been done by using several devices. A widely known device is a modified type oedometer. It is an oedometer with a thin walled ring instrumented with strain gauges. This thin walled ring is known as the "Lateral Swelling Pressure Ring (LSPR)" and was mainly presented by Komornik, A. and Zeitlen J., G. in 1965.

The Lateral Swelling Pressure Ring is an oedometer ring made of stainless steel, with an internal diameter of 81.4mm and a height of 42.0mm (Figure 2.24). The ring has the middle of its section trimmed to a thickness of 0.7mm. The trimmed section, 15mm high, is instrumented with 4 strain gauges of 350 ohm in a full bridge configuration, attached to the ring at mid – height of this section. The ring is calibrated by clamping it between end plates, introducing air under pressure to the inner part of the ring and recording the corresponding strain with a digital strain indicator and a strain recorder.

Figure 2.24: Lateral Swelling Pressure Ring

Ofer (1981) has conducted some comparative tests by using this lateral swelling pressure ring. The aim of its comparative study was to show that the possibility of lateral movement is a situation not simulated in nature and will lead to errors in lateral pressure measurement. The lateral swelling pressures determined with the lateral pressure ring has been compared with the test results obtained by means of an in situ swelling pressure probe (Thomas, 2008).

The tests with lateral swelling pressure ring were conducted by compacting the specimen into the ring and then loading and allowing it for consolidation for a period of 24 hours under an applied pressure of 19 kPa. Afterwards, the clay was inundated with water. Horizontal strains and vertical movements were recorded until the sample had stabilized and no further variation in horizontal and vertical strains was noted. Figure 2.25 shows the results of the tests. From the LSP ring test results, it was anticipated that for a clay compacted to a density of 1,45t/m³ at an initial moisture of 15,2% and loaded with a vertical pressure of 17 kPa, a lateral swelling pressure of 100 kPa and a swell of 8% would develop.

A schematic drawing of the in situ swelling probe is given as Figure 2.26. The in-situ swelling pressure probe consists of a cutting edge at the bottom, a hollow cylinder above with an inner diameter of 70mm and thinned wall of 0.6mm. Connected with a water reservoir at the surface, two water supply rings were mounted at each end of the measuring module. The pressure transducer is a cylinder which has an airtight chamber at mid-height. Holes are provided to allow connection of tubes from an air pressure system and to allow passage of electric leads from the strain gage to a strain indicator. Ofer et. al. (1984) have further developed the in - situ pressure probe having a double shear vane added on it. This further development gave the possibility to determine the variation of the shear strength simultaneous to swelling pressure (Ofer, 1981), (Ofer et. al., 1984), (Thomas, 2008).
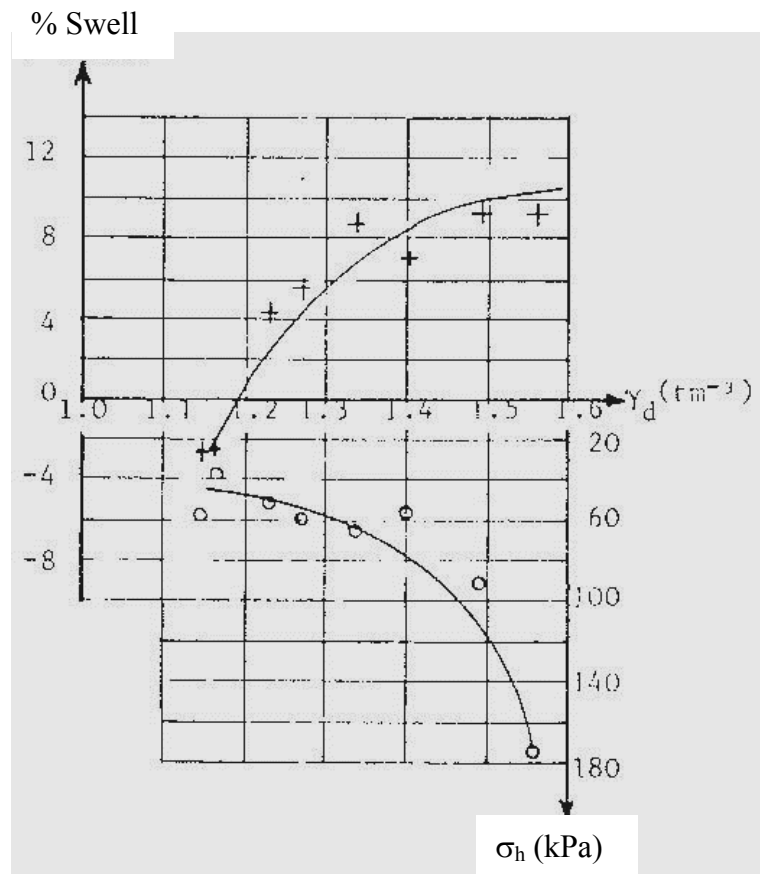
Figure 2.25: Density v.s % Swell – Lateral Swelling Pressure Relation for the LSP Ring Test (Ofer, 1981)
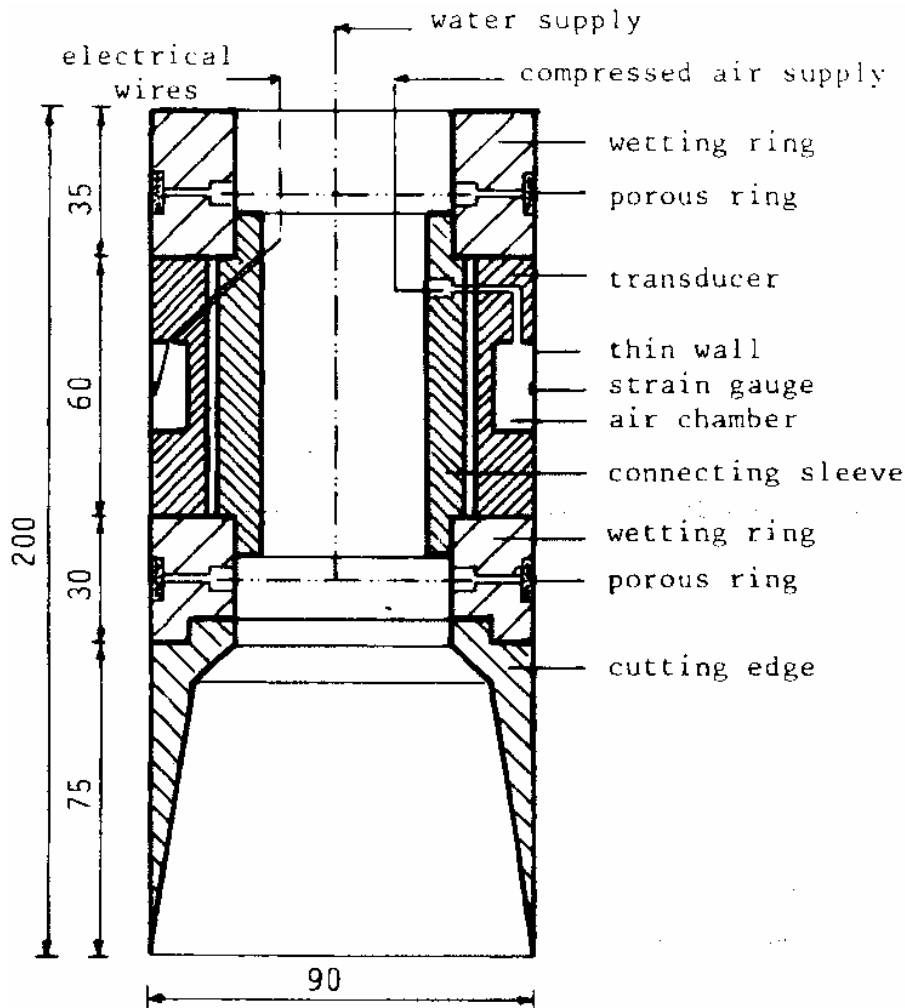
Figure 2.26: In Situ Swelling Pressure Probe (Ofer, 1981)

In the contrary to the test results obtained by the lateral swelling pressure ring, the results of the in-situ probe reveal much higher values. Lateral swelling pressures up to 575kPa were recorded after 8 days with a limited percent swell of 2.9% (Ofer, 1981).

Ofer (1981) has reported that the degree of confinement together with the dimension of the specimen, are major factors affecting the lateral swelling pressure. Ofer and Komornik (1982) have determined that lateral swelling pressure decreases rapidly with the increase in lateral strain.

Based on Ofer's findings, Thomas (2008) states in his study that Ofer has enhanced the ability of the lateral swelling pressure ring by introducing air pressure into the system to counterbalance any lateral swell strain. The air pressure was applied from a second circular cell confining the thin walled ring (Figure 2.27).
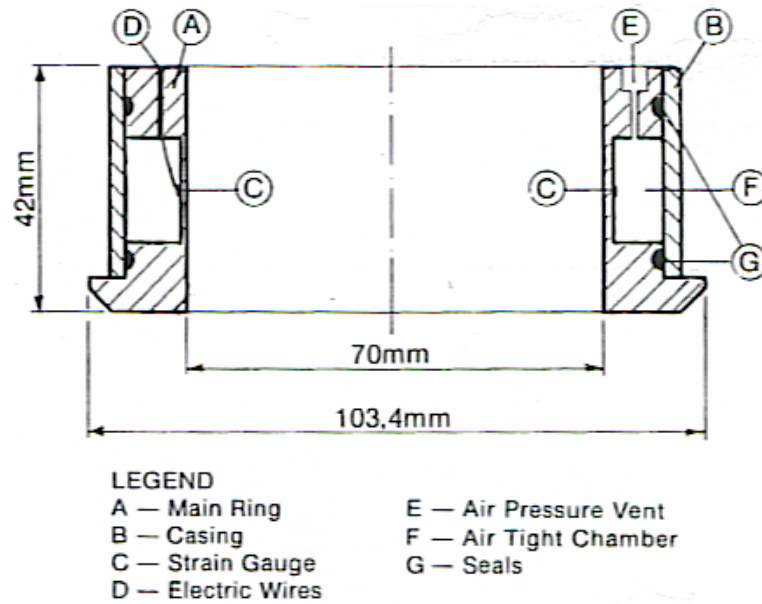
Figure 2.27: The Lateral Pressure Ring of Ofer (Thomas, 2008)

Ertekin (1991) constructed a lateral pressure measuring flexible ring oedometer as described by Komornik and Zeitlin (1965). Edil and Alanzy (1992), Erol and Ergun (1994), Ergüler (2001), Ergüler and Ulusay (2003), Sapaz (2004) and Avşar et al. (2009) have conducted a number of swelling tests with a similar or a modified version of this equipment. For the tests that have been conducted within this thesis, a modified version of the thin walled oedometer ring has been used. The modified ring in this study has been based on the lateral pressure ring of Ertekin (1991).

Ertekin (1991), has rebuild the lateral pressure ring in the Middle East Technical University. This ring, which is a thin walled oedometer ring is similar to the one developed by Komornik and Zeitlen in 1965. The main ring of the device is made of high quality alloy steel. The material Code is Ç4140, which is equal to DIN 42 Cr Mo 4. The internal diameter of the ring is 63,5mm. The wall thickness and the height of the ring are 0,35mm and 78mm, respectively. A Wheatstone bridge was made up by means of mounting four strain gauges 90° apart on the outer wall of the ring. The thin wall of the oedometer was protected against shocks by installing pivot bolts through three holes staggered as 120° apart from each other. Since the calibration of the device is made by means of applying fluid pressure on to the ring, the outer ends of the ring body are screw threaded. These ends are designed to hold top and bottom caps fluid tight during the calibration process. The fluid tightness of the caps is supported with o – rings. The ring body was subjected to a head treatment and hardening process, in order to avoid any deformations after release of

pressure during testing. The setup has been protected against rust by galvanization. A cross – section of the set up of Ertekin is shown in Figure 2.28 and a photograph of the device is shown in Figure 2.29.
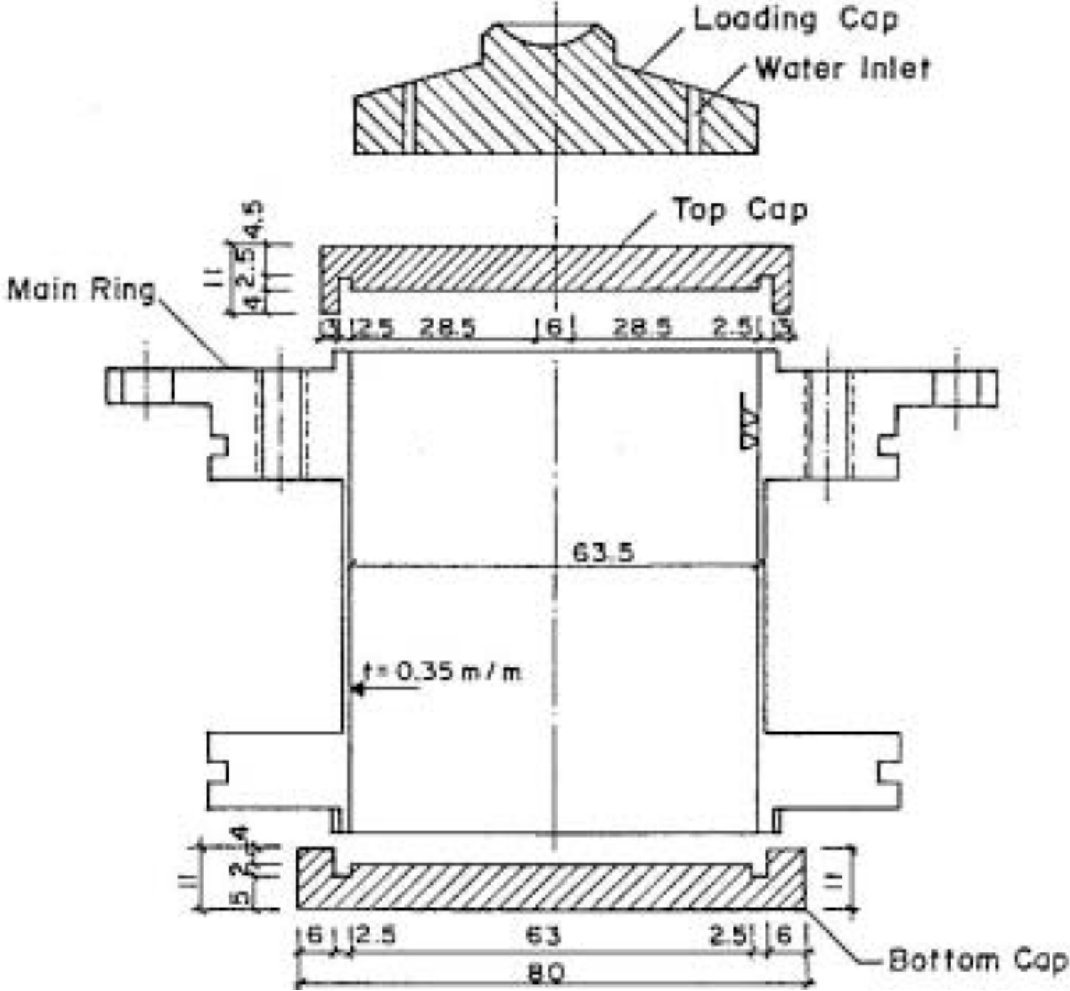
Figure 2.28: Lateral Swell Pressure Test Set Up of Ertekin (Ertekin, 1991)

Figure 2.29: Photographs of the Lateral Swell Pressure Test Set Up of Ertekin

The electrical strain gauges, which are mounted on the exterior surface of the ring, measure the lateral swelling pressure. Four 120ohms electrical strain gauges are installed to the mid – height of the ring. Cu – Ni alloy foil is the sensing element of the strain gauge which is fixed into epoxy carrier. Operational temperature range is between -20° to +80° C. Strain limit of this gauge type and gauge factor are 3% maximum and 2.1, respectively. The gauge length is 10mm (Sapaz, 2004), (Ertekin, 1991).

Katti and Katti (1987) determined in 1987 that the saturated expansive soil behaves unusually with respect to the development of lateral pressure both at active and at

rest conditions. Considering this aspect of Katti and Katti, (1987), Erol and Ergun (1994) performed constant volume swell tests and swell overburden tests on statically compacted clay samples from the Aegean Coast of Turkey.

In the constant volume test procedure, the specimen was left for relaxation for some time after it was placed into the ring. Then, the specimen was inundated with water, and the swelling of the specimen in vertical direction was avoided by means of gradually increasing the applied vertical pressure. The test continued until the termination of swelling. Continuous records of lateral pressures were obtained throughout the experiments. At the equilibrium, the vertical and lateral stresses are defined as swelling pressures. The rebound characteristics were obtained by reducing the vertical pressures in decrements.

In the swell overburden test, a predetermined surcharge pressure was applied to the specimen in dry, and kept for one hour for equilibrium. Then the sample was inundated with water and allowed to swell while registering the lateral pressures continuously. The ultimate swell percent under particular surcharge and variations in the lateral stresses were obtained.

Samples with identical dry densities and varying initial water contents in the range between 27% and 43% weresubjected to the CVS test. According to the results shown in Figure 2.30, the rate of development of vertical pressure is faster in comparison to the lateral swell pressure. This behavior is more dominant with increasing water content. On the contrary, the development of lateral swell pressure continuous to increase at faster rates after the development of vertical pressure slows down. The lateral swell pressure reaches values in excess of vertical swell pressure.
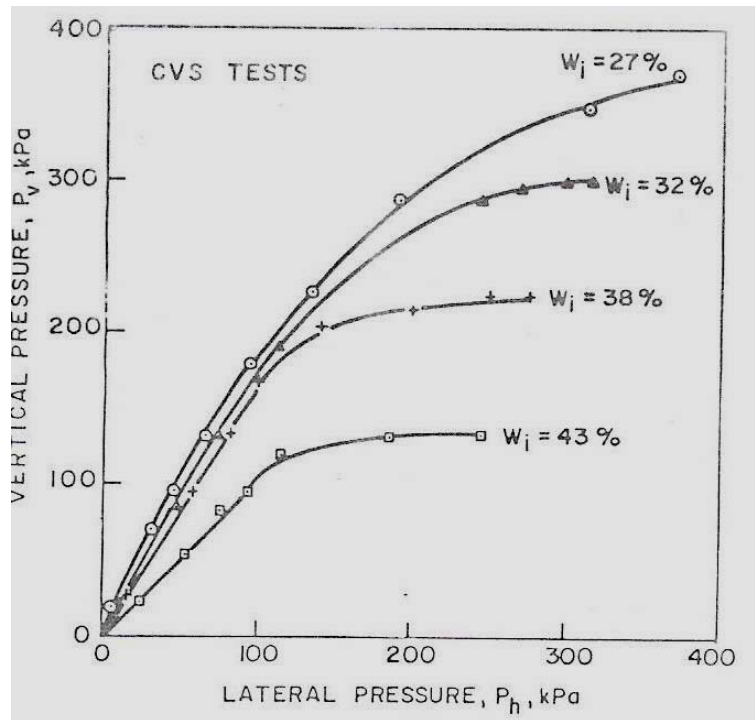
Figure 2.30: Development of Vertical and Lateral Stresses in CVS Tests (Erol and Ergun, 1994)

The variation of Ks (swell pressure ratio) with initial water content obtained at the end of the CVS tests by Erol and Ergun (1994) is given in Figure 2.31. The Ks ratio rises up to 1.55 with the increase of initial water content.
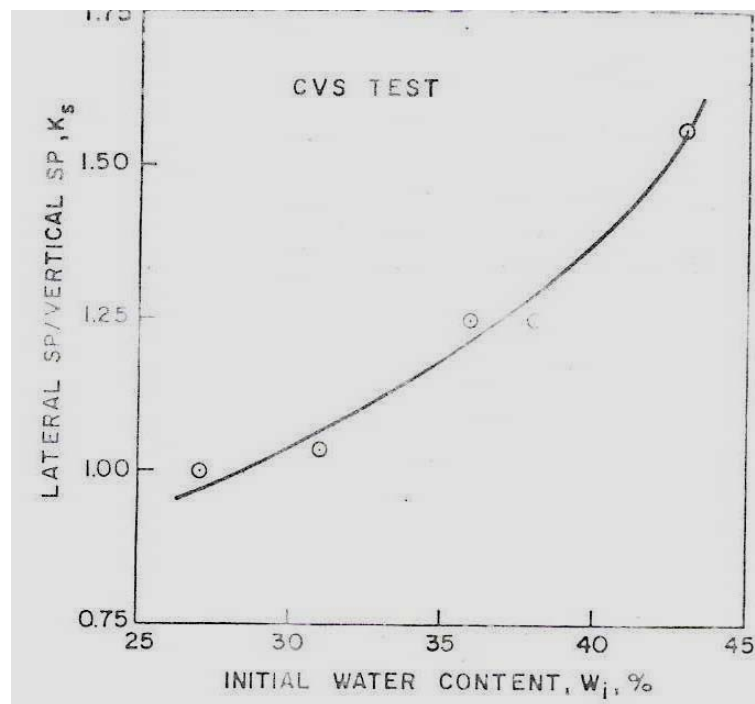
Figure 2.31: Swell Pressure Ratio vs. Initial Water Content in CVS Tests (Erol and Ergun, 1994)

Swell overburden (SO) tests have also been made by Erol and Ergun on compacted samples of the same clay. By employing samples with identical dry density and water content, the development of lateral swell pressure with increasing vertical swell deformation under constant surcharge pressures of 50kPa, 100kPa, 150kPa, and 200kPa has been studied. The investigators have noted that under constant surcharge load, the lateral swelling 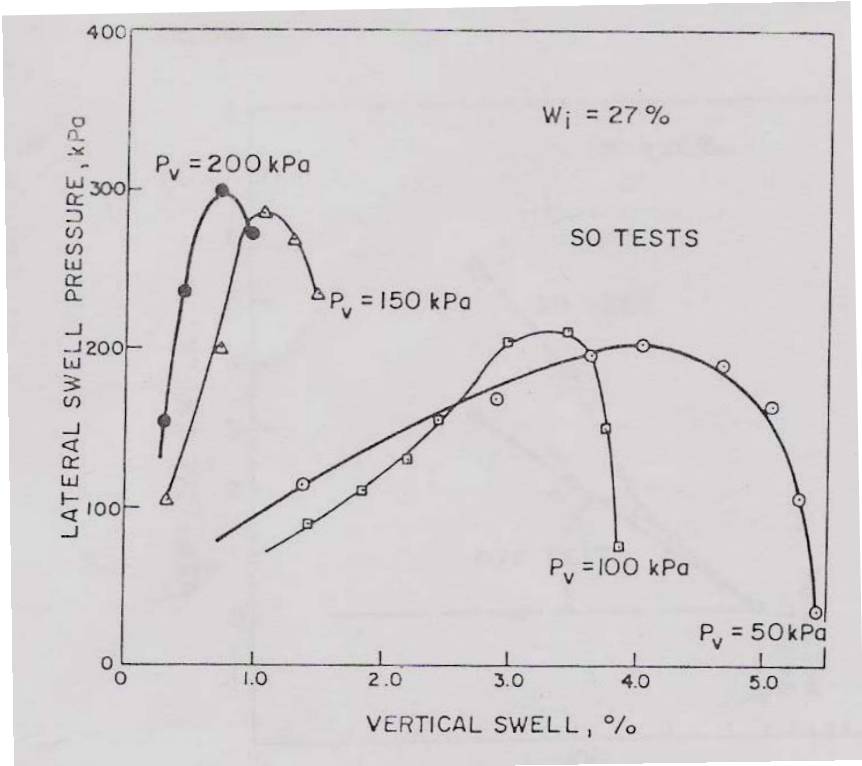pressure increases rapidly with time at the beginning of the saturation phase. Further increase in time and vertical swell deformation ends up with the decrease of lateral swelling pressure. This has been illustrated by the investigators as in Figure 2.32.

Figure 2.32: Typical Lateral Pressure vs. Vertical Swell Behavior in Swell Overburden Tests (Erol and Ergun, 1994)

As it can be seen from Figure 2.32, the decrease of lateral swelling pressure under high surcharge values like 100kPa and 150kPa is very limited in comparison with the decrease of the lateral swell pressure in tests conducted by applying lower surcharge pressures (Erol and Ergun, 1994).

Sapaz (2004) investigated the anisotropic characteristics of the clayey samples encountered in the excavations of the Batıkent – Sincan Metro Line Tunnel in Ankara. Sapaz (2004) has employed compacted clay samples in the tests. The tests have been conducted according to the constant volume test procedure as described in

the ASTM D 4546 – 03. Sapaz (2004) has tabulated the results of the triaxial swelling tests as in Figure 2.33. It should be noted that the constant volume test procedure applied by Sapaz was only restraining the occurrence of strain in the vertical direction. In the contrary, the device used by Sapaz (2004), which is the same device regenerated by Ertekin (1991) as a prototype of the lateral swelling pressure ring of Komornik and Zeitlin (1965), does allow the specimen expand laterally.

		ξ = 1.10 (kg/cm³)	ξ = 1.15 (kg/cm³)	ξ = 1.20 (kg/cm³)	ξ = 1.25 (kg/cm³)	ξ = 1.30 (kg/cm³)
$\square_i$ = 15%	Pv (kg/cm²)	0,66	0,83	1,01	1,91	2,43
	Ph (kg/cm²)	0,45	0,54	0,68	1,20	1,86
	Sr = Ph/Pv	0,68	0,65	0,67	0,63	0,77
	ξ $_f$	48,63	45,48	45,55	43,39	38,66
$\square_i$ = 20%	Pv (kg/cm²)	0,52	0,80	0,90	1,60	2,06
	Ph (kg/cm²)	0,41	0,47	0,62	1,05	1,69
	Sr = Ph/Pv	0,79	0,59	0,69	0,66	0,82
	ξ $_f$	49,99	47,87	43,80	40,89	38,76
$\square_i$ = 25%	Pv (kg/cm²)	0,47	0,69	0,80	1,25	
	Ph (kg/cm²)	0,37	0,45	0,58	0,82	
	Sr = Ph/Pv	0,79	0,65	0,73	0,66	
	ξ $_f$	50,12	48,76	43,51	42,50	
$\square_i$ = 30%	Pv (kg/cm²)	0,40	0,63	0,73		
	Ph (kg/cm²)	0,33	0,41	0,54		Pressure decrease Sr decrease
	Sr = Ph/Pv	0,83	0,65	0,74		
	ξ $_f$	50,84	47,59	44,75		
$\square_i$ = 35%	Pv (kg/cm²)	0,36	0,52			
	Ph (kg/cm²)	0,31	0,37			
	Sr = Ph/Pv	0,86	0,71			
	ξ $_f$	49,95	47,57			
$\square_i$ = 40%	Pv (kg/cm²)	0,31				
	Ph (kg/cm²)	0,27	Pressure Increase			
	Sr = Ph/Pv	0,87				
	ξ $_f$	50,29				

Figure 2.33: Test Results of Sapaz (2004)

As it can be seen Figure 2.33, both lateral and vertical swelling pressures increase with increasing dry unit density. Oppositely, the increase in water content leads to a decrease in swelling pressure. Day (1998) has performed swelling tests on dessicated California Clay samples, which have ended up with similar findings (Avşar et al., 2009).

The test results point out that the development of vertical swelling pressure is much faster than the development of lateral swelling pressure. Figure 2.34 is a typical example visualizing the time shift in the development sequence of vertical and lateral swelling pressure. Sapaz has stated the time necessary for fully development of

lateral swelling pressure as to be recorded within a range of 5000min – 8000min, which corresponds to 4 to 5 days.
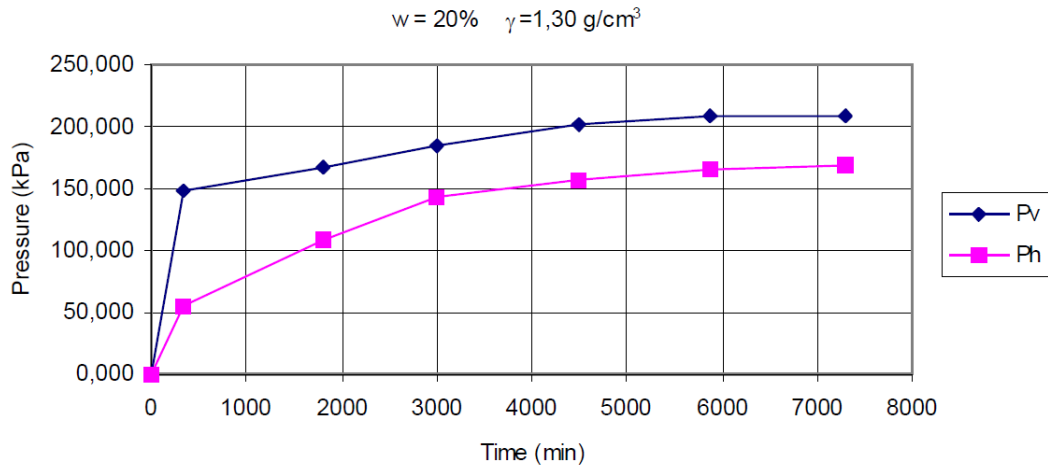

Figure 2.34: Lateral and Vertical Swelling Pressure vs. Time Graph (Sapaz, 2004)

Avşar et al. (2009) have also investigated the anisotropic behavior of Ankara Clay. Districts like Balgat, Çukurambar and Karasunlar in Ankara has been selected as sampling area. The sampling depth has been selected within the active zone, which corresponds to depths varying between 1.0m and 2.4m. The tests have been conducted on disturbed and undisturbed soil samples. Avşar et al. have used a similar, but smaller manufactured version of the thin walled oedometer ring of Ertekin (1991) (Figure 2.35).

According to the results of the study of Avşar et al. (2009), the lateral swelling pressure is lower than the vertical swelling pressure in Ankara Clay. The authors refer to the previous triaxial swelling tests in Ankara Clay, and point out that the swelling pressure ratios (Ph/Pv) within the range of 0.34 – 0.98 are in harmony with the test results having an average swelling pressure ratio of 0.75 as obtained by Sapaz (2004).

Avşar et al. (2009) have also investigated the effect of orientation of the clay particles on anisotropic swelling behavior of clays. They have confirmed that as reported by Chen and Huang (1987), the swelling pressure in the direction perpendicular to particle orientation is greater than that in the direction parallel to particle orientation. Additional to swelling pressure tests, SEM records of the specimen have been obtained for the prediction of this issue.
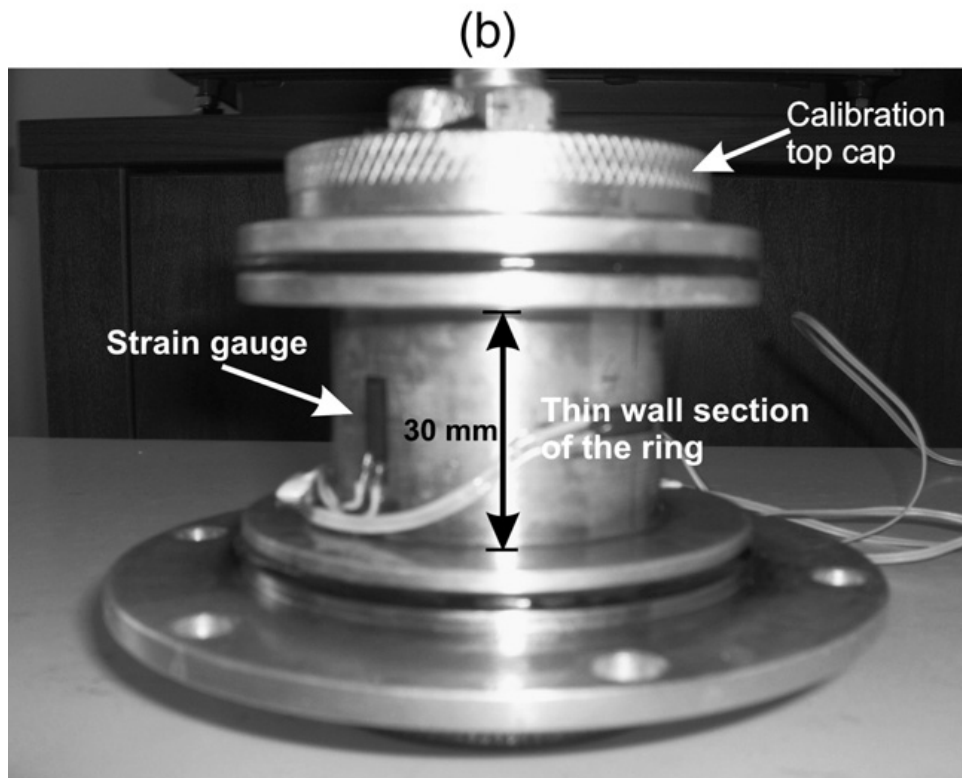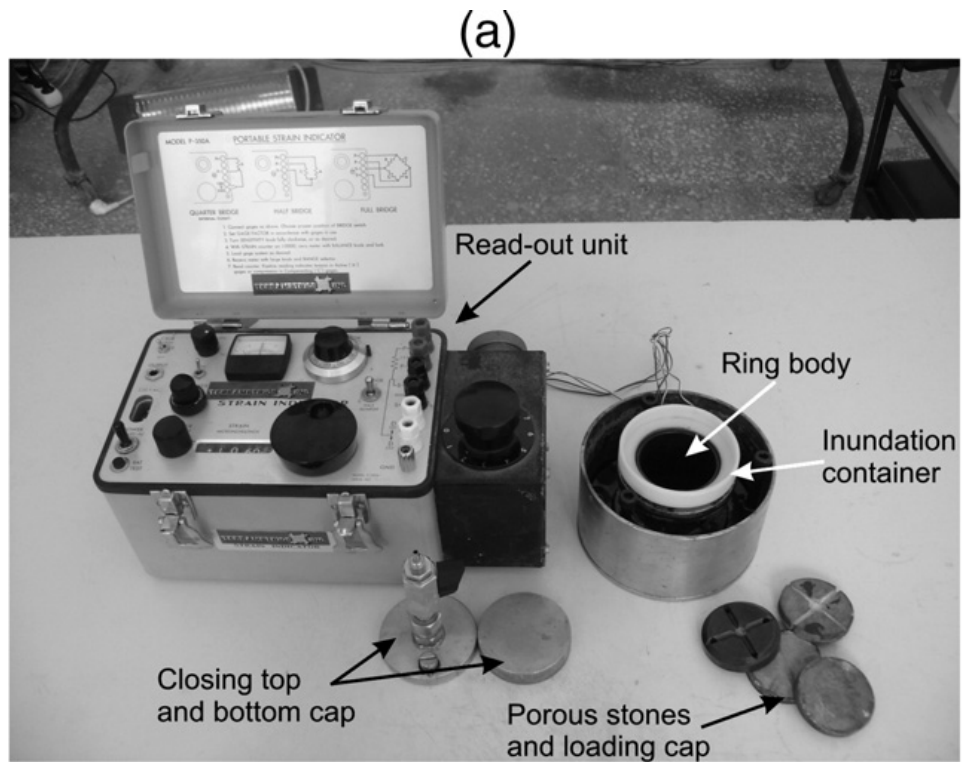
Figure 2.35: Smaller Regenerated Version of the Thin Walled Oedometer
(Avşar et al., 2009)

2.9.2 Other equipment for direct measurement of lateral swelling pressure

Joshi and Katti (1984) have investigated the variation of lateral expansion pressure with a special designed apparatus. They have undertaken a large scale model study in order to simulate the field conditions (Figure 2.36). The height of the model was 2.75m. The setup had lateral pressure measuring units at various depths.   Also the probe plates for measuring vertical movement and the vanes for measuring vane shear strength were embedded at various depths. The sides of the tank were smeared with grease and covered with polyethylene sheets to avoid the effect of side friction.

The authors have investigated the anisotropic behavior of black cotton soil, which is very famous in India for its swelling potential. They have determined that the lateral pressure at the site surface was negligible as the shear strength of the specimen. Then, the lateral pressure and the shear strength of the soil increased rapidly with increasing depth up to 0.92m. Below this depth, both the lateral pressure and the shear strength remain constant. The recorded lateral pressure in 0.92m depth, which is relatively shallow, was 287kPa. These results have made them realize that the lateral pressure characteristics of the expansive soils are different than conventional soils.
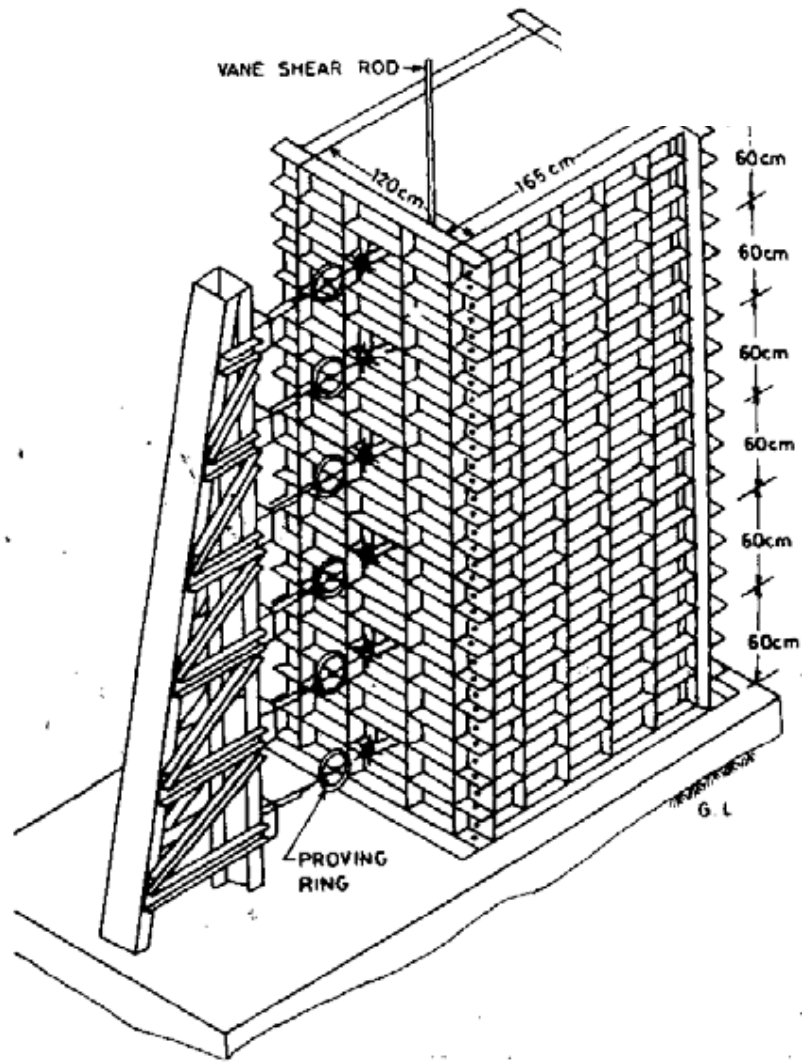
Figure 2.36: Large Scale Model (Joshi and Katti, 1984)

So, a second device (Figure 2.37) was designed, for the study of lateral pressure characteristics under varying dead load surcharges. This second equipment consists of a container fabricated out of 6.4mm thick mild steel plates having internal dimensions of 0.31m x 0.31m x 0.46m (width x length x height). Lateral pressure measuring unit of the device is a piston sleeve, which is fixed to the side of the container. The piston is connected to a dial gauge. The desired surcharge is applied via a lever arm.

49
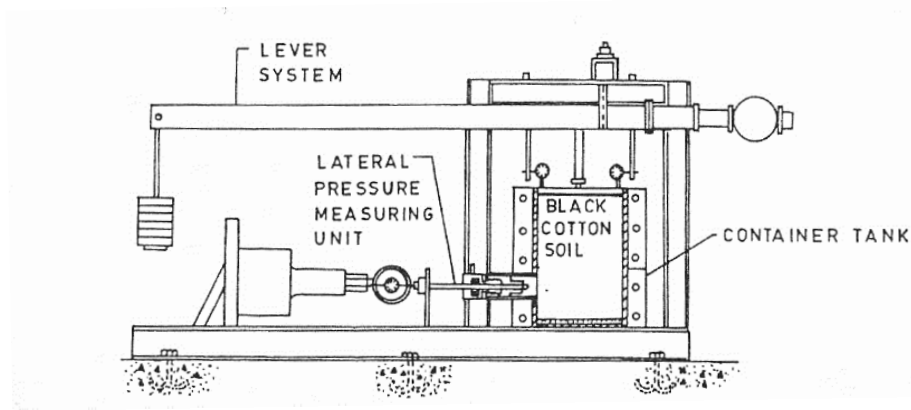
Figure 2.37: Equipment for the Measurement of Lateral Pressure under Dead Load Surcharges

Similar to the test results obtained by Ofer (1981) in the lateral pressure ring, the lateral pressure increased rapidly with time in the beginning of saturation process. Then the rate of increase slowed down and the lateral pressure attained a peak value. Afterwards, the lateral pressure decreased down to a value where it remained constant (Figure 2.38).
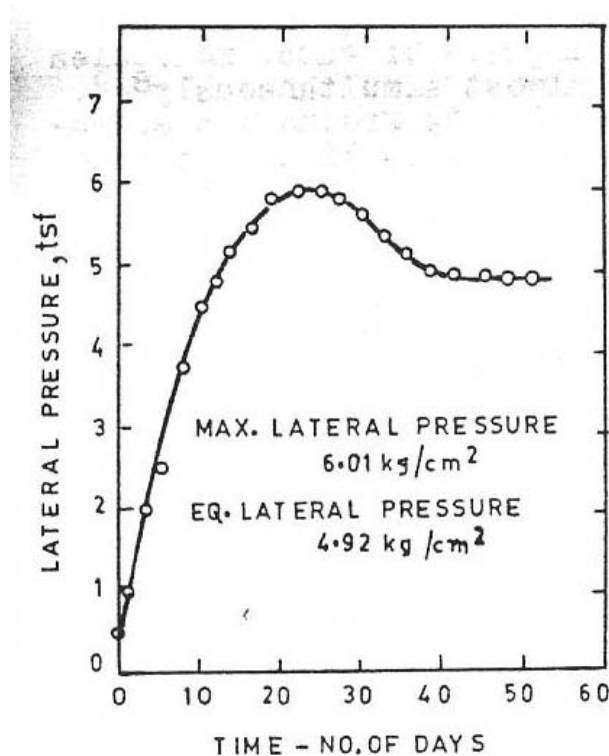
Figure 2.38: Development of Lateral Expansion Pressure under an Initial Surcharge with Time (Joshi and Katti, 1984)

Figure 2.39 shows the increment of equilibrium lateral pressure due to the increment of dead load surcharge. The ratio of increase in lateral pressure to the corresponding increase in dead load surcharge is more than 1.0 in case of increments up to the swelling pressure of the soil. For the incremental surcharges beyond the swelling pressure the ratio works out to be 0.2. This indicates that the basic nature of development of lateral pressure within the swelling pressure range is different from the basic nature of development of lateral pressure beyond the swelling pressure range of soil. Equilibrium of lateral pressure is equal 10 times the vertical pressure until a depth of 0.28m. For a dead load surcharge of 95.8 kPa this ratio decreases down to 3.25. It continues to reduce and reaches the value of 1.19 for a dead load surcharge of 479 kPa (Figure 2.40) (Joshi and Katti, 1984).
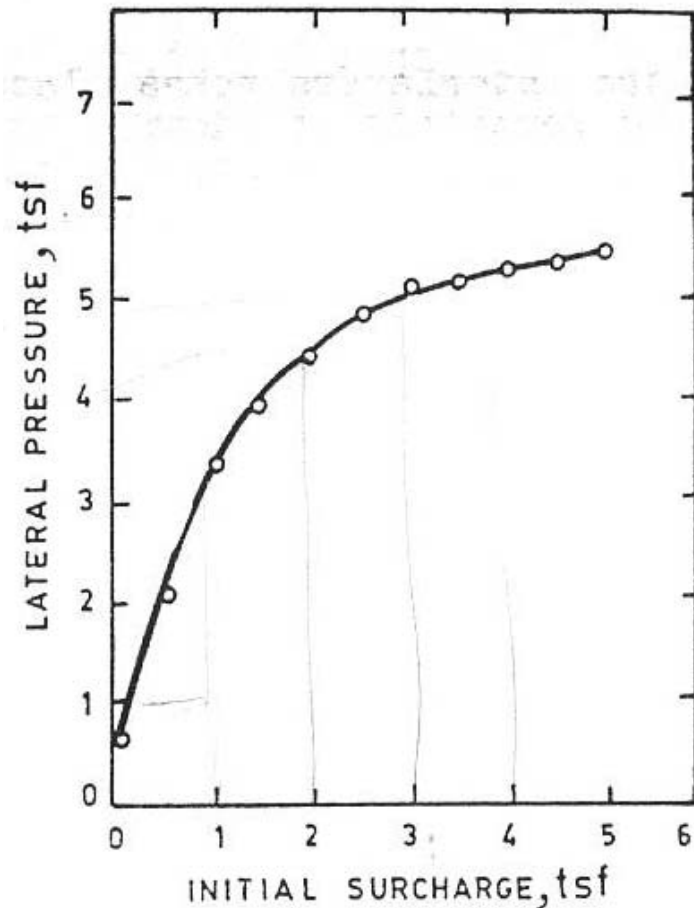
Figure 2.39: Initial Surcharge v.s Lateral Pressure (Joshi and Katti, 1984)
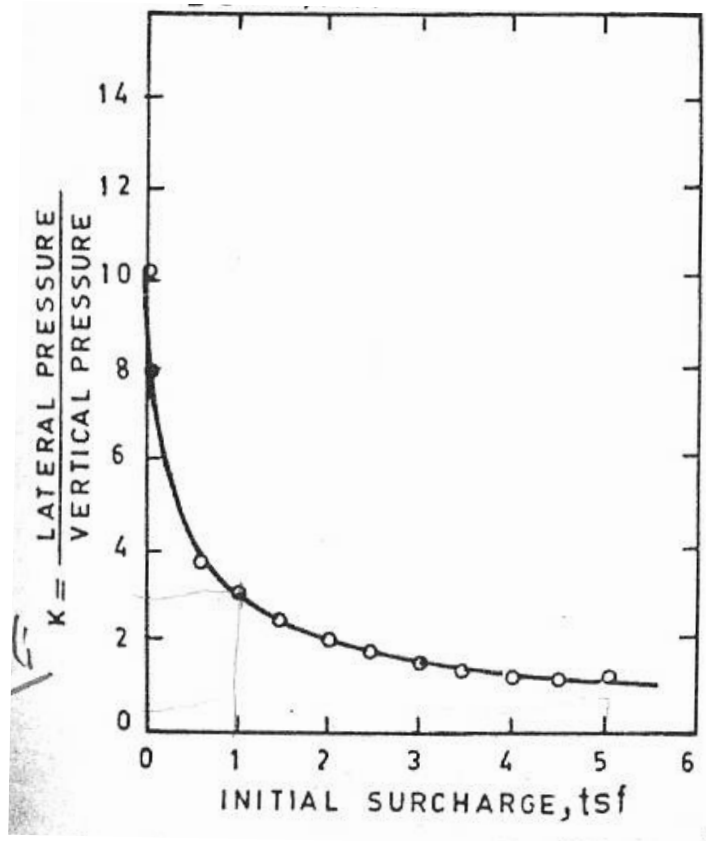
Figure 2.40: K Ratio vs. Initial Surcharge (Joshi and Katti, 1984)

Fourie (1989) has defined a new laboratory technique to determine lateral swelling pressures in expansive clay. Fourie has made his tests by using a Bishop – Wesley (1975) hydraulic triaxial apparatus. The sample was confined with a lateral strain belt like as it had been described by Bishop and Henkel (1962).

A modernized Bishop – Wesley Type Triaxial Apparatus is being produced by GDS Instruments. A schematic drawing showing pictures, together with the working sequence of the Bishop – Wesley Type Triaxial Apparatus is given in Figure 2.41. This device is equipped with an improved strain belt confining the specimen and provides therefore an increased pressure / volume control during the test (URL – 2).
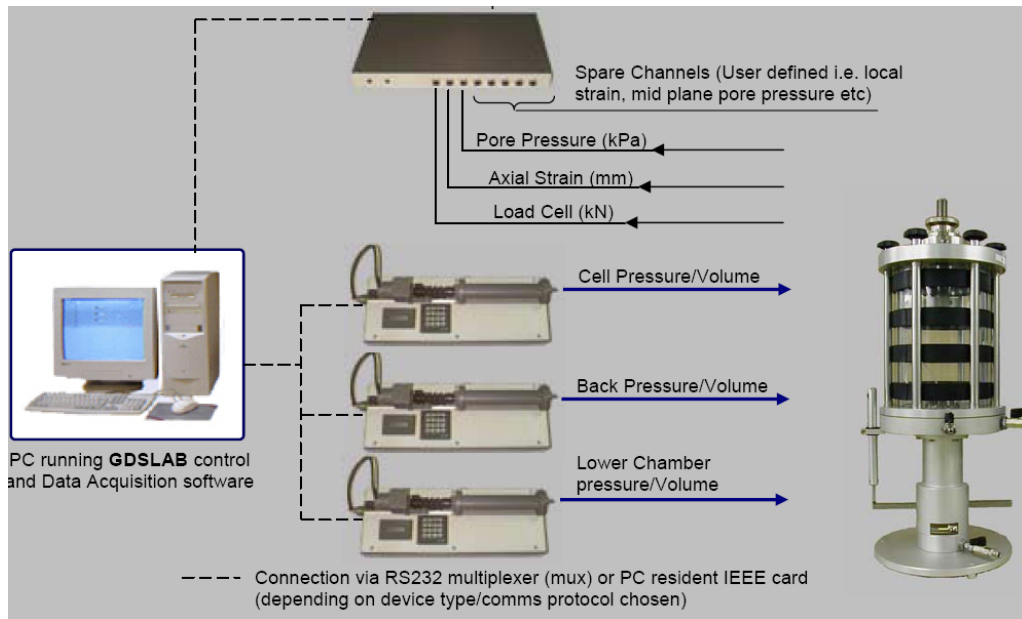
Figure 2.41: Modified Bishop – Wesley Type Triaxial App. (URL–2)

Fourie (1989) has further developed and adopted the "Method of Equilibrium Void Ratios" method discussed by Sridharan, et al. (1986) for lateral swelling pressure determination. The major advantage of the triaxial apparatus is that a confining pressure can be applied to the swelling clay sample. So, based on the same principle, the lateral swelling pressure probe has been built-up by adding a pressure cell around it. The technique originally put into practice the continuous increase of cell pressure. The strain belt detects the increase of the diameter of the sample due to the ingress of water. It was found impossible to avoid overcompensating and thus the sample was compressed beyond its original diameter. To prevent strain based failures, Fourie (1989) modified the technique so that lateral strains under varying constant confining pressures could be recorded. Then, lateral swelling pressure has been determined by drawing the lateral strain vs. lateral pressure curve. Based on Fourie's (1989) technique, the lateral pressure point, where the curve intersects the zero strain axis is the lateral swelling pressure (Figure 2.42).
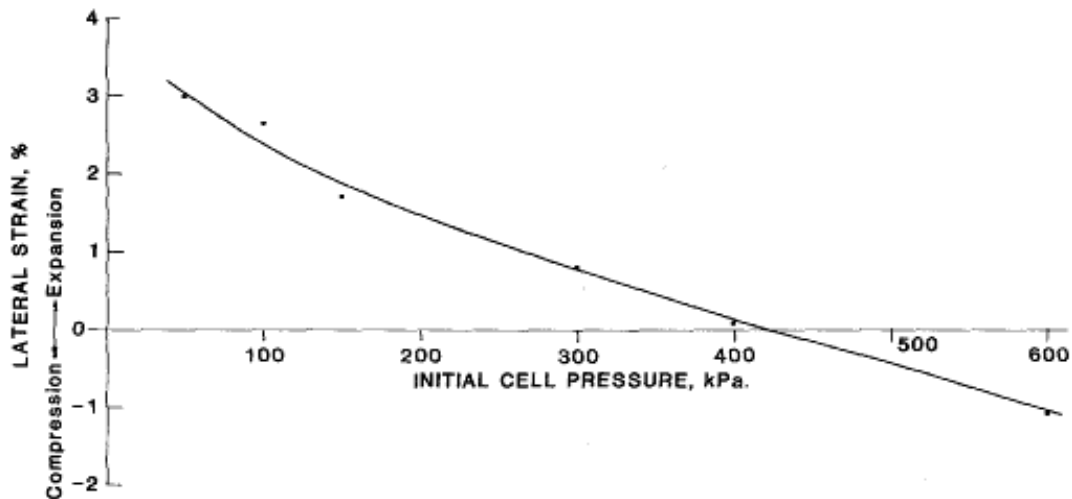
**Figure 2.42:** Initial Cell Pressure vs. Lateral Strain (Fourie, 1989)

Snethen and Haliburton (1973) measured lateral swelling pressures of two type of Oklahoma Clay. They used a device consisting of a pressure transducer and strip chart recorder. In the device, the compacted expansive soil sample was surrounded by a filter paper and a rubber membrane. The soil samples were not allowed to deform in lateral and in vertical directions. Influences of initial moisture content, dry density and compacted soil structure on lateral swelling pressure have been investigated. They have found that the swelling ratio of lateral swelling pressure to vertical swelling pressure approximately equal to 1.0 at moisture content above optimum for both soil types (Aytekin, 1992).

İkizler et. al. (2008) investigated the effect of using a compressible material, which was EPS Geofoam in this example, between the retaining wall and clay backfill with high swelling potential on lateral swelling pressure. They have conducted triaxial swelling tests using a self developed swelling pressure measuring steel box. The steel testing box, with dimensions as 250mm x 250mm x 300mm has a wall thickness of 3mm (Figure 2.43). The box is fitted with a pressure transducer on each side. Lateral and vertical swelling pressures were measured with the help of the pressure transducers. Water absorption of the specimen was maintained by the porous stones which were mounted on the sides of the testing box. The study concludes that there is a remarkable decrease in lateral swelling pressure with the placement of the compressible EPS Geofoam between the retaining system and the swelling clay backfill (Figure 2.44).
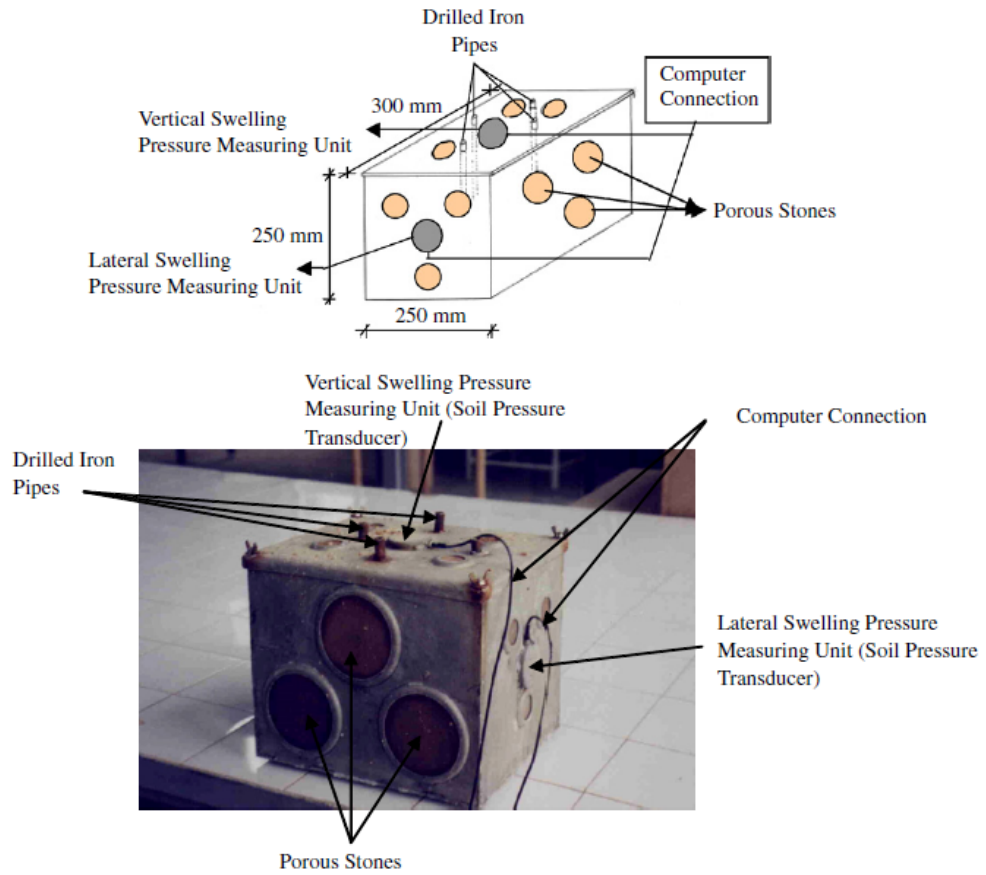
Figure 2.43: Steel Testing Box Developed by İkizler et al. (2008)
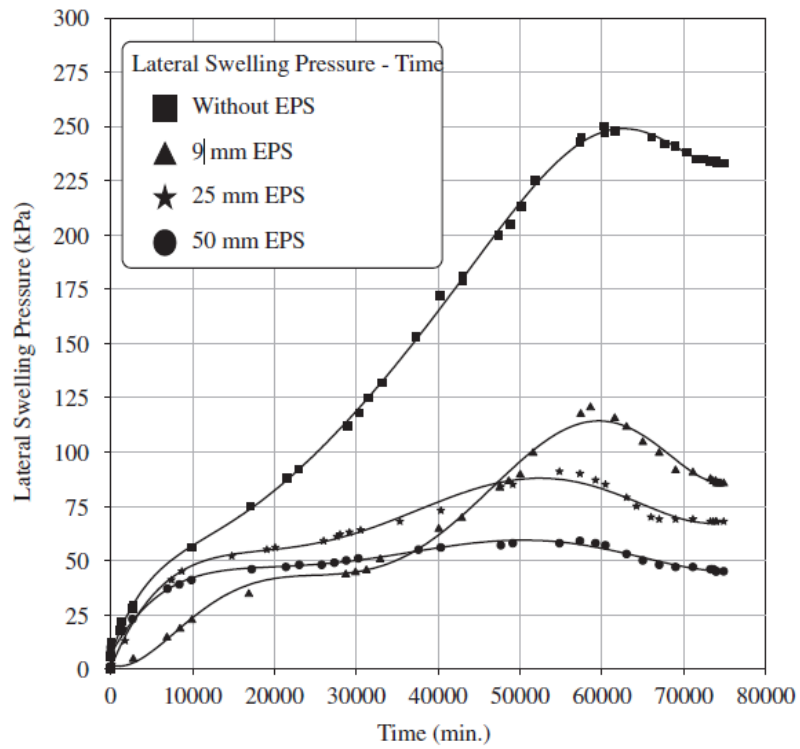
Figure 2.44: Lateral Swelling Pressure vs. Time (İkizler et al., 2008)

Wattanasanticharoen et al.in 2007, studied three-dimensional anisotropic stress conditions of swelling clays using a modified triaxial cell equipment. This triaxial cell can be classified as a combination of the lateral swelling pressure ring and the modified Bishop – Wesley Triaxial Apparatus. The sample is placed in a membrane, instead of thin walled ring. The membrane together with the sample is placed into an airtight triaxial cell where a confining pressure can be applied via water pressure (Figure 2.45). Vertical load is applied using a conventional consolidometer system of weights and lever arms. Swell strains in the lateral direction are measured immediately at the completion of the test by measuring the sample. (Thomas, 2008)
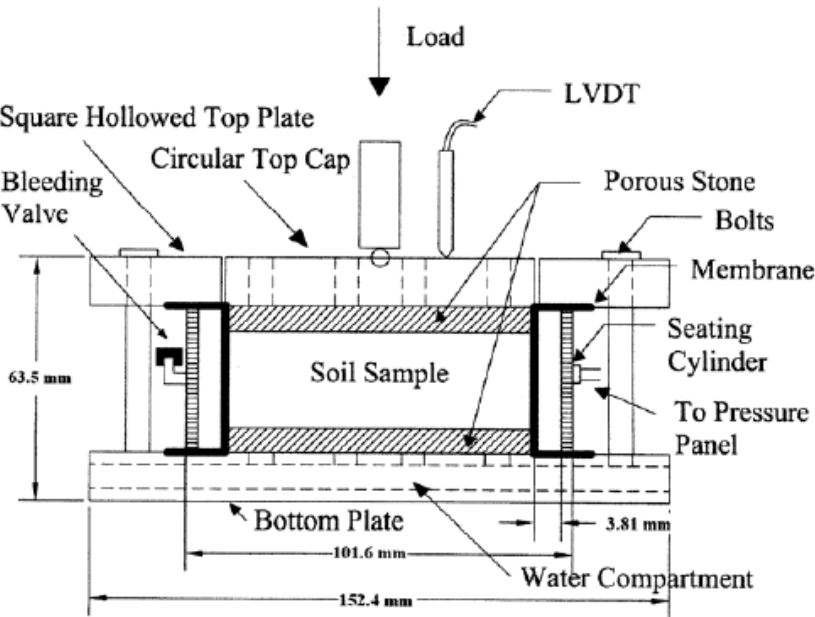
Figure 2.45: Triaxial Swelling Pressure Device of Wattanasanticharoen et al. (2007)

2.9.3 Triaxial swelling behavior of rock

Especially in tunneling design, the triaxial swelling behavior of rock layers has major importance. Since swelling of rock has great importance in tunneling, which is consequently within the scope of this thesis, some studies from the literature will be presented in the following paragraphs.

Sadisun et. al., (2002), Hawlader et. al. (2003), Barla (2007) and Schwingenschloegl and Lehmann (2008) are some of the investigators who have studied the three axial swelling behavior of rock in recent years.

Sadisun et. al. (2002), have fabricated an unconfined swelling test device, which is able to measure the strains caused by swelling of cubic or cylindrical shaped rock

specimens in all three dimensions. A schematic drawing of the device is shown in Figure 2.46.
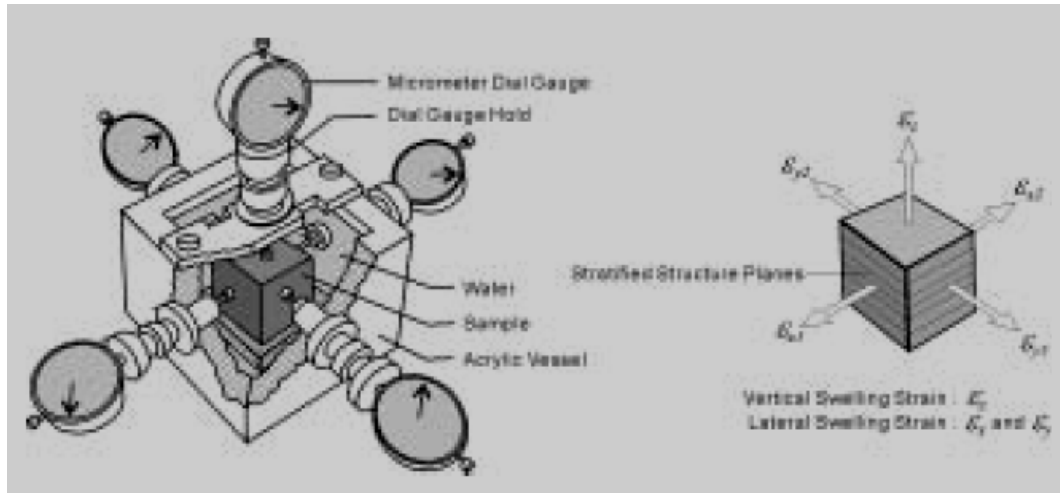
Figure 2.46: Unconfined Swelling Test Equipment (Sadisun et. al., 2002)

Hawlader et. al. (2003) have investigated the triaxial swelling behavior of Quenstone shale rock samples obtained from the Niagara Falls at depths between 80m and 120m. They conducted tests by using the modified testing device of Lo and Lee (1990) and the biaxial testing.

3. TEST MATERIAL AND EQUIPMENT

3.1 Test Material

All swelling pressure tests presented within this thesis have been performed with compacted clay samples. The clay used in the tests has been taken in a disturbed condition from ISBAS (Istanbul Thrace Free Zone) in the Çatalca Region at the western part of Istanbul City. As mentioned in the early paragraphs, the Çatalca clay is volcanic in origin. The thicknesses of these Oligosen aged clay layers are around 150m (Sağlamer, 1991).

### 3.1.1 Visual characteristics of the sample

The clay sample subjected to swelling tests is brown – grey colored and has hard consistency. Although the natural water content of the sample could not be measured because of being in disturbed condition, the fissures at the surface of the block samples indicate that the clay sample was dry.

3.1.2 Grain size distribution

To designate the grain size distribution of the clay sample, sieve analyses and hydrometer tests have been performed. Results of the tests have shown that the samples consist of 100% silt + clay sized particles. A typical grain size distribution graph of the sample is given in Figure 3.1.

3.1.3 Atterberg limits

The index properties of clays are basic indicators of the swelling potential. Therefore, Atterberg limits of the Çatalca clay were determined in the laboratory. Table 3.1 shows the results of these tests.
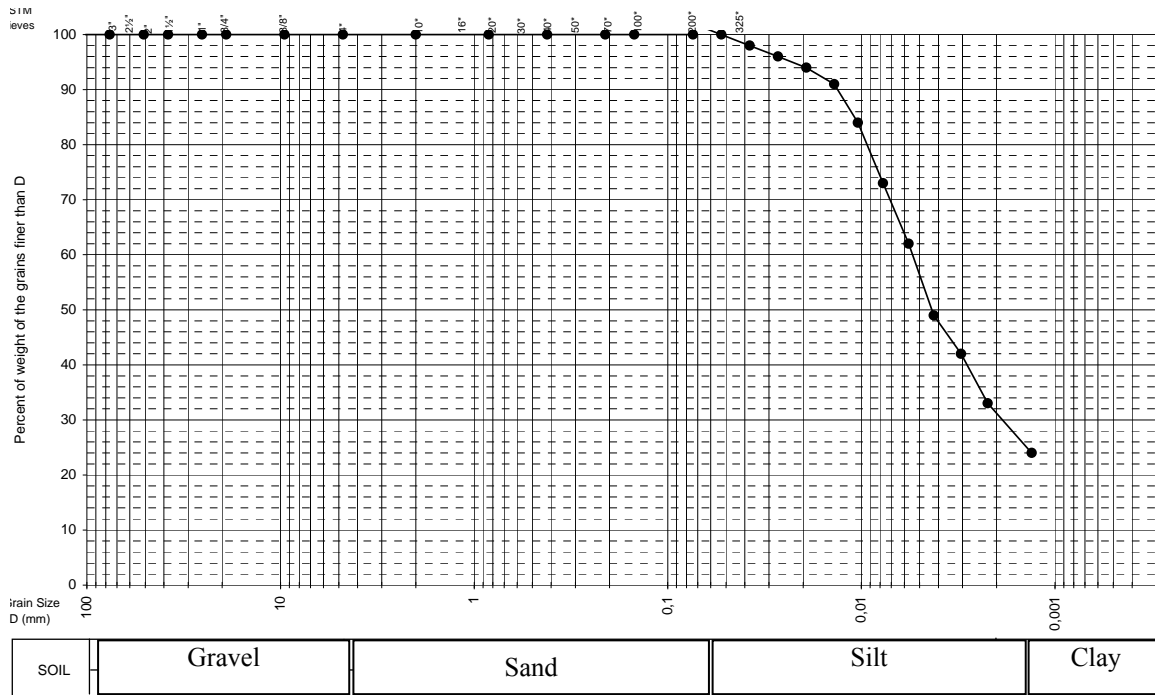
Figure 3.1: Grain Size Distribution of ISBAS Site Clay Sample

Table 3.1: Index Properties of ISBAS Site Clay Sample

Sample No.	1	2	3
Liquid Limit (%) w_L	70	71	68
Plastic Limit (%) w_P	36	35	33
Plasticity Index (%) Ip = w_P - w_L	34	36	35

A comparison of the results summarized in Table 3.1, with the plasticity index and liquid limit intervals given in Table 2.3, reveals that the clay sample taken from ISBAS site has high swelling potential.

According to Figure 3.1, the amount of the clay sized particles inside the tested clayey soil is about C = 32%. Utilizing this value in Equation 2.6, the activity of the sample is calculated as follows;

$$Activity = \frac{PI}{C-10} = 35 \, / \, (32\text{-}10) = 1.6$$

Employing the given results above in the classification chart given in Figure 3.2, the swelling potential of the ISBAS sample is found to be S = 10% - 15%, which corresponds to a highly expansive soil. The swelling potential of the ISBAS sample has also been determined using Equation 2.1 as:

$$S = 60K(PI)^{2.44} = 60 * (3,6 * 10^{-5})*(35)^{2,44} = 12.65.$$

S = 12.65 corresponds to high swelling potential.

60
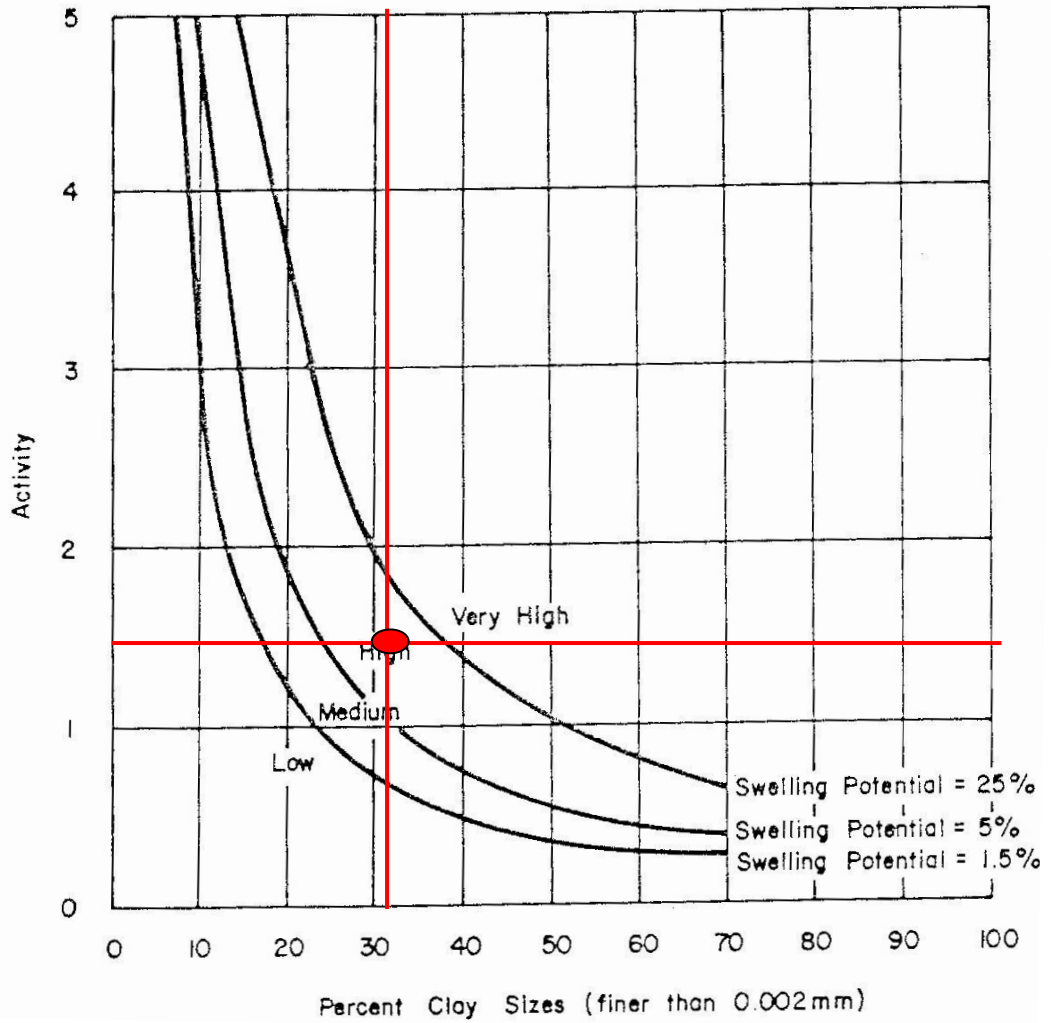
Figure 3.2: The Swelling Potential of ISBAS Sample Regarding its Activity

3.1.4 Mineralogy

Mineralogical specifications of the clay sapmle, subjected to lateral swelling tests has been identified with a X – Ray diffraction test. The X – Ray diffraction test was made in the Marmara Research Center of Tubitak (The Scientific and Technological Research Council of Turkey).

Based on the X – Ray diffraction test results, the mineralogical composition of the clay sample that has been used in the tests is as follows: 56.18% calcite, 32.02% quartz, 4.49% montmorillonite, 3.93%feldspar, 2.25%kaolinite and 1.13% illite. Although the montmorillonite content of the sample is not as much as expected, the clay sample has high swelling potential.

3.1.5 Standard Proctor tests

Since compacted samples have been employed in all the swelling tests within the scope of this thesis, optimum moisture content and the maximum dry unit weight of the clay material had to be determined. It has been decided to work with compacted samples prepared within a standard proctor mold, since it was easier to cover undisturbed swelling samples from this mold instead of the present modified proctor mold in the laboratory.

All standard proctor tests within the coverage of this study have been made in accordance with the ASTM D 698–07; Standard Test Methods for Laboratory Compaction Characteristics of Soil Using Standard Effort.

To prepare the clay samples for proctor tests, they have been laid to dry into the oven for a period longer than 24 hours. Then they have been pulverized. Finally, two standard proctor tests have been performed on them. The results of the standard proctor tests are given in Table 3.2, where one representative graph is given as in Figure 3.3.

Table 3.2: Standard Proctor Test Results

| $\gamma_{dry,max}$ (t/m^3)	w_{opt} (%)
1.32	32
1.37	29

3.1.6 Uniaxial swell test

Prior to subjecting the clay samples to triaxial swelling tests, uniaxial swelling pressure tests following the constant volume procedure (CVS) and the free swell method have been made in accordance with the ASTM D 4546– 03. Two samples were prepared in the laboratory; both compacted with the standard proctor procedure. Initial water content of the samples were ω_o = 19% and 20%, respectively.

Two specimens have been taken from the first sample and subjected to a constant volume swell test. The tests began on 04.11.2009 and have reached equilibrium at 06.11.2009 after a period of 48 hours. Final swelling pressures were determined at the end of these tests as 153kPa and 150kPa. The final moisture contents of the specimens were ω_{final} = 37% and ω_{final} = 39%.

Two specimens recovered from the second sample with an initial water content of ω_o = 19% were subjected to free swell test. The specimens have been saturated and left

to swell freely starting from 12.11.2009 until 19.11.2009 in the conventional oedometer. Subsequent to the termination of swelling, a pressure of 200kPa for each specimen had to be applied, so that the initial volume of samples could be achieved. In other words, the free swell tests resulted with a swelling pressure of 200kPa.
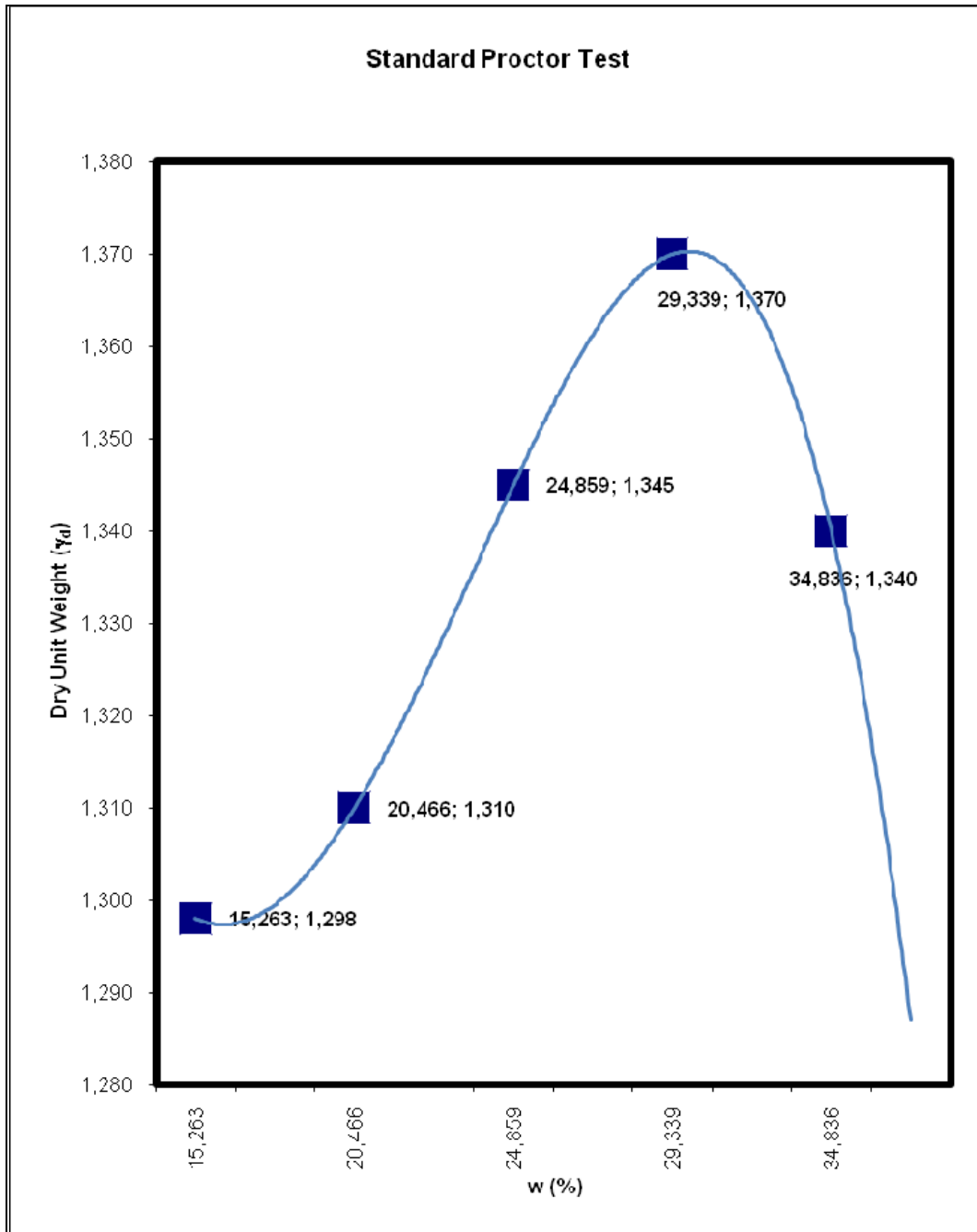
Figure 3.3: Dry Unit Weight – (%) Water Content Graph obtained from Standard Proctor Test

3.2 Test Set Up

3.2.1 Lateral swelling pressure probe used in this thesis

The main idea was to design and to manufacture a lateral pressure probe, mainly a thin walled oedometer with a pressure cell added around it. This probe is based on the investigations of Komornik and Zeitlin (1965), Ofer (1981), and Ertekin (1991) in principle. As mentioned earlier, Komornik and Zeitlin (1965) designed and used the Lateral Swelling Pressure ring, and Ofer in 1981 has further developed the ring and added a back pressure cell around this ring. Ertekin (1991) has rebuilt a device similar to that of Komornik and Zeitlin's thin walled ring in the laboratories of Middle East Technical University. The specifications of the device developed by Ertekin (1991) are given in details in Paragraph 2.9.1.

The device, that has been built for this study is based more on the investigations of Ofer (1981) and is therefore equipped with a confining back pressure cell. As stated previously, the results of the tests made with the In-Situ Probe by Ofer reveal different values than the results obtained from the tests with the Lateral Swelling Pressure Ring. With 2.9% swell, a lateral swelling pressure of 575kPa was recorded in the test with the In Situ Probe, where a test with a sample of the same soil in the thin walled oedometer had terminated with a peak lateral pressure value of 100kPa and a swell strain of 8%. So it was obvious that the degree of confinement and the amount of strain had major roles in the development of swelling pressure.

As mentioned before, Bishop and Wesley (1975) type hydraulic triaxial apparatus which allows stress controlled loading of both axial and radial pressures has been founded due to equal considerations represented in Ofer's (1981) study and can be accepted as an alternative testing equipment serving for the same purpose.

The main reason of deciding to rebuild and further develop a thin walled ring rather than the hydraulic triaxial apparatus was the ease of capturing undisturbed samples for the thin walled ring with limited height in comparison to cover specimens for the triaxial apparatus. Especially with compacted samples, conducting tests with a thin walled lateral pressure ring has always been more practical.

3.2.2 The production phase of the lateral swelling pressure probe

A schematic drawing showing the lateral pressure measurement device that has been utilized is given in Figure 3.4. The device has been manufactured in the workshop of Kurtuluşlar Hava Sinai Ltd. Şti. The device is a modified version of the device used by Ertekin (1991). The thin walled ring and its top and bottom collars have been shaped from a single cylindrical block.

One other consideration during the manufacture sequence was to increase the height of the specimen. This has been made to avoid the limiting effect of the top and bottom boundaries on the deflection of the thin walled ring. In other words, the surface with decreased rigidity has been increased so that the confining effect of the ring can be minimized. So, it has been tried to maintain an unconfined swelling option for the specimen in lateral direction and it has also been tried to retain a suitable condition for the direct effect of the back pressure to be applied on the specimen.

The inner diameter and the height of the ring are 70mm. Different than the ring of Komornik A. and Zeitlen J. (1965), the new ring has a thickness of 0.35mm, like the one of Ertekin (1991). The code of the ring material is Ç4140, which is equal to DIN 42 Cr Mo 4. The Shock protection has been made by installing pivot bolts through three holes staggered as 120° apart from each other, as in the device of Ertekin (1991). The ring has a top and a bottom collar. Following the completion of the production, the device has been covered with chrome in order to avoid rusting.
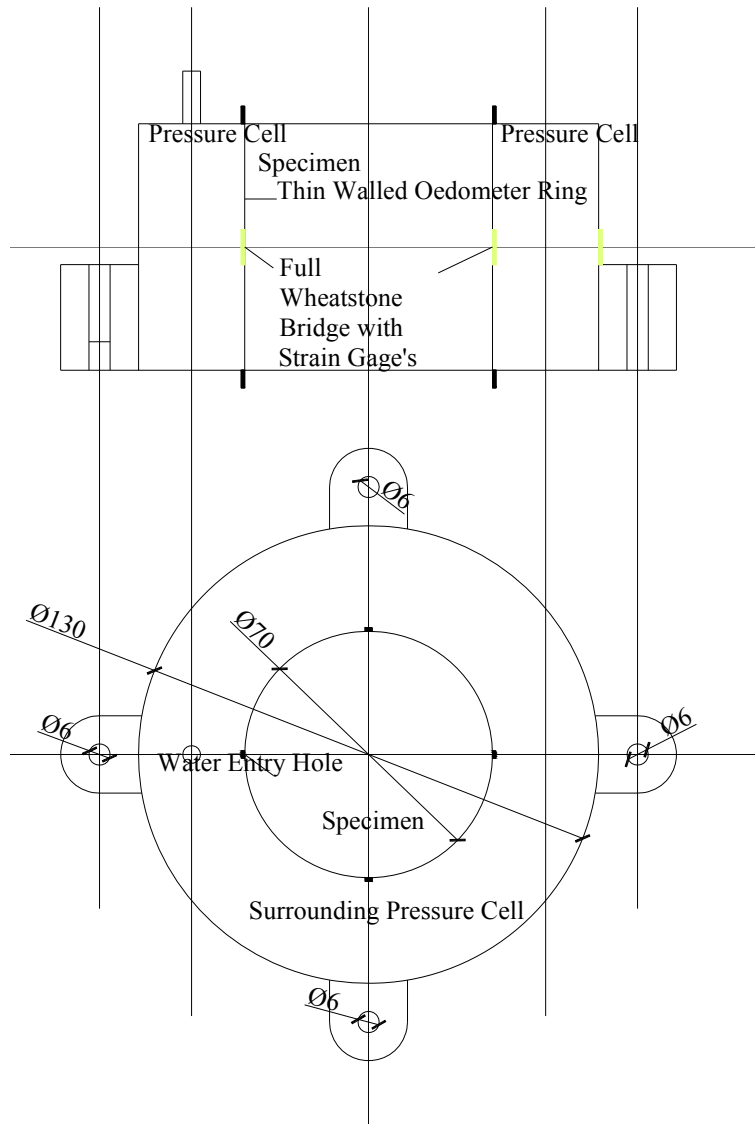
Figure 3.4: Drawing of the Regenerated Device

Both ends of the ring body are screw threaded. This screw treatment is provided for the installation of the calibration caps. The ring body with its collars is shown in Figure 3.5.

Figure 3.5: The ring body, top and bottom collars and the pivot bolts

The back pressure cell is a cylinder with a diameter of 130mm. The top and bottom openings of the back pressure ring were sealed with o – ring. A valve is mounted on the periphery of the back pressure cell, on which the pipe of the regulator is mounted during the test. The back pressure cell is shown in Figure 3.6.

The calibration of the strain gauges is made by sealing the top and bottom caps of the ring. Water pressure is used for the calibration. After the completion of the calibration of the strain gauges, the specimen is being placed into the ring and the ring body is being placed inside the back pressure cell. Finally, a top cap of the pressure cell, with a cyclic gap, as large as the specimen diameter, is placed. The completed set up is placed under a conventional oedometer lever arm holder, by applying vertical pressure to the specimen. Figure 3.7 is a photograph of the sealed test setup.

Figure 3.6: Back Pressure Cell

Figure 3.7: The sealed test set up

The strains and pressures on the thin walled ring are measured via waterproof strain gauges, which are mounted on the ring. The back pressure is provided by applying water pressure from a pressure regulator.

3.2.3 Read – out and data logging

As mentioned before, water proof strain gauges are mounted on the thin walled ring. Instead to build up a full Wheatstone bridge as in the original testing equipment, quarter bridges have been assembled with the strain gauges. The quarter-bridge type I, which has been designed for data collection measures either axial or bending strain. It was sufficient to obtain the axial strain alone. Figure 3-8 shows the type of strain gauges used in the Quarter Bridge Type I.
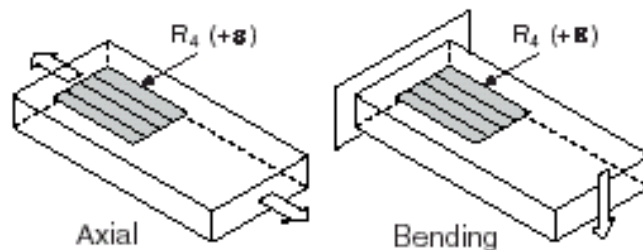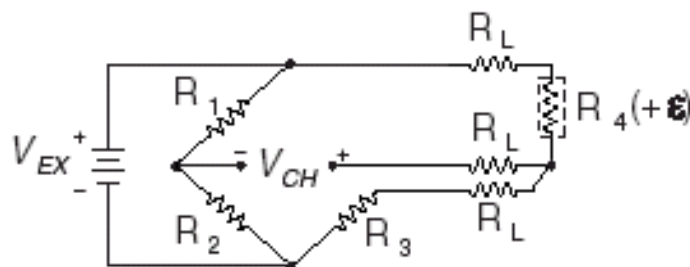

Figure 3.8: Quarter-Bridge Type I Measuring Axial and Bending Strain

Main characteristics of a quarter bridge type I are as follows:

- A single active strain-gauge element is mounted in the principle direction of axial or bending strain.
- A passive quarter-bridge completion resistor (dummy resistor) is required in addition to half-bridge completion.
- Temperature variation in specimen decreases the accuracy of the measurements.
- Sensitivity at 1000 me is ~ 0.5 mVolt/ VEX input.

Figue 3–9 shows the circuit diagram of a Quarter Bridge Type I.

Figure 3.9: Quarter-Bridge Type I Circuit Diagram

• R_1 and R_2 are half-bridge completion resistors.
• R_3 is the quarter-bridge completion resistor (dummy resistor).
• R_4 is the active strain-gauge element measuring tensile strain (+e).

The disadvantage of using a quarter bridge is that the data accuracy was susceptible to temperature changes. Therefore, the tests have been conducted in an temperature conditioned test room with limited temperature variation. The advantage and the progressing step of the quarter bridge in comparison to the full bridge is that particular readings could be taken from each strain gauge instead of taking one reading from all four strain gauges. So, this gave us the ability to see the time depending non-homogeneous behavior of the clay specimens.

Although the back pressure was given through the pressure regulator in the laboratory, a pressure cell has been mounted on the outer periphery of the back pressure cell, right over the valve, to see the deviation of the back pressure throughout the duration of the test. This has shown how proper the pressure regulator has worked during the test. A milivolt output pressure transducer of Omega Electronics has been used for this purpose (Figure 3.10).

The vertical pressure that was applied to the specimen via the lever arm of the oedometer has been measured by means of a cylindrical load cell. Also the load cell has been provided from Omega Electronics. The surface mounted type load cell has a capacity of 50kN (Figure 3.11).

Figure 3.10: Pressure Transducer

Figure 3.11: Surface Mounted Load Cell

The whole data has been collected via a four channel collector connected to a desktop computer. Detailed descriptions of the data logger and the evaluation of the data has been given in the related paragraphs..

3.2.4 The installation phase in the laboratory

The lateral pressure measuring modified oedometer ring has been put into service in that manner that it has been installed into a existing oedometer apparatus in the Soil Mechanics Laboratory of Istanbul Technical University. Therefore, the load transferring arms of the conventional oedometer apparatus were also subjected to small modifications. The width between the two arms of the set up was increased so that enough space could be provided for a aluminum pot holding water. The test setup shown in Figure 3.7 has been mounted into this pot (Figure 3.12).

To prevent direct contact between the specimen bottom and the pot base and to uphold drainage during the swelling process, a porous stone with a diameter, 0,5cm smaller than the specimen's diameter is placed at the bottom of the specimen. Also the top of the specimen iss sealed with a porous stone and a hard plastic cylindrical shaped elevating equipment with tubes on top of it. The load cell is placed to the top of this elevating cylinder (Figure 3.13). The elevating cylinder is essential in avoiding the contact of the cables of the load cell with water.

Figure 3.12: Test Apparatus
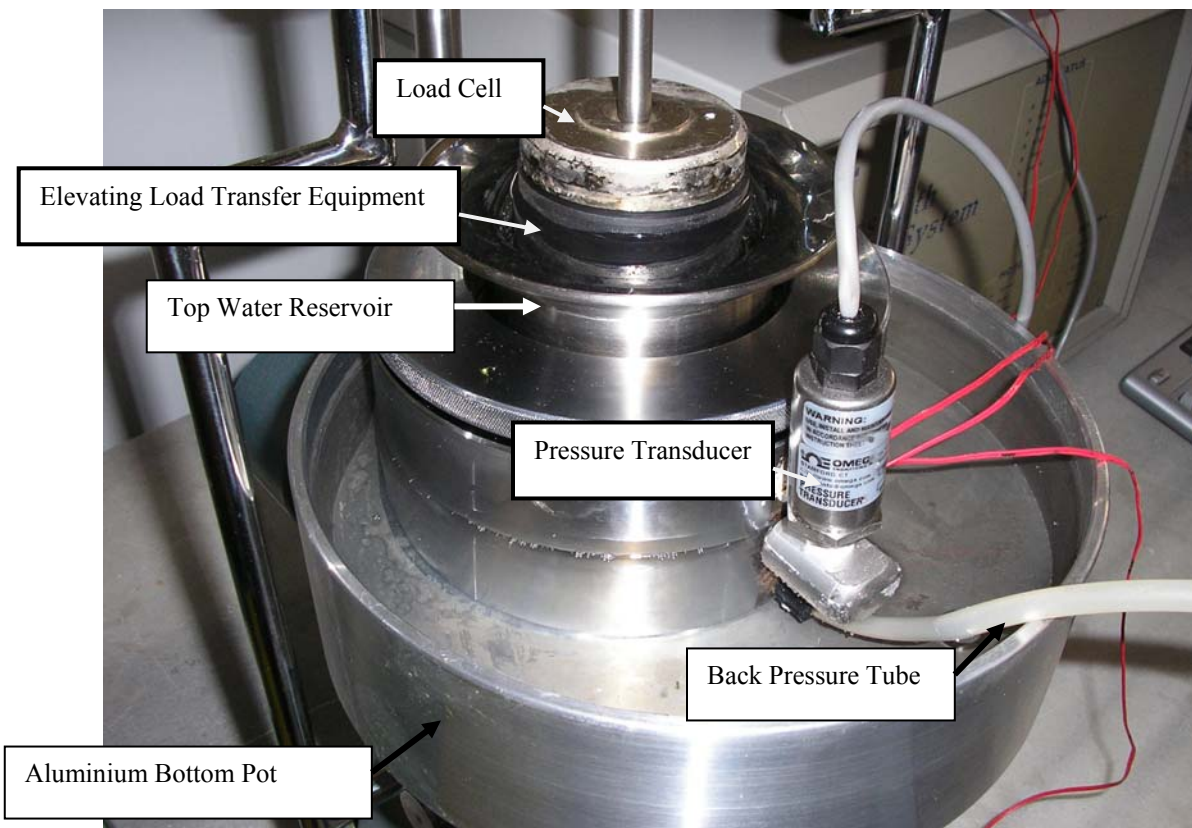
Figure 3.13: Big Scale Picture of the Test Apparatus

As it can be seen from Figure 3.13, the water reservoir on the top of the pressure cell is established via a cone shaped hollow cylinder. This cone is threaded so that it can be screw fixed. Conclusively, the specimen is saturated from the top and the bottom.

While the applied vertical pressure is measured with the help of the load cell, the pressure transducer that is screwed on the back pressure cell is used for back pressure measurement.

3.2.5 Calibration

The load cell which is used for vertical pressure readings was calibrated in the manufacturing factory. The strain gauges and the back pressure cell have been calibrated in the soils laboratory. Calibration of both strain gauges and back pressure cell were made by separating the ring body from the back pressure cell.

For the calibration of the strain gauges, the top and bottom of the ring body has been sealed via the screw fixed caps. On the top cap, a valve is built up which is connected to the water pressure regulator (Figure 3.14). Afterwards, the strain gauges were connected to the data logger, their calibration was made by increasing and decreasing the water pressure in stages of 50kPa. It was sufficient to select a pressure range of 0.00kPa – 500kPa for the calibration of the strain gauges.

Figure 3.14: The top calibration cap

The standby duration in each loading and unloading stage was selected as 2 minutes in the calibration of the set up in our case. The setup duration has been determined

as the duration necessary for the damp of the oscillation of the strain gauge readings. In order to gain a reliable calibration curve, the process which has been described above was repeated for three times. The pressure – strain diagram showing the calibration curves of the strain gauges is shown in Figure 3.15.
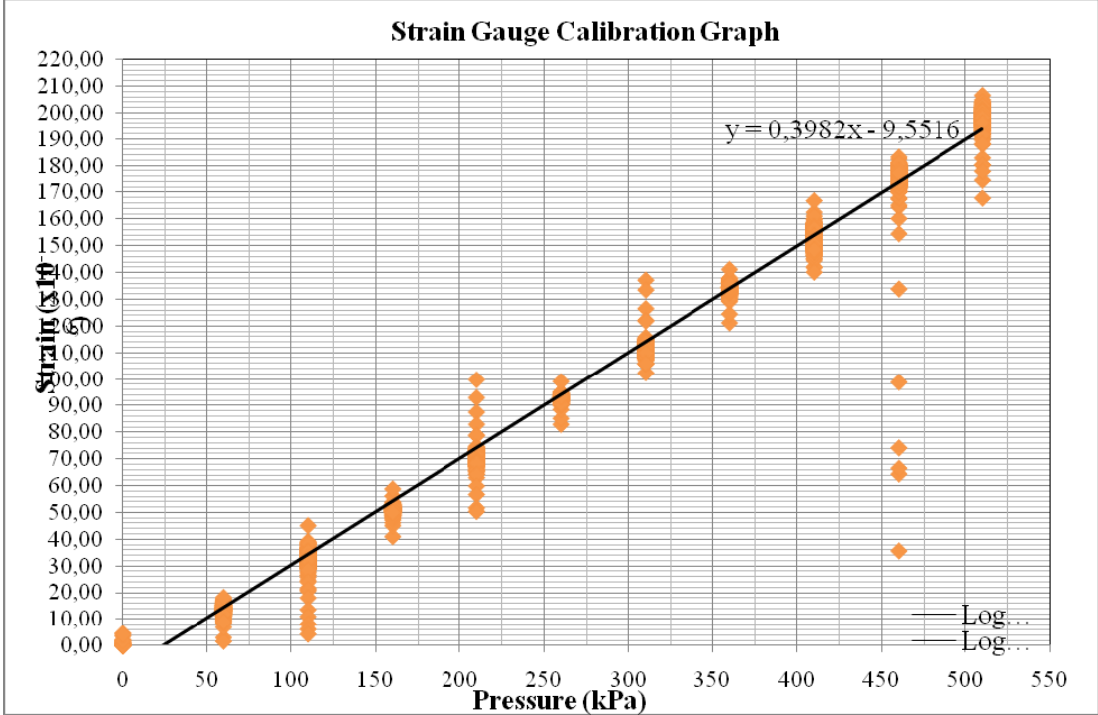
Figure 3.15: Strain Gauge Calibration Curve

Similar to the calibration of the strain gauges, the pressure transducer was calibrated with applying water pressure to the sealed ring body. For the calibration of the pressure transducer, the valve at the top calibration cap was removed, and the pressure transducer was screw fixed to the cap. Then again, three cyclic loading and unloading steps have been utilized to determine the calibration curve of the pressure transducer.

3.2.6 Sample preparation

The clay samples, which have been subjected to the swelling tests for this study were taken as disturbed samples from a construction site at Thrace Free Trade Zone, in Çatalca. Properties of the clayey soil samples, which were determined by means of laboratory tests, have already been given in detail above.

The clay samples were stored in an oven and kept there until they were dry. Afterwards, oversized grains (sand and gravel) were sieved and the remaining

cohesive soil were pulverized. It was restored again in an oven for duration of 24 hours, to ensure that the sample is dry.

A dried clay sample was mixed prior to compaction with an amount of water bringing it to a determined water ratio. The water ratio of the specimens were selected as to below the optimum water ratio. The water content was kept around $\omega = 20\%$. Then, the operation has followed with compaction of the pulverized clay particles within a proctor mold. The compaction of the clay sample has been made in accordance with the ASTM D 698 "Standard Test Methods for Laboratory Compaction Characteristics of Soil Using Standard Effort (12 400 ft-lbf/ft3 (600 kN-m/m3))".

Following the compaction, the prepared specimen was taken out from the standard proctor mold and it was put into a desiccator for at least 24 hours, in order to maintain the homogeneity of the samples water ratio (Figure 3.16).
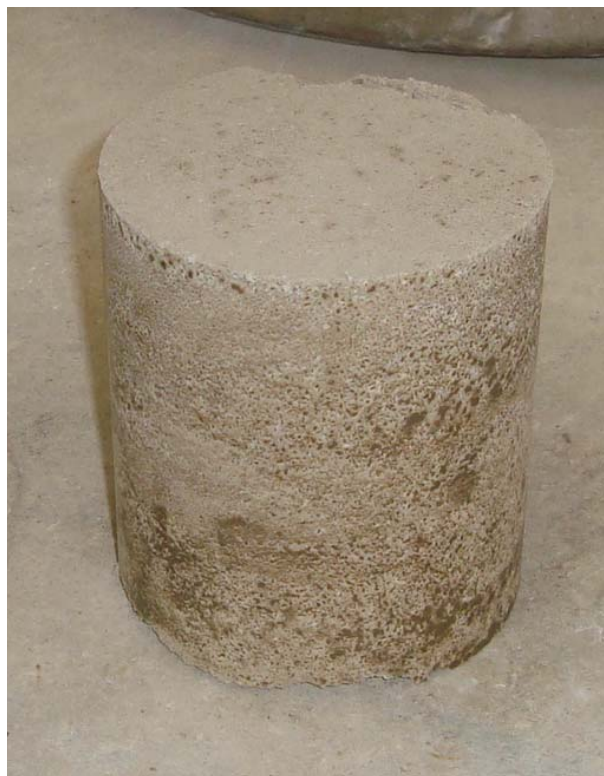
Figure 3.16: Compacted Sample

After taking the artificially prepared clay sample out from the desiccator, the specimen was recovered from the compaction sample by means of penetrating the a specially manufactured sampler as shown in Figure 3.17, into the compacted clay sample.

Figure 3.17: A Photograph Taken During the Penetration of the Sampler into the Specimen

Finally, the specimen within the sampler was transferred into the thin oedometer ring via a hard plastic pull having a base diameter 2mm lesser than the sample diameter.

The strain gauges mounted on the thin ring were readjusted after the installation of the specimen in all tests, so that the residual strains that may have been accumulated on the ring during the specimen transfer do not affect the zero readings which will be taken from the strain gauges. Briefly, the residual strains occurred up to the starting stage have been accepted as zero strain, and the lateral pressure readings have been based on the further strains which occur during the test.

3.2.7 Data collection, evaluation and presentation

The test data consists of vertical pressure, vertical displacement, lateral swelling pressure, lateral cell pressure and lateral strain. To collect the whole data, a four channel data logger of National Instruments has been used. Since the channel

number of the data logger was limited, vertical displacements have been monitored via a manual micrometer. Moreover, only two strain gauges of three could be employed during the tests, while the load cell and the pressure transducer were connected to the third and fourth channel of the data logger.

As data logger, the NI-USB 9162 of National Instruments has been used in the tests (Figure 3.18). The standard software of NI, Lab View 3.0 has been used for data interpretation. The software has recorded strain and volt data with 0,51 second intervals. Since, data measurements with such short intervals were not necessary for the evaluation of the swelling behavior; a data reduction has been made via transforming the saved files into Microsoft Excel files. Finally, read-outs per minute interval have been listed and visualized in time – swelling graphs. The results of swelling tests that have been conducted within this thesis will be presented in the related paragraphs.

Figure 3.18: Four Channel Data Logger

3.2.8 Test methodology

Swelling tests in vertical direction have been made in correspondence with ASTM D 4546 – 03, "Standard Test Method for One Dimensional Swell or Settlement Potential of Cohesive Soils". Three different test methods known as; Method A or Free Swell, Method B, and Method C or Constant Volume Swell (CVS), are described in ASTM standard.

Method A, the Free Swell Method: The specimen is inundated, and is allowed to swell in the vertical direction, under a seating pressure of at least 1kPa (20 lbf/ft2). The seating pressure is applied as the sum of the weight of the top porous stone and the load plate. The load on the specimen is increased after primary swell has completed up to the value consolidating it to its initial volume (height).

Method B: A vertical pressure exceeding the seating pressure is applied to the specimen before placement of free water into the consolidometer. The magnitude of vertical pressure is usually equivalent to the in situ vertical overburden pressure or structural loading, or both, but may vary depending on the application of the test results. Afterwards, access of free water to the specimen is given. This may result with swell, swell then contraction, contraction, or contraction then swell. The amount of swell or settlement is measured at the applied pressure when the settlement or swell of the specimen reaches a negligible speed.

Methods C: This is defined as the Constant Volume Swell Method (CVS). In this method, the specimen is preserved at a constant height by adjustments of vertical pressure. A consolidation test is subsequently performed in accordance with Test Method ASTM D 2435-04. The Rebound data is used to estimate the potential heave.

The above summarized test methods of ASTM, are swelling tests methodologies mainly generated for one directional swelling tests conducted in the oedometer. Some of these methodologies has been implement to the triaxial testing device used in this thesis. The tests have been conducted in groups following the below described groups.

Some initial tests have been conducted as free swell tests. During these tests, the specimen was left free to swell on both vertical and lateral directions. It has been observed that the specimen tends to swell in vertical direction and thus no lateral swelling pressure was observed.

In the following group of tests, the swelling of the specimen in vertical direction has been prevented by load adjustment in vertical direction after the specimen was inundated like as in the CVS (ASTM 2435-04, Method C) type swelling pressure test. Simultaneously, the specimen has been let to swell in lateral direction. Both vertical and lateral swelling pressures have been recorded. The vertical swelling

pressure has been accepted as to be the applied pressure to maintain zero vertical swelling strain, where the lateral swelling pressure has been calculated by employing the recorded lateral strain values into the calibration curve given in Figure 3.15.

The third test method preserves the volume of the specimen in both, vertical and lateral directions. As like the vertical pressure regulation, lateral pressure adjustment has been made via applying hydraulic cell pressure on to the thin walled lateral pressure ring.

The fourth group tests were based on the test methodology of Windal and Sharour (2002). A vertical surcharge has been adopted to the specimen and the lateral swelling has been measured. This problem has been considered as to be a typical swelling pressure problem acting on buried structures such as tunnels, basement walls, retaining system of deep excavations, etc. The specimen was consolidated under varying vertical surcharge pressures between 100kPa and 200kPa. Afterwards, the specimen was inundated and the mobilized lateral and vertical pressures were determined.

The fifth group of tests represents the adoption of the method of equilibrium method generated by Fourie (1989) for swelling tests made with a modified triaxial testing device.

4. TEST RESULTS

The results of the tests are presented in this chapter under subtitles based on the testing methodogy. Solely, test results will be presented in this chapter without any comments. Evaluation of the test results are presented in the next chapter.

4.1 Free Swell Tests in Vertical and Lateral Directions

During these type of tests no lateral swelling can be recorded. Nevertheless, the tests done as free swell tests were useful in a way in a way that the vertical heave of the specimen must be restricted by applying vertical pressure.

4.2 Vertically Restrained Laterally Free Swell Tests (VR-LFST)

Several tests were made by employing this method in order to monitor the lateral swelling behavior of the specimen. Restrain of swelling in vertical direction was maintained by applying gradually increased vertical stress to the specimen. So, by means of gradual increment of vertical loading, vertical displacement was kept as zero as in the CVS (constant volume swell) testing method in an conventional uniaxial swelling test.

The first test according to this methodology was made on 02.06.2009. The initial and final water contents of the specimen and the recorded lateral and vertical swelling pressures are depicted on Figure 4.1 and Figure 4.2, respectively.
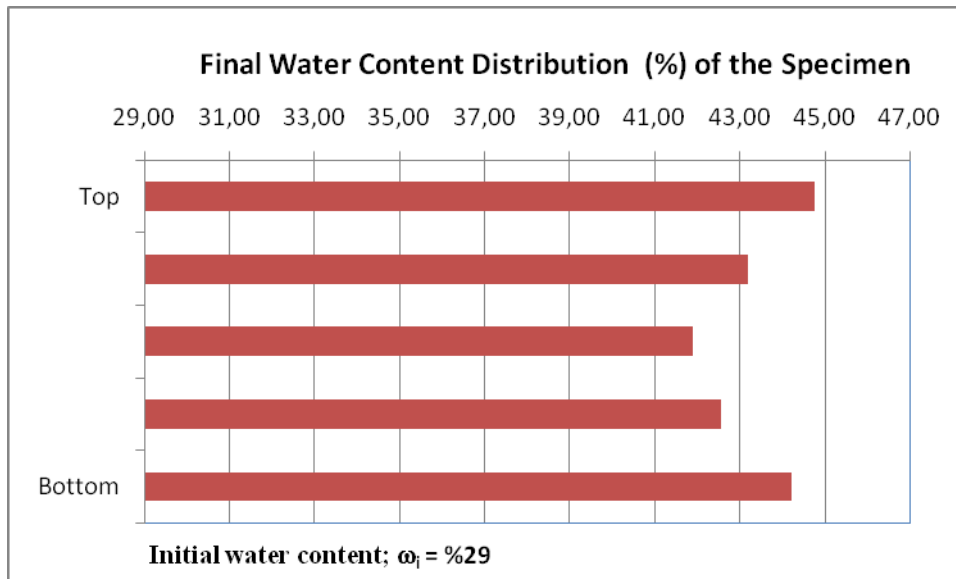
Figure 4.1: Initial and Final Water Contents, (Test: 02.06.2009)
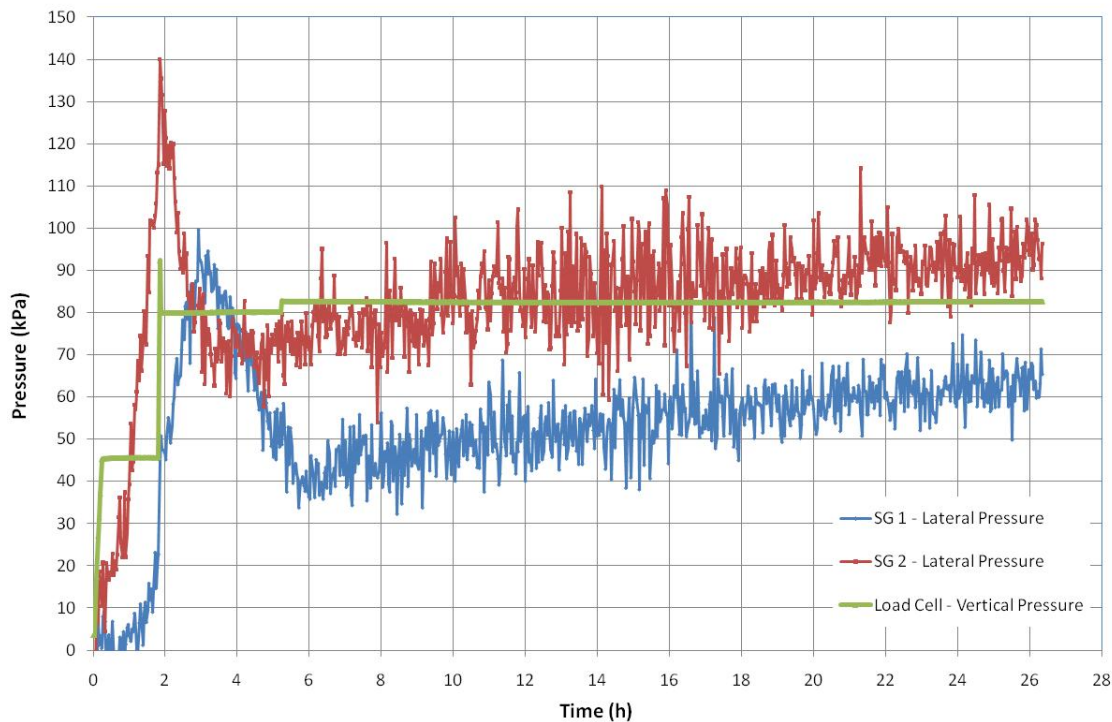
Figure 4.2: Pressure versus Time Graph (Test: 02.06.2009)

As it can be seen from Figure 4.1, the initial water content of the clay sample was $w_{i,ave} = 29\%$ in average. Water content measurements made at the end of the test on the uncovered sample, by slicing it into five pieces from top to bottom have shown a water content increase varying between $\Delta w = 12\% - 15\%$. This test has been finalized with an average water content of $w_{f,ave} = 43\%$. Water content distribution of the specimen clearly indicates that water ingress into the sample is from the top and the bottom.

Further tests with this method have been made on 28.08.2009, 02.09.2009, 05.09.2006, 16.10.2009. Results of five tests in this group are given on Table 4.1. Figure 4.1 and Figure 4.2 reveal the results of one test that was conducted on 02.06.2009, out of these five tests.

Table 4.1: Summary of the Test Results made with Vertical Strain Limitation

Test Date:	Stratification	Average Initial Water Content w_i(%)	Average Final Water Content w_f(%)	Vertical Swelling Pressure (kPa)	Lateral Swelling Pressure (kPa)		$\sigma r = \sigma_{sL}/\sigma_{sv}$	Total Test Duration (h)	Duration of Vertical Swelling Pressure Mobilization	Duration of Lateral Swelling Pressure Mobilization
02.06.2009	Horizontal	29	41	80	90	70	1,00	26	2	3
28.08.2009	Horizontal	19	46 - 39	70	120	120	1,71	68	5	68
02.09.2009	Horizontal	19	45 - 39	80	110	90	1,25	29	2	29
05.09.2009	Horizontal	19	39 - 45	80	115	115	1,44	72	4	58
16.10.2009	Horizontal	19	38 - 43	120	150	150	1,25	52	20	49

Additionally, three tests on 09.09.2009, 13.09.2009 and 16.09.2009 have been made using the same method. In these tests, the sample was recovered from the compacted sample in the horizontal direction. This has been made to investigate the effect of stratification on swelling. The initial water content of the specimens have been kept within a range of $w_{i,ave}$ = 19% - 20% in all of these tests. The results of the tests have been visualized as graphical outputs and enclosed to the thesis.

The swelling tests have been terminated after the full mobilization of the swelling pressure, Final water contents of the specimens have attained values within a range of $w_{f,ave}$ = 40% - 42% in all of the tests. Considering that the initial water content of the specimens was around $w_{i,ave}$ = 19%, all specimens doubled their water content by soaking water.

The vertical swelling pressure range of the specimens has varied in vertically encapsulated specimens between 70kPa and 120kPa. Swelling behavior of the specimens in vertical direction terminated before than lateral direction. The full vertical swelling pressure has mobilized within durations varying between 5 to 8 hours in all the tests. On the contrary, mobilization of lateral swelling pressures has continued up to 72 hours. The recorded lateral swelling pressures were between 100kPa to 150kPa. The specimens behaved almost homogenous in the horizontal direction.

As mentioned before, three additional tests were made by utilizing the same method on samples recovered horizontally from the compacted clay block. In other words, vertical direction of the sample has been rotated, so that the surcharging axis and the lamination plain were perpendicular. Related time – swelling and water content variation graphics are given in the attachment of this thesis. The results of these tests are summarized in Table 4.2. Vertical swelling pressures have been determined as 70 – 105kPa, where the recorded lateral swelling pressures were above 110kPa.

Table 4.2: Results of the Tests on Vertically Laminated Specimens Subjected to Vertically Restrained Swelling Tests

| Test Date:	Stratification	Average Initial Water Content w_i(%)	Average Final Water Content w_f(%)	Vertical Swelling Pressure (kPa)	Lateral Swelling Pressure (kPa)		$\sigma r = \sigma_{sL}/\sigma_{sv}$	Total Test Duration (h)	Duration of Vertical Swelling Pressure Mobilization	Duration of Lateral Swelling Pressure Mobilization
09.09.2009	Vertical	19	39 - 45	105	130	140	1,29	47	18	6
13.09.2009	Vertical	19	39 - 45	70	110	110	1,57	46	2	14
16.09.2009	Vertical	19	38 - 42	110	180	220	1,82	54	6	50

4.3 Constant Volume Swelling Pressure Tests (CVS)

In these tests, the volume change in both, vertical and horizontal directions was restricted. In the vertical direction, the swelling of the specimen was avoided in the conventional way, by surcharging the specimen gradually if the sample had a tendency to swell. The horizontal swell strains were monitored through the strain gauges. The hydraulic cell pressure prevented the occurrence of any lateral strain. The pressure transducer measured the applied lateral pressure.

The first test with this method was made on 01.07.2009. The initial water content of this test was selected as $w_{i,ave}$ = 30,5%. The mobilization of the lateral and the vertical swelling pressures were completed more or less simultaneously after 4 hours. At the end of the test, the water content at the top and bottom of the specimen have increased about 3% to 5%. At the mid-height of the specimen the increase in water content was limited with 2%. A lateral swelling pressure of 140kPa was recorded in this test together with a vertical swelling pressure of 60kPa. The resulting graphics of the test held on 01.07.2009, including the variation of strain with time are given in Figure 4.3, Figure 4.4 and Figure 4.5.
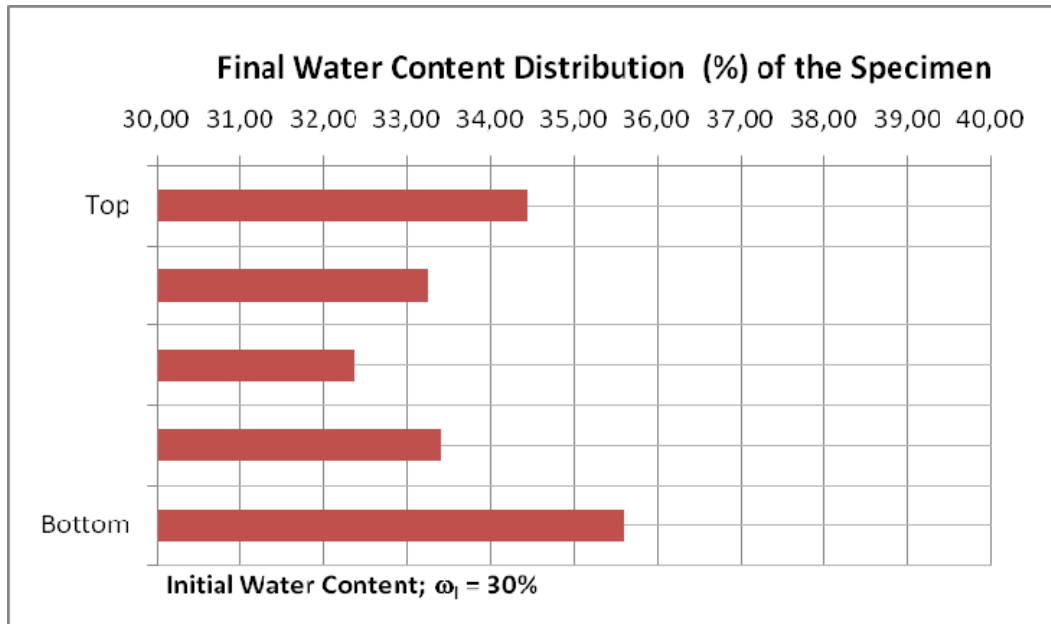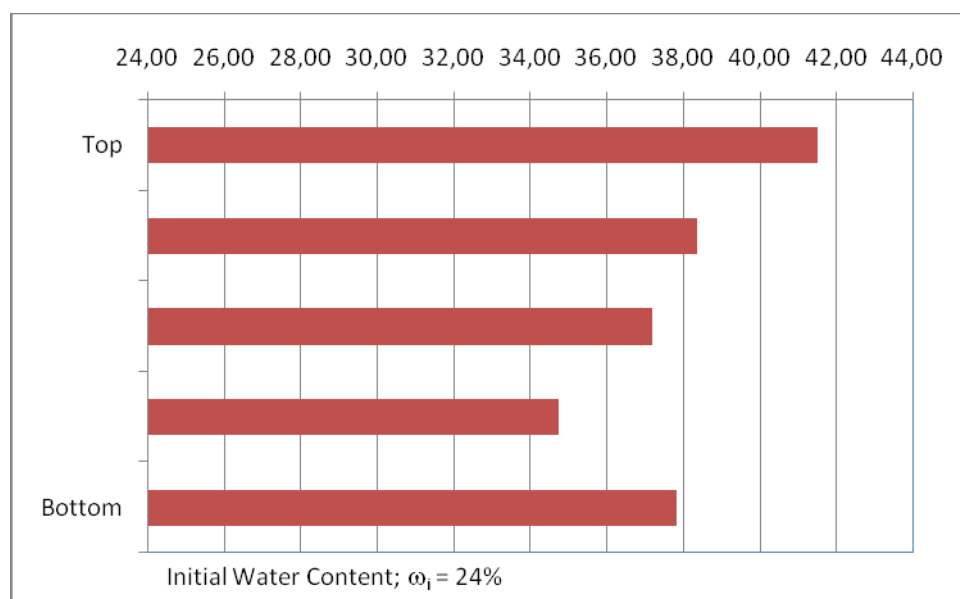
Figure 4.3: Initial and Final Water Contents, (Test: 01.07.2009)
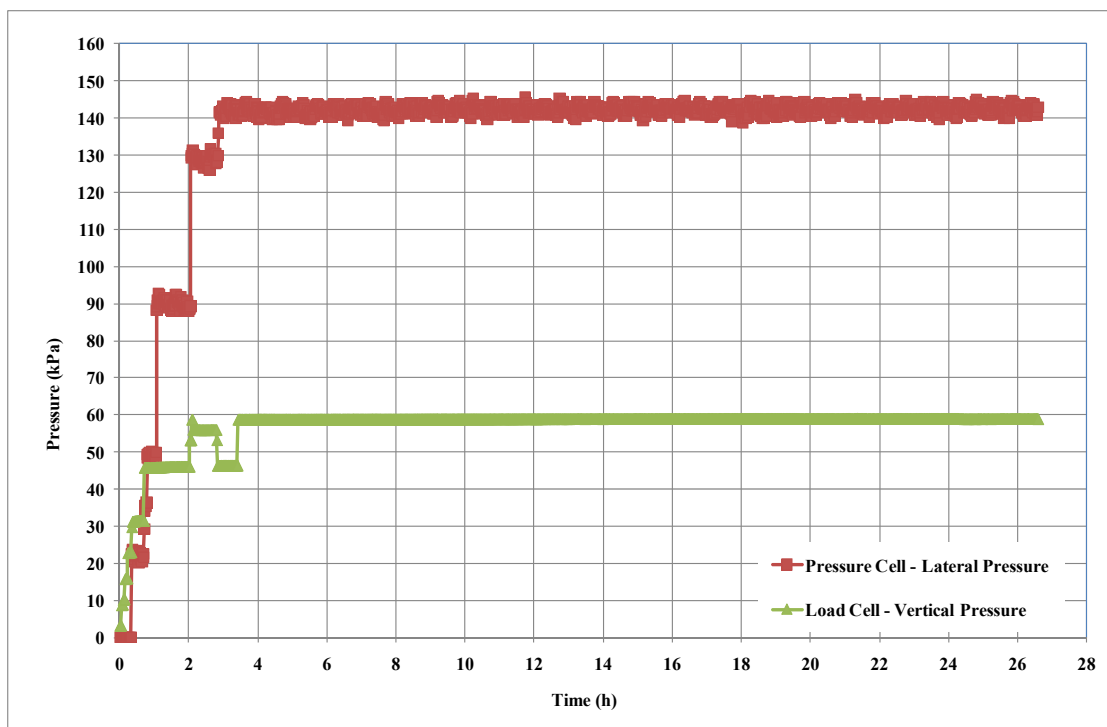
Figure 4.4: Pressure vs. Time Graph (Test: 01.07.2009)

85
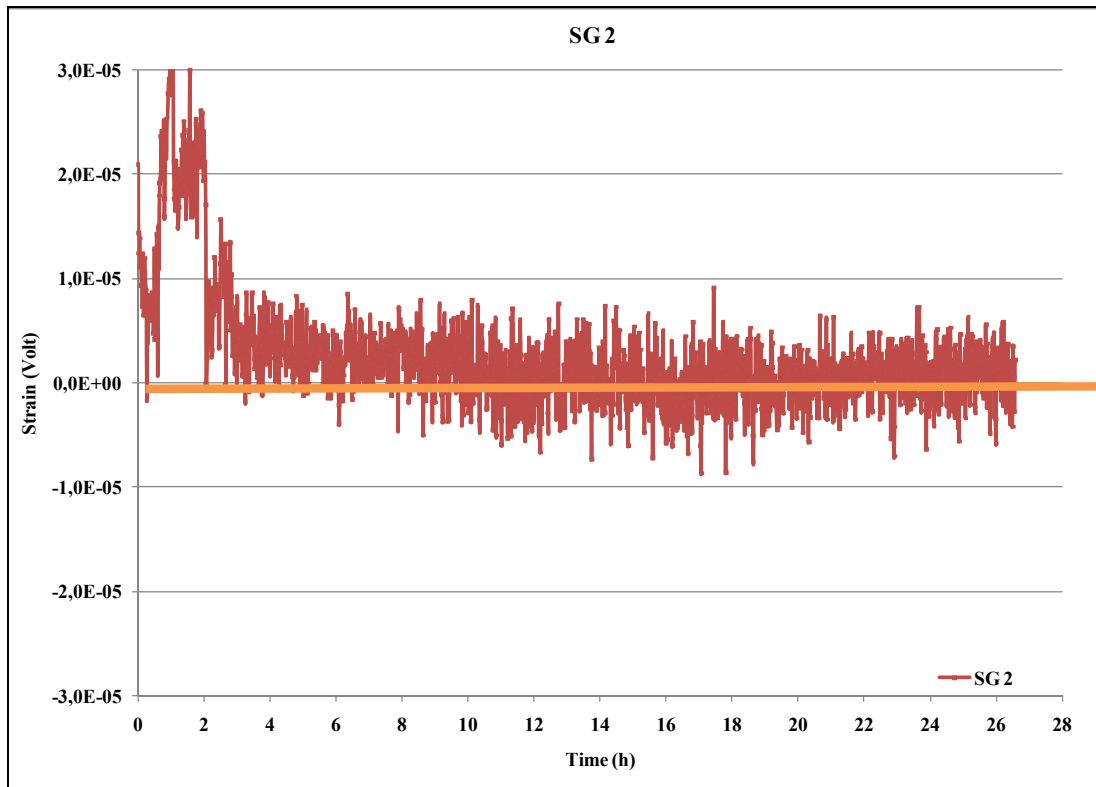
Figure 4.5: Lateral Strain vs. Time Graph (Test: 01.07.2009)

Additional constant volume tests were made on 07.07.2009, 09.07.2009, 13.08.2009, 17.08.2009, 25.09.2009, 02.10.2009 and 08.10.2009. Furthermore, three swelling tests on samples recovered from with rotated block were conducted on 20.08.2009, 22.08.2009 and 26.08.2009. Outputs of these tests in graphical form are given in the attachment of this thesis. Results of the horizontally laminated specimens are summarized in Table 4.3 and the results of the tests on vertically stratified samples are given in Table 4.4.

4.4 Tests under Constat Vertical Surcharge [(CS – LFST) and (CS-ZLST)]

These tests are based on the study of Windal and Sharour (2002). These tests can be considered as simple examples to the swelling problems faced in tunneling or a retaining wall construction. Similar as in these tests, the swelling pressures will act to the retaining system or to the tunnel lining in one plane while the generation of them will be hindered in the perpendicular plane by the effect of the earth pressure acting from overburden.

A vertical surcharge of 200kPa was applied to the dry specimen inside the test set up in the first tests. Then, the settlement of the specimen has been monitored and

recorded. Following the completion of the settlements, the specimen has been inundated. After the inundation of the specimen some further settlements have occurred, where simultaneously the swelling progress has started. The clay sample has swelled laterally, since the vertical swelling pressure of the specimen was not great enough to resist the vertical surcharge. Only limited vertical pressure has been recorded in these tests. The results of these tests, conducted on 05.06.2009 and 10.06.2009 are given below on Figures 4.6 ~ 4.11.

Table 4.3: Results of the Constant Volume Tests (Horizontally Laminated)

Test Date:	Stratification	Average Initial Water Content $w_i(\%)$	Average Final Water Content $w_f(\%)$	Vertical Swelling Pressure (kPa)	Lateral Swelling Pressure (kPa)	$\sigma r = \sigma_{sL}/\sigma_{sv}$	Total Test Duration (h)	Duration of Vertical Swelling Pressure Mobilization	Duration of Lateral Swelling Pressure Mobilization
01.07.2009	Horizontal	30	33 - 36	60	140	2,33	27	3	3
07.07.2009	Horizontal	25	42 - 35	65	105	1,62	24	3	3
09.07.2009	Horizontal	23	41 - 34	70	120	1,71	30	20	4
13.08.2009	Horizontal	17	23 - 46	95	95	1,00	29	8	23
17.08.2009	Horizontal	17	47 - 40	85	60	0,71	30	7	7
25.09.2009	Horizontal	18	37 - 43	120	80	0,67	57	24	24
02.10.2009	Horizontal	17	39 - 44	75	90	1,20	98	8	72
08.10.2009	Horizontal	18	39 - 45	80	85	1,06	52	24	24

Table 4.4: Results of the Constant Volume Tests (Vertically Laminated)

| Test Date:	Specimen Encapsulation Direction	Average Initial Water Content $w_i(\%)$	Average Final Water Content $w_f(\%)$	Vertical Swelling Pressure (kPa)	Lateral Swelling Pressure (kPa)	$\sigma r = \sigma_{sL}/\sigma_{sv}$	Total Test Duration (h)	Duration of Vertical Swelling Pressure Mobilization	Duration of Lateral Swelling Pressure Mobilization
20.08.2009	Vertical	17	45 - 41	100	135	1,35	46	2	26
22.08.2009	Vertical	17	43 - 41	90	260	2,89	28	4	5
26.08.2009	Vertical	17	46 - 43	65	150	2,31	29	20	23
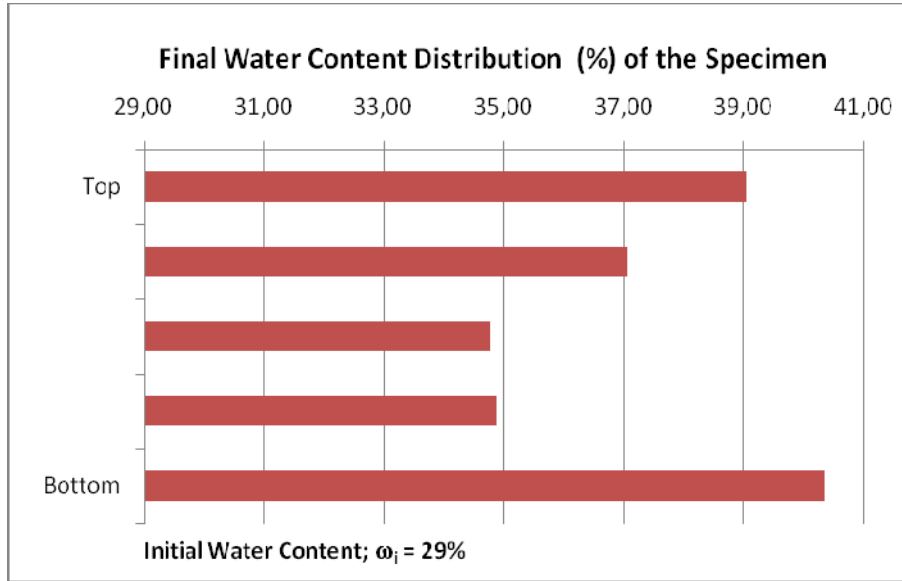
Figure 4.6: Initial and Final Water Contents, (Test: 05.06.2009)
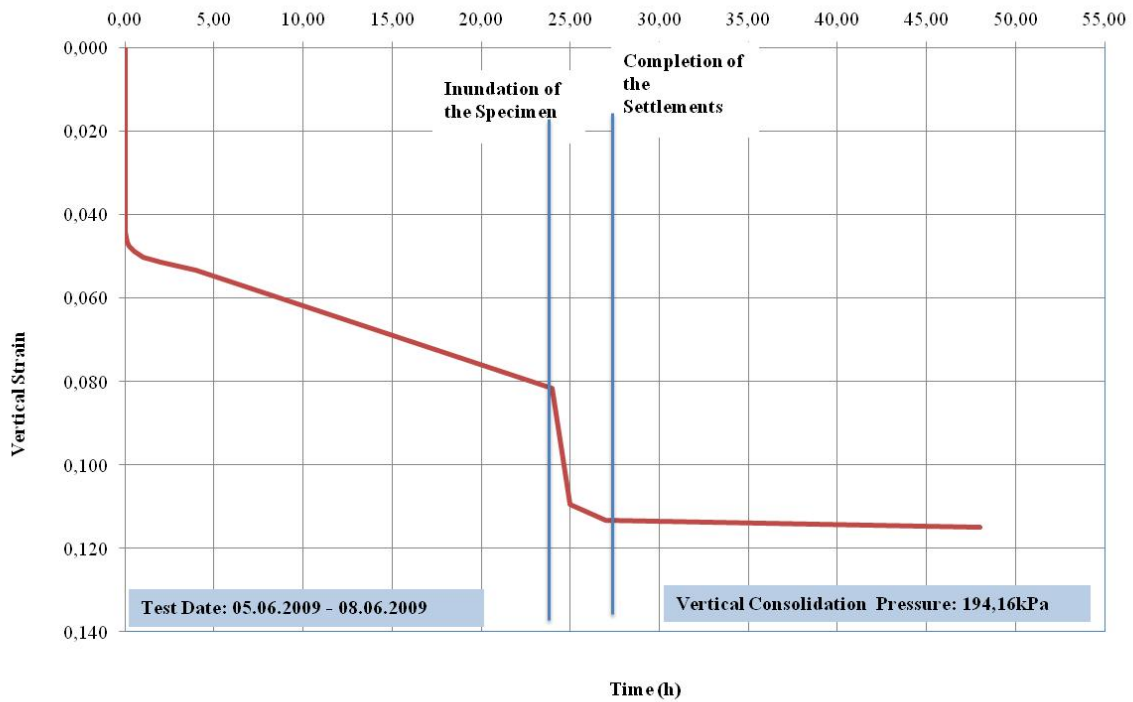
Figure 4.7: Vertical Strain vs. Time Graph (Test: 05.06.2009)

88
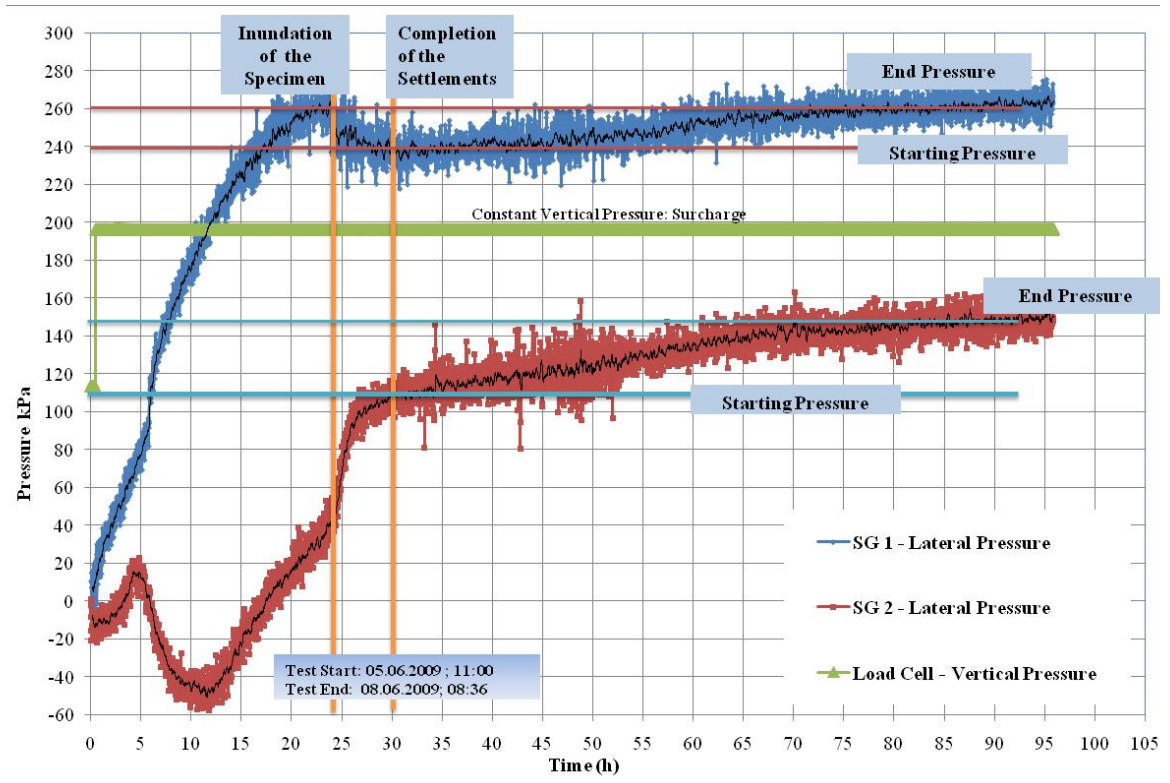
Figure 4.8: Pressure vs. Time Graph (Test: 05.06.2009)

Figure 4.9: Initial and Final Water Contents, (Test: 10.06.2009)

First test by employing a pre-described vertical surcharge was made on 05.06.2009. The initial water content of the specimen was w= 29%. In this test, the consolidation of the specimen was completed in 24 hours. Following the inundation of the specimen, some further settlements occurred, which were completed in 28th hours (Figure 4.7). As shown on Figure 4.8, the behavior of the specimen was non –

homogeneous up to this stage. Nevertheless, beginning from the 28th hour until the end of the test, strain gauges have revealed a parallel increase in vertical strain. Accepting the 28th hour as to be the stage where the lateral swelling pressure is zero, the lateral swelling pressure of the clay sample under the constant surcharge pressure of 194,6kPa has been recorded by the strain gauges SG 1 and SG 2 as 20kPa and 35kPa, respectively. The variation of the water content of the specimen at the end of the test is shown in Figure 4.6.

The test has been repeated by employing the same constant surcharge pressure of 194,6kPa. In this second test the initial water content of the specimen was dropped down to 24% (Figure 4.9).

Compared with lateral pressure values obtained under constant vertical surcharge given in similar previous studies, the lateral pressure values recorded in the test on 05.06.2010. So, this has forced us to revise the test methodology.

A reevaluation of the present test sequence has shown that letting the specimen consolidate within the test device causes some residual strains on the ring, which decreases the accuracy of lateral pressure readings. Hence, the decision was to consolidate the specimen in the sampling tube under the constant vertical testing surcharge and to transfer the specimen to the measuring equipment following the completion of consolidation. Now, the specimen was overconsolidated and only minor settlements have occurred after surcharging the specimen following its transfer to the test set up. The specimen reached an equilibrium condition in the test setup prior to inundation. Then the strain gauges were adjusted to zero and the test progressed with the inundation of the specimen.

Total 7 tests under constant vertical surcharge pressures varying between 75kPa to 125kPa have been made. All of the specimens have been consolidated inside the sampling tube. After transferring the specimens into the testing equipment, the same surcharge pressure have been applied. The specimens have been inundated right after they have been left to relaxation for a short time after the transfer. Vertical settlement or heaves of the specimens have been observed through an analog micrometer. The results of the first tests made with this method on 21.10.2009 are given on Figure 4.10 to Figure 4.12.
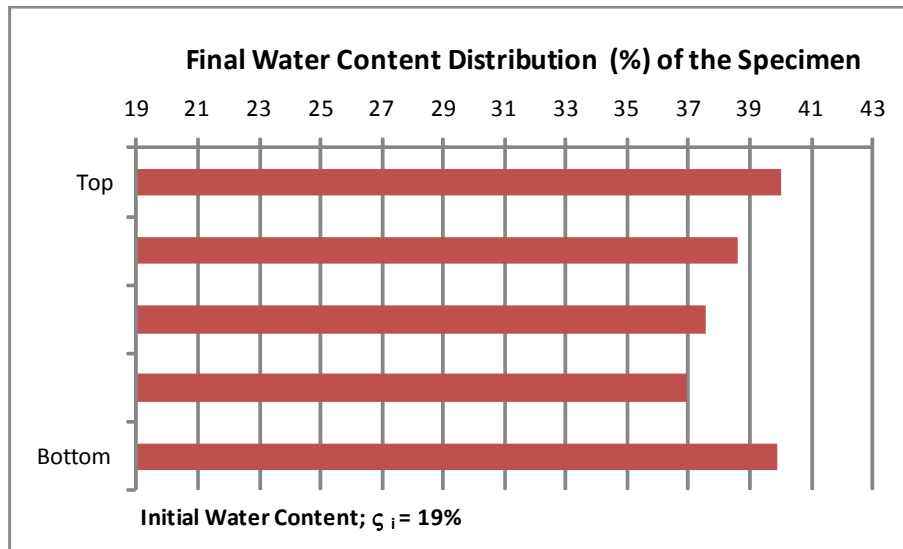
Figure 4.10: Initial and Final Water Contents (Test: 21.10.2009)
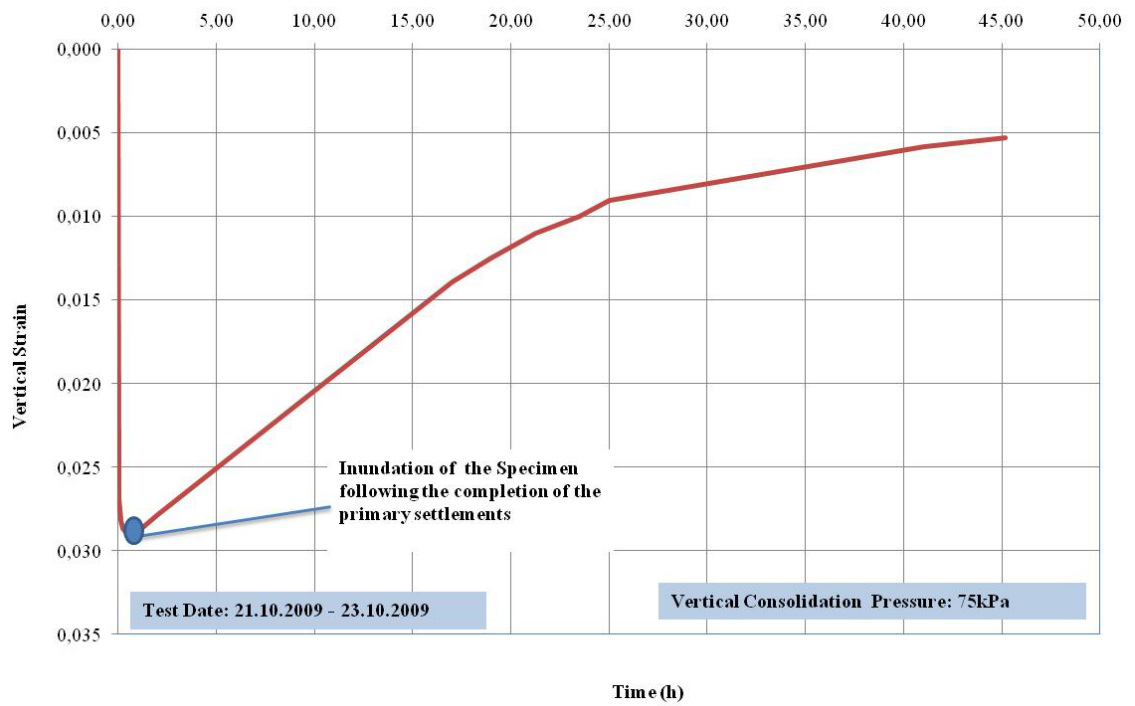
Figure 4.11: Vertical Strain vs. Time (Test: 21.10.2009)
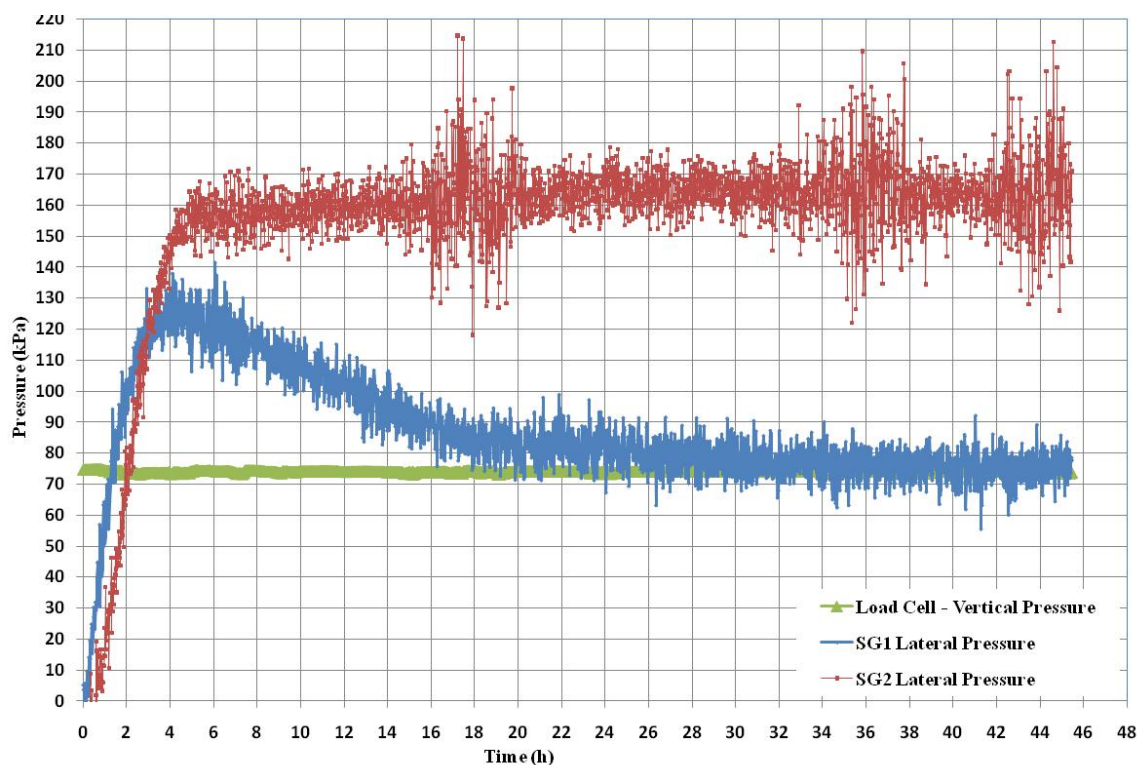
Figure 4.12: Pressure vs. Time (Test: 21.10.2009)

The test performed on 21.10.2009 with the revised technique under constant vertical surcharge pressure has resulted successfully, revealing a lateral swelling pressure of 160kPa, as it can be seen in Figure 4.12. It should also be noticed that the vertical swelling pressure of the specimen has exceeded the applied constant surcharge pressure. Figure 4.11 represents the vertical heave that has occurred during the test. The decrease of lateral swelling pressure in the SG 1 strain gauge is related to the increasing volume of the specimen in the vertical direction. On the contrary, the second strain gauge has reached the peak lateral swelling pressure value. The behavior of the second strain gauge is normally unexpected.

As mentioned before, additional six tests have been conducted with this methodology. The results of these tests are summarized in Table 4.5 and the graphical outputs envisioning the pressure – time variations are given in the attachment. In all the tests, with vertical surcharge pressure lower than 165kPa, the vertical swelling pressure of the specimen were greater than the applied surcharge. Being related to the volume increase ability of the specimens, lateral swelling pressure has dissipated in the later stages of the tests.

92

Table 4.5: Results of the Lateral Free Swell Tests made under Constant Predetermined Vertical Surcharge (CS-LFTS)

Test Date:	Average Initial Water Content ω_i(%)	Average Final Water Content ω_f(%)	Vertical Surcharge Pressure (kPa) (constant)	Lateral Swelling Pressure (kPa)		$\sigma r = \sigma_{sL}/\sigma_{sv}$	Total Test Duration (h)	Duration of Lateral Swelling Pressure Mobilization (h)
21.10.2009	19	37 - 40	75	170	120	1,93	48	4
24.10.2009	19	38 - 41	72	70	100	1,18	75	12
28.10.2009	19	36-41	100	100	160	1,30	125	5
03.11.2009	19	36 - 40	100	260	260	2,60	52	50
04.12.2009	19	37 - 39	125	100	100	0,80	72	10
08.12.2009	19	37 – 38	125	160	110	1,08	96	10
12.12.2009	19	32 – 34	165	180	180	1,09	52	26
29.12.2009	19	37 – 38	170	160	160	0,94	46	24

The tests have been repeated under similar constant vertical surcharge pressures with restraint lateral strain. In these tests, the vertical swelling pressure has been assumed to be equal to the lateral back pressure applied to the specimen to keep the initial lateral strain. Lateral pressure measurements have been made via a pressure transducer. The results of this second group of tests under constant vertical surcharge have been summarized in Table 4.6. Comparison of the results of the tests performed under zero lateral strain condition with the test results given in Table 4.5, shows the slight increase in the vertical swelling pressure/lateral swelling pressure ratios.

Table 4.6: Results of the Tests made under Constant Predetermined Vertical Surcharge with Lateral Cell Pressure Application (CS-LR)

Test Date:	Average Initial Water Content ω_i(%)	Average Final Water Content ω_f(%)	Vertical Surcharge Pressure (kPa) (constant)	Lateral Swelling Pressure (kPa)	$\sigma r = \sigma_{sL}/\sigma_{sv}$	Total Test Duration (h)	Duration of Lateral Swelling Pressure Mobilization (h)
19.01.2010	19	36 - 37	112	95	0,85	54	32
28.01.2010	19	36 - 40	138	98	0,71	30	28
02.02.2010	18	38 - 39	85	70	0,82	50	8
05.02.2010	17,5	40	85	50	0,59	50	7
09.02.2010	18	37	85	105	1,24	72	54
13.02.2010	17	37-40	115	115	1,00	25	8

4.5 Lateral Swelling Pressure Tests with Fourie Method

Fourie's (1989) method has been followed in the fifth group of tests. Considering that strain based failures may have a significant effect on the lateral swelling pressure determination, the lateral strains under varying lateral back pressures have been recorded.

Fourie has investigated the lateral swelling pressures of expansive soils based on the "Method of Equilibrium Void Ratios" of Sridharan et al. (1986). Fourie (1989) has conducted the tests in a hydraulic triaxial cell under varying initial cell pressures. The fifth group of tests within this thesis, which will be mentioned in the following paragraphs have been made following the same methodology. The similarity of the modified thin lateral pressure ring used in this study with the triaxial apparatus of Bishop and Wesley (1975) having the Bishop and Henkel (1962) strain belt has given the possibility of adopting the testing methodology followed by Fourie (1989) to this study.

Varying back pressures have been applied to the samples and they were allowed to change the volume until an equilibrium under a constant surcharge of 125 kPa was achieved. Since predicting the lateral swelling pressure was the main intention, a constant surcharge has been applied in all of the tests performed within this group. A total number of eight tests have been made within this group. The test results have been tabulated on Table 4.7. Related graphics illustrating the results of the tests are given in the attachment. The observed lateral strains and the related cell pressures are given in Chapter 5.

Table 4.7: Results for Lateral Swelling Pressure Tests Made in Accordance with "Method of Equilibrium"

Test Date:	Average Initial Water Content ω_i(%)	Average Final Water Content ω_f(%)	Vertical Surcharge (kPa)	Lateral Back Presure Pressure (kPa)	Average Lateral Strain
19.02.2010	19	38 - 41	125	4	0,000030
24.02.2010	19	35 - 37	125	25	-0,000010
27.02.2010	17	33 - 35	125	20	0,000030
03.03.2010	18	35 - 37	125	35	0,000025
06.03.2010	19	32 - 34	125	40	0,000030
10.03.2010	17	38 - 39	125	95	-0,000010
13.03.2010	20	34 - 35	125	115	-0,000020
17.03.2010	17	33 - 34	125	25	0,000020

Only one set of tests have been conducted by using the "Method of Equilibrium". Additional tests may be conducted by applying different vertical surcharges on clay samples.

5. EVALUATION OF TEST RESULTS

Results of the tests that have been conducted with the modified thin walled oedometer have been summarized in Chapter 4. The test results have been evaluated in this chapter. Findings given in this Chapter also represent the reliability of different test methods that may be followed when using the thin walled lateral swelling pressure ring. Applicability of different test methods shall also be discussed.

As mentioned previously, the inspiration of concentrating this study to lateral swelling pressure was based on the idea to design a testing device so that test results to be obtained from this device can directly be employed in geotechnical design. To be more precise, the aim was,

- to predict the swelling pressure without any overestimation as in the conventional uniaxial test methodologies

- to predict the anisotropic swelling behavior and to find out the ratio of lateral swelling pressure to vertical swelling pressure

- to investigate the variation of lateral swelling pressure with depth for a given soil profile

- to represent the variation of the lateral pressure with the rigidity of a retaining structure or a tunnel lining. In other words, to demonstrate the attenuation of the swelling pressure with deformation.

Prior to the start of the evaluations of the test results, it will be helpful to review the test results explained previously in the following paragraphs.

All of the tests have been conducted on compacted samples that have been prepared in the laboratory, under similar conditions and using the same clayey soil. The samples have been compacted under equal compaction energy in accordance with

ASTM D4546 – 03 "Standard Test Method for One Dimensional Swell or Settlement Potential of Cohesive Soils".

The effect of initial water content on swelling pressure is well known. Hence, the subject of this thesis was to present a method on the determination of lateral swelling pressure, and the variation of the swelling pressure due to the variation of the initial moisture content is not a matter of subject in this study. For this reason, the initial water content of the samples has been kept constant in the tests. Generally, the initial water content values of the specimens vary between 17% and 19%. Only a few samples in the trial tests had higher initial water content values. The laboratory program has been generated so that all the tests have been repeated once at least. The test results have been verified in this manner.

The tests performed within the scope of this research have been evaluated under groups according to their stress – strain conditions as illustrated in the schema below (Figure 5.1).
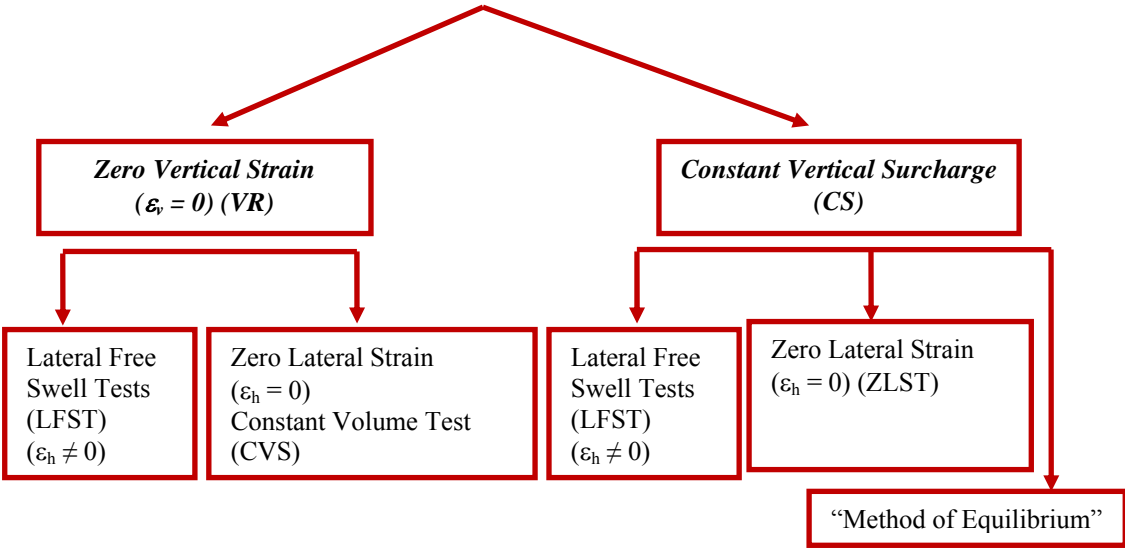
Figure 5.1: Stress - Strain Conditions of the Tests Performed for this Study

5.1 Lateral Swelling Tests Based on the Method C in ASTM 4546-03

Two types of lateral swelling tests have been made, based on the Method C in ASTM 4536-03. In the first group of tests, swelling of the specimen in vertical direction has been prevented by load adjustment in vertical direction following the inundation of the specimen. Simultaneously, the specimen swelled in lateral direction. The vertical swelling pressure has been accepted as the value of surcharge necessary to

prevent the swelling of the specimen in vertical direction. Lateral swelling pressure has been determined by calculating the corresponding pressure from the occurred lateral strain. These tests are defined as "vertically restrained - lateral free swell tests – (VR-LFST)" (Figure5.2). These tests are alike the Method C given ASTM 4536-04 in restaining the vertical strain of the specimen. However, they do differ from Method C, in that the specimen swells free in lateral direction.

Similar to these tests, a group of tests have been made in which both, the vertical strain and the lateral strain have been kept zero ($\varepsilon_h = \varepsilon_v = 0$). The vertical strain was kept as zero as in the previous VR-LFST tests. Hydraulic cell pressure restrained the occurrence of lateral strain. These tests satisfy completely the requirements of ASTM D4546 -03, Method C and are defined as "constant volume tests – (CVS)" (Figure5.2).
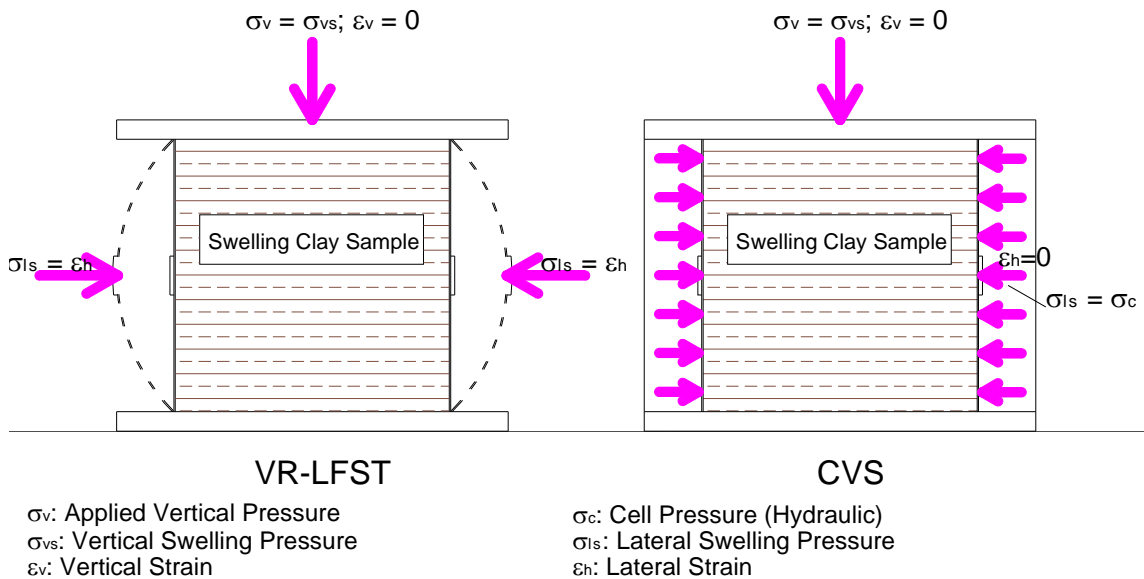
Figure 5.2: Comparison of VR-LFST and CVS Tests

The tests within this group were necessary to understand the effects of modifications made on the testing device as a part of the research program. In view of the fact that most of the previous studies have also used similar techniques, the results of swelling tests conducted in this research are comparable with the results of other studies on swelling behavior of soils.

5.1.1 Validation of initial test results in contrast to the results of previous studies

The origin of the testing device developed and used within this study bases the device designed by Komornik and Zeitlin (1965). Ertekin has regenerated Komornik and Zeitlin's device in 1991. As mentioned in the paragraphs above, Erol and Ergun (1994) and Sapaz (2004) have conducted a number of swelling tests with Ertekin's (1991) device.

The testing device developed for this thesis is different than the one regenerated by Ertekin (1991) in a way that it can measure lateral swelling pressure under zero lateral strain by its ability to apply cell pressure in lateral direction. Applying the lateral cell pressure is an option that can either be used or not. Another major change is that the dimensions of the thin walled ring have been increased from 63.5mm / 50mm (diameter / height) to 70mm/70mm by the author. As already cited in the related paragraphs above, especially the ring height has been increased to reduce the effect of the rigid top and bottom plates on the deformability of the thin walled ring at its mid height where the strain gauges are mounted.

Before reviewing the complete results obtained from the tests within this study, it will be useful to compare the results of initial tests with the results of similar tests. In other words, a validity check on the dependability of the new test equipment has been made.

Results of the VR-LFST tests based on Method C, which were made without the application of cell pressure are compared. First of all, the distribution of lateral swelling pressures versus vertical swelling pressures obtained in these tests are illustrated in Figure 5.3.
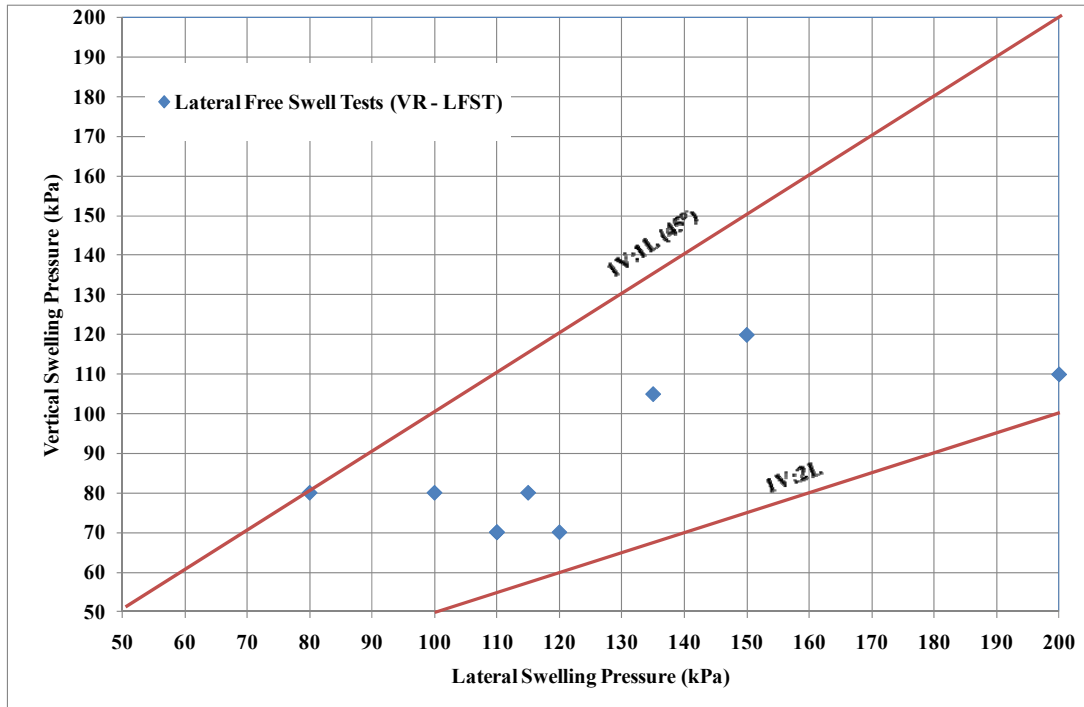
Figure 5.3: Results of VR-LFST

The results reveal that clays has an anisotropic swelling behavior. The results depicted in Figure 5.3 match the swelling pressure ratios mentioned by Mc Dowell (1956) and Crilly (1992). The lateral swelling pressure is greater than the vertical swelling pressure and is in a range between $\sigma_L/\sigma_v = 1 \sim 2$. The results depicted in Figure 5.3 have also been depicted in Figure 5.4 showing the results of earlier studies as well.

In addition to the results of Sapaz (2004) and Erol and Ergun (1994), the test results of Erguler and Ulusay (2003) and Avşar et al.(2009) reflecting the anisotropic behavior of Ankara clay have been shown in Figure 5.4 as a basis for comparison.

Different than rest of the investigators, Avşar et al. have made triaxial swelling tests by using a testing device similar to that of Ertekin's ring in a smaller scale. The diameter of the shrunken ring was 54.5mm and the height was 30mm. Avşar et al. have resized the ring in order to raise the ring rigidity and by this way avoiding the lateral deformation in a different way than a back (cell) pressure applicable device as Ofer (1980) has generated.

Avşar et al. have realized the tests in accordance with the Method B in ASTM 4546 – 03 (2003). Briefly, the specimen is left to swell under a vertical surcharge corresponding to its natural geological overburden stress at the beginning. Then,

after completion of swell, vertical pressure was applied until the specimen was recompressed to its initial height. The magnitude of applied vertical pressure is accepted as the vertical swelling pressure.

Even though the test method of Avşar et al. was different than the rest of the investigators and the test method followed in this thesis, the results have been considered to be significant and have been presented therefore in this thesis for comparison. The primary vertical pressure under which the specimens of Avşar et al. (2009) had been left to swell freely was 4kPa.

The peak values of the swelling pressures mobilized in lateral and vertical directions during the tests of the studies mentioned above have been depicted in Figure 5.4.
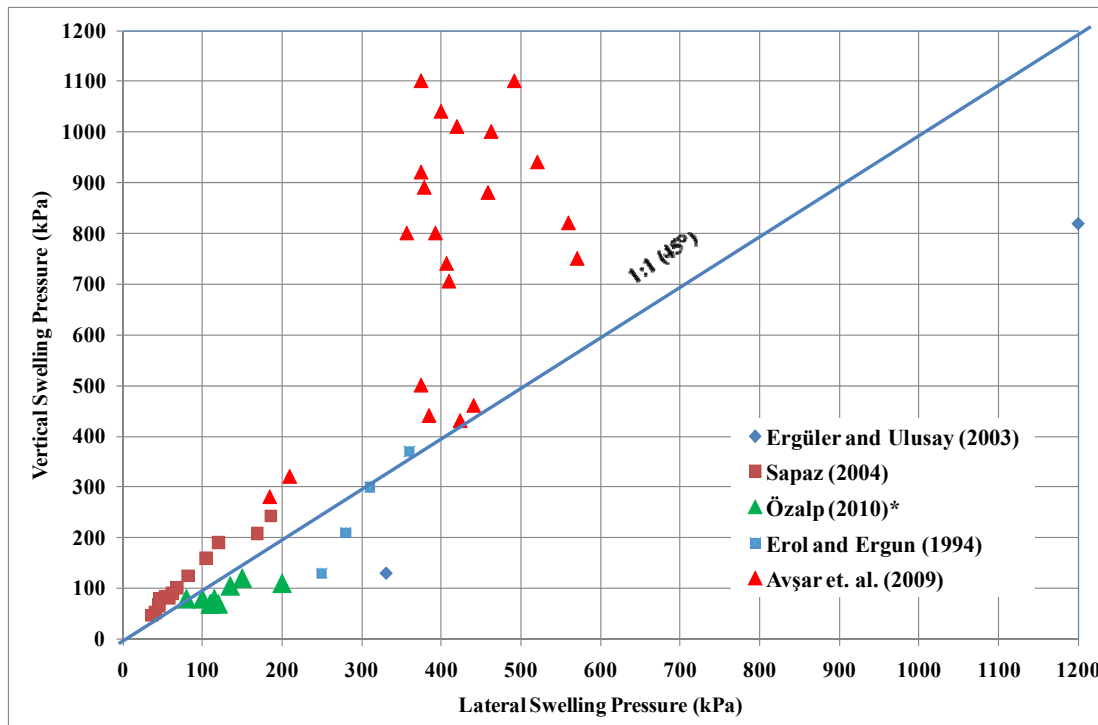
Figure 5.4: Peak Vertical Swelling Pressure vs. Lateral Swelling Pressure

The tests of Sapaz (2004) have terminated with higher vertical swelling pressures than lateral. On the contrary, the samples taken from the Aegean coast by the investigators Erol and Ergun (1994) have exposed grater lateral swelling pressures than vertical swelling pressures alike the clay used in present research. The general distribution of the test results is around the equality line ($\alpha = 45°$). As mentioned in the previous paragraphs, the volumetric strain ratio of a swelling samples yields to $\varepsilon_l/\varepsilon_v = 1$.

An important fact that could be noted from Figure 5.4 is that the lateral swelling pressures obtained from the tests with the shortened thin walled lateral pressure ring of Avşar et al. (2009), have been accumulated in an upper limit within the range of 500kPa to 600kPa. For tests with respectively low vertical swelling pressures, the ratio of vertical to lateral swelling pressure is slightly over 1.0. With the increase of vertical swelling pressures, the ratio increases rapidly to the constant lateral swelling pressure values within the range of 500kPa – 600kPa. This may be attributed because of the limited deformation ability of the testing device due to the decrease of the ring height. Although, the ring wall is as thin as the ring used in this thesis, the short height of the ring may be effected from the rigid top and bottom plates. Based on this matter, the ring starts to act as a normal oedometer ring after reaching a certain lateral displacement and the swelling pressure build up continues merely in the vertical direction.

On the contrary, the height of the ring used in this study has been increased up to 70mm. So, the effect of the rigid top and bottom plates on the thin walled oedometer ring has been minimized. The increase of the ring height may raise the question that the ease of bending the thin walled ring may lead to overestimated lateral swelling pressure. As stated by Azam (2009), especially the loading induced volume decrease or limitation may force the specimen to shear, leading to overestimated lateral swelling pressures. To avoid the overestimation of lateral swelling pressure due to the shear of the specimen, a pressure cell has been added to the ring. With the help of this pressure cell surrounding the thin walled ring, constant volume tests can be made with the recently generated testing device.

To conclude, the lateral swelling pressure test results of the tests conducted with the device designed for this study agree with the results of tests that were carried out with the same method and simliar testing devices, previously. This comparison has validated the reliability of the test set up.

5.1.2 Comparison of laterally restrained and lateral free swell tests based on ASTM 4546-03, Method C

The addition of the cell around the thin walled oedometer ring is one of the major developments that has been accomplished in the test device that were used in this study. The aim of designing such a testing device was to see the effect of lateral

strains on swelling pressure development. For this reason, the lateral swelling pressures obtained from lateral free swell tests have been compared with the results of the tests, in which the lateral strain has been kept in its initial state ($\varepsilon_h = 0$) by applying cell pressure. As stated before, the lateral swelling pressure has been determined by reading the corresponding pressure from the strain − pressure calibration curve of the thin walled ring (Figure 3.15).

Figure 5.5 depicts the results gathered from specimens tested by both methods. In the first group of tests, samples were restrained in vertical direction with lateral free swell and in a second group of tests, the samples were triaxially confined.
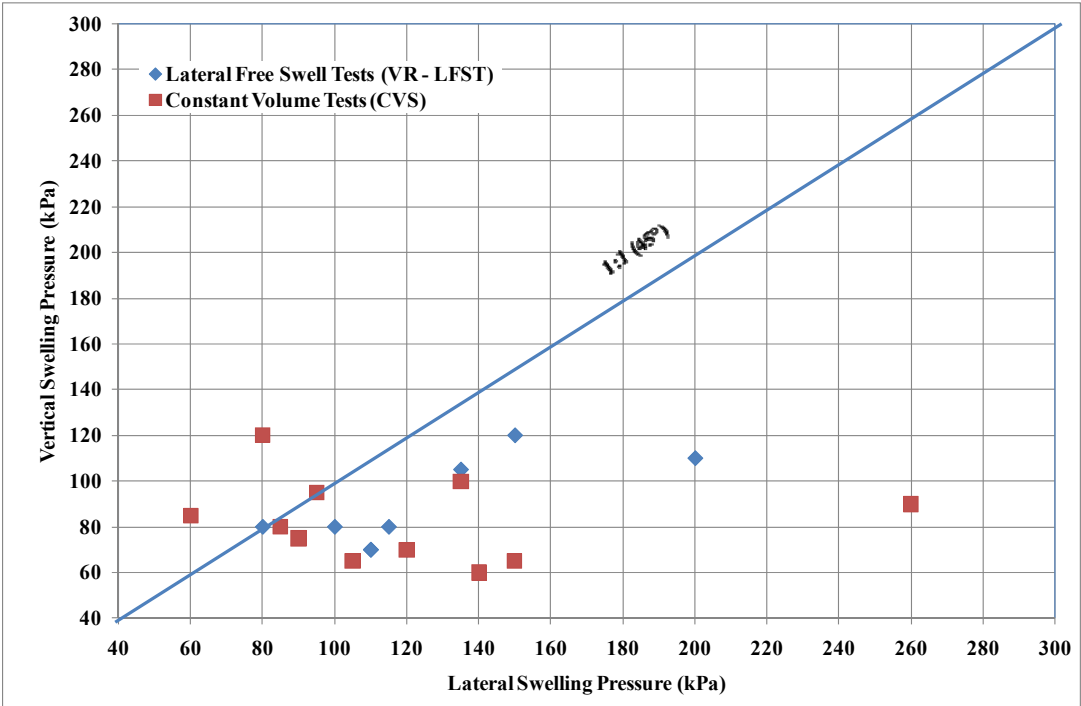
Figure 5.5: Comparison of LFST - CVS test results

Against the expectations, the variations in the test results were minor. As depicted in Figure 5.5, the range of lateral swelling pressures vary within a range of 80kPa to 150kPa in both test methods. To reflect the test results in a better way, the test swelling pressure ratios (σ_{sh}/σ_{sv}) observed for different vertical swelling pressure values have been illustrated in Figure 5.6 and Figure 5.7.
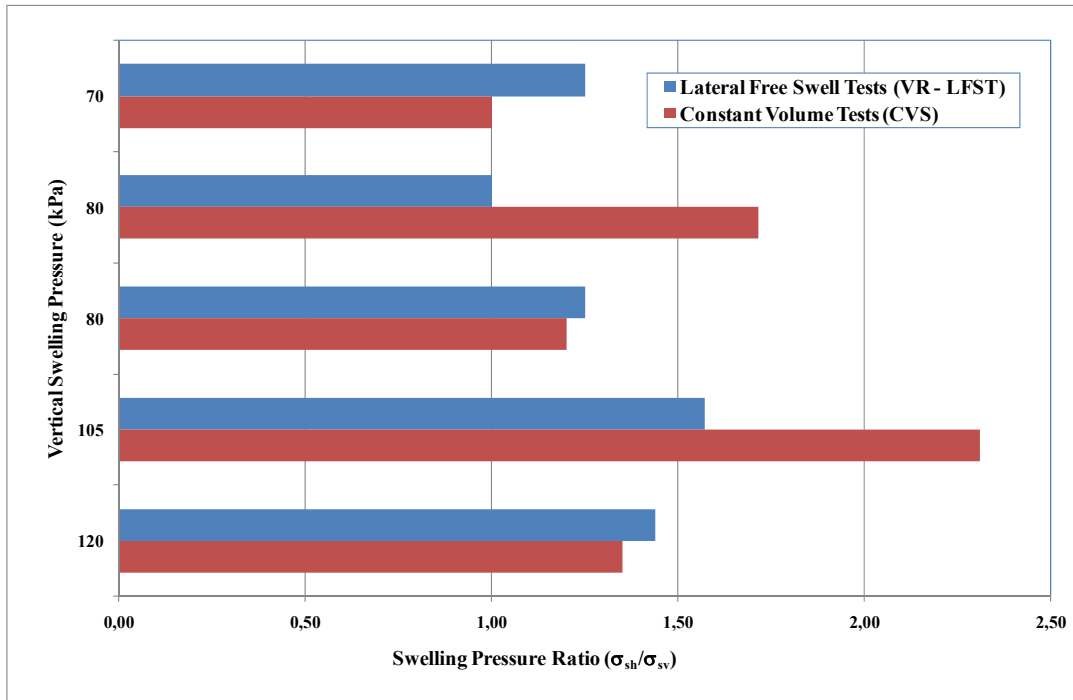
Figure 5.6: Comparison of swelling pressure ratios
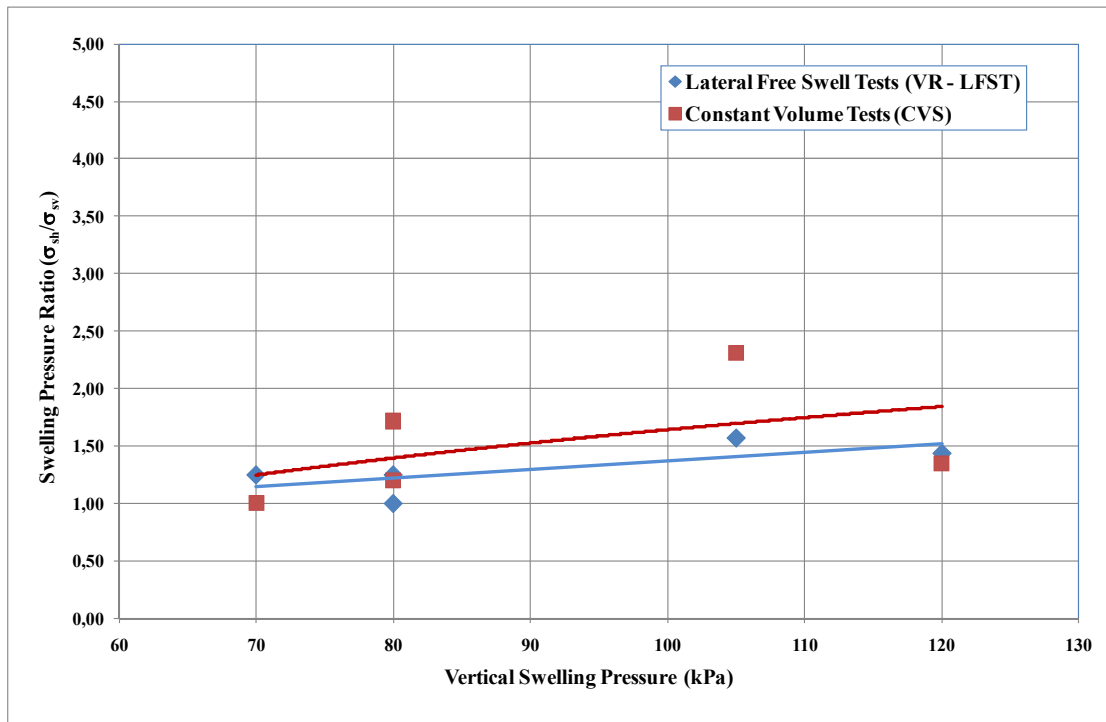
Figure 5.7: Comparison of swelling pressure ratios

Figure 5.6 and Figure 5.7 illustrate the variation of swelling pressure ratios, which are defined as the ratio of lateral swelling pressure to vertical swelling pressure. Some constant volume tests have resulted with higher swelling pressure ratios. Especially Figure 5.7 shows that the average of the swelling pressure ratios obtained from the constant volume tests are higher than those obtained from the lateral free

105

swell tests. On the contrary, Figure 5.6 compares the tests results for different vertical swelling pressures in particular groups. Based on the comparisons on Figure 5.6, the difference between the test methods may be neglected, since, some of the LFST tests have resulted with higher lateral swelling pressures as well.

A potential reason for having almost similar results (Figure 5.5) obtained from the triaxial swelling tests that were realized with and without restrained lateral strain, may be the limited swelling potential of the clay type that were used in the experiments. The variation in the test results may be more pronounced for a clay type soil that has a much higher swelling potential.

Moreover, the volume of the specimens has been kept constant by increasing vertical and lateral pressures gradually so that no vertical and lateral strains occur. As the vertical and lateral pressure increase has been made manually, a small amount of strain has occurred first, than the occurred strain has returned to its initial state by increasing the vertical and lateral pressure. On the contrary, Windal and Shahrour (2001), and Ofer (1981) have stated that even a small amount of deformation highly decreases the lateral swelling pressures. So, instead of applying back pressure manually, implementing a strain induced automatic cell pressure triggering may possibly raise the accuracy of the triaxial swelling pressure test results to be obtained from the thin walled swelling pressure device used in this thesis.

As observed in several studies, the swelling pressure of the same specimen can vary in a free swell or a constant volume test. Usually, higher swelling pressures are obtained in free swell tests than in constant volume swell test. Results of the uniaxial tests conducted in this thesis given in Subtitle 3.1.6 confirm this conclusion. The uniaxial constant volume test results have reached a peak swelling pressure value of 136kPa, while the specimen taken from the same compaction mold has ended up with a vertical swelling pressure of 200kPa in free swell test. The vertical swelling pressure established in the free swell test is 47% more than the vertical swelling pressure determined by the constant volume test.

Like in the vertical direction, the degree of limitation of strain in the lateral direction may have an effect on swelling pressure. Prior to analyzing this matter, the difference in the physical conditions in both cases has to be set well.

As mentioned before, in the swelling tests within this group, the vertical strain has been kept as zero by increasing the vertical pressure gradually. No cell pressure has been applied in these tests. The lateral swelling pressure has been obtained by utilizing the final lateral strain value in to the calibration chart and lateral swell pressure has been determined indirectly. Since no cell pressure was applied in lateral direction, these tests are lateral free swell tests (LFST).

The explanations below are quite informing about the reason of higher swelling pressure observations in uniaxial - vertical free swell tests than in uniaxial - vertical constant volume tests. Lambe (1966) has set the following relationship:

$$\sigma = \sigma' + u + (R - A) \tag{15.1}$$

Where;
σ: total stress
σ': intergranular (or particle to particle) stress;
u = pore water pressure;
$(R - A)$ = net repulsive or attractive force between particles due to Coulomb or Van der Waal's forces.

"For the case of dispersed soils, there is no interparticle contact. This may not be the case for highly precompressed clays but for a constant volume condition it may be reasonable to assume that the value of the term remains constant. For this case, the following relationship is obtained

$$\sigma' = \sigma - u = (R - A) \tag{5.2}$$

For a given electrolyte concentration, type of absorbed ion, and temperature, there is a unique curve of net interparticle force versus particle spacing (Lambe, 1953, 1958; Scott, 1963). Thus, in a constant volume consolidation test, the value of $(R - A)$ cannot change. The load added in a constant volume consolidation test merely balances the negative pore pressure, which is released due to immersion. Thus, the immersion water has the same ion concentration as the free pore water, the value of $(R - A)$ remains constant and, by equation (5.2), the effective stress must also remain constant. In the case of a free swell test, the pore pressure again goes to zero with time after immersion and the value of $(R - A)$ decreases due to an increased particle spacing until an equilibrium is reached with the confining pressure. (Hardy, 1965; Noble, 1965).

The different swelling mechanism in the uniaxial free swell test and the uniaxial constant volume test is one of the major causes for the disagreeing test results. Another cause may be the change in structure of the soil during the recompression stage of the free swell test. Seed et. al. (1962) has highlighted the reality that in attempting to measure the total swelling potential in a constant volume consolidation test, it should be recognized that even small changes in volume would greatly affect the measured swelling pressure.

In a triaxial swelling test with a thin walled swelling pressure ring, the case is different from the classical free swell test as described above. At first, it is still not a total free swell test in that the volume change of the specimen has to be avoided in the vertical direction by whether staged incremented or constant applied vertical surcharge. The specimen is laterally free to deform and strain is developed in lateral direction. However, a ring confines the sample, although this is a thin wall ring. Conclusively, the volume change and the related increase in particle distances is limited and the decrease in (R – A) is not as high as in the vertical free swell test.

One other fact to emphasize is that the swelling pressure in a lateral free swell test is calculated from the recorded lateral strain. Therefore, the soil structure is not recompressed and deformed, like in the vertical free swell test.

5.2 Lateral swelling tests under constant surcharge

Lateral swelling pressures acting on structures in shallow depths (in active zone) may be solved by soil improvement or soil replacement. The increase of depth in swelling pressure problems such as swelling pressures acting on earth retaining systems in deep excavations, tunnels or buried pipes entails the necessity to predict the variation of swelling pressure with depth. To be more explanatory, the distribution of swelling pressure with depth has to be known for design of structures in expansive soils.

Windal and Sharour (2002) have made lateral swelling pressure tests under constant vertical surcharge. The vertical surcharge employed in a test represents the overburden pressure corresponding to that depth. As a part of this research, several tests have been made based on Windal and Sharour's (2002) test methodology. Some of the tests have been made by employing cell pressure increase during the

test, while some of them have been made as lateral free swell tests, i.e., not applying any the cell pressure.

Prior to testing, the specimens have been consolidated under varying vertical surcharge pressures in a range of 100kPa to 200kPa. Swelling tests have started after inundating the consolidated specimen. In eight of these tests, the specimens have been let to swell free laterally and six of them were conducted under zero lateral strain ($\varepsilon_h = 0$) condition, or otherwise said, under cell pressure.

5.2.1 Principles of the method followed in lateral swelling pressure tests under constant vertical surcharge

Prior to discussing the test results, the test procedure will be explained. As mentioned in Paragraph 4.14, in the primary tests under constant vertical surcharge, the artificially prepared specimens have been consolidated inside a thin walled ring.

Figure 4.8 reveals that only minor lateral swelling pressures have been observed in these tests. In order to prevent the overestimation of lateral swelling pressure, the lateral strain tha might cause some shear strain in the specimen during the consolidation phase has been neglected. As shown in Figure 4.8, the strain already occurred until the completion of the consolidation of the specimen has been accepted as zero.

Even though, these tests resulted with noticeable lateral swelling pressures, the accuracy of these results is doubtful. It is easy to realize that the rigidity of the thin walled ring will be higher than in the zero strain condition since it is already been strained under the shear force acting from the specimen. So, to overcome this kind of problems, the testing procedure has been modified. The intention of the modified testing procedure was to maintain minor or almost zero strain condition at the beginning of the test. This has been realized by pre-consolidating the specimen inside the encapsulation tube. After the completion of the consolidation phase under the constant vertical surcharge pressure to be applied during the swelling test, the specimen has been transformed into the thin walled ring. Then the specimen has been left to swell under the previously applied surcharge.

Figure 5.8 illustrates the vertical strain range of the swelling tests made under constant vertical swelling pressure. By consolidating the compacted samples in the

sampling tube prior to swell tests have succeeded in that the vertical strains recorded in these tests have fitted into a narrow range between -1% and +3%.   The limited vertical strains occurred in the tests under constant vertical surcharge pressures are substantiate the reliability of the lateral swelling pressure values obtained at the end of the tests.   The vertical strain values recorded in the tests on which the specimens were consolidated inside the test ring instead of the sampling tube were in a range between 7% to 15% (Figure 4.7).
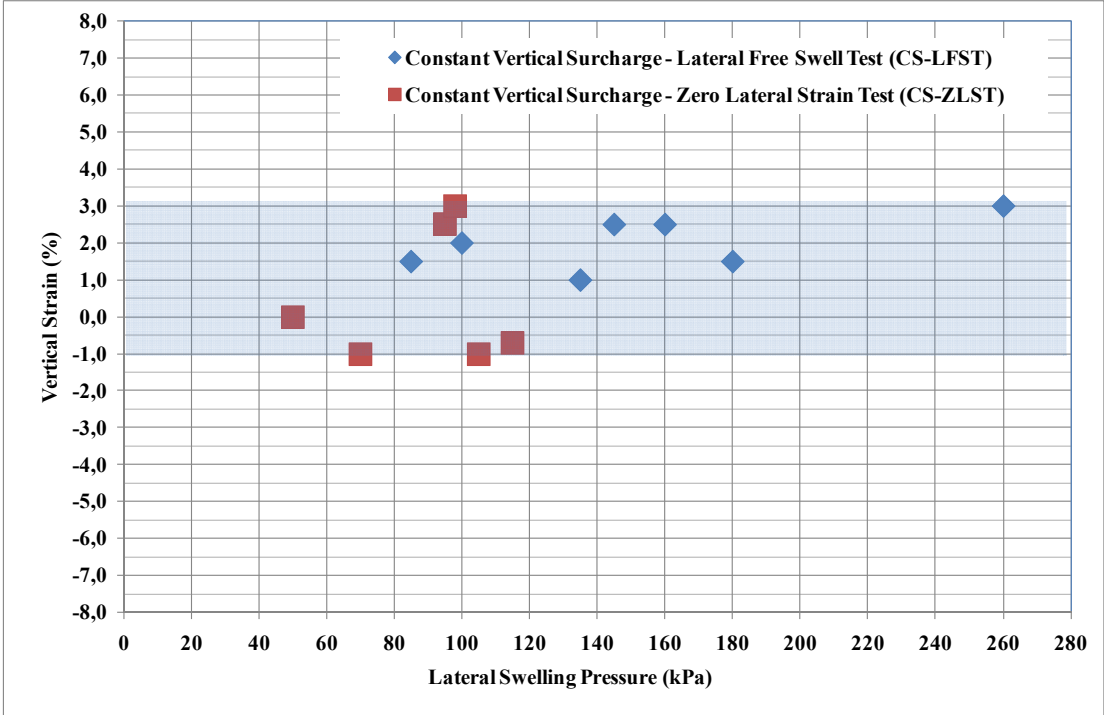
Figure 5.8: Recorded Vertical Strain Values vs. Lateral Swelling Pressure of Swelling Tests under Constant Vertical Surcharge

5.2.2 Comparison of lateral swelling pressures in various tests under constant vertical surcharge

As stated above, one of the aims of this study was to reflect the effect of strain on swelling pressure development.   Therefore, a pressure cell surrounds the swelling pressure ring in the test set up.   As well as the tests according to Method C, also in the tests under constant vertical surcharge, both test methods have been followed to achieve comparable results.

In Figure 5.9, the results of the tests conducted under zero lateral strain conditions $(\varepsilon_h = 0)$, and the results of the lateral free swell tests are shown together.

Figure 5.9 and Figure 5.10 show that greater lateral swelling pressures are obtained from Lateral Free Swell Tests under constant surcharge when compared with tests under Zero Lateral Strain Condition, in general.

The expectations were that the tests under lateral cell pressure would end up with higher lateral swelling pressures than the tests on which the specimen have been left free to swell in lateral direction. On the contrary, results of the tests on which the specimen has been left free to swell in lateral direction have resulted with slightly higher lateral swelling pressures than the tests under zero lateral strain condition. Regarding the fact that the difference is negligible, it is concluded that magnitude of ultimate swell pressure is not affected by the test method.

Results of these tests are in agreement with the results obtained from the tests in accordance with Method C. As a parallel statement to the evaluations made in Paragraph 5.1.2, the occurrence of even very small strains leading to volumetric increase in sample causes significant decrease in lateral swelling pressure.

Evaluating all the test results together reveal that a strain induced automatic cell pressure triggering for lateral swelling pressure prediction under zero lateral strain conditions is necessary for greater accuracy. If, automatic cell pressure triggering is not present, which is the case in this study, the adjustment of a testing technique like "The Method of Equilibrium (Fourie, 1989)", will avoid side effects of possible failures of lateral stress adjustment by the cell pressure increase. The lateral swelling pressure is obtained from a set of tests under different constant lateral cell pressures in "The Method of Equilibrium" suggested by (Fourie, 1989).
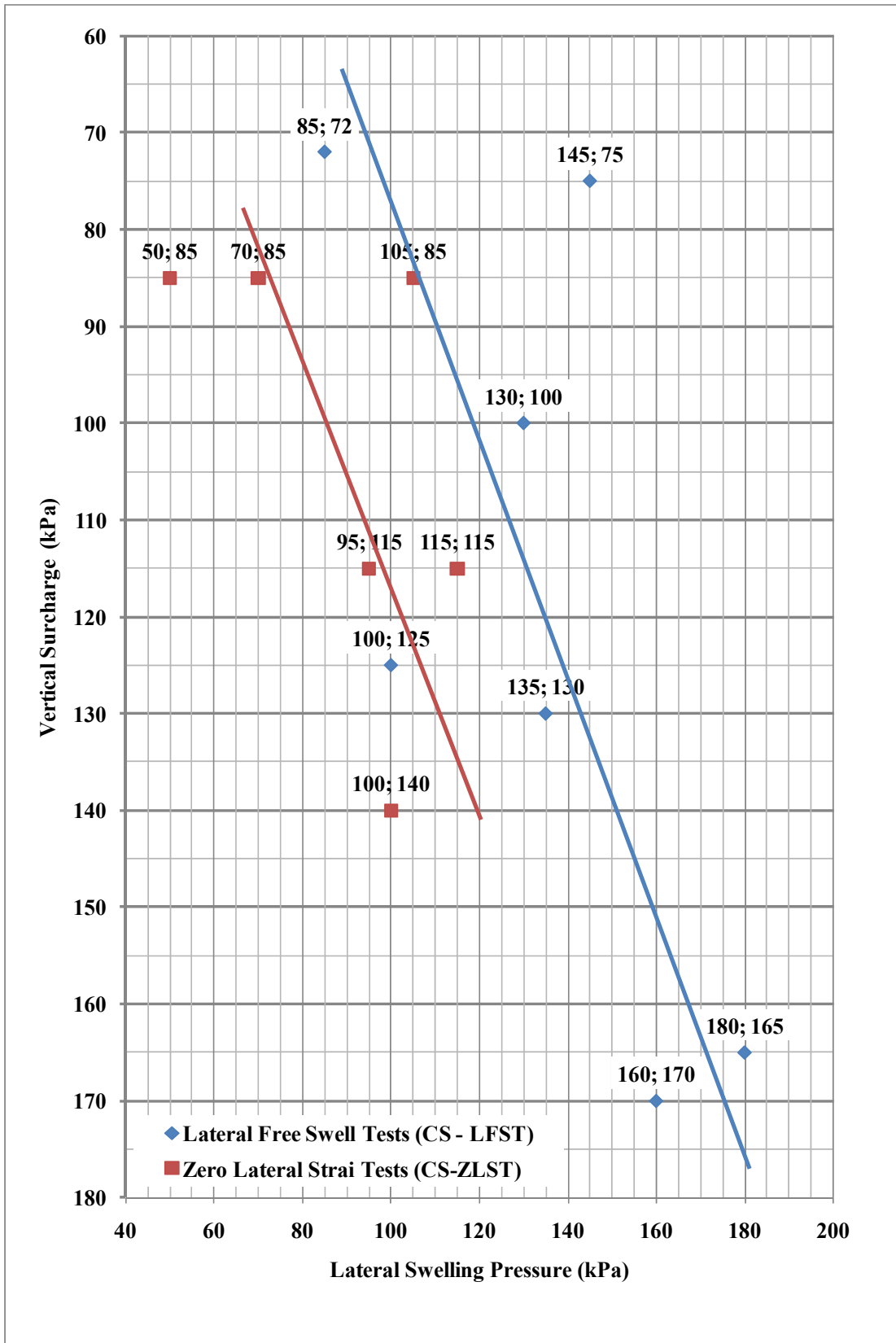
Figure 5.9: Lateral Swelling Pressure under Varying Constant Vertical Surcharge

112

A series of tests in accordance with the "Method of Equilibrium" have been made within this study and the results of these tests are given in sub-title 4.5. An evaluation of the results obtained from these tests will be given in the following paragraphs.

5.2.3 Variation of lateral swelling pressure with variation of vertical surcharge

Test results shown on Figure 5.9, point out a certain increase in lateral swelling pressure with increasing vertical surcharge. Simply, two straight lines drawn on Figure 5.9 show that there is a well defined increase in lateral swelling pressure, as the vertical stress increases.

Hence, Joshi and Katti (1984) and Windal and Shahrour (2002) have conducted lateral swelling pressure tests under varying vertical surcharge pressures. So, the test results given on Figure 5.9 have been compared with the test results of these researchers in Figure 5.10. Similar to the test results obtained within this study, the results of Joshi and Katti (1984) and Windal and Shahrour (2002) also reflect a significant increase in lateral swelling pressure with increasing vertical surcharge. The lateral swelling pressure has an asymptotic behavior with increasing vertical surcharge and reaches an ultimate value as an upper limit in the tests.

The ratio of Lateral swelling pressure to the vertical surcharge is shown on Figure 5.11. Again, as in the results of the previous, gradually loaded swelling pressure tests in vertical direction, pressure ratios within a range in between 0.60 and 1.30 have been obtained in most of the tests. Figure 5.11 clearly reveals that the average ratio σ_{sl}/σ_v ratio is 1.00. The average value of the σ_{sl}/σ_v ratio points ones more out that the lateral and vertical swelling pressures are almost equal.

As in the results the tests under constant surcharge within this study, the tests of Joshi and Katti (1984) and Windal and Shahrour (2001) have resulted with mobilization of increasing lateral swelling pressures under increasing vertical surcharge. Considering the vertical surcharge as the overburden pressure, the lateral swelling pressure increases to a certain depth. From this point on the increase in depth, i.e., the overburden pressure has no effect on lateral swelling pressure. Of course, this conclusion is valid only for a specific type of clay in the soil profile having the same natural (initial) water content. Higher plasticity indices and

decreasing water contents of the swelling clay certainly lead to higher swelling pressures.

Figure 5.10 gives also an impression that the depth, which happens to be a major factor for the variation of lateral swelling pressure, may increase with the increased swelling potential of the clay layer. To be certain at this point it is necessary to conduct a certain number of tests with clay samples having different swelling potential.

On the contrary to the test results obtained within this study, the results of the aforementioned researchers have revealed that the lateral swelling pressure/vertical surcharge ratio (σ_{sl}/σ_v) is much greater (up to 6) for tests conducted under lower vertical surcharge pressures. Based on the fact that Joshi and Katti (1984) have realized their tests on a large scale model, their test results may be evaluated as to be more accurate. The test results depicted on Figure 5.11 do also reflect a slight decrease in the lateral swelling pressure/vertical surcharge ratio with increasing vertical surcharge, i.e. increasing overburden. Swelling pressure/vertical surcharge ratios (σ_{sl}/σ_v) obtained by Joshi and Katti (1984), Windal and Shahrour (2002) and the in this study are depicted together on Figure 5.11.
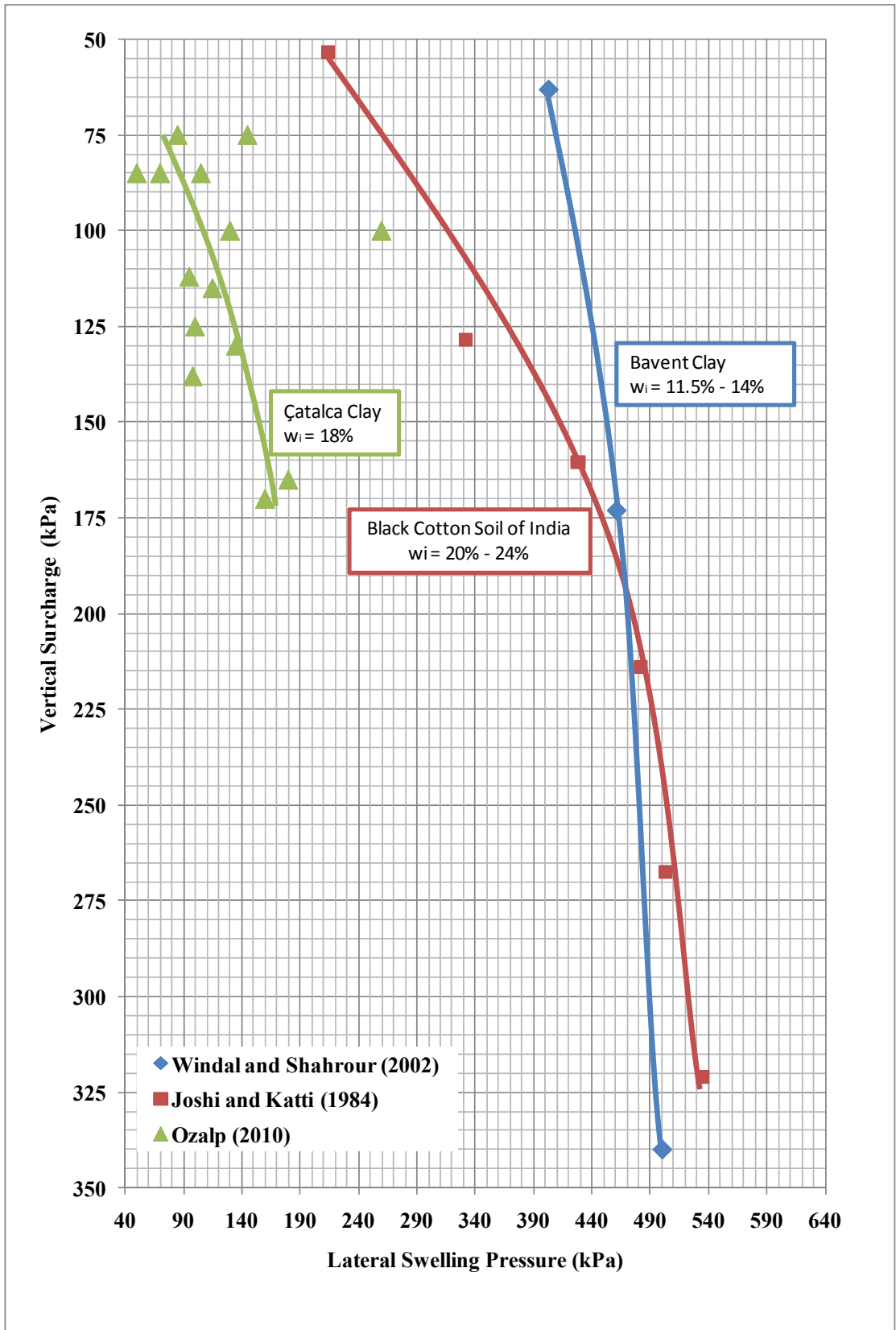
Figure 5.10: Lateral Swelling Pressure under Varying Constant Vertical Surcharge
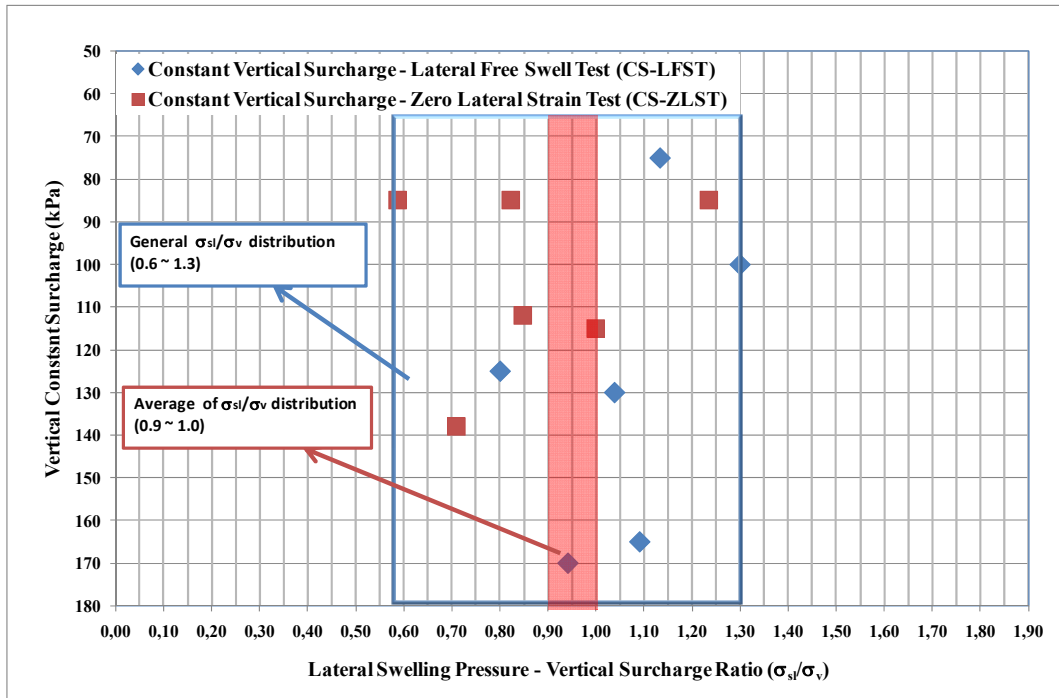
Figure 5.11: Vertical Surcharge vs. Lateral Swelling Pressure
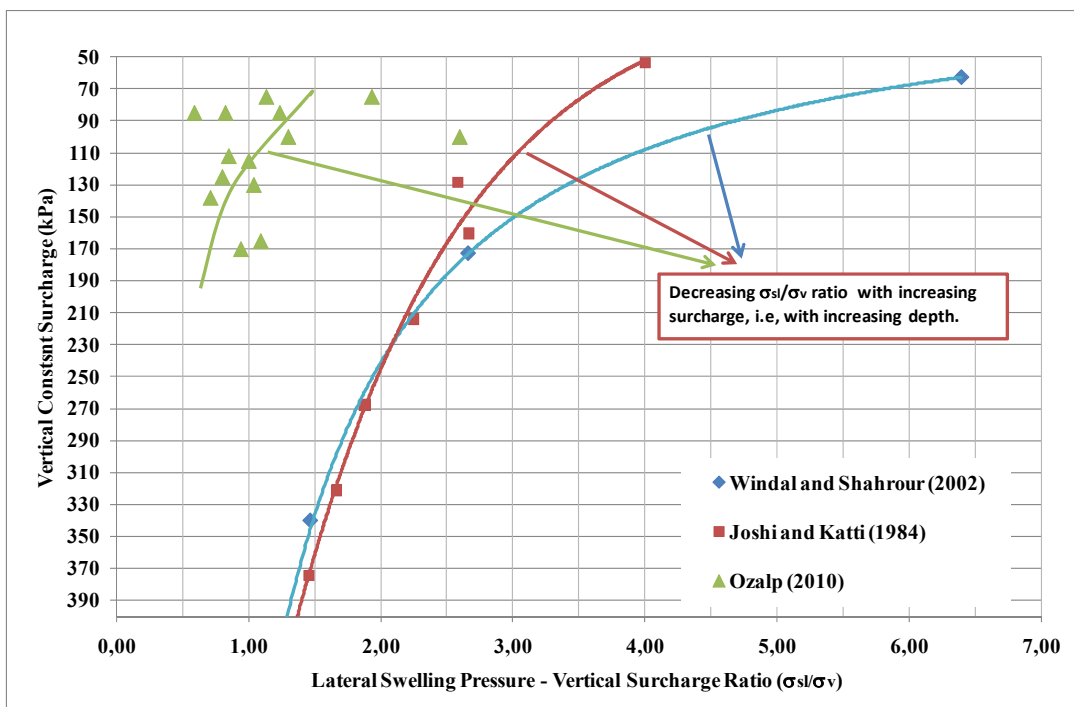
Figure 5.12: Comparison of Vertical Surcharge vs. Lateral Swelling Pressure Distributions

Again, the tests under varying vertical surcharges have resulted with almost similar lateral swelling pressures as the constant vertical strain tests evaluated in the first part of this paragraph.. Based on the test results of Ofer (1981) and Windal and Shahrour (2002), the expectations were to obtain greater lateral swelling pressures in cell

116

pressure applied tests. The increase in the lateral swelling pressures with increasing ring rigidity can be seen in Windal and Shahrour's (2002) test results (Figure 5.10). The cell pressure applied to keep the lateral strain in its initial state increases the rigidity of the thin walled ring in a way. So, the reason for not obtaining a similar increase in lateral swelling pressure must be questioned.

Several factors have been considered so far affecting the results of swelling pressure tests under zero lateral strain conditions. The affect of manual cell pressure application was already mentioned in the paragraphs above. The lateral cell pressure has always been applied following the development of some lateral strain. Since the lateral pressure increase was not automatic triggered by the lateral strain occurrence there was no way to prevent the occurrence of these small lateral strains.

In addition, the lower swelling potential of the clay used in this thesis against the much higher swelling potential of the expansive clay samples in the compatible studies, may also lead to similar results on tests performed under zero and free lateral strain conditions.

As a final reason, the specimens employed in the tests of this study were prepared by compaction in the laboratory. So, the specimens employed in the tests are not alike each other as the undisturbed samples of other researchers.
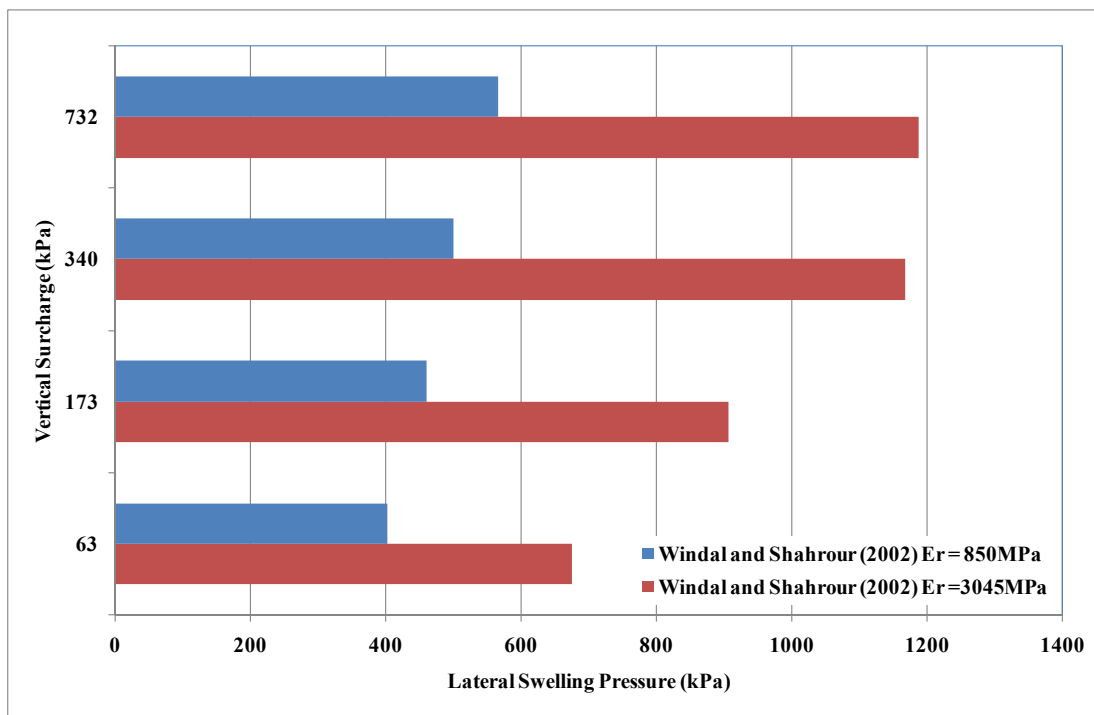
Figure 5.13: Lateral Swelling Pressure Test Results of Windal and Shahrour (2002)

5.3 The Effect of Stratification on Swelling Pressure

To determine the effect of lamination to swelling pressure, some of the samples have been encapsulated laterally, after the compacted sample has been removed from the compaction mold, while the rest of the samples have been encapsulated directly by penetrating the encapsulation mold into the compaction mold. Hence, the stratification in the laterally recovered specimens were in vertical direction. The vertical and lateral swelling pressures observed in swelling tests that have been conducted on the horizontal and vertically laminated samples are illustrated on Figure 5.11.
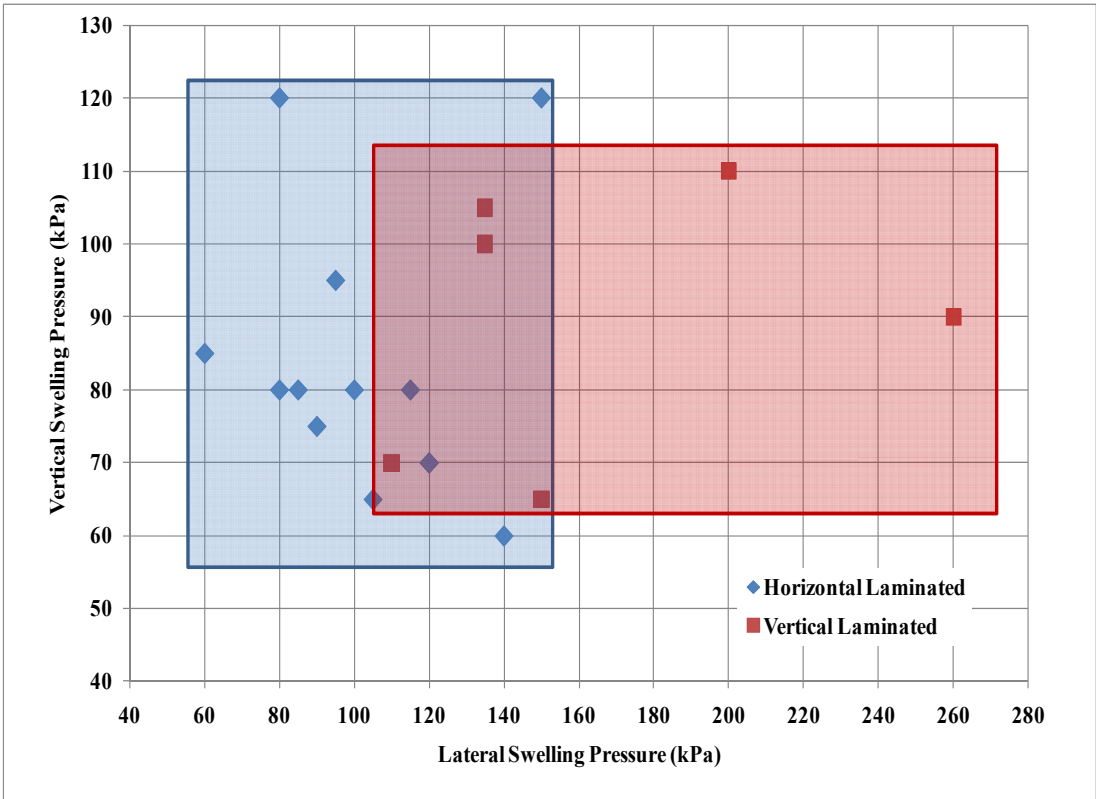
Figure 5.14: Effect of Sample Lamination on Swelling Pressure

Vertically laminated specimens having vertical water flow paths have resulted with higher lateral swelling pressures. Furthermore, considering that a horizontally encapsulated specimen consists of multiple vertical plates, which tend to bend, enables to understand the increase in the lateral swelling even better.

5.4 Recommended Test Method for Lateral Swelling Pressure Prediction: "The Method of Equilibrium"

To equip a thin walled lateral pressure ring with a surrounding cell and to maintain tests in which the volume of the specimen is kept in its initial state has been a major objective in this study. However, different than anticipated, the presence of a surrounding ring alone was not enough to reflect the effect of strain occurrence on swelling pressure development. As pointed out in the evaluations above, the cell pressures was applied manually. In other words, the cell pressure increase was after observing a lateral strain increase in the specimen, i.e, thin ring around the specimen. The recorded magnitudes of lateral strain were always very small in these tests, and the volume of the specimen reduced to its initial state with cell pressure increase. Even this very small magnitude of strain may have resulted with a remarkable decrease in swelling pressure.

In order to find out the most reliable testing technique to be employed for tests made with the lateral pressure testing equipment that has been used in this study, the technique followed by Windal and Shahrour (2002) with rings of varying stiffness has been considered. The major difference was that the stiffness of the rings on Windal and Shahrour (2002)'s tests were present from the beginning of the test. In other words, the expansion ability of the specimen inside the stiffer ring was limited from the beginning of the test.

So, based on the reality that to limit the expansion causes mobilization of an increased lateral swelling pressure, the "Method of Equilibrium" testing technique has also been adopted in this research program. Fourie (1989), has conducted several triaxial swelling pressure tests according to "Method of Equilibrium" with a modified triaxial testing device. The test methodology described by Fourie (1989) has the similar rigidity effect as depicted in the test of Windal and Shahrour (2002).

The "Method of Equilibrium" is a method to obtain the lateral swell pressure from a group of test without manually intervening to the device following the start of the test. From another point of view, to follow the "Method of Equilibrium" testing method has also avoided the possible accuracy problems that may occur due to the absence of integrated strain based automatic cell pressure triggering system.

In all of the tests conducted to obtain the lateral swelling pressure by following the method of equilibrium, the lateral strain of the specimen under constant cell pressures has been recorded. Then, the lateral swelling pressure has been determined by a graphical method that is based on lateral strains and corresponding cell pressures (Figure 5.12).
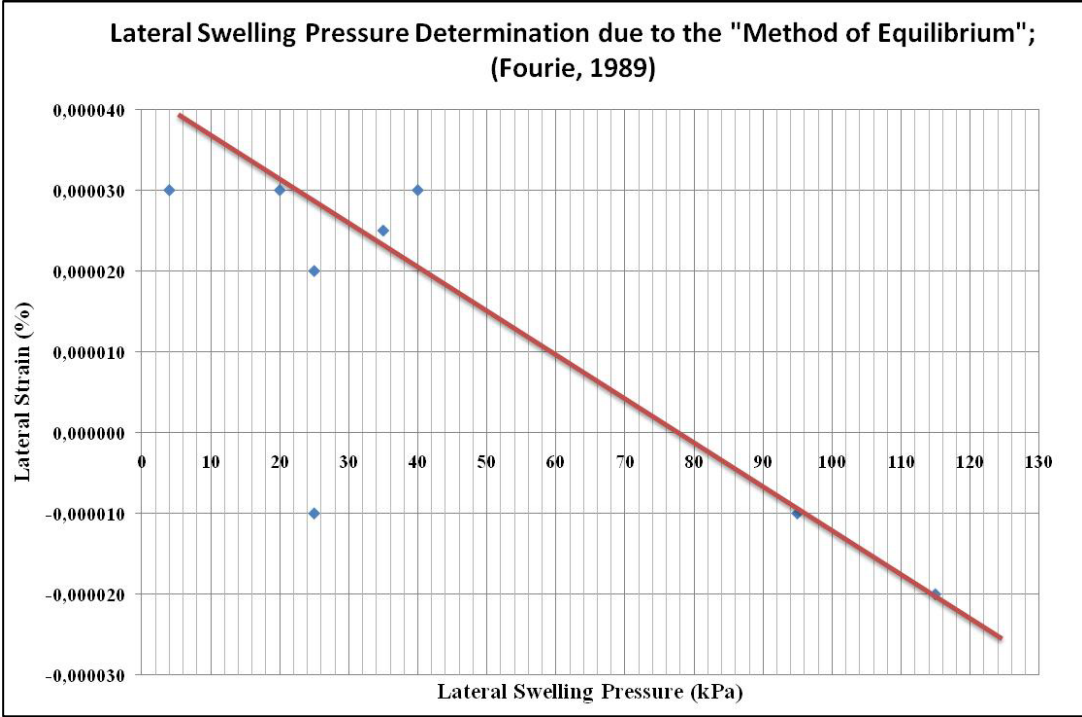
Figure 5.15: Lateral Swelling Pressure Determination according to "Method of Equilibrium

The intersecting point at zero lateral strain of the straight line drawn through the points on the graphic on Figure 5.12 has been accepted as the lateral swelling pressure. One group of tests has been made under a vertical surcharge of 112kPa to obtain the lateral swelling pressure by the method of equilibrium. The test results reveal that the lateral swelling pressure at zero strain is 80kPa (Figure 5.12).

It is concluded that the most reliable method for predicting the lateral swelling pressure for a clay sample with a specified initial water content would be to conduct swelling tests by the "Method of Equilibrium" technique in the testing apparatus designed and used in this research program.

6. CONCLUSION

This study is on the determination of the triaxial swelling behavior of soils. A testing equipment that can measure lateral swelling pressures on real time basis has been designed and manufactured for this study. The test equipment is based on the thin walled oedemoter rings designed and used by Komornick and Zeitlin (1965), Ofer (1981) and Ertekin (1991).

The testing apparatus has been equipped with a confining back pressure cell. The height of the ring is designed as 70mm whereby the flexibility of the ring has been increased. The thickness of the ring is kept as 0.35mm, like the one of Ertekin (1991). The back pressure cell is a cylinder with a diameter of 130mm, surrounding the thin walled lateral swelling pressure (oedometer) ring. Strains and pressures on the thin walled ring are measured via three waterproof strain gauges, mounted on the ring. With quarter bridge connection, each strain gauge on the ring is a separate indicator. One pressure transducer is present at the outer surface of the pressure cell.

All swelling pressure tests have been performed on compacted clay samples. The clay has been taken in a disturbed condition from ISBAS (Istanbul Thrace Free Zone) in the Çatalca Region of Istanbul City. The initial water content of the samples have been kept constant in the tests. Generally, the initial water content values of the specimens vary between 17% and 19%.

The tests performed within the scope of this research are assembled in five groups according to their stress-strain conditions (see Figure 5.1).

Two types of lateral swelling tests have been made, based on the Method C in ASTM 4536-03. In the first group of tests, swelling of the specimen in vertical direction has been prevented by load adjustment in vertical direction, while laterally the specimen has been let to swell (VR-LFST). In the second group of tests both the vertical strain and the lateral strain have been kept as zero ($\varepsilon_h=\varepsilon_v=0$) (CVS). The lateral strain has been restrained by applying hydraulic cell pressure.

Three group of tests have been made under constant vertical surcharge pressure. One group of the tests have been made by employing cell pressure increase during the test, while the other group have been made as lateral free swell tests, i.e., not applying any cell pressure. Finally, to see the real effect of the limitation of lateral expansion, " the Method of Equilibrium" (Fourie, 1989) testing technique has been adopted into the research program.

The conclusions of this study are summarized below:

- Test results obtained from this study utilizing the specially designed and manufactured apparatus agree with the results of previous studies, in general. This comparison has validated the reliability of the test set up.

- A comparison of the results of the present study with previous studies has shown that to increase the height of the thin walled ring has minimized the restrainment effect of the rigid top and bottom plates of the ring on the lateral deformation ability of the ring. So, lateral strains caused by the swelling of the specimen could be recorded with a greater accuracy due to the increased flexibility of the ring.

- The range of vertical and lateral swelling pressures obtained from all of the tests vary within a range of 80kPa to 150kPa. As well as the tests under zero vertical strain ($\varepsilon_v = 0$), the tests under constant vertical surcharge pressure have resulted with lateral swelling pressures fitting into the same range.

- Full mobilization of vertical swelling pressures took 5 to 8 hours during the tests. On the contrary, the mobilization of lateral swelling pressure has continued up to 72 hours.

- Swell pressures obtained from triaxial tests against the swell pressures recorded on uniaxial tests performed on likewise prepared samples of the ISBAS clay has shown that uniaxial swell tests (conventional swell tests) may result with overestimated swelling pressures. The outcomes of the uniaxial swelling pressure tests were σ_{sv}=150kPa–200kPa.

- Average range of the swelling pressure ratios (σ_{sL}/σ_{sV}) obtained from vertically restained (VR) tests are in the range of 1.0 – 2.0. CVS tests, which were preformed by applying hydraulic cell pressure restraining the lateral strain of the

specimen have resulted with slight higher swelling pressure ratios than the lateral free swell tests (VR-LFST). Nevertheless, the difference between the two test methods was less significant than expected.

- The average range of the lateral swelling pressure to surcharge ratio (σ_{sL}/σ_{ss}) observed from the swelling pressure tests under constant surcharge was equal to 0.9 to 1.0. No great difference was recorded between CS – ZLS and CS LFST tests.

- Based on the test results of Ofer (1981) and Windal and Shahrour (2002), the expectations were to obtain greater lateral swelling pressures in cell pressure applied tests. The cell pressure keeps the lateral strain in its initial state and increases the rigidity of the thin walled ring.

- Similar test results on LFST and ZLST and CVS tests are consequences of manual cell pressure application. During the tests, a small amount of strain has occurred first, than the occurred strain has returned to its initial state after increasing the cell pressure. On the contrary, even a small amount of deformation highly decreases the lateral swelling pressures. Therefore, to obtain satisfactory test results, automatic cell pressure triggering is necessary.

- Similar to the test results of Windal and Shahrour (2002) on Bavent Clay and Joshi and Katti (1984), the results of the tests under constant surcharge within this study, have resulted with mobilization of increasing lateral swelling pressure under increasing vertical surcharge. Considering the vertical surcharge as the overburden pressure, the lateral swelling pressure increases to a certain depth. From this point on the increase in depth, i.e., the overburden pressure has no effect on lateral swelling pressure.

- The lateral swelling pressure is also determined by a group of tests by employing the "Method of Equilibrium". One group of tests has been made in accordance with the "Method of Equilibrium". The constant vertical surcharge was kept 112kPa in those tests and the lateral swelling pressure at zero strain has been determined as 80kPa from the diagram shown in Fig. 6.1. The swelling pressure ratio is 80kPa/112kPa = 0,71.

- The "Method of Equilibrium" testing method avoids the possible accuracy problems that may occur due to the absence of strain based automatic cell pressure triggering system.

- No manual intervention to the cell pressure is necessary for the swelling pressure tests according to "Method of Equilibrium". Therefore, tests to be made with the testing apparatus designed and used in this research program is readily capable of performing reliable swelling tests in accordance with the "Method of Equilibrium" technique.

REFERENCES

Al - Shamrani, M. A., and Dhowian, A. W., 2003. "Experimental Study of Lateral Restraint Effects on the Potential Heave of Expansive Soils" *Engineering Geology*, Volume **69**, Issues 1-2, April, p. 63 – 81.

ASTM D 4546 – 03, 2003. "Standard Test Method for One Dimensional Swell or Settlement Potential of Cohesive Soils", USA.

ASTM D 698 – 07; 2007. "Standard Test Methods for Laboratory Compaction Characteristics of Soil Using Standard Effort (12 400 ft-lbf/ft3 (600 kN-m/m3))", USA.

ASTM D2435 – 04, 2004. "Standard Test Methods for One-Dimensional Consolidation Properties of Soils Using Incremental Loading", USA.

Avşar, E. Ulusay, R., Sönmez, H., 2009. "Assessments of swelling anisotropy of Ankara Clay" *Engineering Geology*, Vol.**105**, pp. 24 – 31.

Aytekin, M., 1992. "Finite Element Modeling of Lateral Swelling Pressure Distribution Behind Earth Retaining Structures" *Ph. D. Thesis*, Texas Tech University, Texas, USA.

Azam, S., 2009. "Discussion on: Assessments of swelling anisotropy of Ankara Clay" *Engineering Geology*, Vol.**108**, pp. 304-305.

Barla, M., 2007. "Numerical simulation of the swelling behavior around tunnels based on special triaxial tests" *Tunneling and Underground Technology*, Vol. **23**, pp. 508–521.

Ben-Dor E. et. al., 2009. "Using Imaging Spectroscopy to study soil properties" *Remote Sensing of Environment* **113**, pp. S38–S55.

Bishop, A.W., Wesley, L.D.; 1975. "A Hydraulic Triaxial Apparatus for Controlled Stress Path Testing", *Geotechnique*, **25**(4), 657 – 670.

Borden, D., and Giese, R. F., 2001. "Baseline Studies of the Clay Minerals Society Source Clays: Cation Exchange Capacity Measurements by the Ammonia – Electrode Method" *Clays and Clay Minerals*, Vol. **49**, Nol. 5, p. 444 – 445.

Bowles, J. E., 1996. "*Foundation Analysis and Design*", McGraw Hill, New York, USA.

Chabrillat, S. et. al., 2002. "Use of hyperspectral images in the identification and mapping of expansive clay soils and the role of spatial resulotion" *Remote Sensing of Environment* **82**, pp. 431 – 445.

Chen, F. H., 1988. "*Foundations on Expansive Soils*", Elsevier Scientific Publishing Company, Amsterdam, The Netherlands.

Chen, F. H., Huang, D., 1987. "Lateral Expansion Pressure on Basement Walls", *Proceedings of the 6th International Conference on Expansive Soils*, New Delhi, India, Vol. **I**, pp. 55-59.

Crilly, M. S., Driscoll, R. M., and Chandler, R., J., 1992. "Seasonal ground and water movement observations from an expansive clay site in the UK" *Proceedings, 7th International Conference on Expansive Soils*, Dallas, Texas, USA, pp. 313-318.

Day, R.W., 1998. "Swelling Behavior of Dessicated Clay" *Environmental and Engineering Geoscience* **IV**, pp.124-129.

Delage, P., Howat, M. D., Cui, Y. J., 1998. "The relationship between suction and swelling properties in a heavily compacted unsaturated clay", *Engineering Geology*, Vol. **50**, pp.31-48.

Dhowian, A. D, Erol, O. and Youssef, A., 1990. "Evaluation of Expansive Soils and Foundation Methodology in The Kingdom of Saudi Arabia", *General Directorate of Research Grants Programs – King Abdul Aziz City for Science & Technology*, Riyadh, Saudi Arabia.

Dohrmann, R., 2006. "Cation Exchange Capacity Methodology I: An Efficient Model for the Detection of Incorrect Cation Exchange Capacity and Exchangeable Cation Results" *Applied Clay Science*, Volume **34**, Issues 1-4, October, p. 105-124.

Edil, T.B. and Alanzy, A.S., 1992. "Lateral Swelling Pressures" *Proceedings 7th International Conference on Expansive Soils*, Dallas, pp.227-232.

Ergüler. Z. A. Ulusay R., 2003. "A simple test and predictive models for assessing swelling potential of Ankara Clay", *Engineering Geology*, Vol. **67**, pp. 331-352.

Ergüler. Z. A., 2001. "Ankara Kilinin Şişme Davranışının ve Örselenmenin Şişmeye Etkisinin İncelenmesi, Şişme Potansiyelinin Görgül Yaklaşımlarla Belirlenmesi (Turkish)", *M. Sc. Thesis*, Department of Geology, Hacettepe Universitesi, Ankara, Turkey.

Erol, A., O., Dhowian A., and Youssef, A., 1987. "Assessment of Oedometer Methods for Heave Prediction", *Proceedings 6th International Conference on Expansive Soils*, New Delhi, India, pp. 99-103.

Erol, O., Ergun, U; 1994. "Lateral Swell Pressures in Expansive Soils", *XIII ICSMFE*, New Delhi, INDIA.

Ertekin, Y., 1991. "Measurement of Lateral Swell Pressure with Thin Wall Oedometer Technique" *M. S. Thesis*, The Graduate School of Natural and Applied Sciences, Middle East Technical University (METU), Ankara, Turkey.

Erzin, Y., Erol, O., 2007. "Swell pressure prediction by section methods", *Engineering Geology*, **92**(2007) 133 – 145.

Fourie, A. B., 1989. "Laboratory Evaluation of Lateral Swelling Pressure" *Journal of Geotechnical Engineering*, Vol. **115**, No. 10, October 1989, pp. 1481-1486.

Gill, W. R., and Reaves, C. A., 1957. "Relationship of Atterberg limits and cation exchange capacity to some physical properties of soil" *Mechanics Research Communications*, Volume **29**, Issue 5, September-October, pp. 375-382.

Gourley, C. S, Newill, D. and Schneider, H. D., 1993. "Expansive soils: TRL's research strategy. *Proceedings of First International Symposium on Engineering Characteristics of Arid Soils*, City University, London, UK.

Gürtuğ, Y., 2004. "Effect of Compaction Energy on the Behavior of Fine Grained Soils" *Ph. D. Thesis*, Eastern Mediterranean University, Gazimağusa Northern Cyprus.

Hardy , R.M., 1965. "Identification and Performance of Swelling Soil Types" *Canadian Geotechnical Journal*, **2**, pp. 141-153.

Hawlader, B. C., Lee, Y. N., and Lo, K.Y.., 2003. "Three Dimensionla Stress Effects on Time – Dependent Swelling Behaviour of Shaly Rocks" *Canadian Geotechnical Journal*, Vol: **40**, pp. 501-511.

2003. "Three – dimensional stress effects on time – dependent swelling behavior of shaly rocks" Canadian Geotechnical Journal, Vol. 40, pp. 501-511.

Holtz W., Gibbs H., 1956. "Engineering properties of expansive clays", *Transactions*, *ASCE*. **121**(1). page 641-663.

Holtz. R. D., and Kovacs, W. D., 1981. *"An Introduction to Geotechnical Engineering"* Prentice – Hall Inc., New Jersey, USA.

İkizler, S.B., Aytekin, M., Nas, E., 2008, "Laboratory Study of Expanded Polystrene (EPS) Geofoam Used with Expansive Soils", *Geotextiles and Geomembranes,* Vol. **20**, pp. 189 - 195.

Johnson, L.D., Snethen, D.R., 1978. Prediction of potential heave of swelling soils. *Geotechnical Testing Journal* **1**, 117–124.

Joshi, R. P., and Katti, R. K., 1984. "Lateral Pressure Development Under Surcharges" *Proceedings of the Fifth International Conference on Expansive Soils*, Adelaide, SOUTH AFRICA, p. 227-241.

Kariuki, P. C., Van der Meer, F., 2004. "A Unified Swelling Index for Expansive Soils" *Engineering Geology*, Volume **72**, Issues 1-2, March, p.1-8.

Kassif, G. Ben Shalom, A., 1971. "Experimental relationship between swell pressure and soil suction" *Geotechnique*, Vol. **21**, pp. 245-255.

Kate, D.R., Katti, R.K.; 1987. "Studies on Passive Resistance Development in Saturated Expansive Soils", *Proc. of 6th International Conference on Expansive Soils*, New Delhi, pp:61-66.

Komormik, A., & Zeitlen, J. G., 1965. "An Apparatus for Measuring the Lateral Soil Pressure in the Laboratory", *Proceedings of the Sixth International Conference on Soil Mechanics and Foundation Engineering,* Montreal, Canada, p.107-114.

Lambe, T., 1951. *"Soil Testing for Engineers"*, New York, Wiley, 165 pp.

Lambe, T., 1953. "The Structure of Inorganic Soil." *Proc. ASCE 79*, Separate No. 3316.

Lambe, T., 1958. "The Structure of Compacted Clay" Proc. *ASCE* **84**, SM2.

Lambe, T., 1966. "A Mechanistic Picture of Shear Strength in Clay" *ASCE Proc. Res. Conf. on Shear Strength of Cohesive Soils*.

Mc Dowell, 1956. "Interrelationship of load, Volume Change and Layer Thickness of Soils to the Behavior of Engineering Structures", Highway Research Board, *Proceeding of the Thirty Fifth Annual Meetings*, Publication No. 426, Transportation Research Board Washington D.C., pp. 754 - 772.

Mitchell, J. K.; 1992. *"Fundamentals of Soil Behavior - 2ⁿᵈ Edition"*, John Wiley&Sons Inc., USA.

Muntohar, S., A., 2006. "Prediction and classification of expansive clay", *Expansive Soils; Recent advances in characterization and treatment*, Taylor & Francis, London, Chapter 3, pp.25.

Noble, C. A., 1965. "Discussion: Identification and Performance of Swelling Soil Types" *Canadian Geotechnical Journal*, **2**, pp. 161 – 162.

Ofer, Z., 1981. "Instruments for Laboratory and In Situ Measurement of the Lateral Swelling Pressure of Expansive Clays" *Proceedings of the Fourth International Conference on Expansive Soils*, Volume **I**, Denver Colorado, USA, pp. 45-53.

Ofer, Z., Blight, G. E., and Komornik, A. 1984. "Simultanous Determination of IN Situ Swelling Pressure and Shear Strength" *Proceedings of the Fifth International Conference on Expansive Soils*, Adelaide, AUSTRALIA, pp. 80-84.

O'Neil, M.W., Ghazzally, O.I., 1977. Swell potential related to building performance. Journal of the Geotechnical Engineering Division, *ASCE* **103** (GT12), 1363-1379.

Oregon Natural Hazards Group, 2006. "Polk County Natural Hazards Mitigation Plan", Section 12, Mid – Willamette Valley, USA.

RAO, S. M., 2006. *"Identification and classification of expansive soils"*; Expansive Soil – Recent advances in characterization and treatment, Taylor & Francis, UK.

Raymond, G. P., 1997. "Soil Fines – Clay Minerals", *Geotechnical Engineering Course Notes*, Queens University, Kingston, Ontario, Canada.

Richards, B. G. and Kurzeme, M., 1973. "Earth pressure observations on a retaining wall in expansive clay, Gouger Street Mail Exchange, Adelaide", *Australian Geomechanics Journal*, Vol. **G3**, No. 1.

Richards, L.A., 1941. "Apressure membrane extraction apparatus for soil suction" *Soil Science*, Vol. **51**, pp. 377 - 386.

Sadisun, I. A., Shimada, H., Ichinose, M., Matsui, K., 2002. "An experimental study of swelling strain in some argillaceous rocks by means of an improved unconfined swelling test" *Korean Society for Rock Mechanics (KSRM)*, pp. 227-254.

Sağlamer, A., 1991. "İstanbul Trakya Serbest Bölgesi Geoteknik Raporu" (Turkish) Istanbul Technical University, Structure and Earthquake Application Research Center, Istanbul, Turkey.

Sapaz, B., 2004. "Lateral Versus Vertical Swell Pressures in Expansive Soils" *M. Sc. Thesis*, The Graduate School of Natural and Applied Sciences, Middle East Technical University (METU), Ankara, Turkey.

Schwingenschloegl, R., and Lehmann, C., 2008. "Swellig rock behavior in a rock tunnel: NATM – support vs. Q – support – A comparison" *Tunneling and Underground Technology*, Vol. **24**, pp. 356 – 362.

Scott, R., 1963. "Principles of Soil Mechanics" Addison-Wesley, London, UK.

Seed H.B., Woodward R.J., Lundgren R., 1962. "Prediction of swelling potential for compacted clays", *Soil Mechanics and Foundation Division* **88**, pp. 53–87.

Seybold, C. A., Grossman, R. B., and Reinsch, T. G., 2005. "Predicting Cation Exchange Capacity for Soil Survey Using Linear Models", *Soil Science Society American Journal* **69**, pp.856-863.

Snethen, D. R., and Haliburton, T. A., 1973. "Lateral Swelling Pressures in Compacted Oklahoma Cohesive Soils" Highway Research Board Bulletın No. 429, Washington D.C., USA, pp. 26-28.

Snethen, D. R., Johnson L. D., Patrick, D. M., 1977. "An evaluation of expedient methodolgy for identification of potentially expansive soils" Soil and Pavements Laboratory, *U.S. Army Eng. Waterway Exp. Sta.*, Vicksburg

Sposito, G., 2008. "The Chemistry of Soils – Second Edition", Oxford University Press, New York, USA.

Sridharan, A., and Rao, S., M., 1988. "A Scientific Basis for the Use of Index Tests in Identification of Expansive Soils" *Soil Science Soc. Am. Proceedings* **21**, pp 491- 494.

Sridharan, A., Rao, S., and Sivapullaiah, P. V., 1986. "Swelling Pressure of Clays" *Geotechnical Testing Journal*, Vol. **9**, pp.24-33.

Thomas, M. G., 2008. "Impact of Lateral Swelling Pressure on Retaining Structure Design Using Expansive Cohesive Backfill" *M. Sc. Thesis*, The University of Texas in Arlington, USA.

Thomas, P. J., 1998. "Quantifying Properties and Variability of Expansive Soils in Selected Map Units" *Ph. D. Thesis*, Virginia Polytechnic Institute and State University.

Thomas, P. J., Baker, J. C., Zelazny L. W., 2000 "An Expansive Soil Index for Predicting Shrink–Swell Potential", *Soil Sci. Soc. Am. J.*, Vol. **64** pp. 268-274.

2000. "An Expansive Soil Index for Predicting Shrink–Swell Potential" Soil Sci. Soc. Am. J., Vol. **64**, pp. 268- 274.

TM 5 – 818 – 7, 1983. "Foundations in Expansive Soils", *Headquarters Department of the Arrny*, Washington, USA.

Tombacz, E., Szekeres, M., 2006. "Surface Charge Heterogeneity of Kaolinite in Aqueous Suspension in Comparison with Montmorillonite" *Applied Clay Science*, Volume **34**, Issues 1-4, October, pp. 105-124.

Tonoz M.C., Gokceoglu C., Ulusay R.; 2003. "A Laboratory – scale investigation on the performance of lime columns in expansive clays", *Bulletin of Engineering Geology and Environment*, 62, pp.91-106.

URL - 1 < *http://en.wikipedia.org/wiki/X-ray_scattering_techniques*>, 26.10.2009.

URL - 2 < *http://www.gdsinstruments.com/datasheets/GDSTAS_Datasheet.pdf*>, 20.11.2009.

Wattanasanticharoen, E., Puppala, A. J., and Hoyos, L. R., 2007. "Evaluation of Heaving Behavior of Expansive Soils Under Anisotropic Stress State Conditions" *Geotechnical Testing Journal*, Pending Publication.

Windal, T., and Sharour, I., 2002. "Study of the Swelling Behavior of a Compacted Soil Using Flexible Oedometer" *Mechanics Research Communications*, Volume **29**, Issue 5, September-October, pp. 375-382

Woodward, D., Woodside, A., and Jellie, J., 2002. "Clay in Rocks" SCI Lecture Paper Series, Society of Chemical Industry – Highway Engineering Research Group, Newtonabbey, UK

Yılmaz, I., 2006. "Indirect estimation of the swelling percent and a new classification of soils depending on liquid limit and cation exchange capacity" *Engineering Geology*, 85, pp. 295 – 301.

APENDICES

APPENDIX A :   VERTICALLY RESTRAINED LATERAL FREE SWELL TEST RESULTS (VR – LFST)

APPENDIX B: CONSTANT VOLUME TEST RESULTS (CVS)

APPENDIX C: CONSTANT SURCHARGE LATERAL FREE SWELL TESTS (CS – LFST)

APPENDIX D: CONSTANT SURCHARGE ZERO LATERAL STRAIN TESTS (CS-ZLTS)

APPENDIX E: TESTS IN ACCORDANCE WITH METHOD OF EQUILIBRIUM

APPENDIX A

VERTICALLY RESTRAINED; LATERALLY FREE TO SWELL (VR-LFST)

TEST NO: 16	
Test Start:	
Date:	28.08.2009
Time:	10:45
Test Duration:	68 hours
Test End:	
Date:	31.08.2009
Time:	06:45

Final Water Content Distribution (%) of the Specimen

Initial Water Content; ω_i = 19%
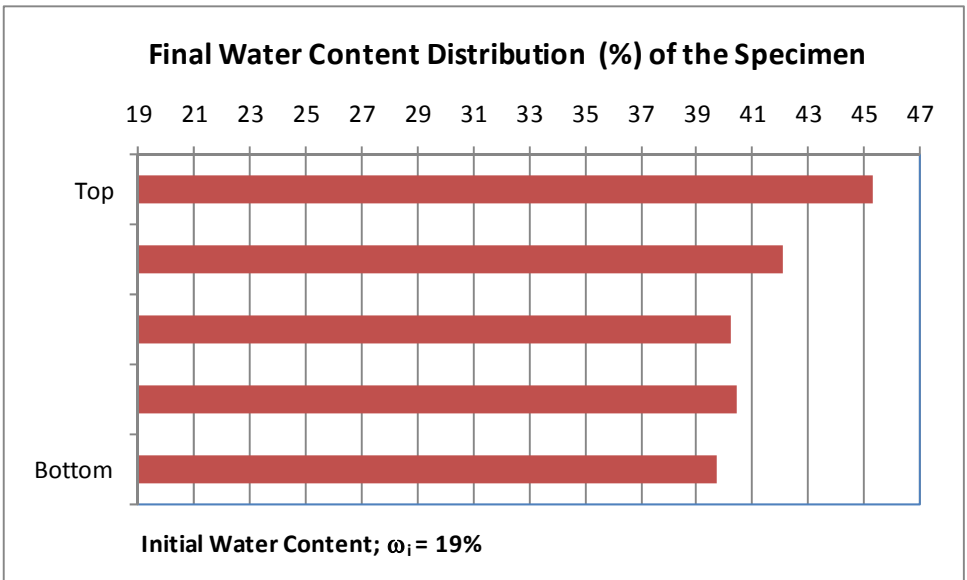
Figure A1.1: Initial and Final Water Contents, Test No: 16; (28.08.2009)
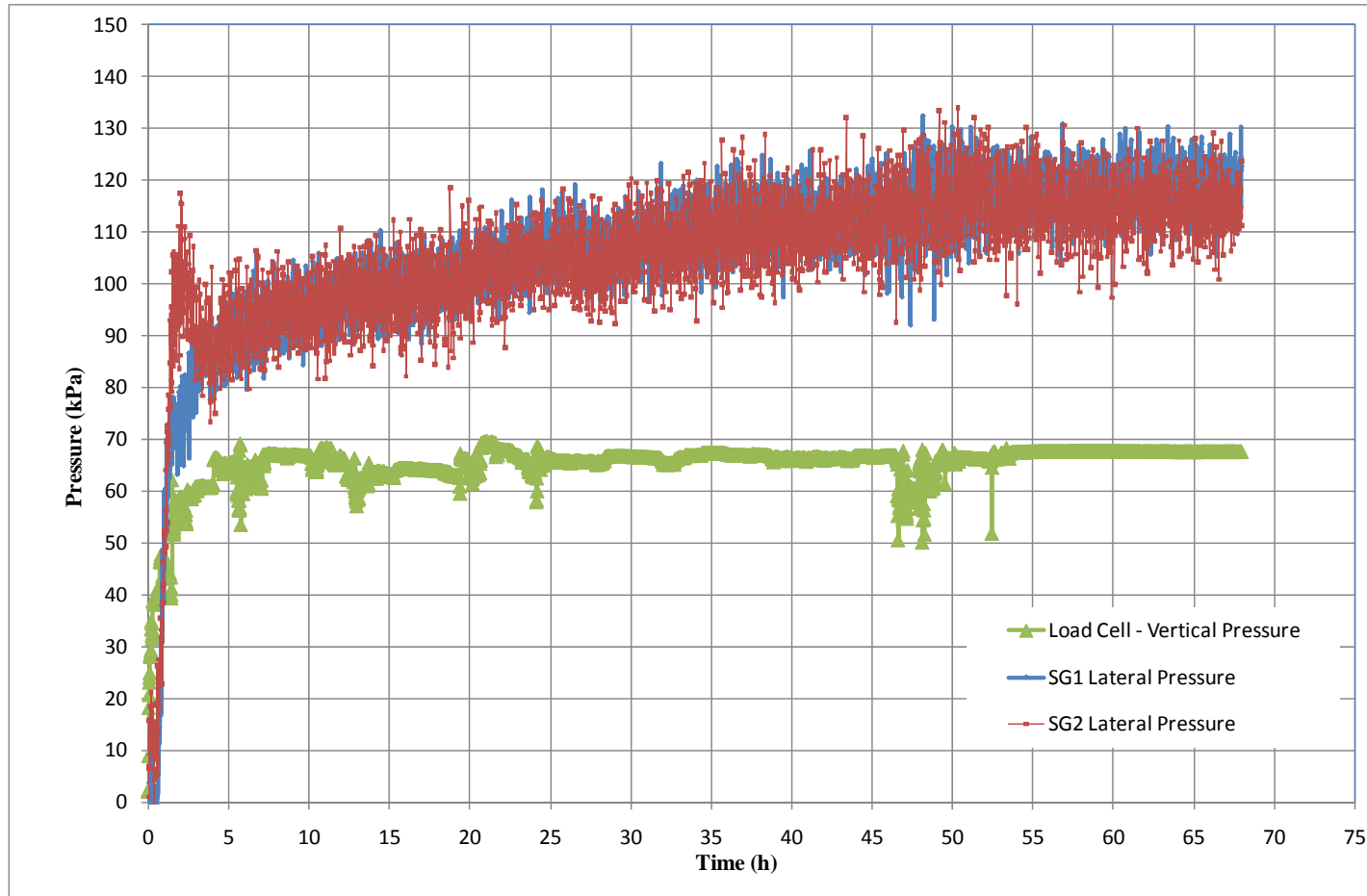
Figure A1.2: Pressure – Time Graph Test No: 16, (28.08.2009)

TEST NO: 17	
Test Start:	
Date:	02.09.2009
Time:	12:00
Test Duration:	29 hours
Test End:	
Date:	03.09.2009
Time:	17:00
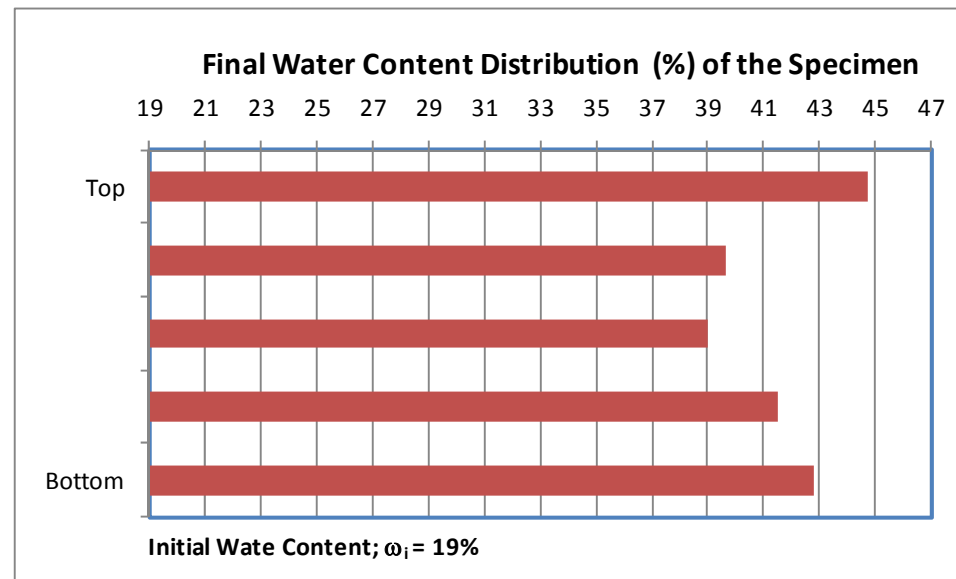
Figure A1.3: Initial and Final Water Contents Test No: 17; (02.09.2009)
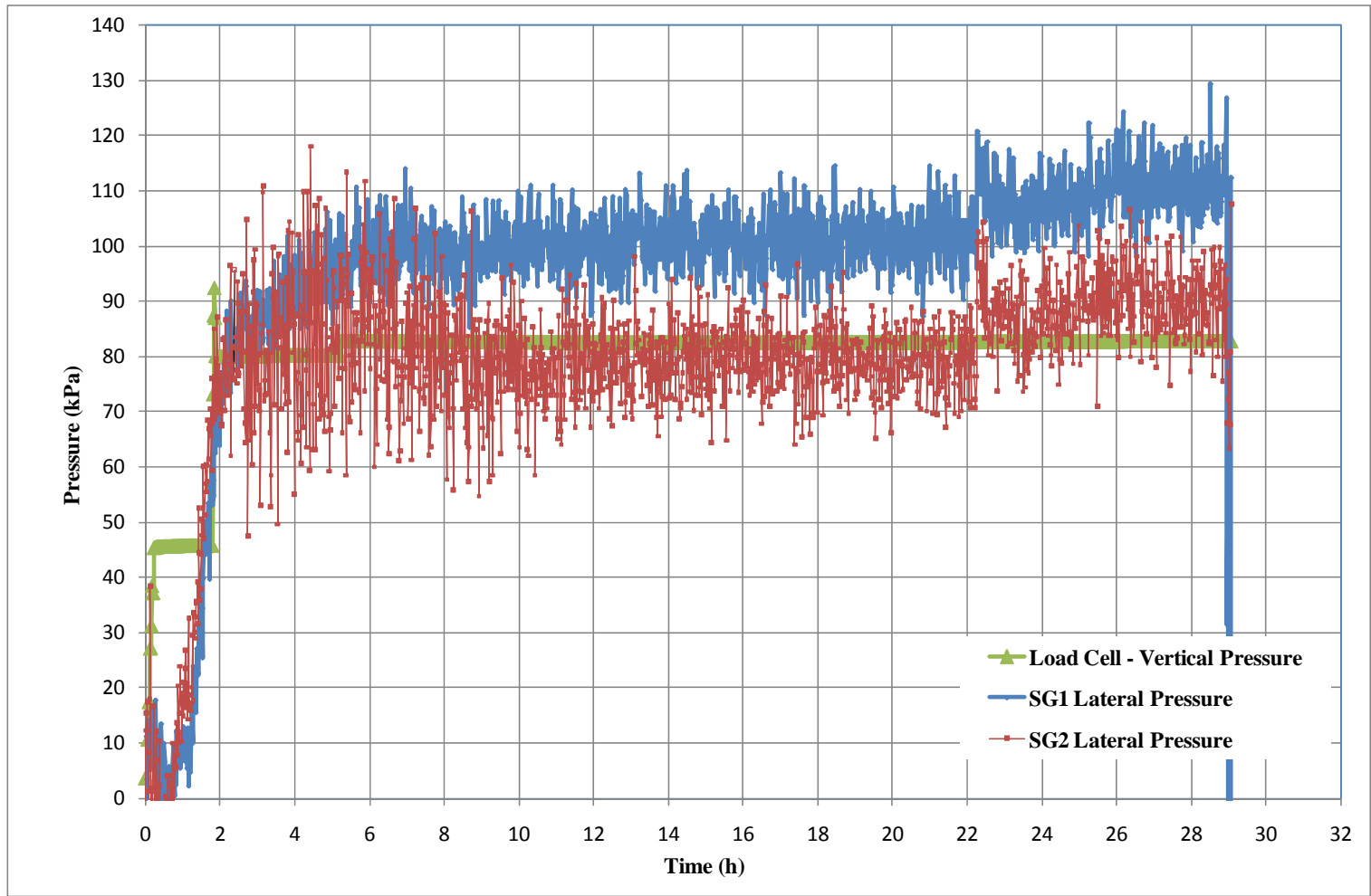
Figure A1.4: Time Graph Test No: 17; (02.09.2009)

TEST NO: 18	
Test Start:	
Date:	05.09.2009
Time:	10:00
Test Duration:	71 hours
Test End:	
Date:	08.09.2009
Time:	09:00
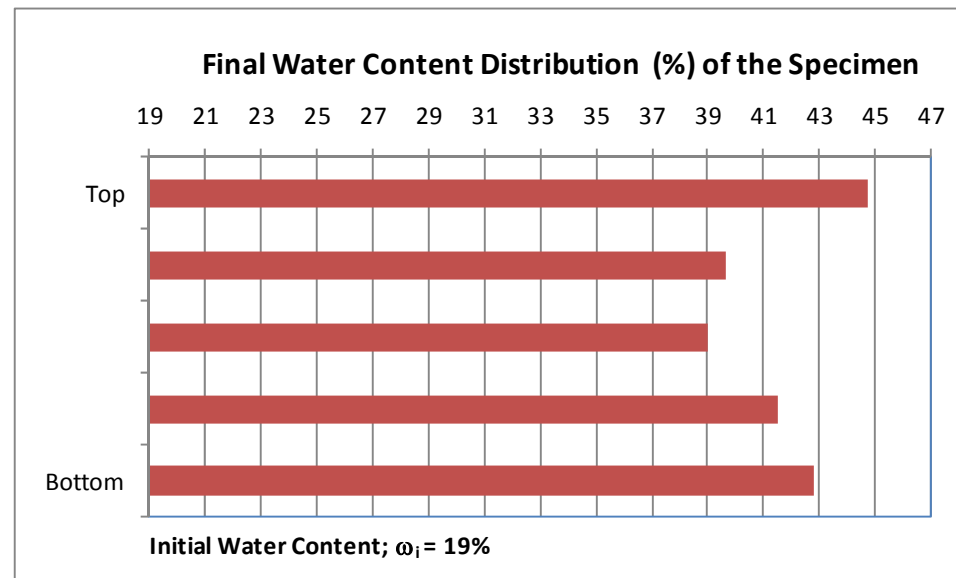
Figure A1.5: Initial and Final Water Contents Test No: 18; (05.09.2009)
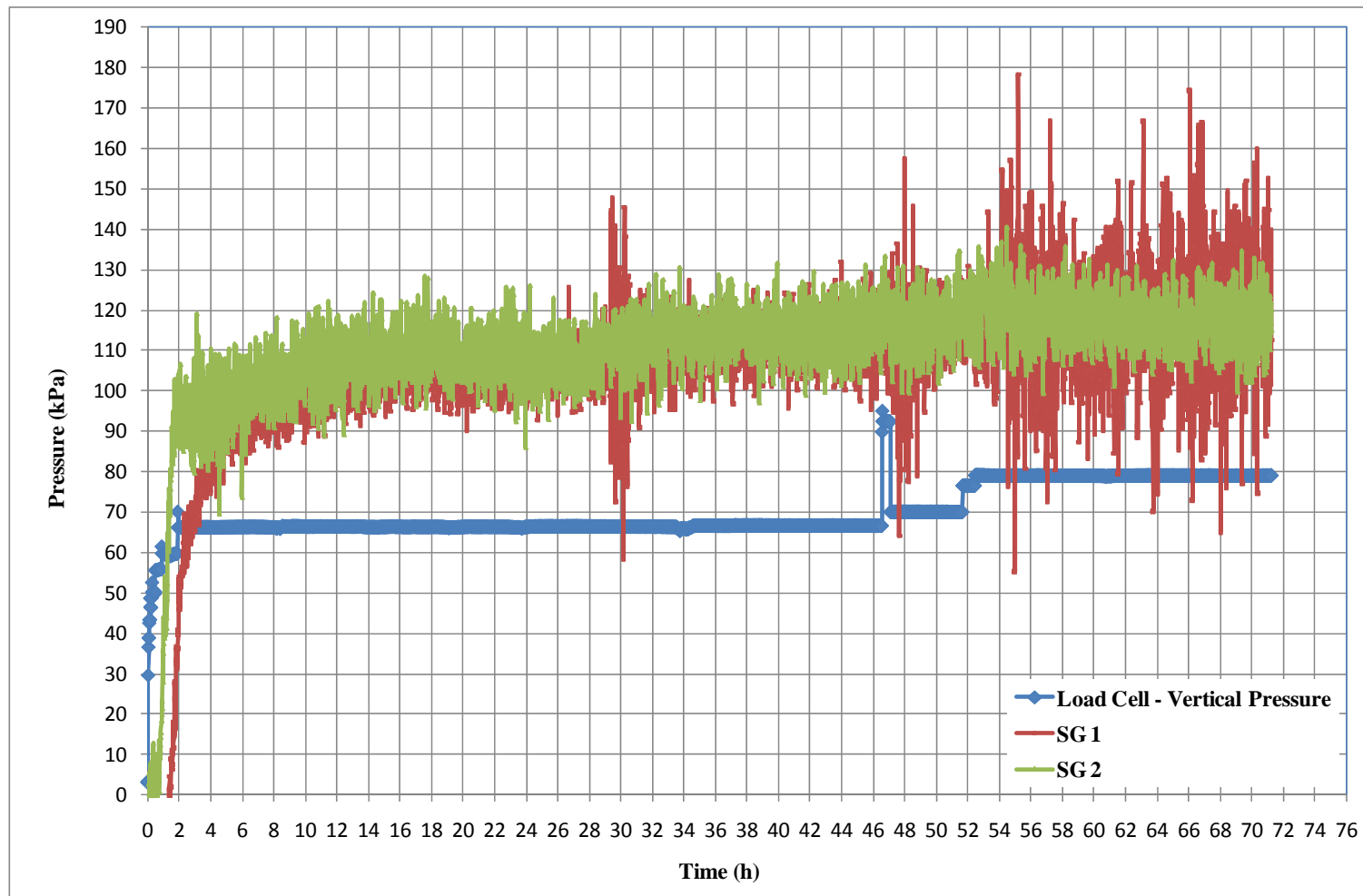
Figure A1.6: Pressure – Time Graph Test No: 18; (05.09.2009)

TEST NO: 25	
Test Start:	
Date:	16.10.2009
Time:	13:30
Test Duration:	49 hours
Test End:	
Date:	18.10.2009
Time:	14:30
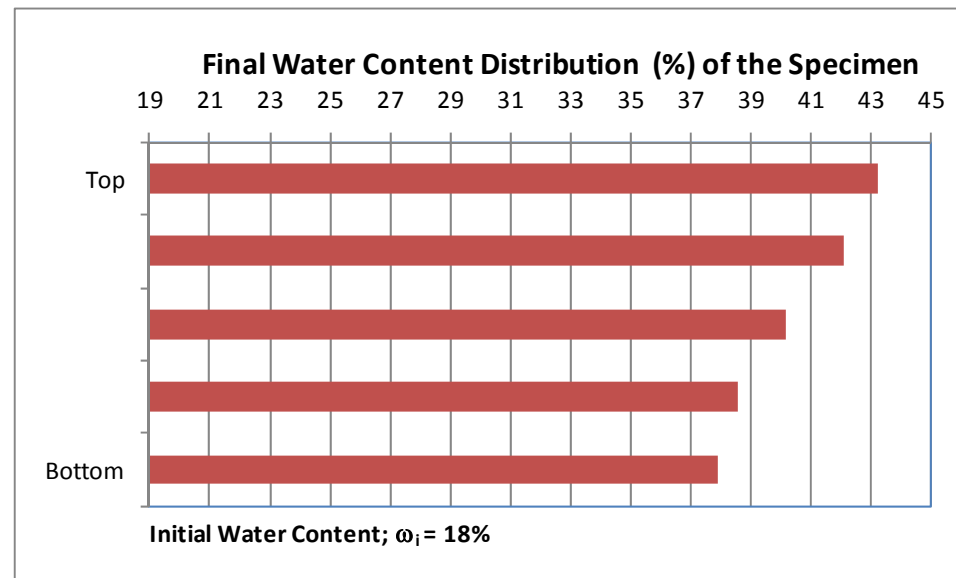
Figure A1.7: Initial and Final Water Contents Test No: 25; (16.10.2009)
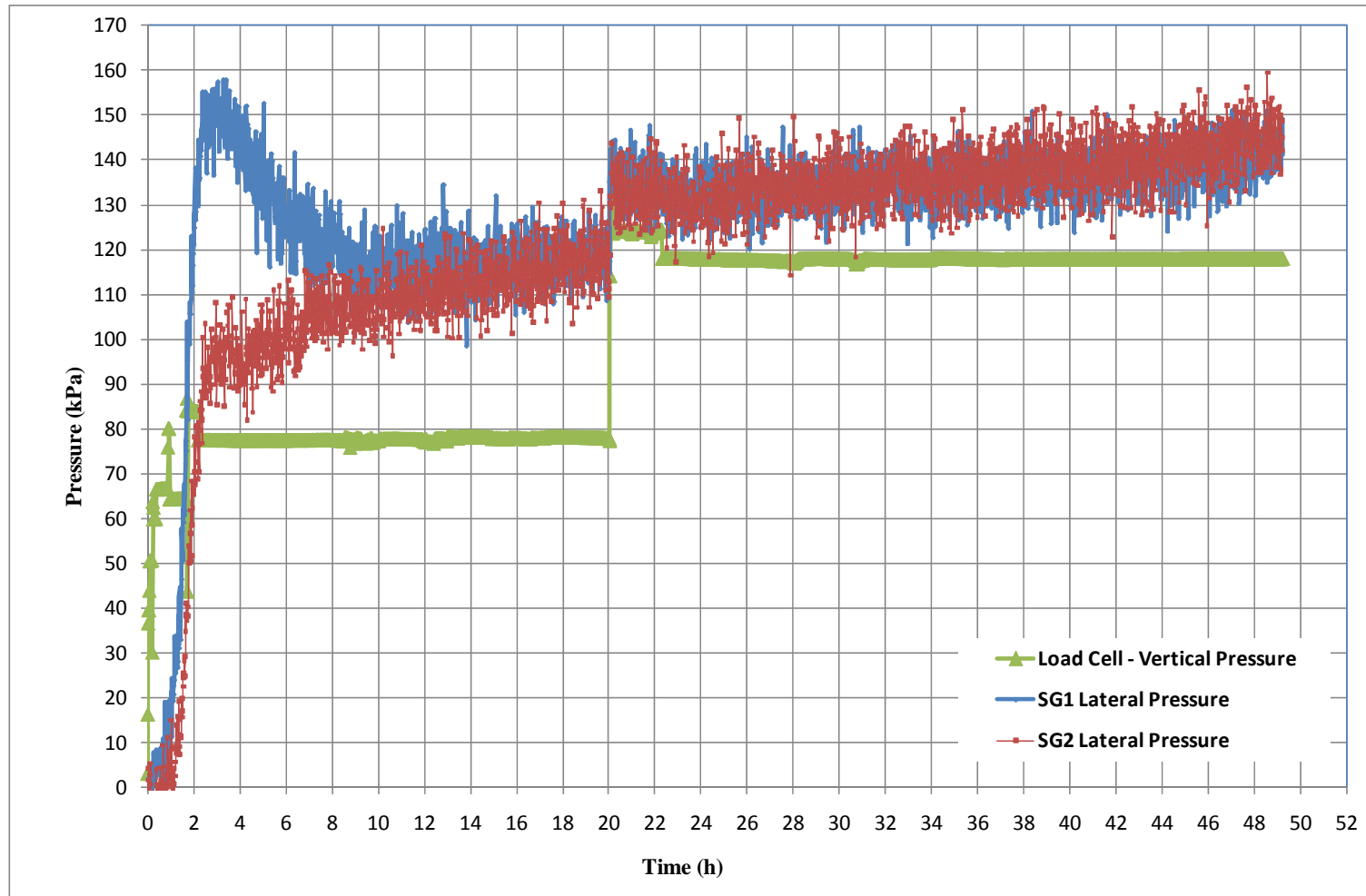
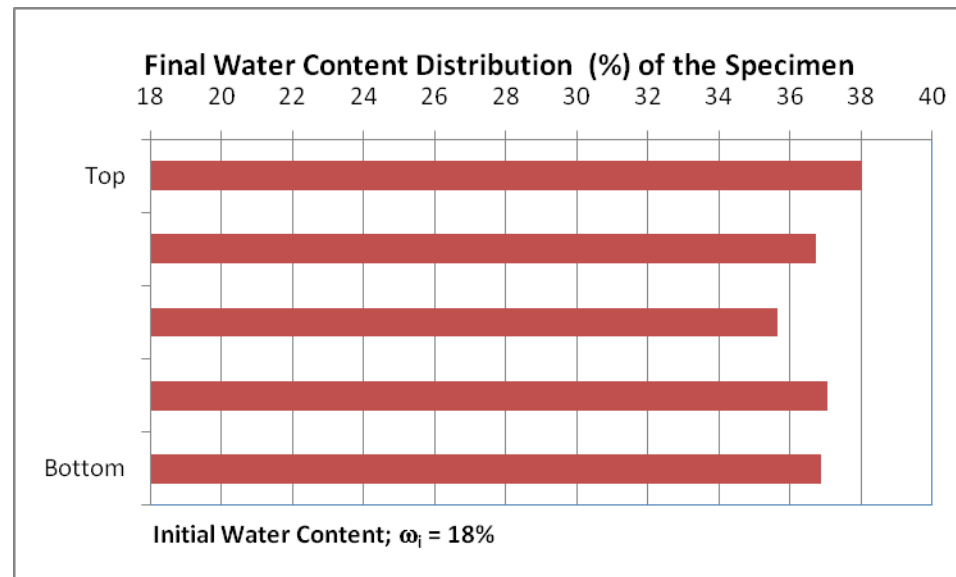**Figure A1.8:** Pressure – Time Graph Test No: 25; (16.10.2009)

TEST NO: 19	
Test Start:	
Date:	09.09.2009
Time:	13:00
Test Duration:	45 hours
Test End:	
Date:	11.09.2009
Time:	10:00
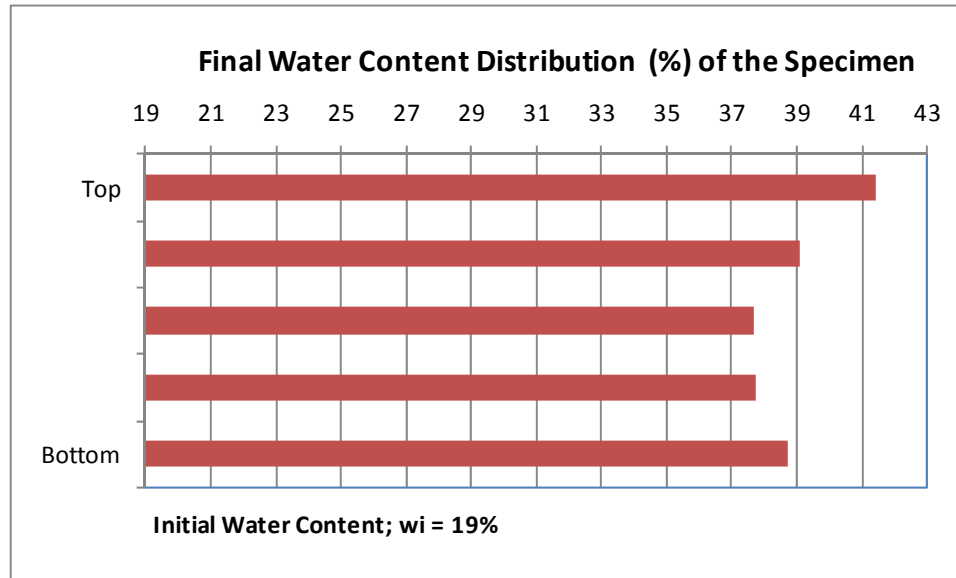
Figure A2.1: Initial and Final Water Contents Test No: 19; (09.09.2009)
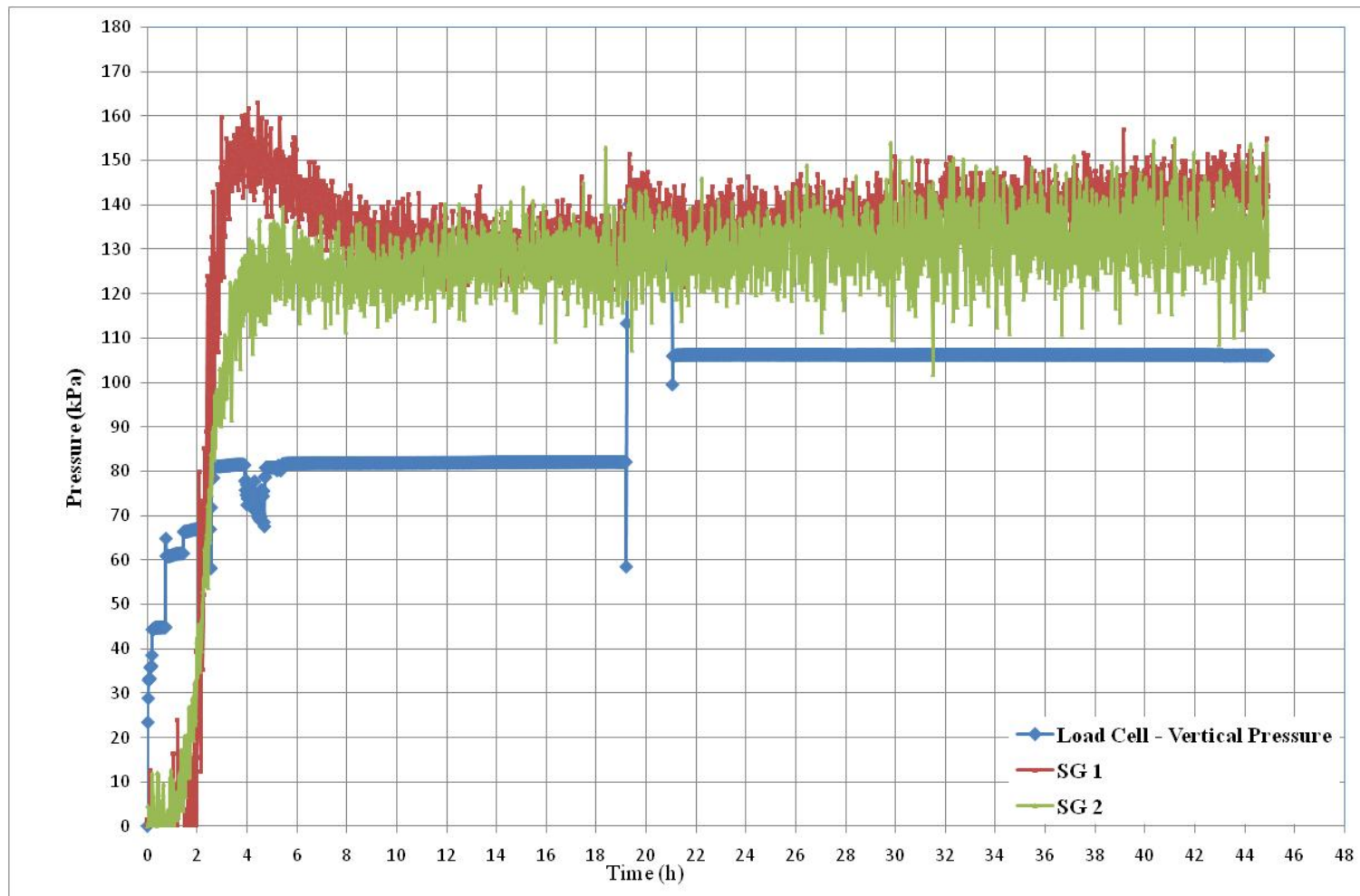
Figure A2.2: Pressure – Time Graph Test No: 19; (09.09.2009)

TEST NO: 21	
Test Start:	
Date:	16.09.2009
Time:	11:00
Test Duration:	53 hours
Test End:	
Date:	18.09.2009
Time:	16:00
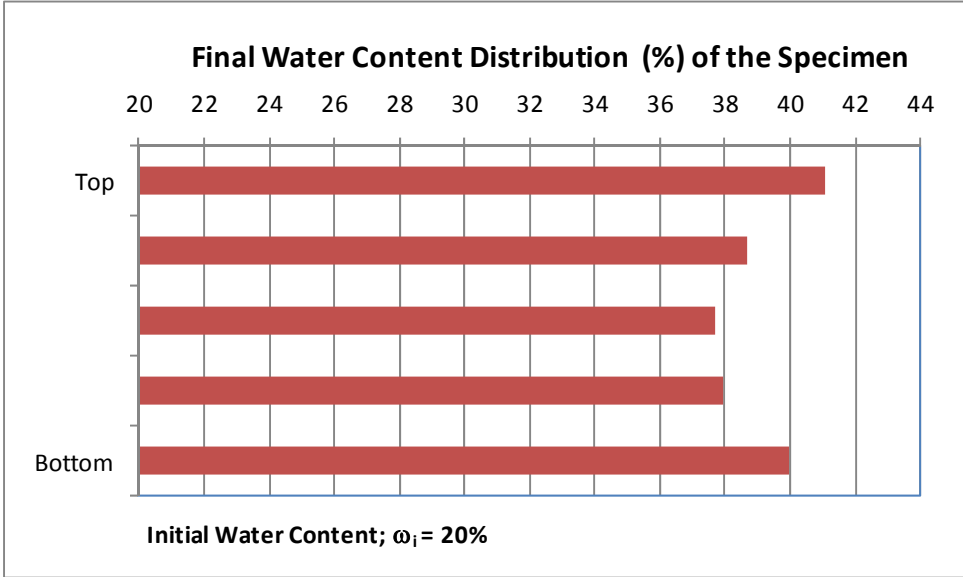
Figure A2.3: Initial and Final Water Contents Test No: 21; (16.09.2009)
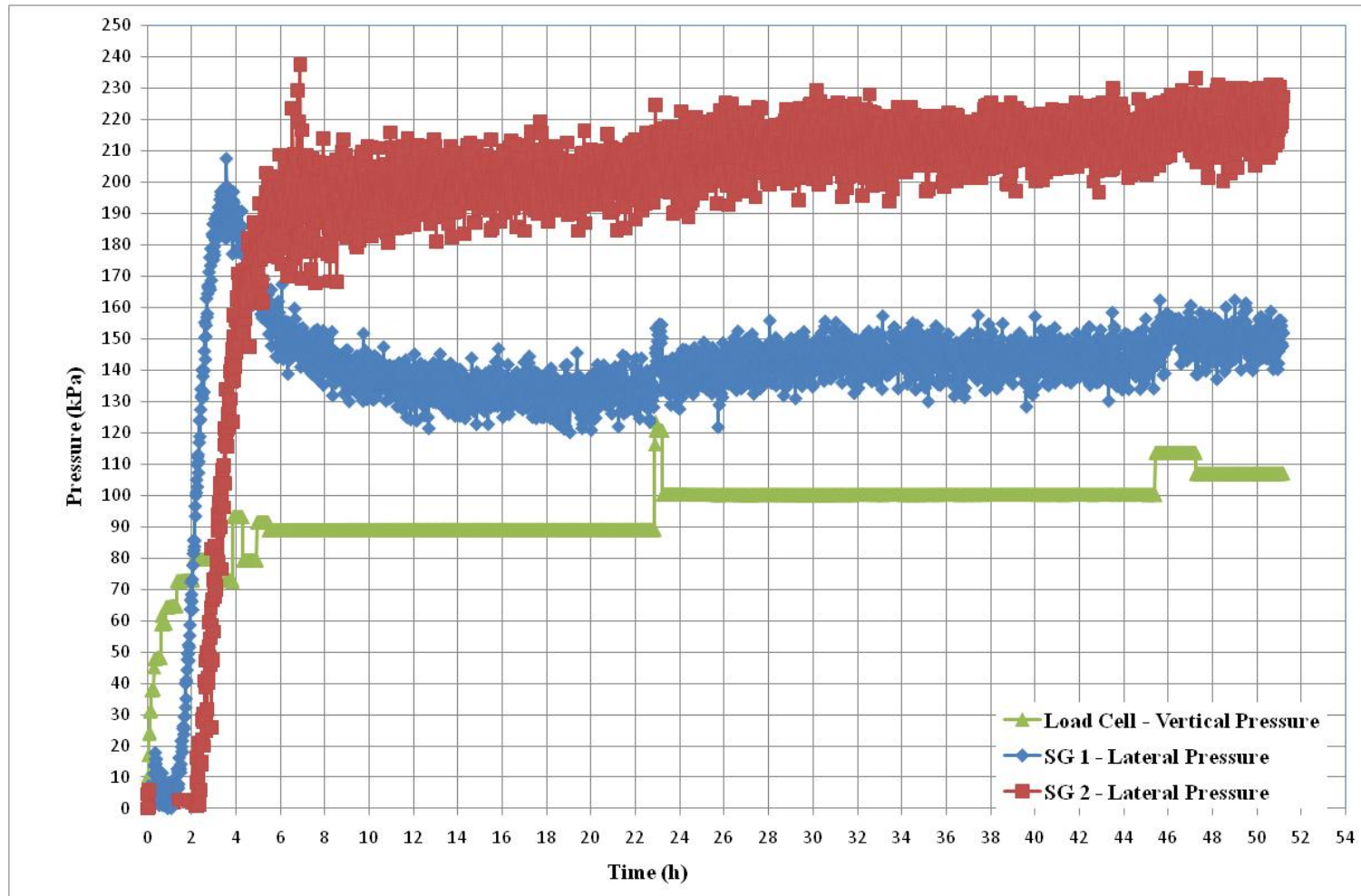
Figure A.24: Pressure – Time Graph Test No: 21; (16.09.2009)

APPENDIX B
CONSTANT VOLUME TESTS (CVS)

TEST NO: 9	
Test Start:	
Date:	07.07.2009
Time:	13:00
Test Duration:	24 hours
Test End:	
Date:	08.07.2009
Time:	13:00
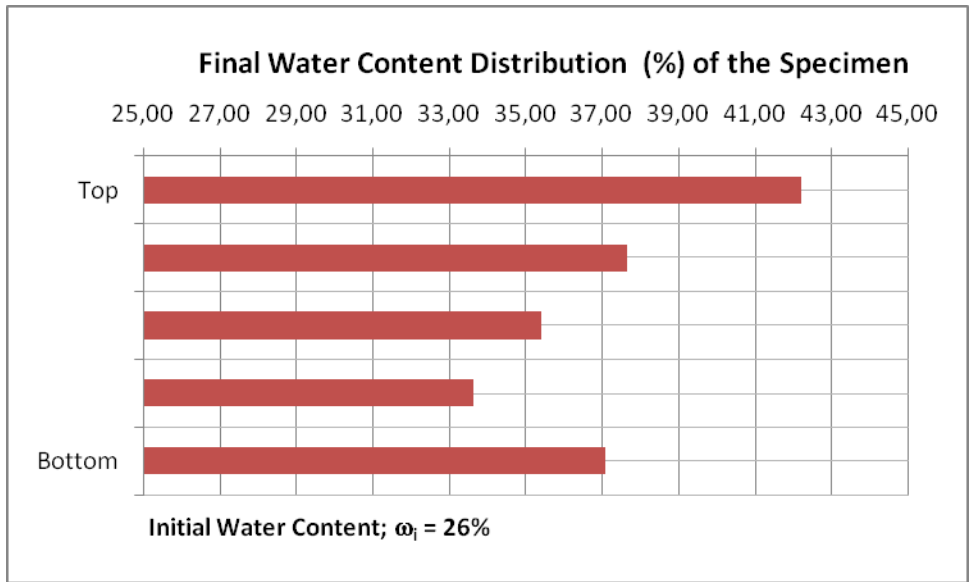
Figure B1.1: Initial and Final Water Contents Test No: 9; (07.07.2009)
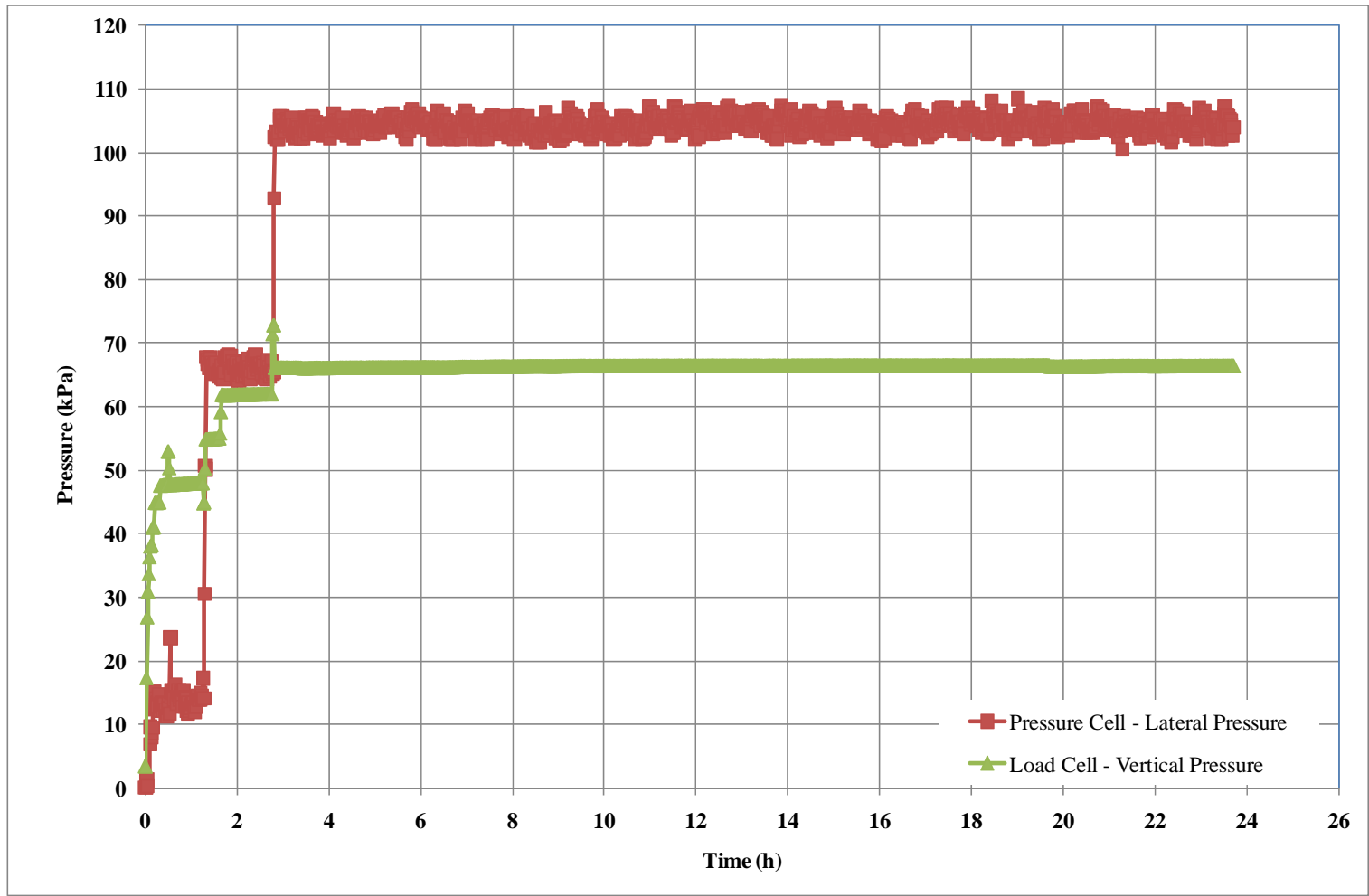
Figure B1.2: Pressure – Time Graph Test No: 9; (07.07.2009)
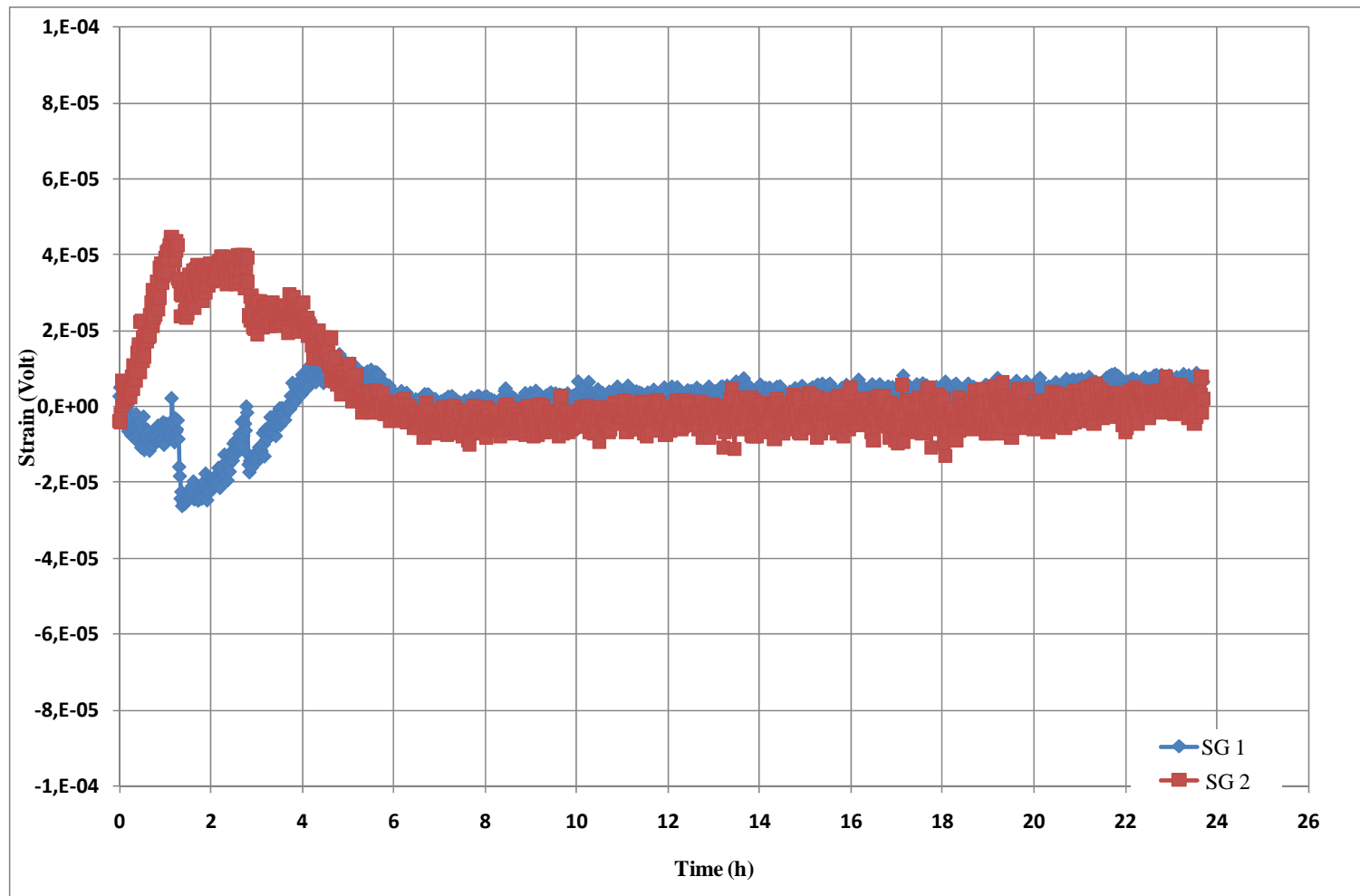
Figure B1.3: Strain – Time Graph Test No:9; (07.07.2009)

TEST NO: 10	
Test Start:	
Date:	09.07.2009
Time:	13:00
Test Duration:	30 hours
Test End:	
Date:	10.07.2009
Time:	19:00
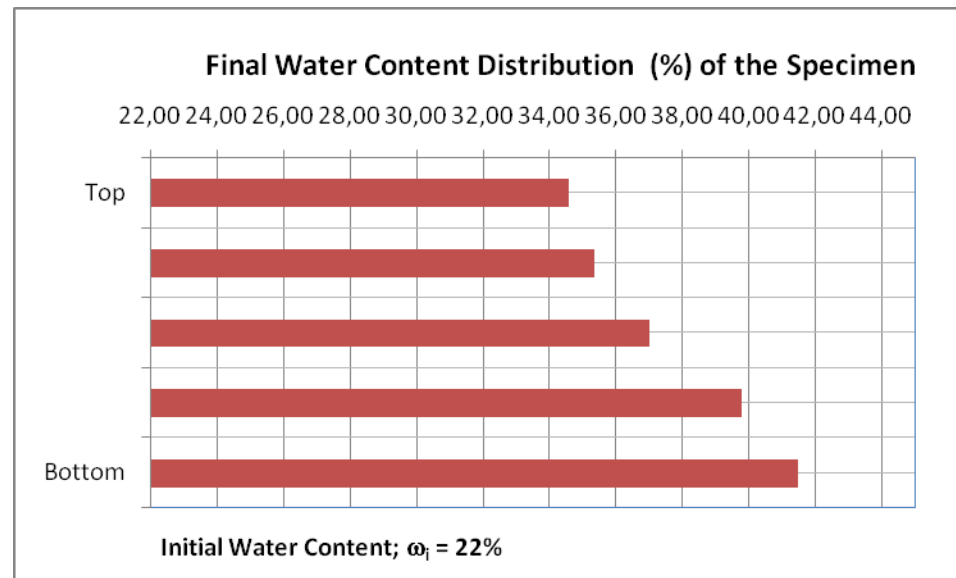
Figure B1.4: Initial and Final Water Contents Test No: 10; (09.07.2009)
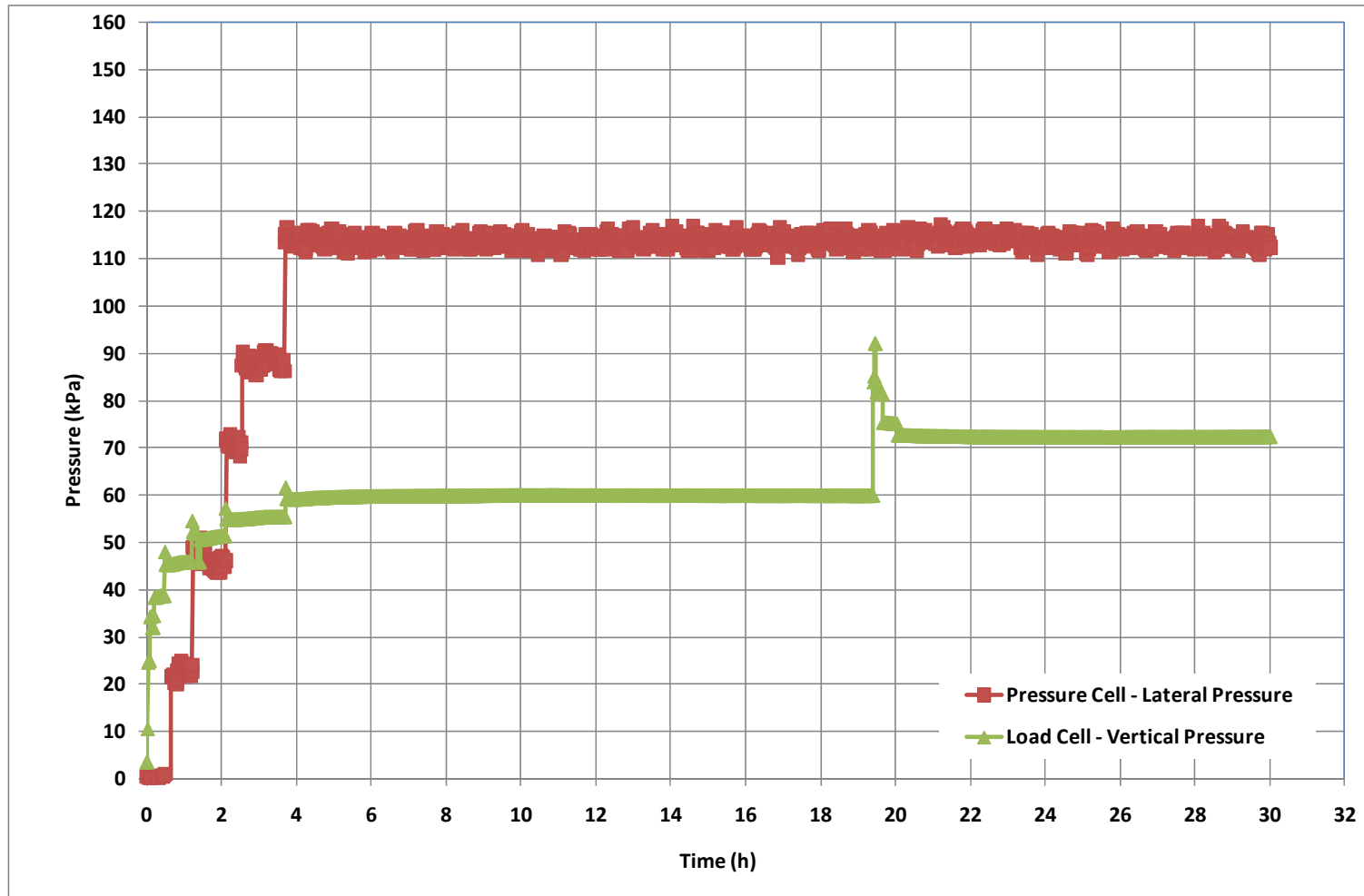
Figure B1.5: Pressure – Time Graph Test No: 10; (09.07.2009)
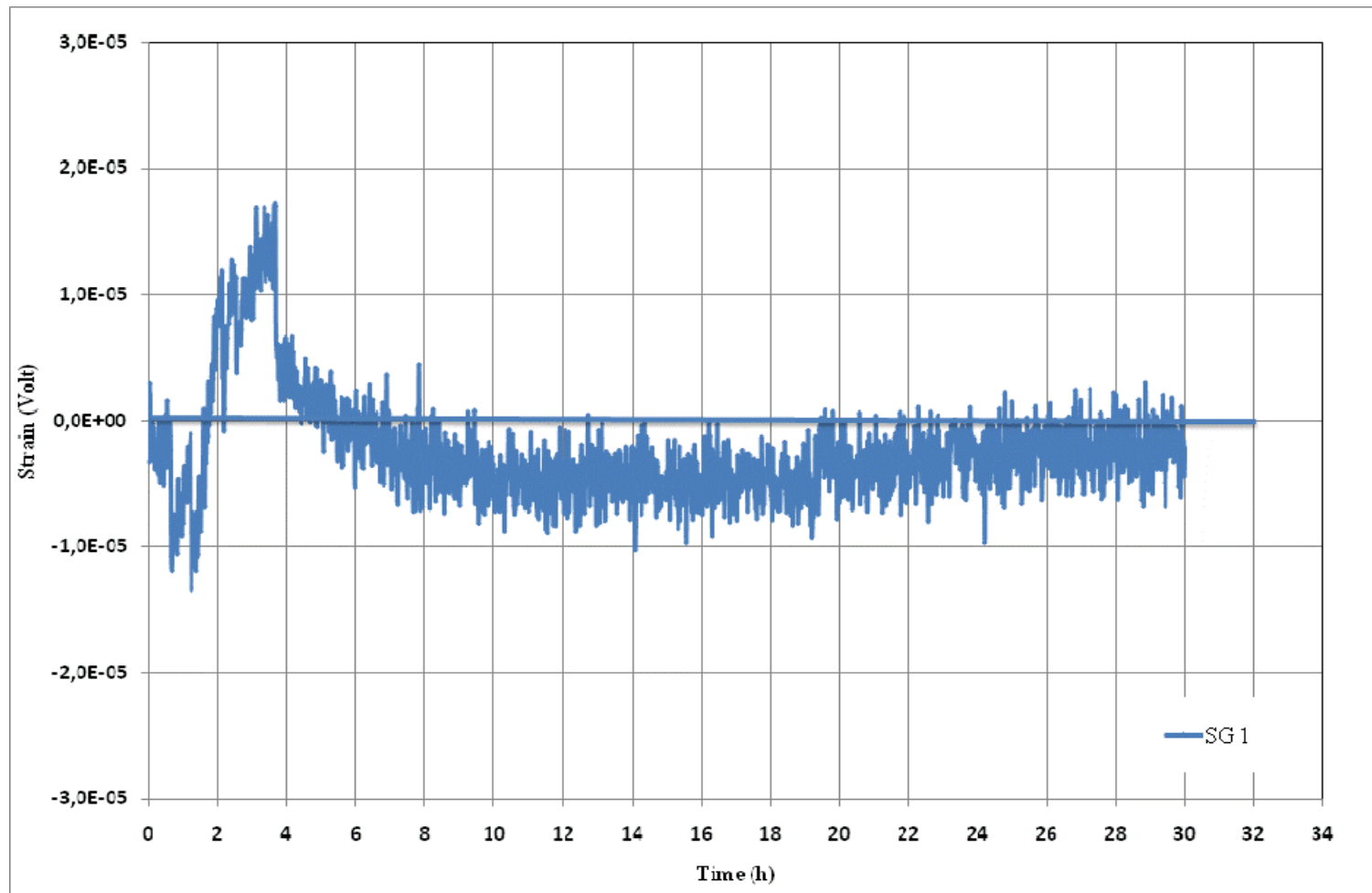
Figure B1.6: Strain – Time Graph Test No:10; (09.07.2009)

TEST NO: 11	
Test Start:	
Date:	13.08.2009
Time:	09:00
Test Duration:	29 hours
Test End:	
Date:	14.08.2009
Time:	14:00
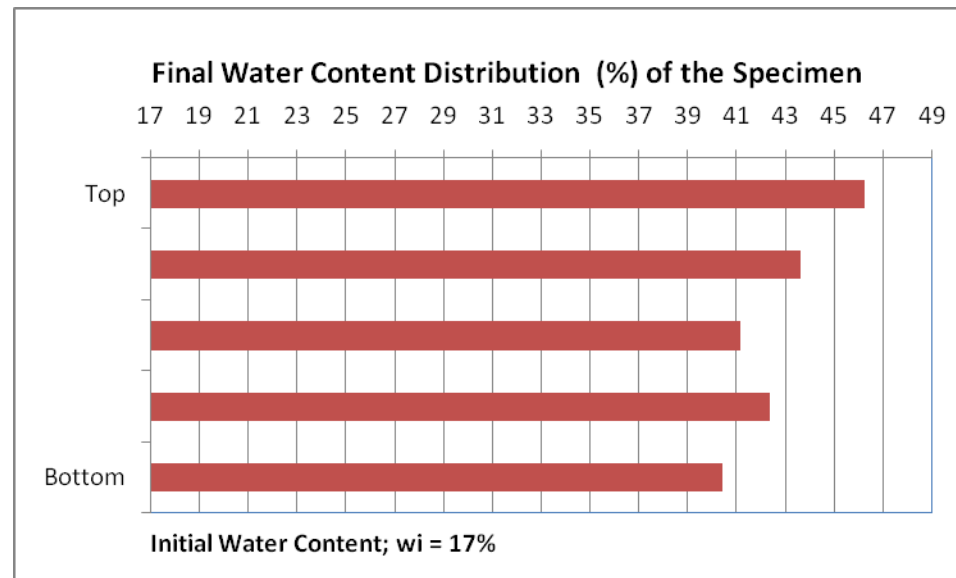
Figure B1.7: Initial and Final Water Contents Test No:11; (13.08.2009)
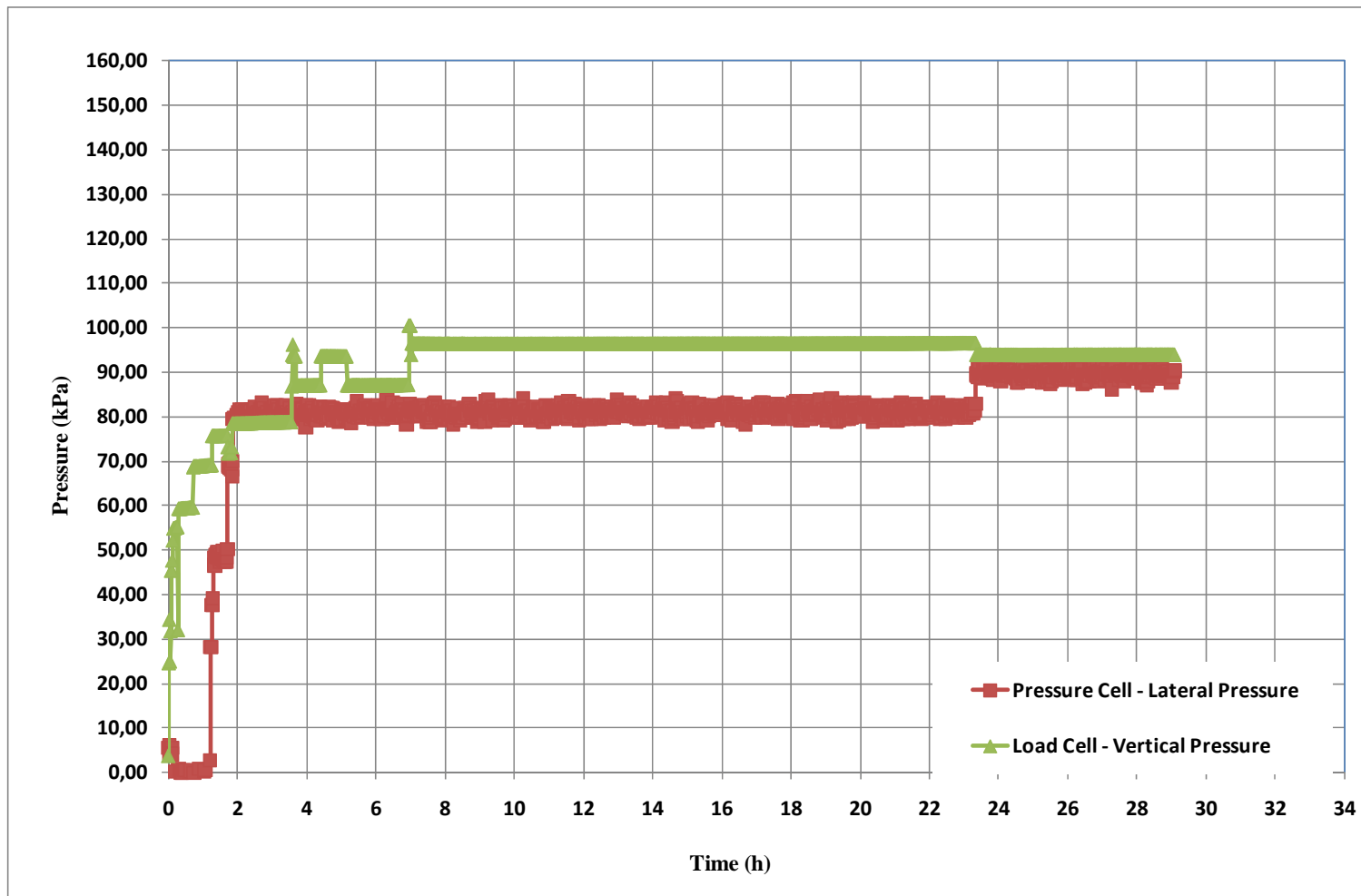
Figure B1.8: Pressure – Time Graph Test No: 11; (13.08.2009)
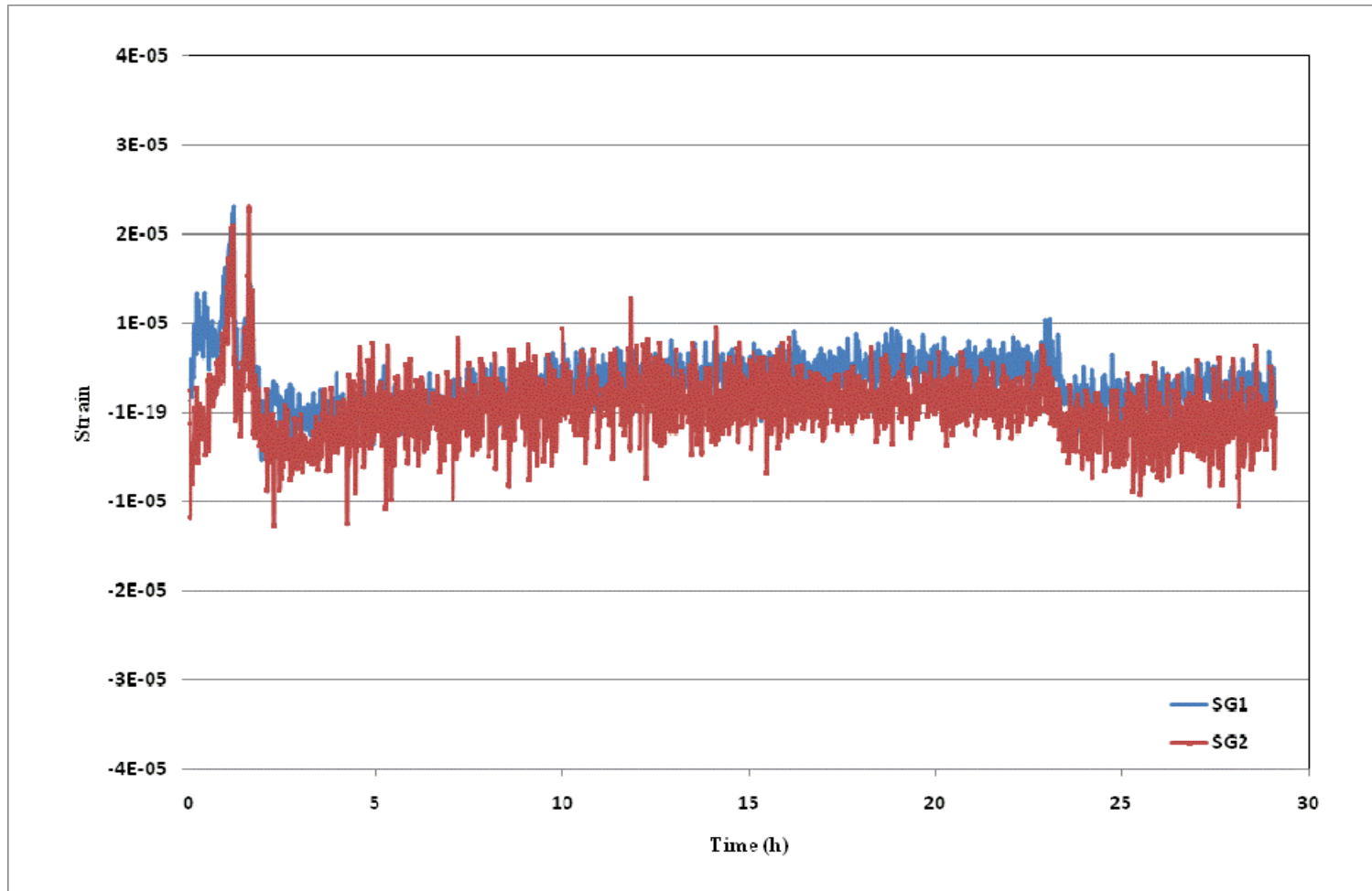
Figure B1.9: Strain – Time Graph Test No: 11; (13.08.2009)

TEST NO: 12	
Test Start:	
Date:	17.08.2009
Time:	15:00
Test Duration:	48 hours
Test End:	
Date:	19.08.2009
Time:	15:00
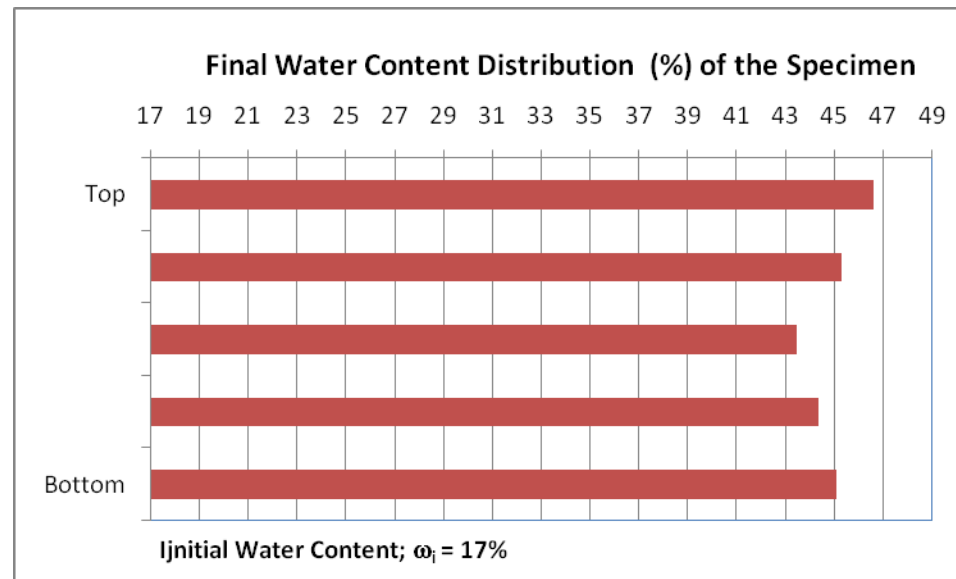
Figure B1.10: Initial and Final Water Contents Test No: 12; (17.08.2009)
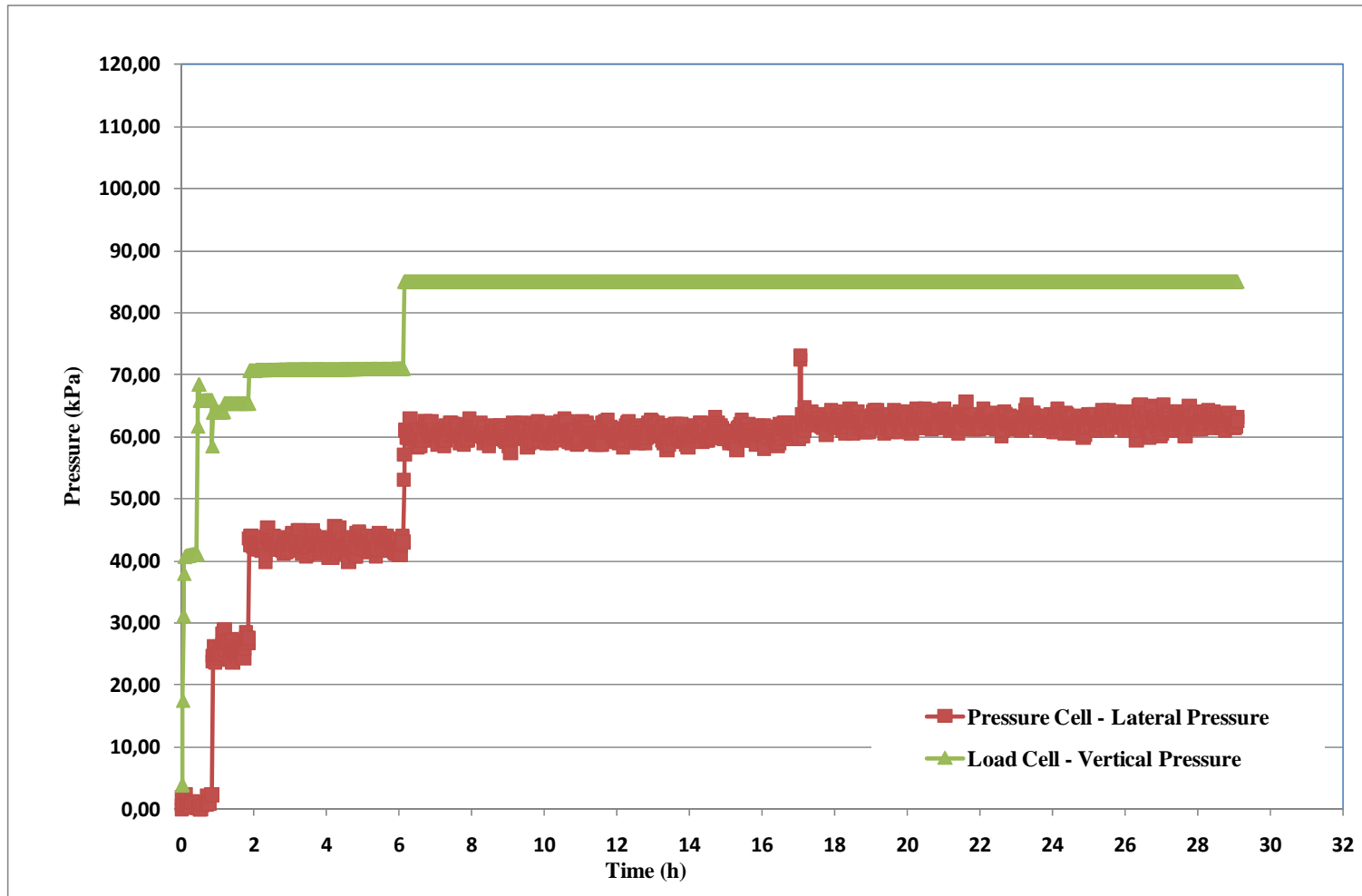
Figure B1.11: Pressure – Time Graph Test No: 12; (17.08.2009)
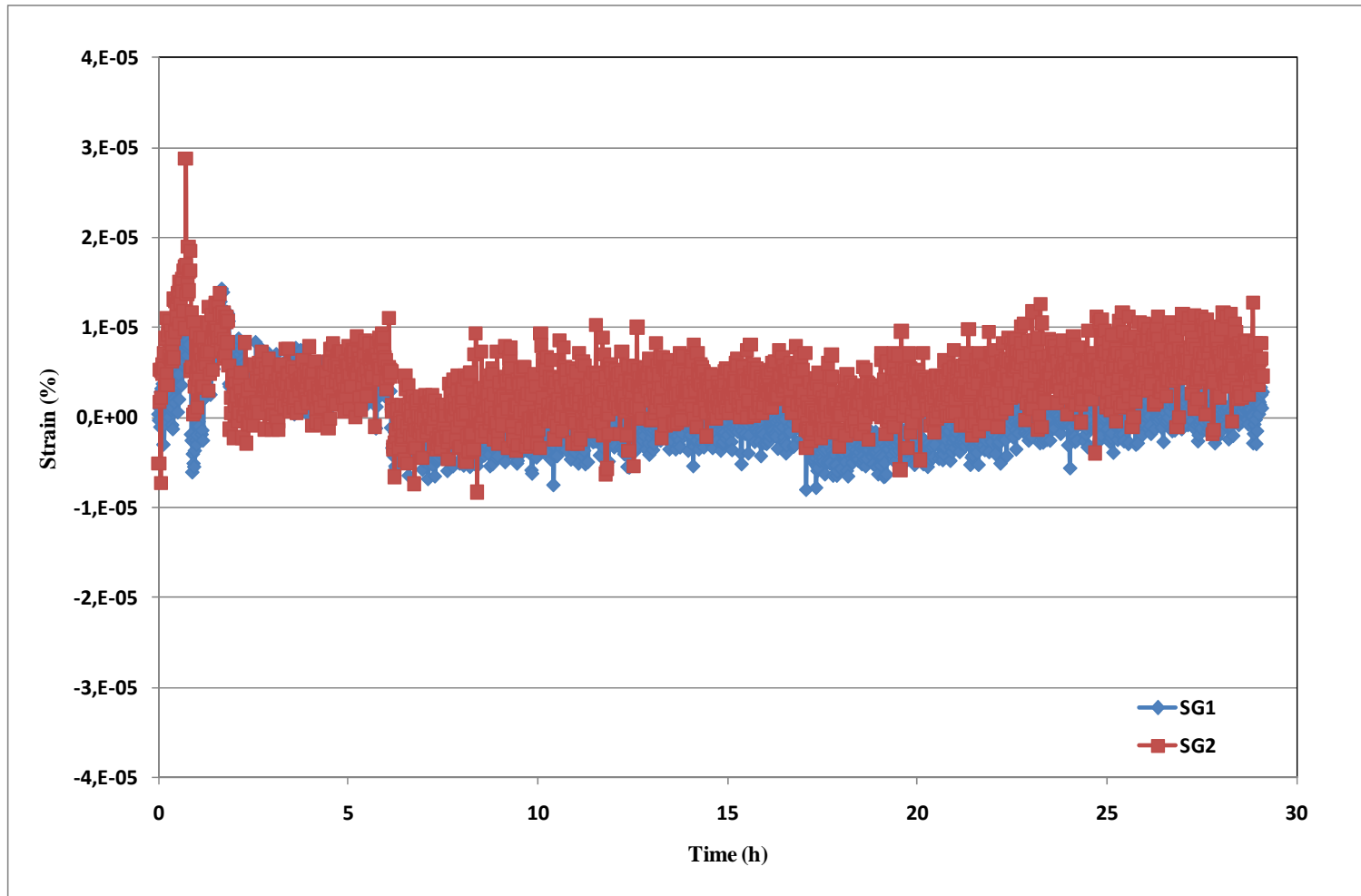
Figure B1.12: Strain – Time Graph Test No: 12; (17.08.2009)

TEST NO: 22	
Test Start:	
Date:	25.09.2009
Time:	09:00
Test Duration:	57 hours
Test End:	
Date:	27.09.2009
Time:	18:00
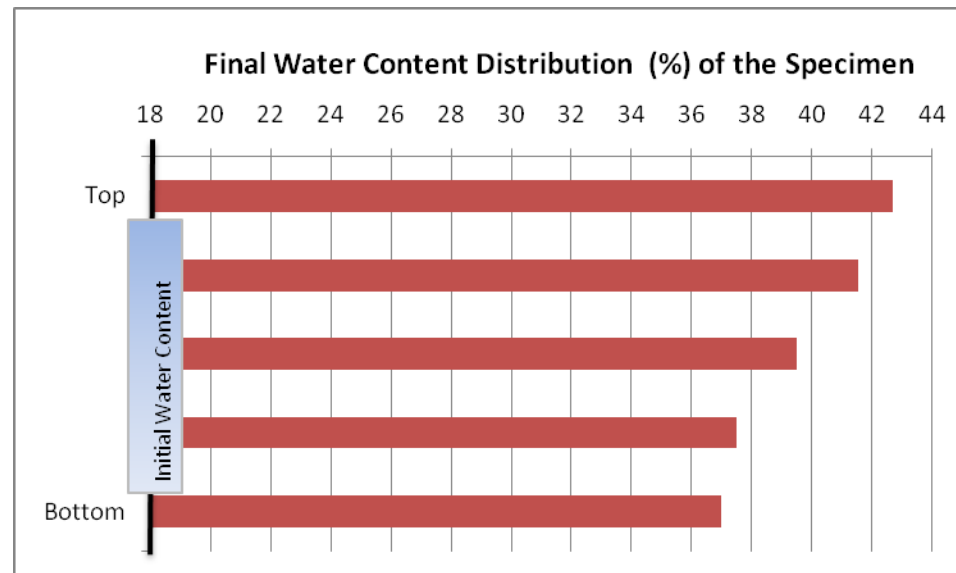
Figure B1.13: Initial and Final Water Contents Test No: 22; (25.09.2009)
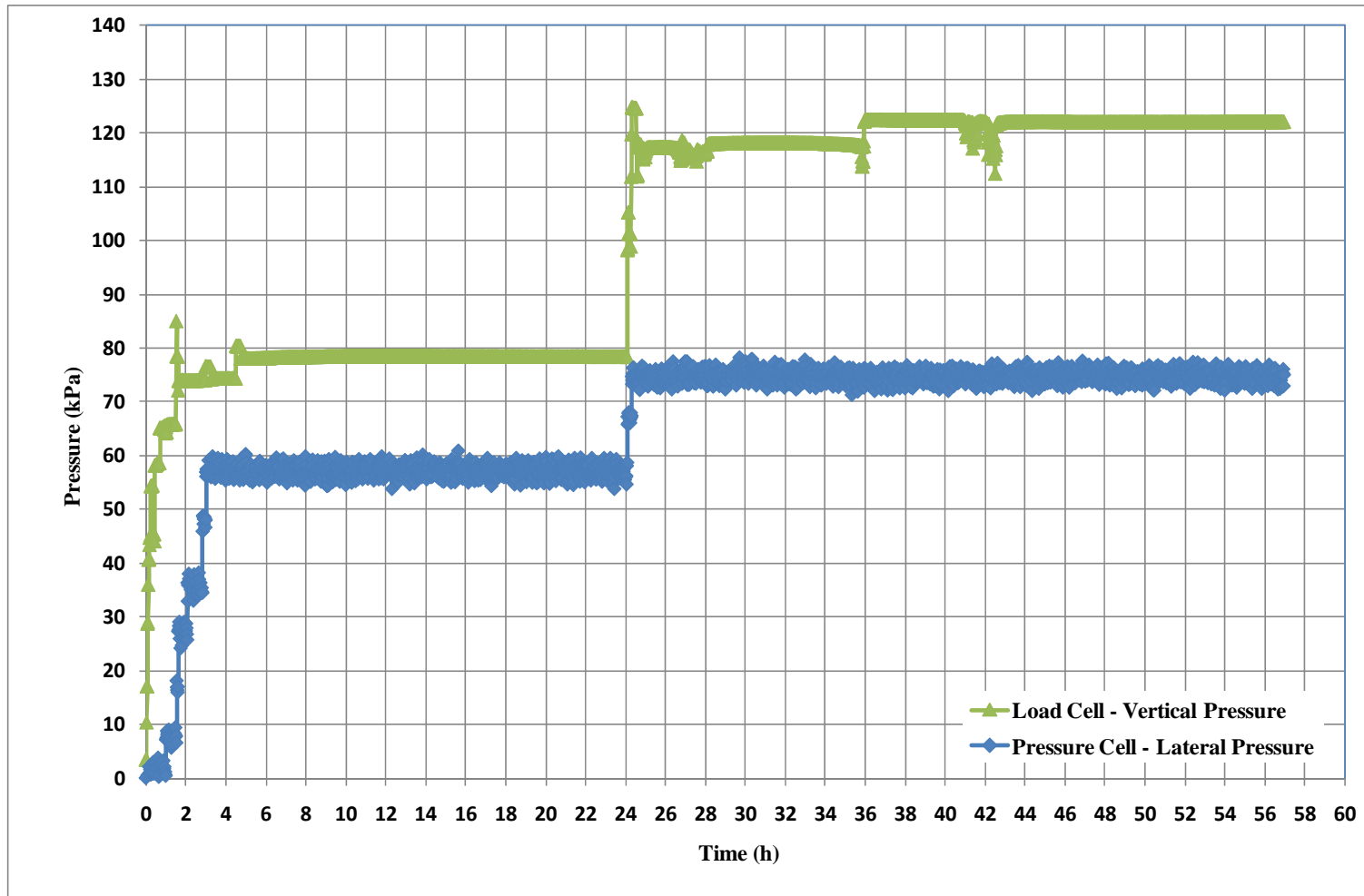
Figure B1.14: Pressure – Time Graph Test No: 22; (25.09.2009)
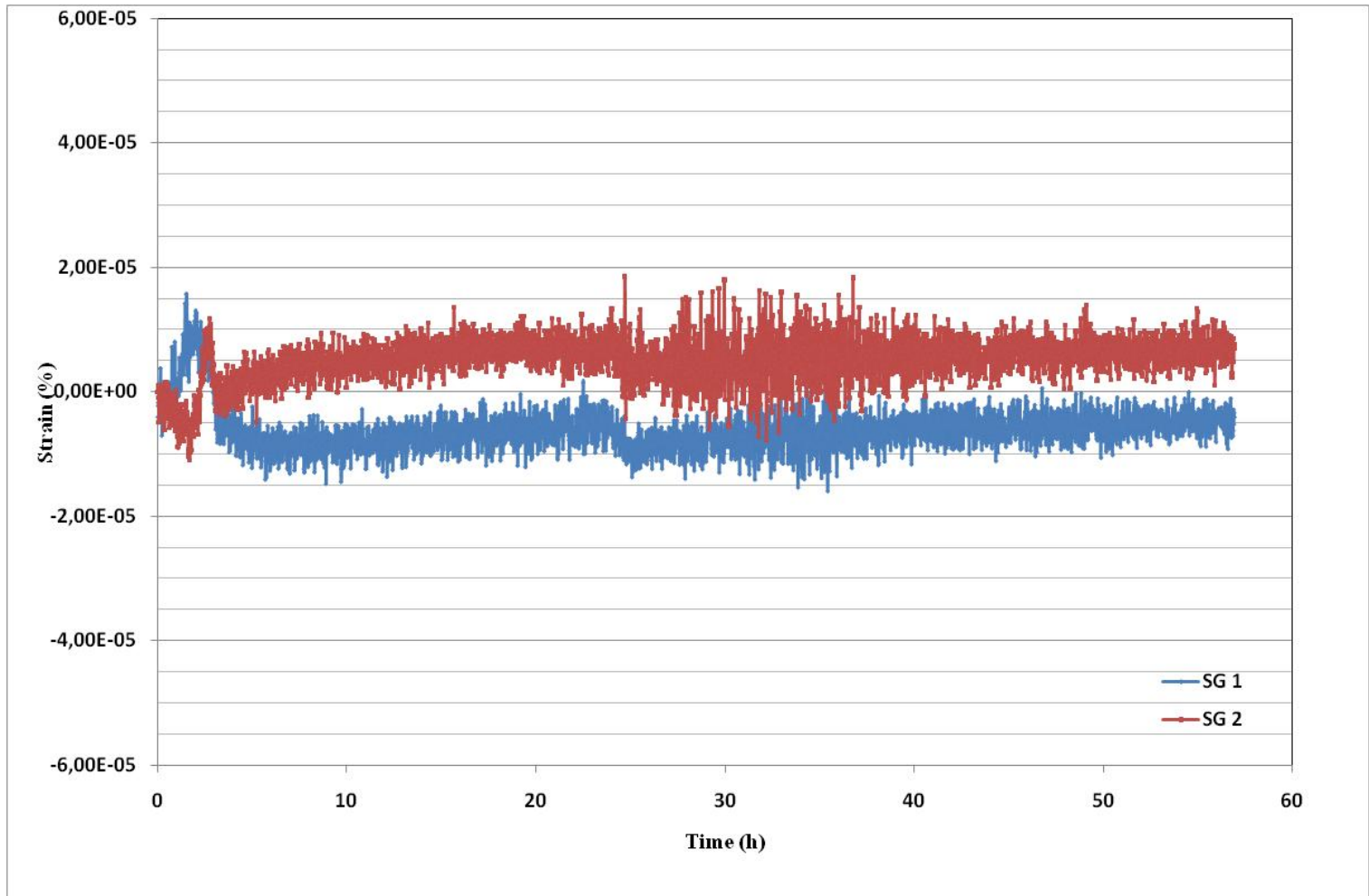
Figure B1.15: Strain – Time Graph Test No: 22; (25.09.2009)

TEST NO: 23	
Test Start:	
Date:	02.10.2009
Time:	08:30
Test Duration:	57 hours
Test End:	
Date:	04.10.2009
Time:	17:30
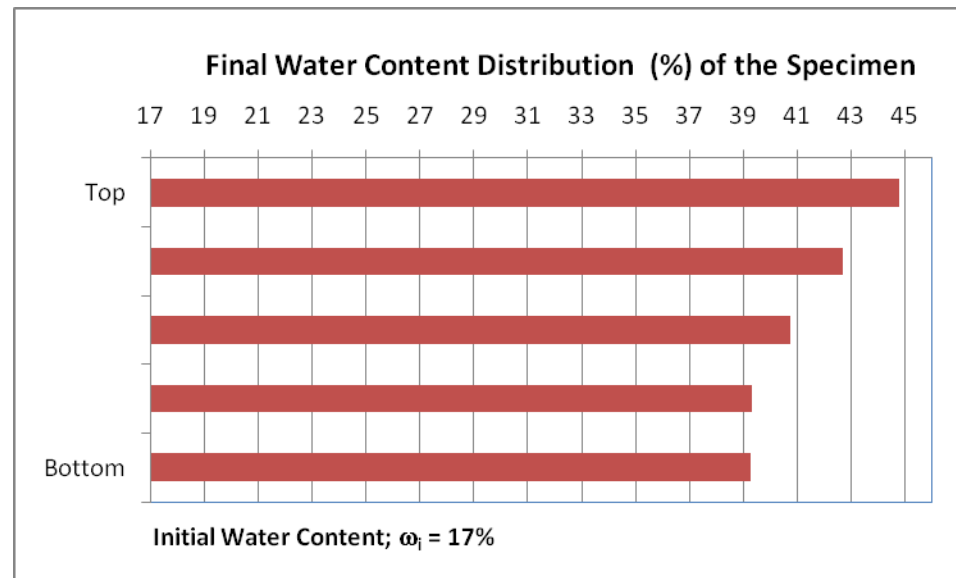
Figure B1.16: Initial and Final Water Contents Test No: 23; (02.10.2009)
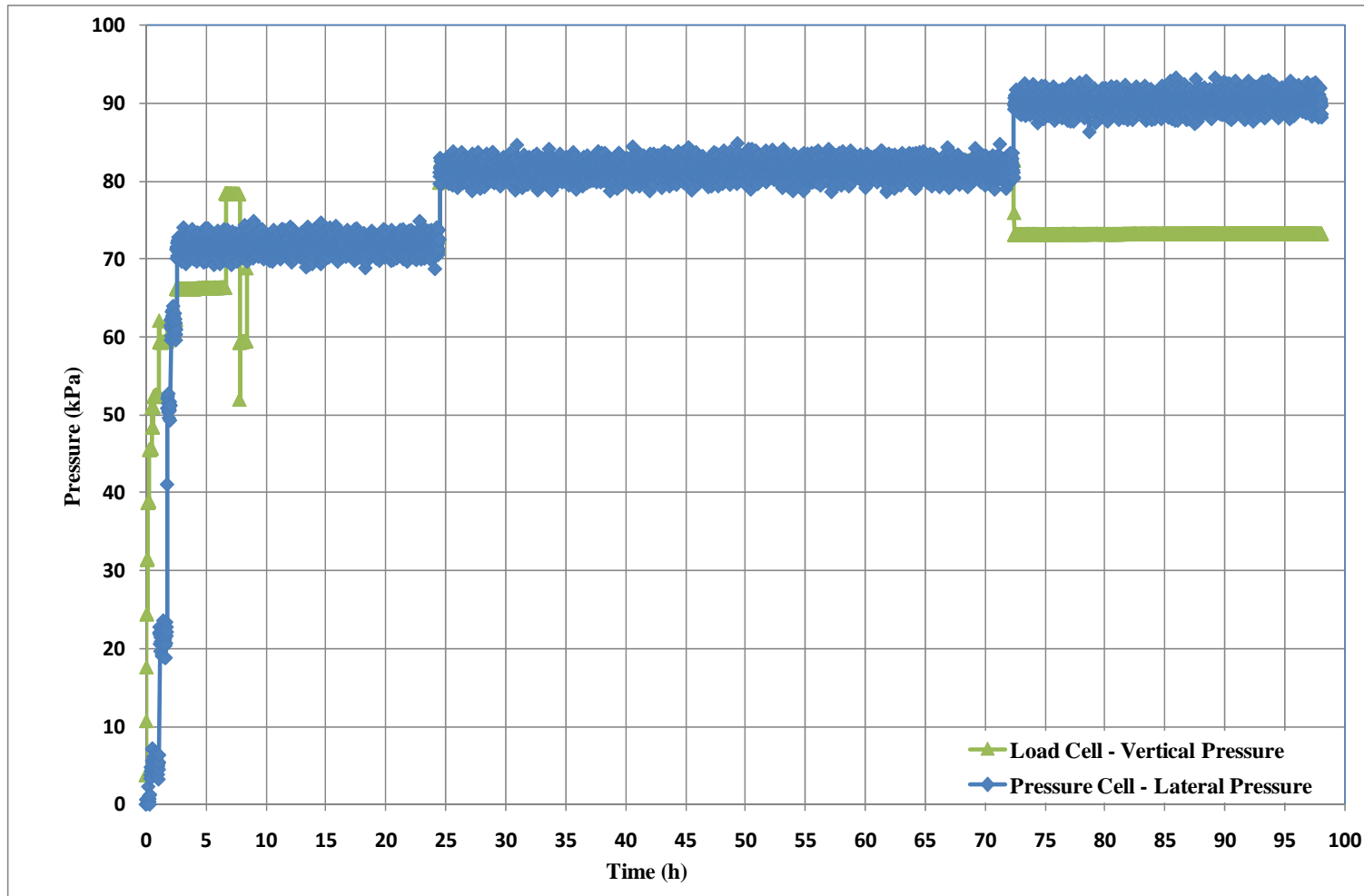
Figure B1.17: Pressure – Time Graph Test No: 23; (02.10.2009)
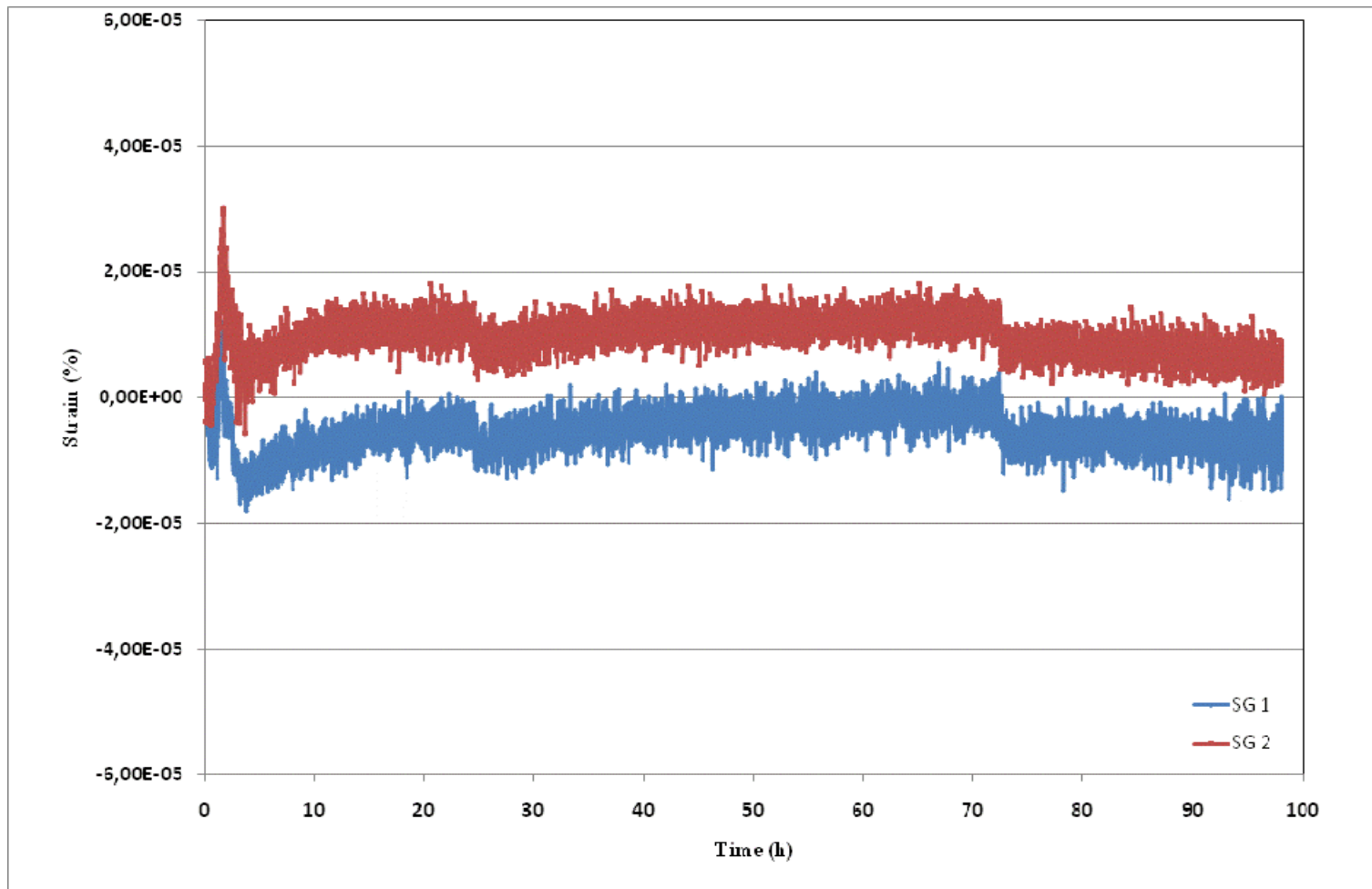
Figure B1.18: Strain – Time Graph Test No: 23; (02.10.2009)

TEST NO: 24	
Test Start:	
Date:	08.10.2009
Time:	10:00
Test Duration:	52 hours
Test End:	
Date:	10.10.2009
Time:	14:00
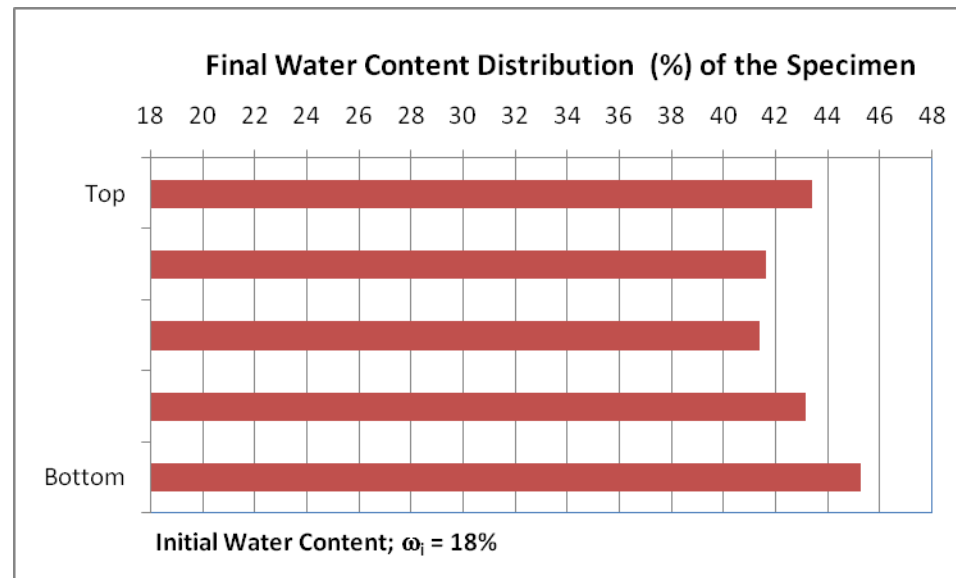
Figure B1.19: Initial and Final Water Contents Test No: 24; (08.10.2009)
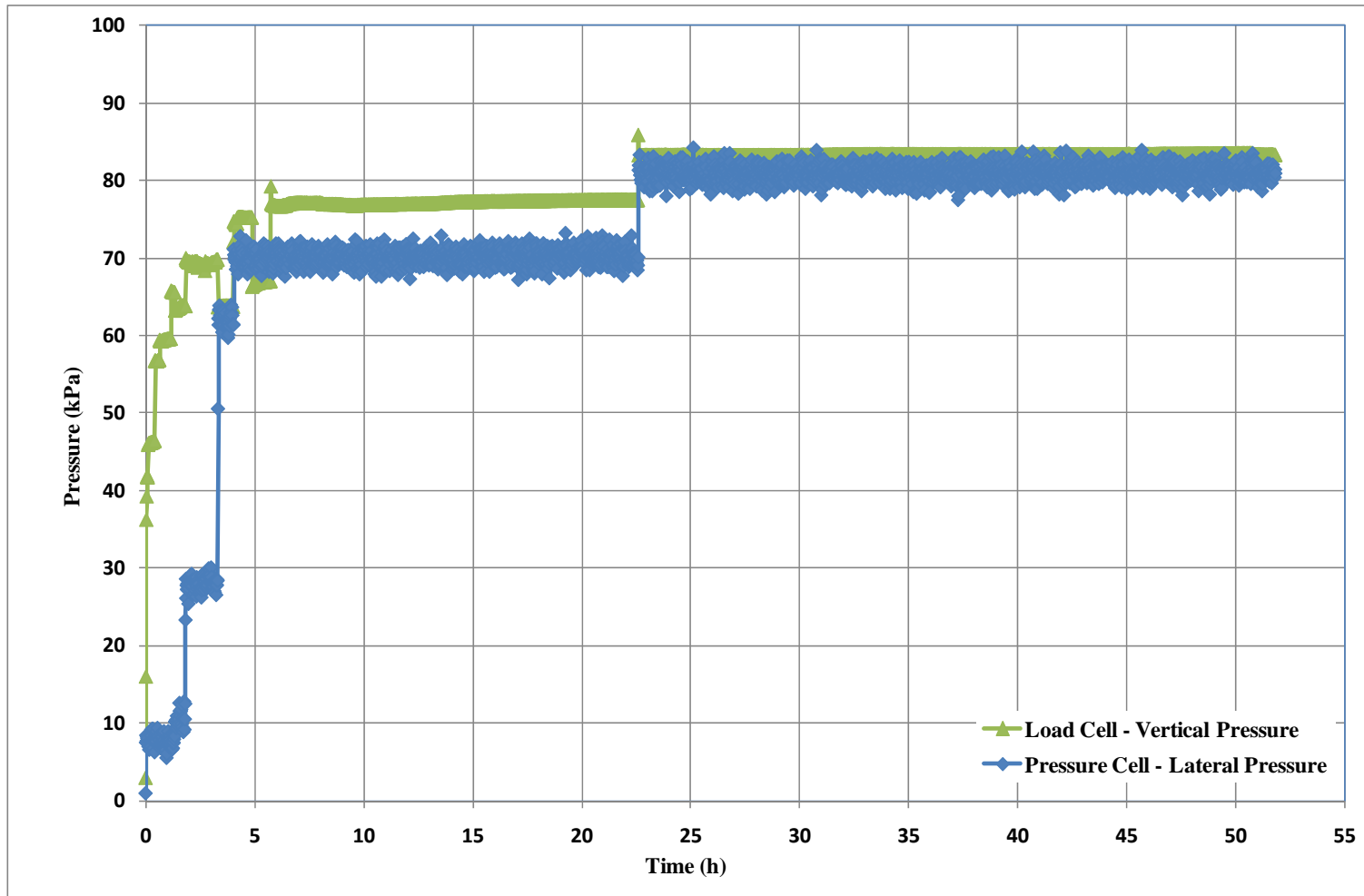
Figure B1.20: Pressure – Time Graph Test No: 24; (08.10.2009)
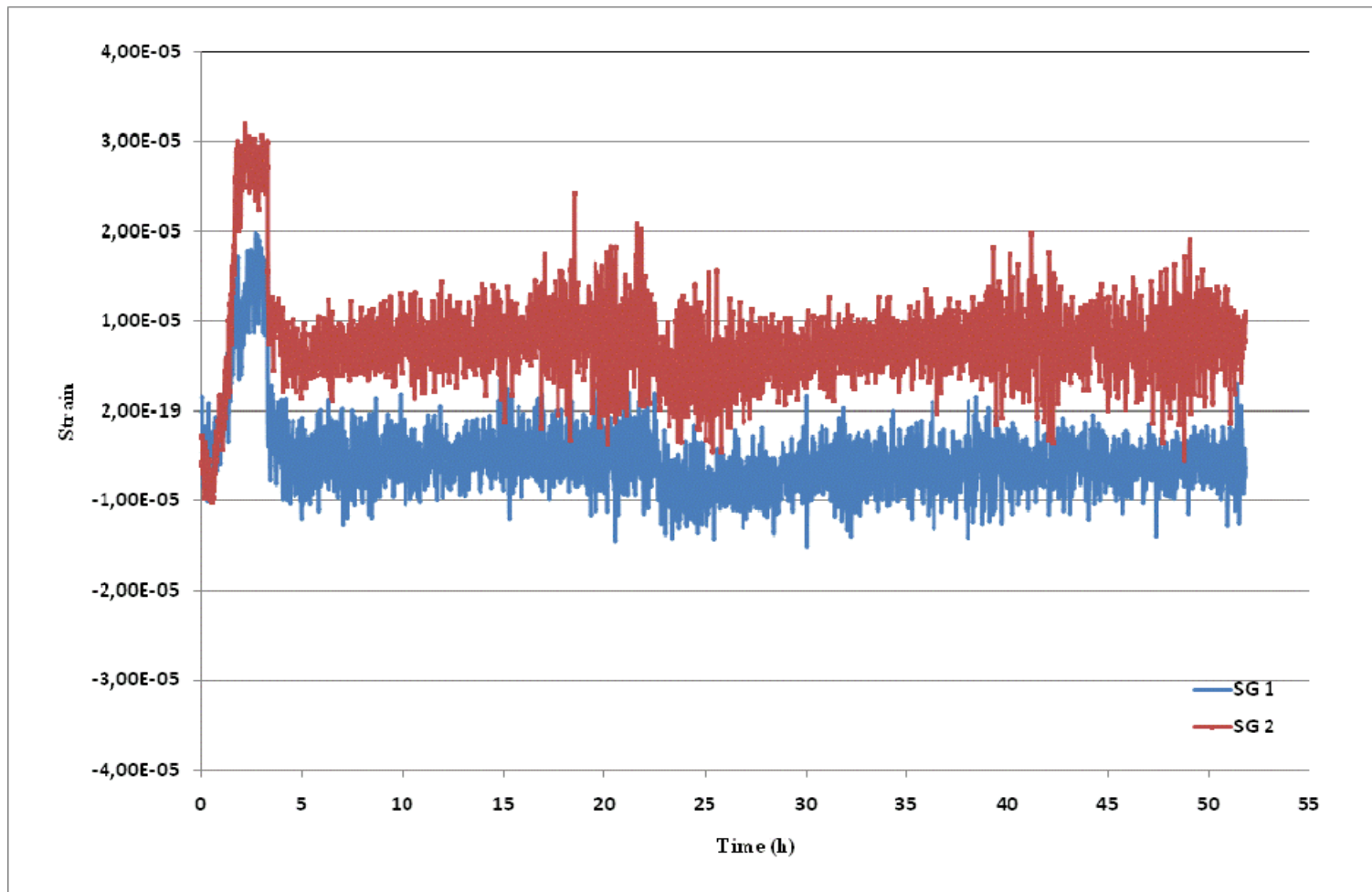
Figure B1.21: Strain – Time Graph Test No: 24; (08.10.2009)

TEST NO: 13	
Test Start:	
Date:	20.08.2009
Time:	12:00
Test Duration:	45 hours
Test End:	
Date:	22.08.2009
Time:	09:00
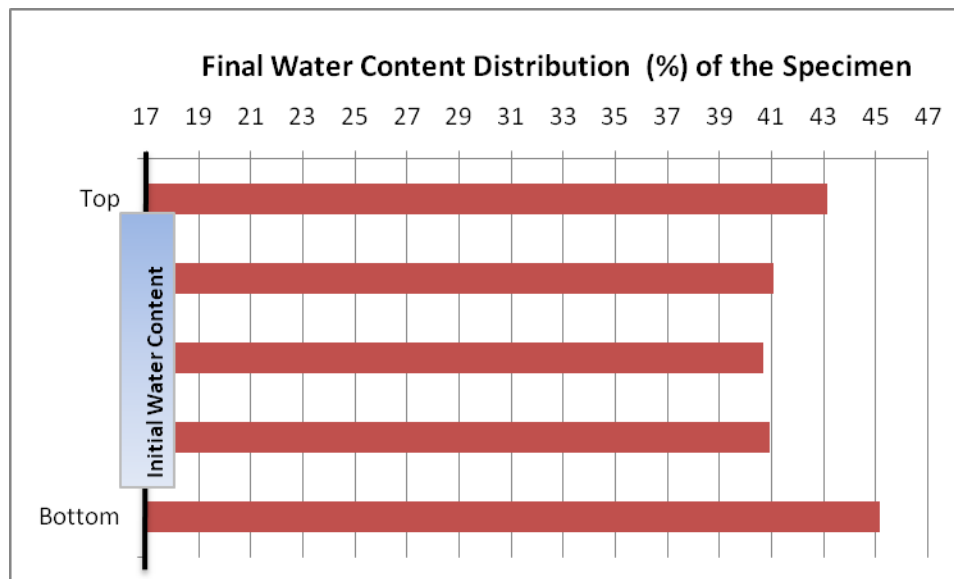
Figure B2.1: Initial and Final Water Contents Test No: 13; (20.08.2009)
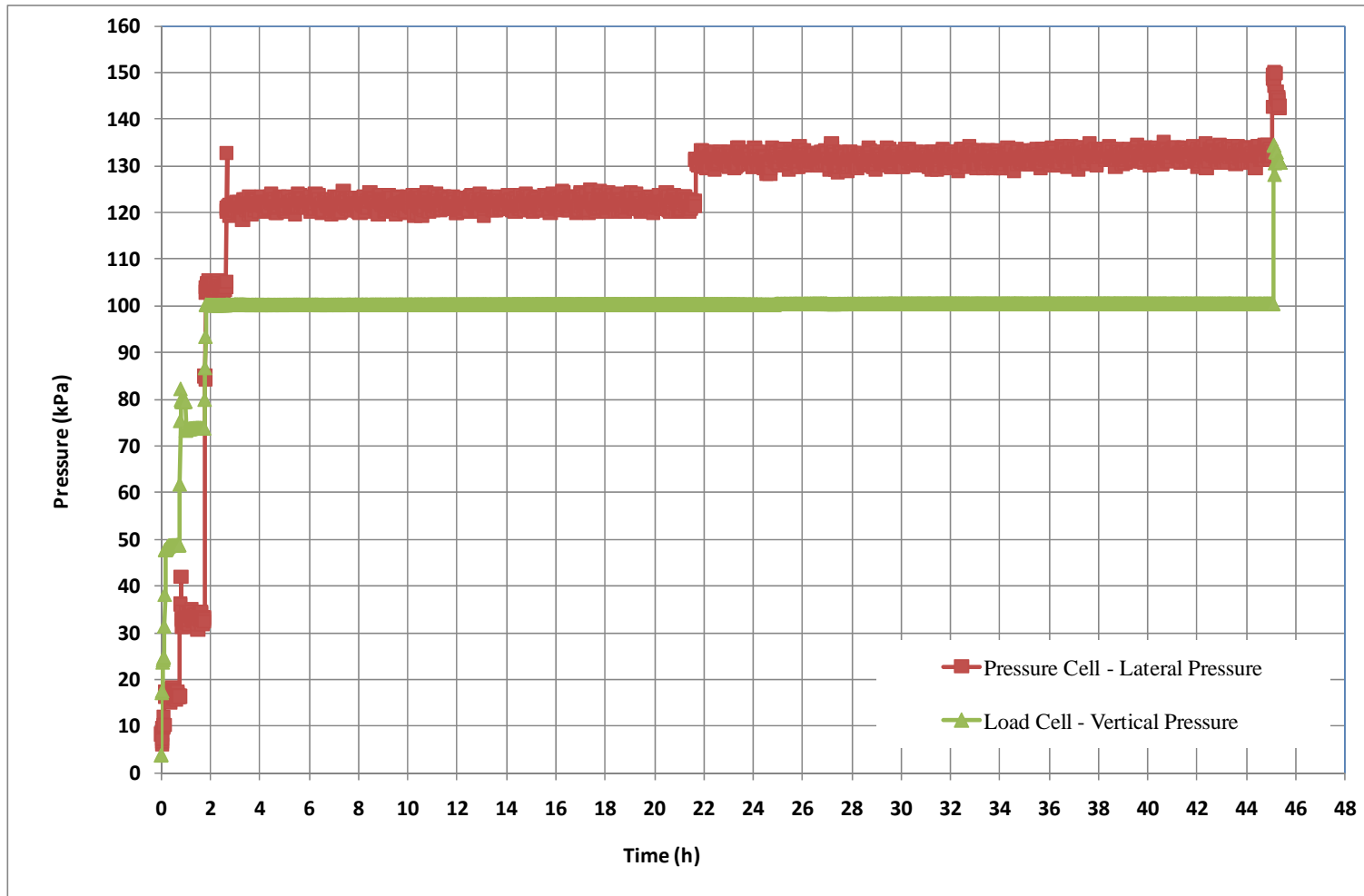
Figure B2.2: Pressure – Time Graph Test No: 13; (20.08.2009)
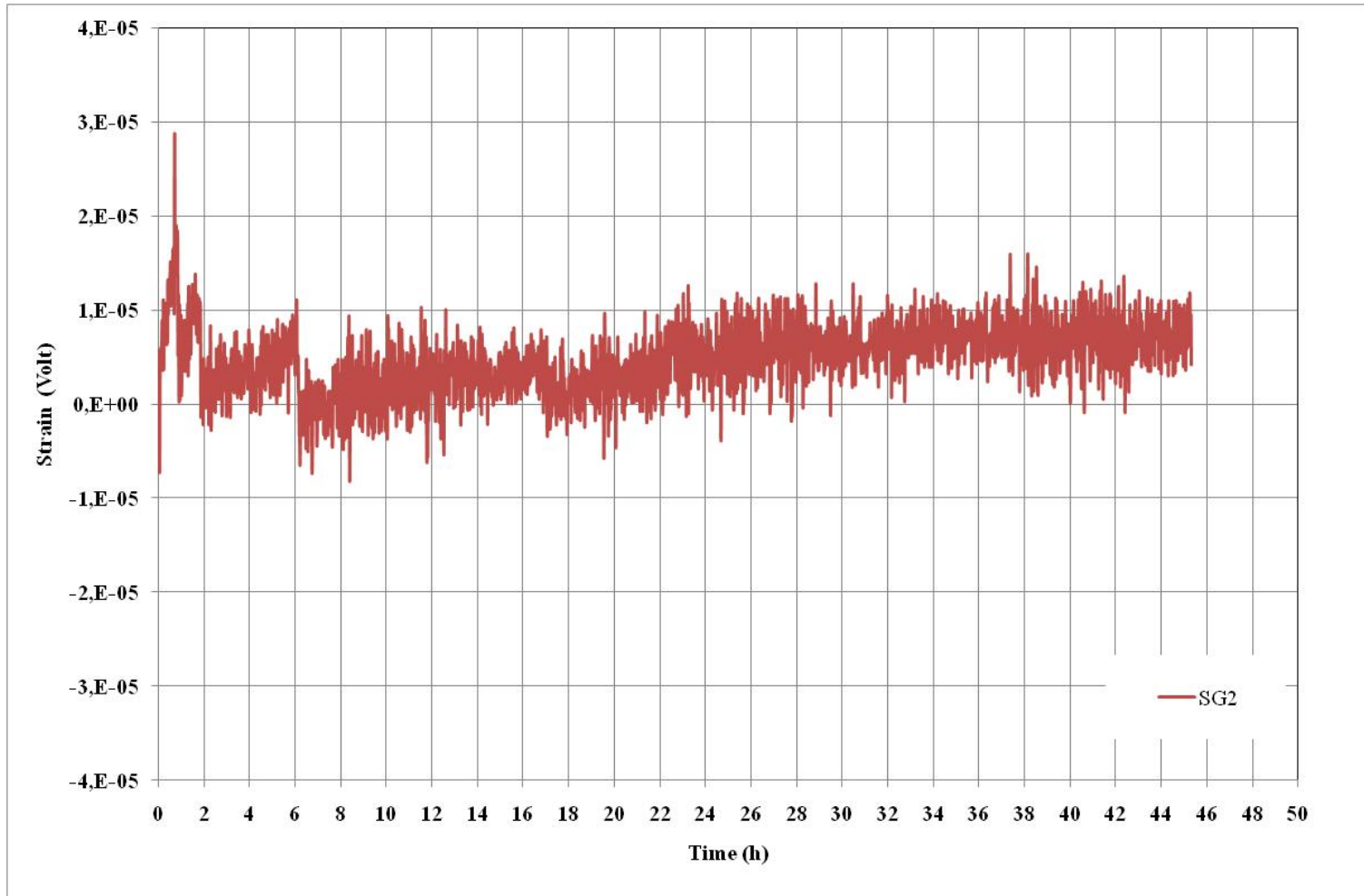
Figure B2.3: Strain – Time Graph Test No: 13; (20.08.2009)

TEST NO: 14	
Test Start:	
Date:	22.08.2009
Time:	10:45
Test Duration:	51 hours
Test End:	
Date:	24.09.2009
Time:	13:45
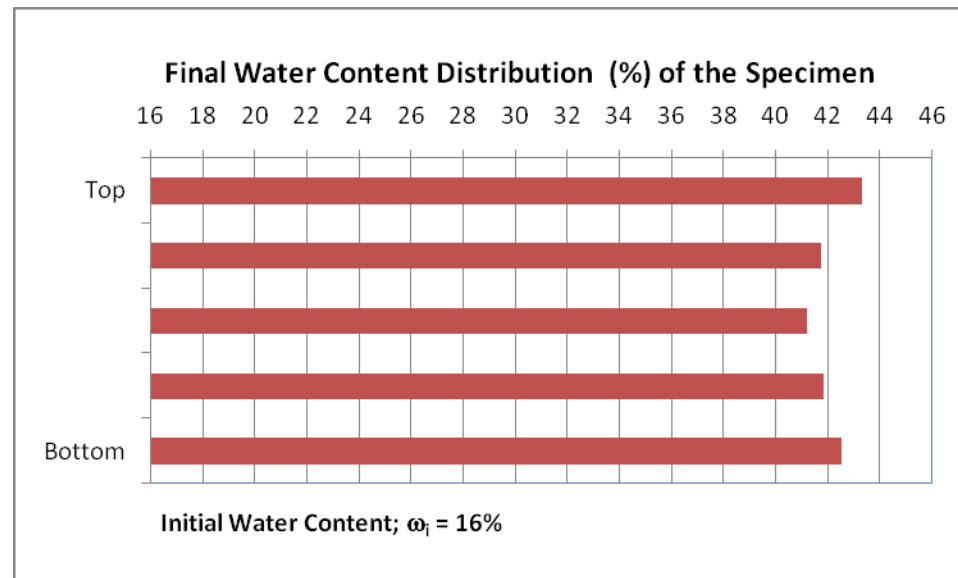
Figure B2.4: Initial and Final Water Contents Test No: 14; (22.08.2009)
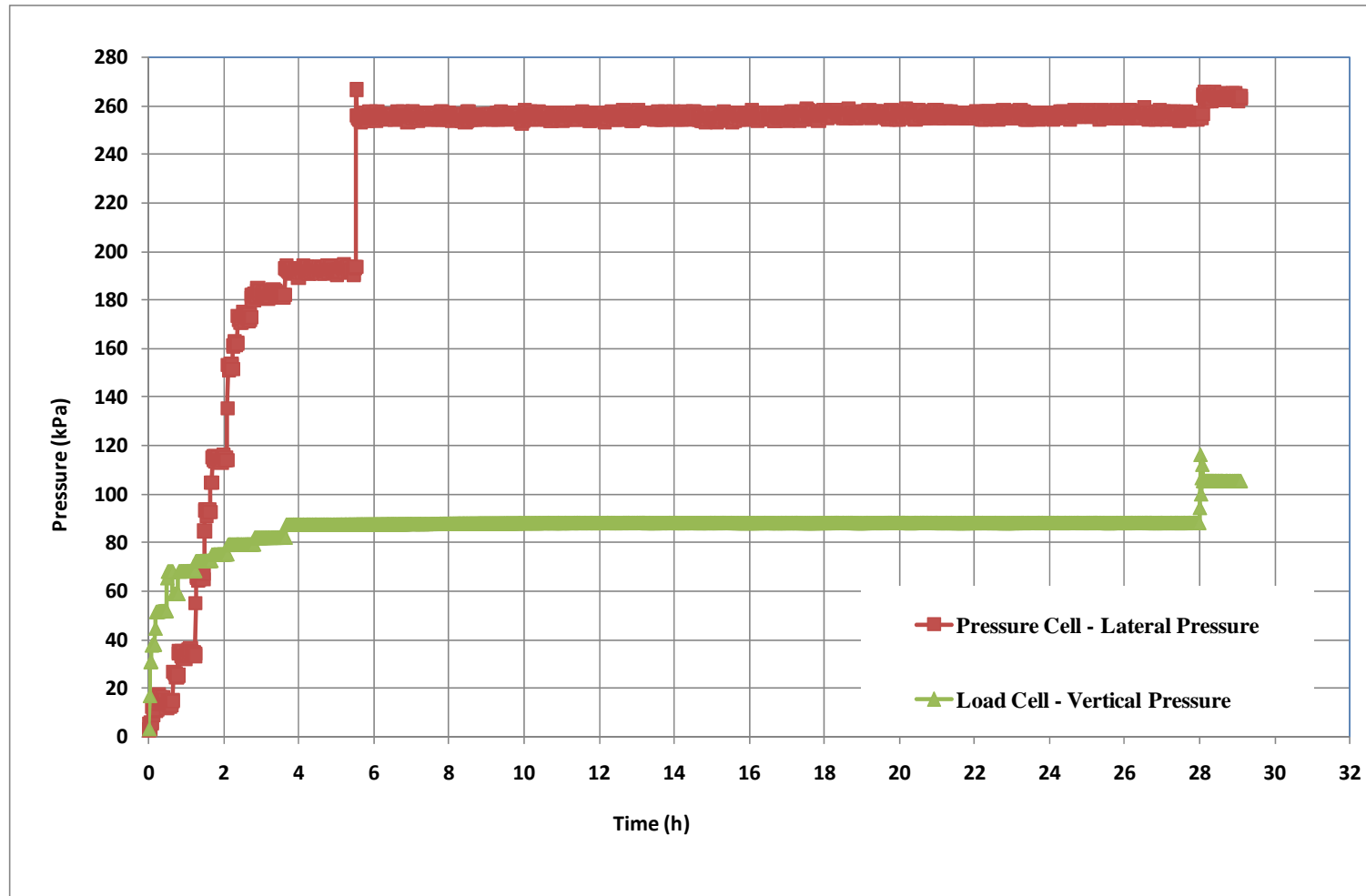
Figure B2.5: Pressure – Time Graph Test No: 14; (22.08.2009)
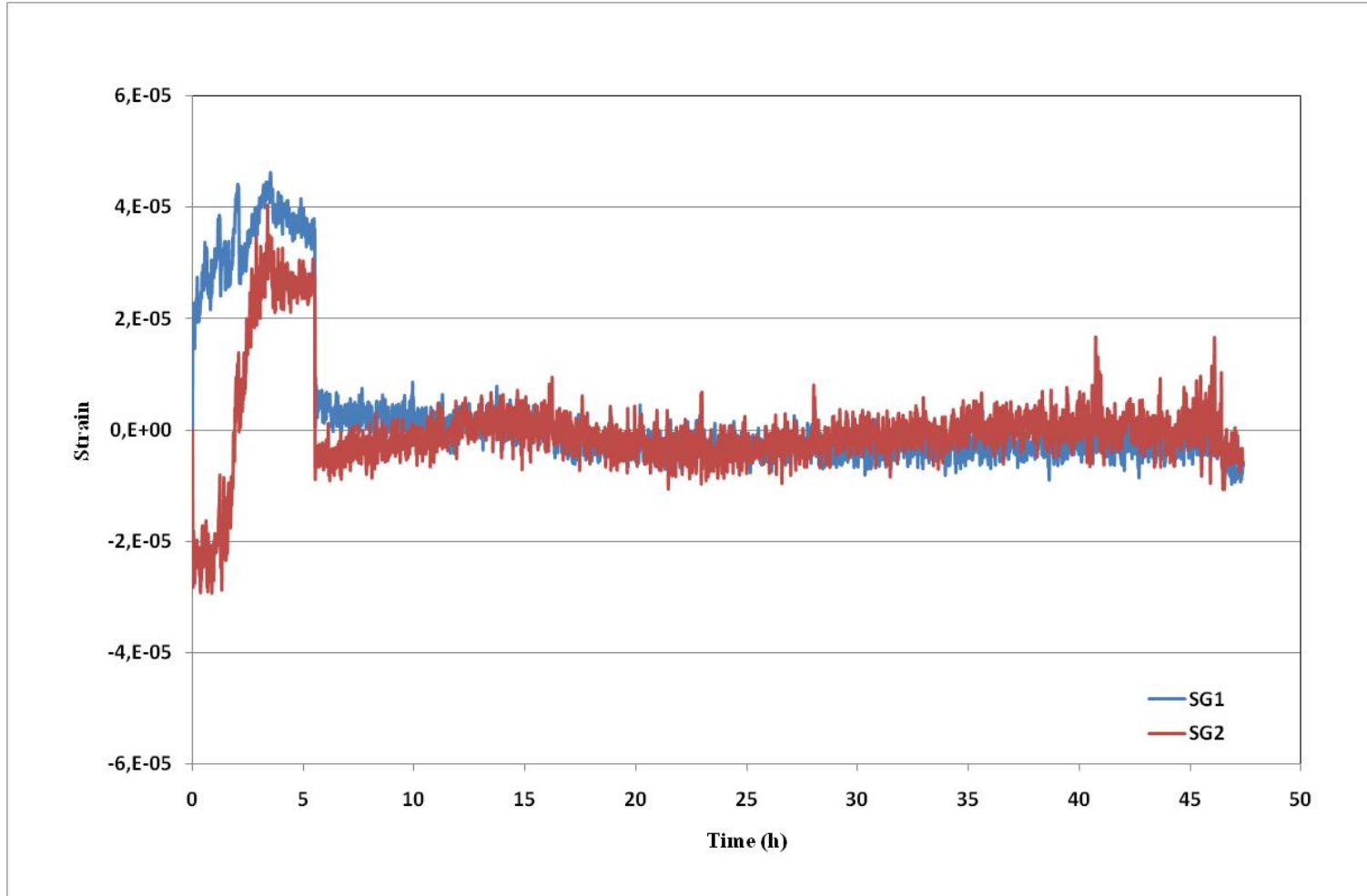
Figure B2.6: Strain – Time Graph Test No: 14; (22.08.2009)

TEST NO: 15	
Test Start:	
Date:	26.08.2009
Time:	11:40
Test Duration:	45,00 hours
Test End:	
Date:	28.08.2009
Time:	08:40
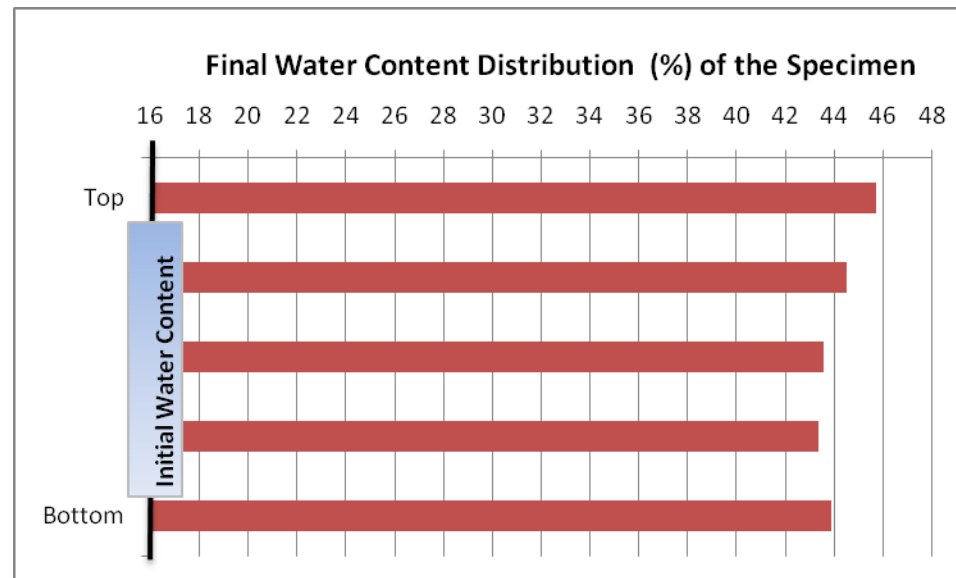
Figure B2.7: Initial and Final Water Contents Test No: 15; (26.08.2009)
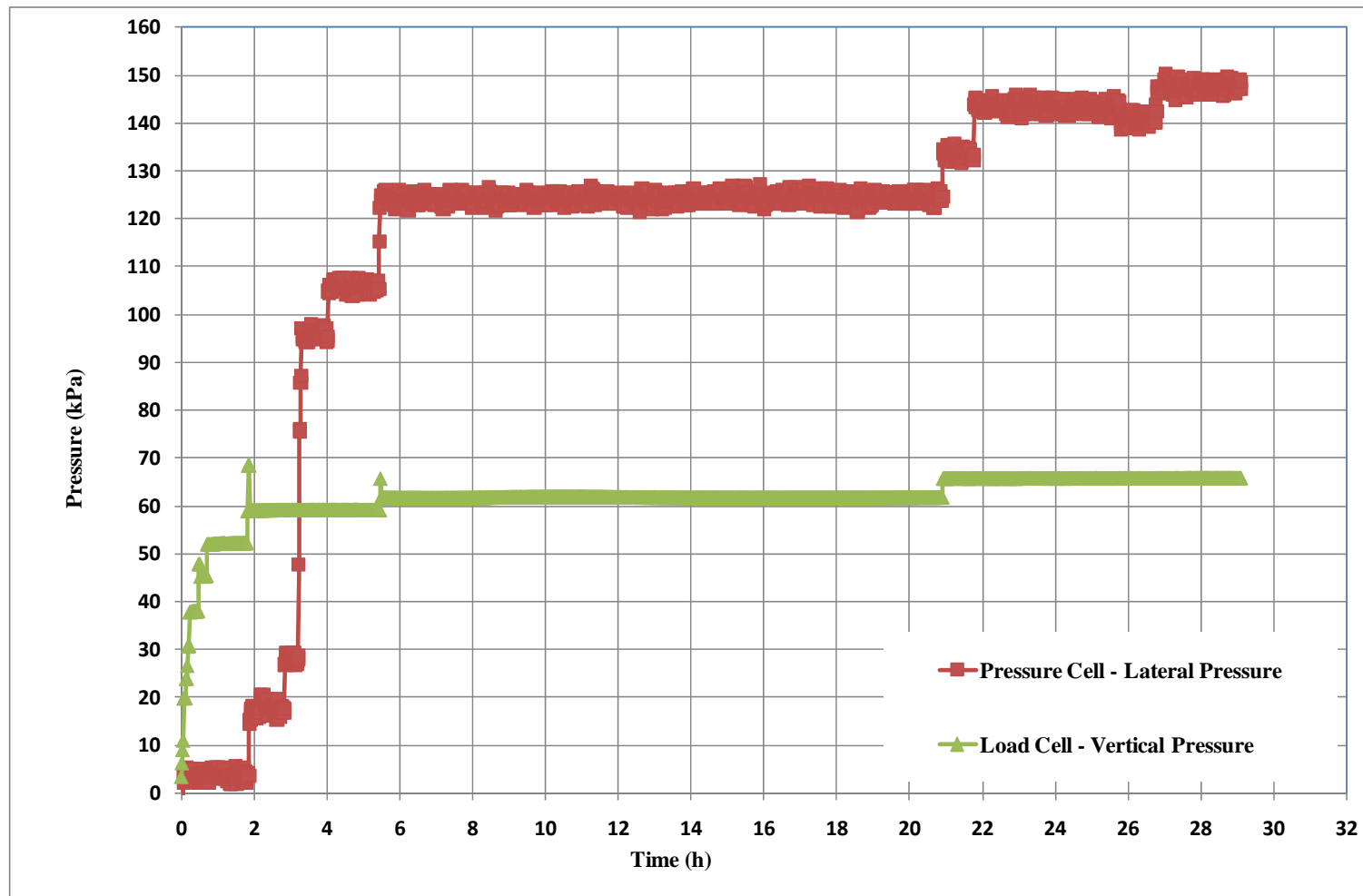
Figure B2.8: Pressure – Time Graph Test No: 15; (26.08.2009)
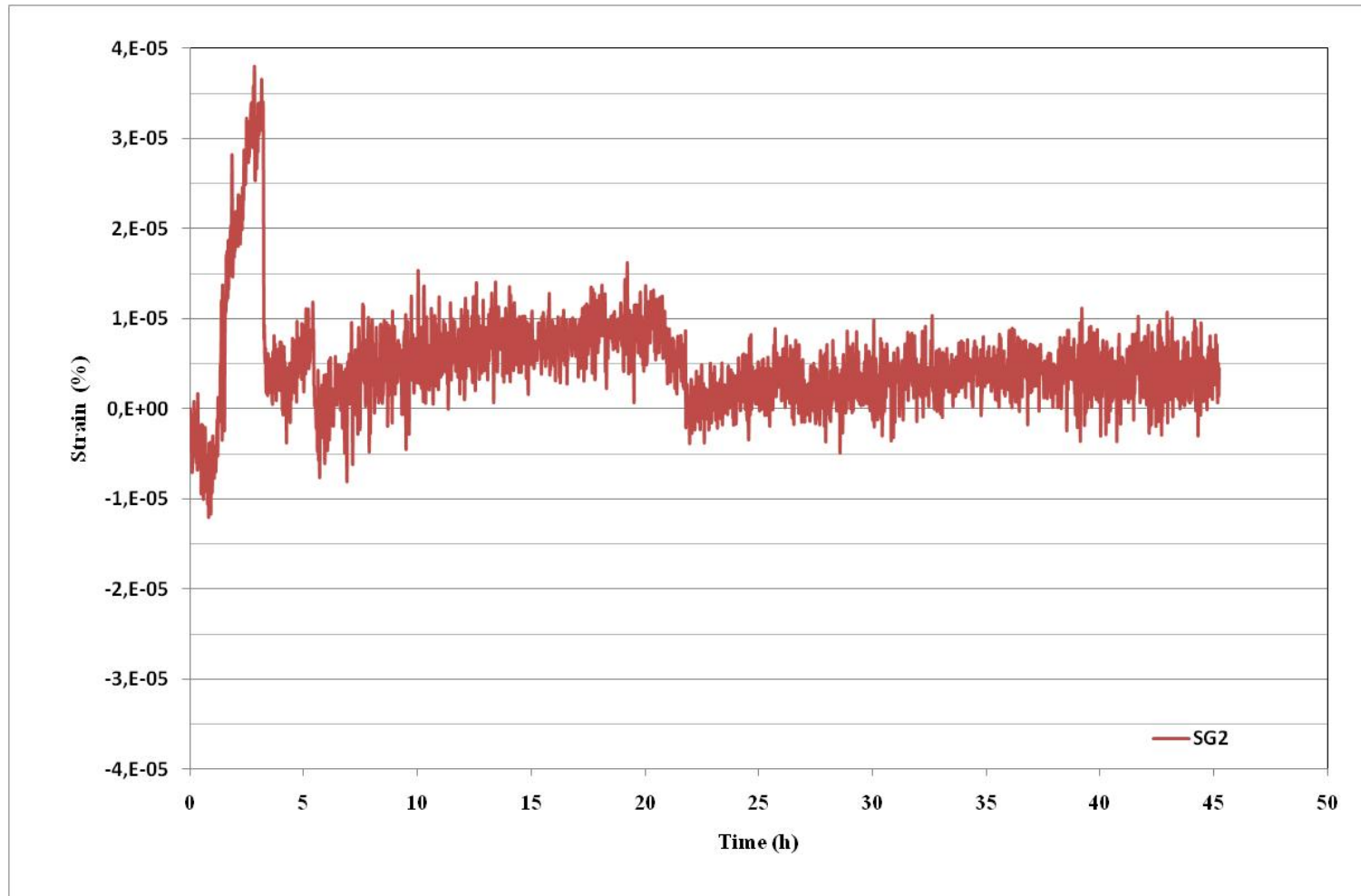
Figure B2.9: Strain – Time Graph Test No: 15; (26.08.2009)

APPENDIX C
CONSTANT VERTICAL SURCHARGE LATERAL FREE SWELL TESTS

TEST NO: 26	
Test Start:	
Date:	21.10.2009
Time:	15:20
Test Duration:	45 hours
Test End:	
Date:	23.10.2009
Time:	12:20
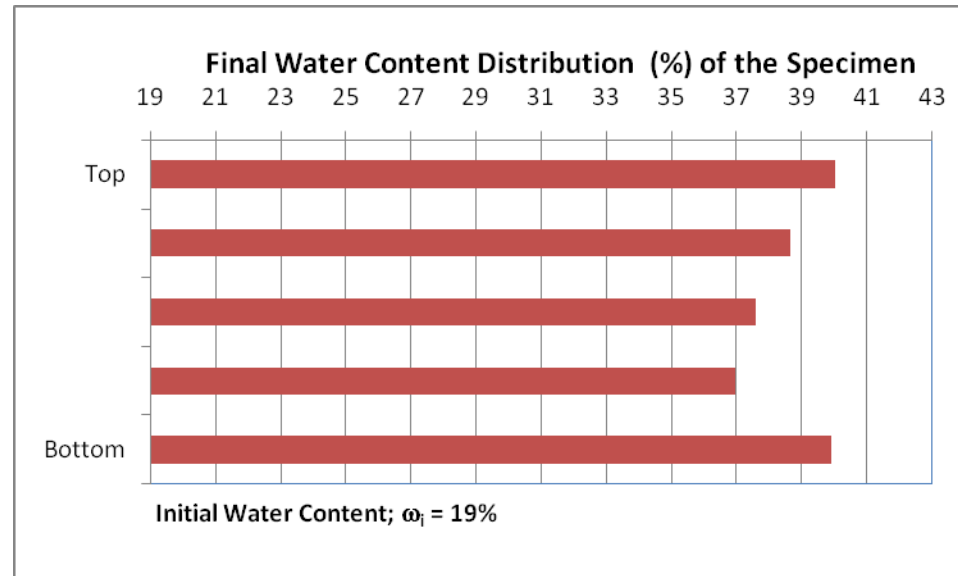
Figure C.1: Initial and Final Water Contents Test No: 26; (21.10.2009)
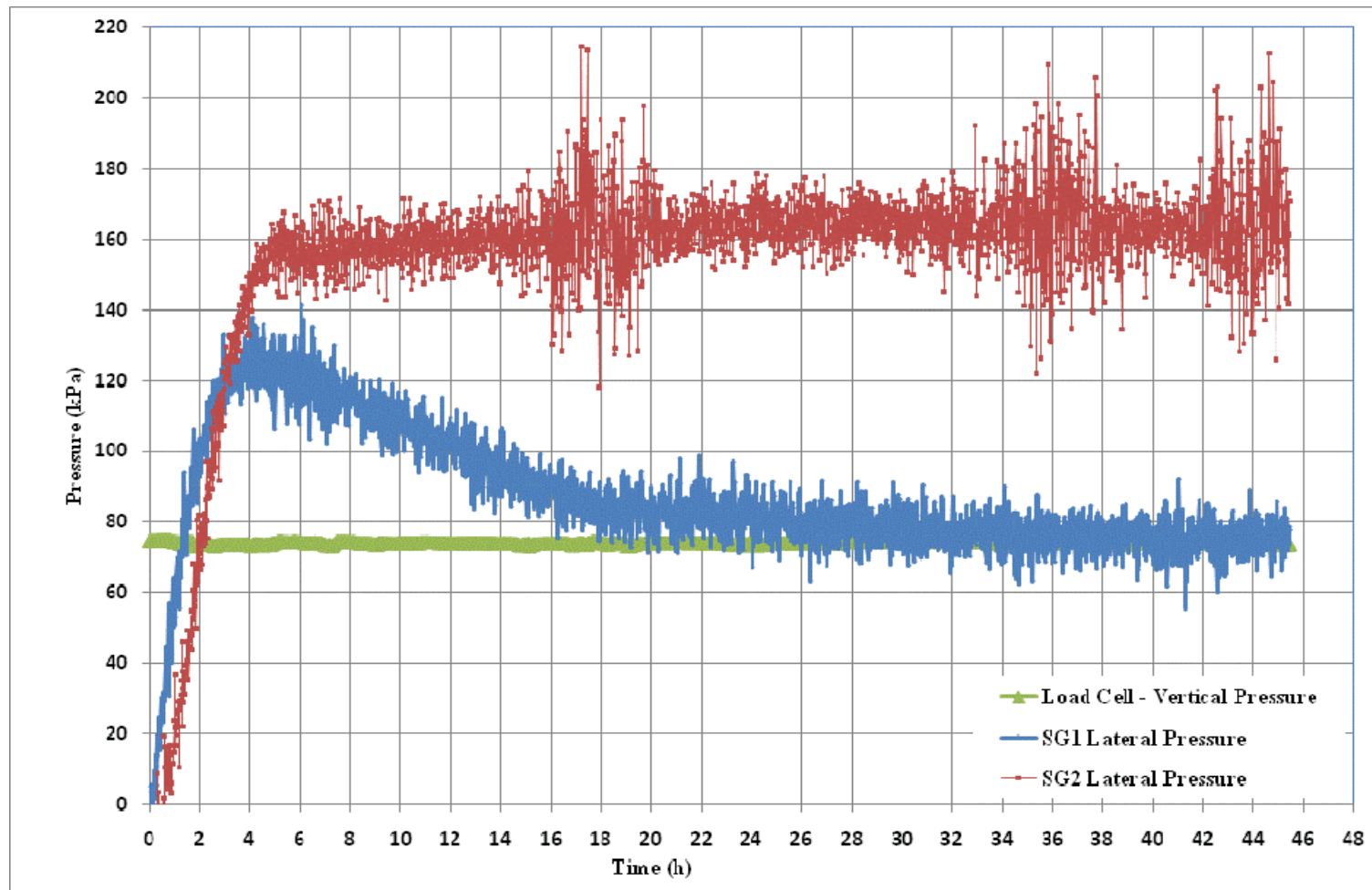
Figure C2: Pressure – Time Graph Test No: 26; (21.10.2009)
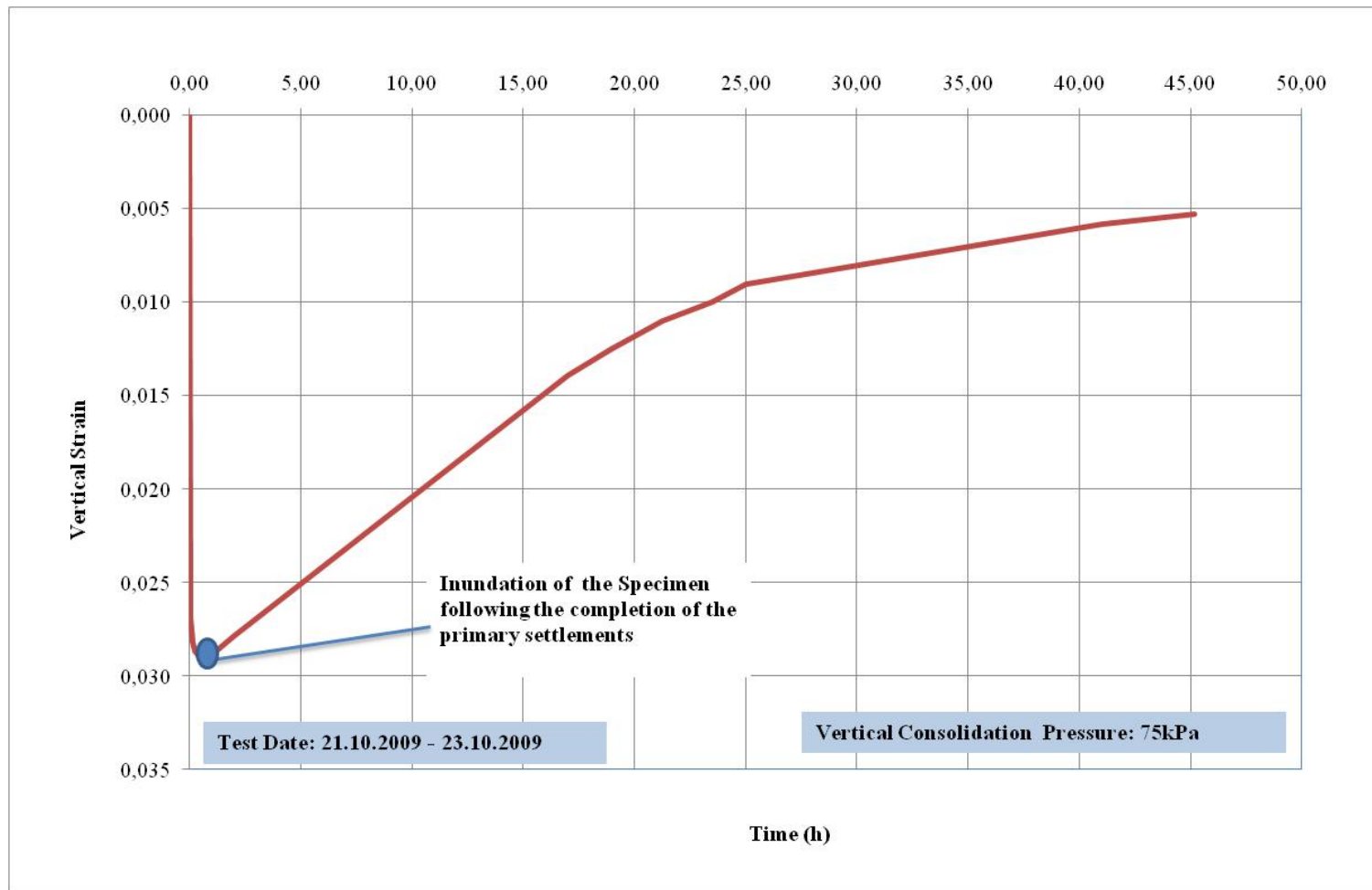
Figure C3: Vertical Strain – Time Graph Test No: 26; (21.10.2009)

TEST NO: 27	
Test Start:	
Date:	24.10.2009
Time:	08:00
Test Duration:	74 hours
Test End:	
Date:	27.10.2009
Time:	10:00
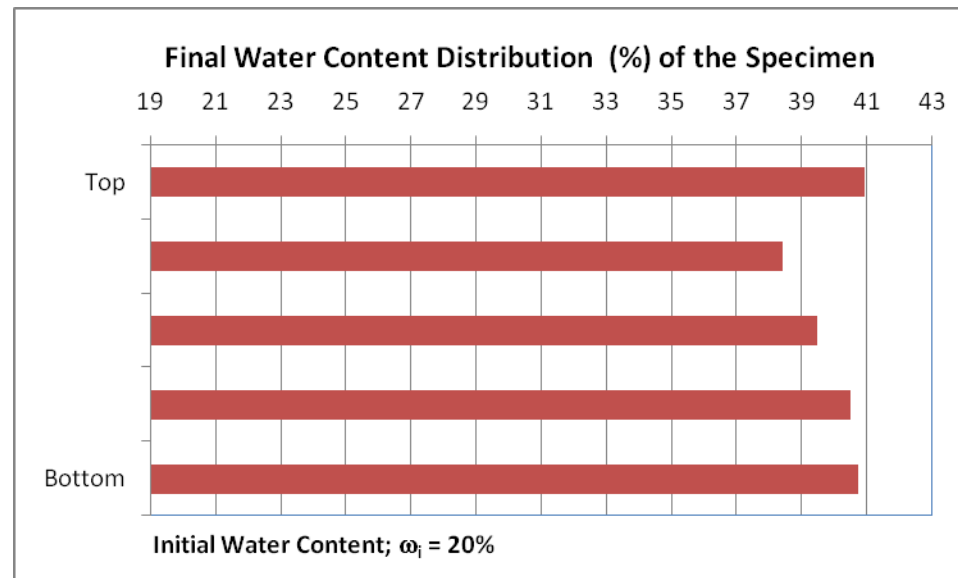
Figure C4: Initial and Final Water Contents Test No: 27; (24.10.2009)
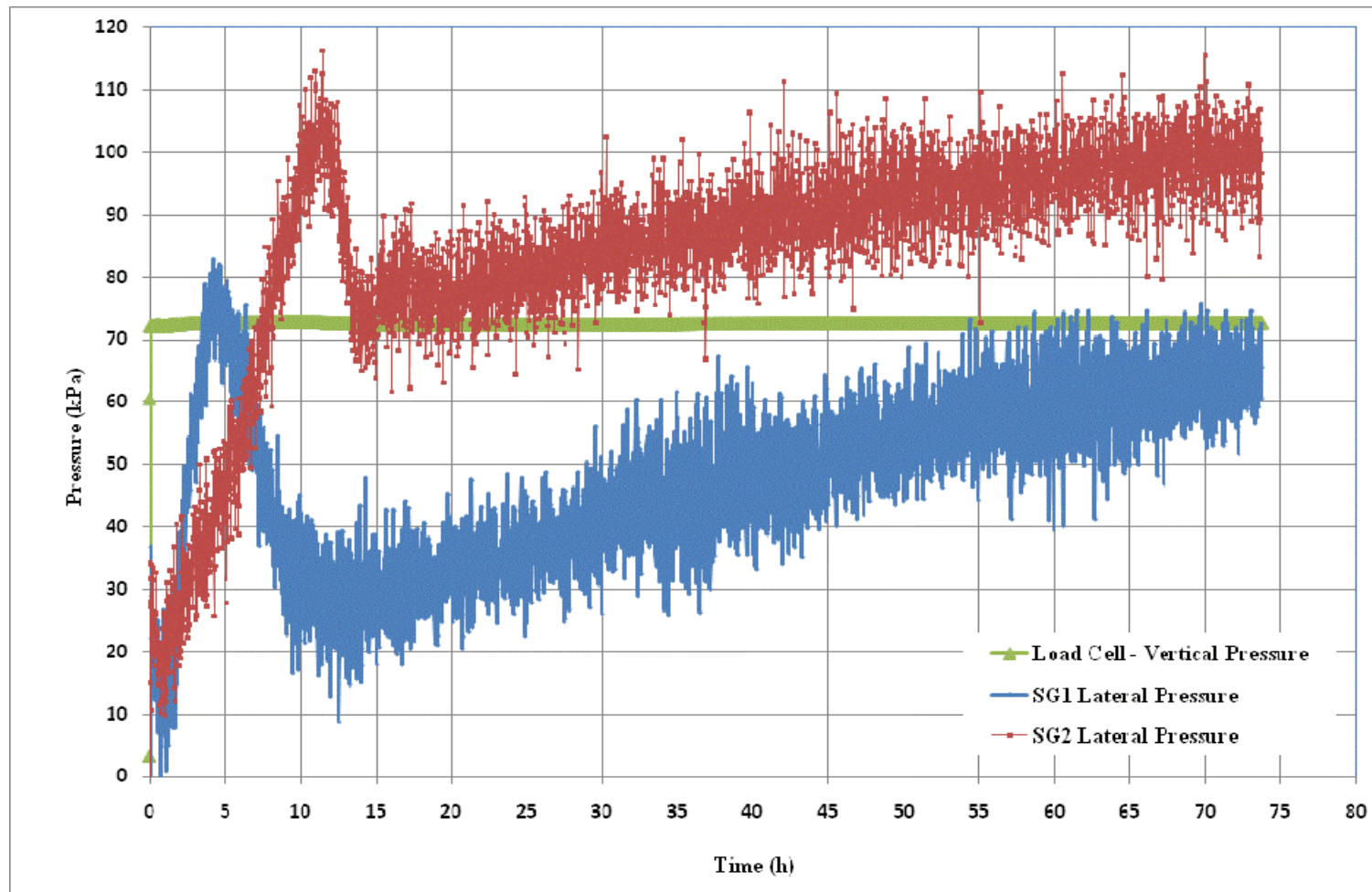
Figure C5: Pressure – Time Graph Test No: 27; (24.10.2009)
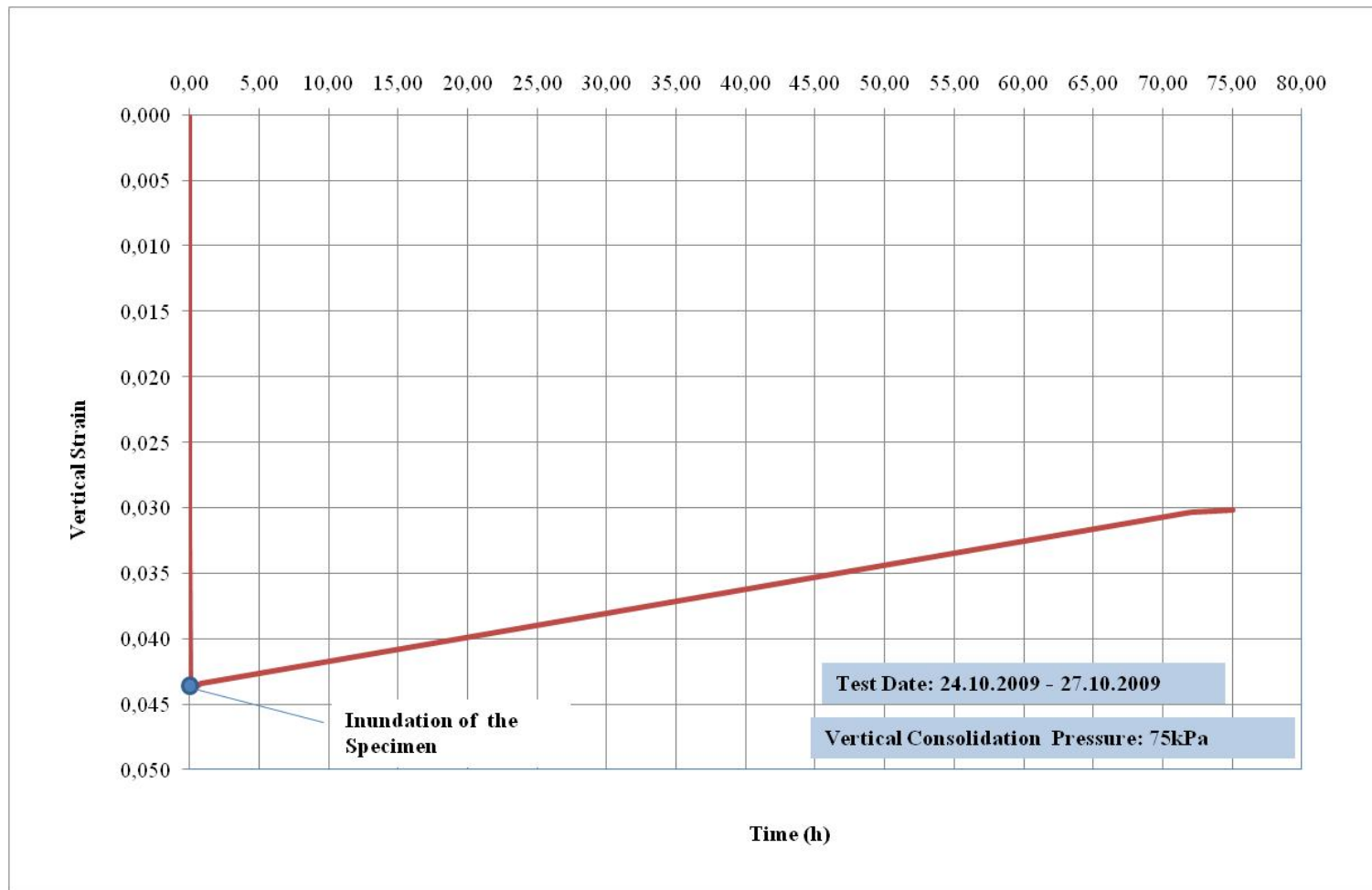
Figure C6: Vertical Strain – Time Graph Test No: 27; (24.10.2009)

TEST NO: 28	
Test Start:	
Date:	28.10.2009
Time:	09:00:00
Test Duration:	125 hours
Test End:	
Date:	02.11.2009
Time:	09:05:00

Final Water Content Distribution (%) of the Specimen

Initial Water Conent; ω_i = 19%
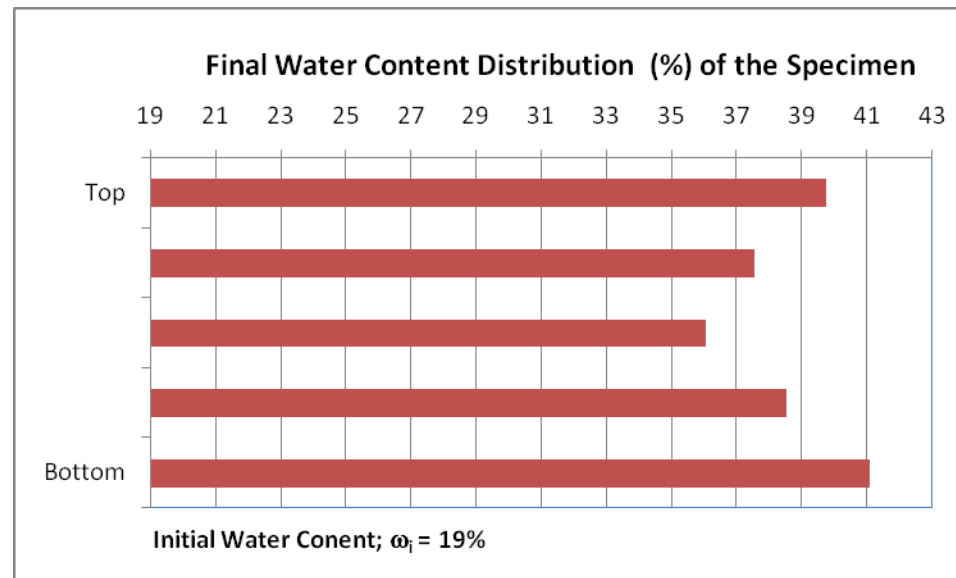
Figure C7: Initial and Final Water Contents Test No: 28; (28.10.2009)
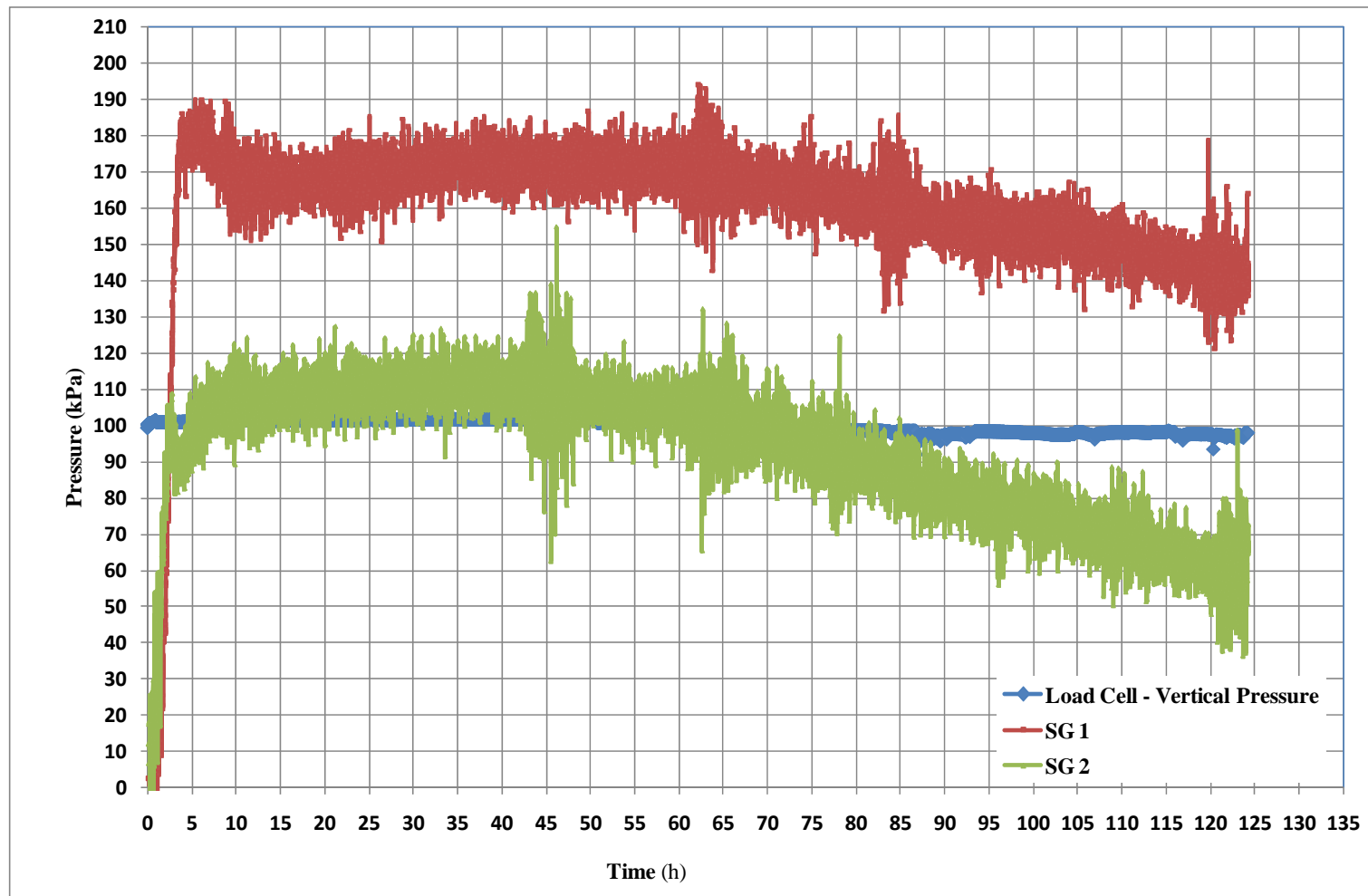
Figure C8: Pressure – Time Graph Test No: 28; (28.10.2009)
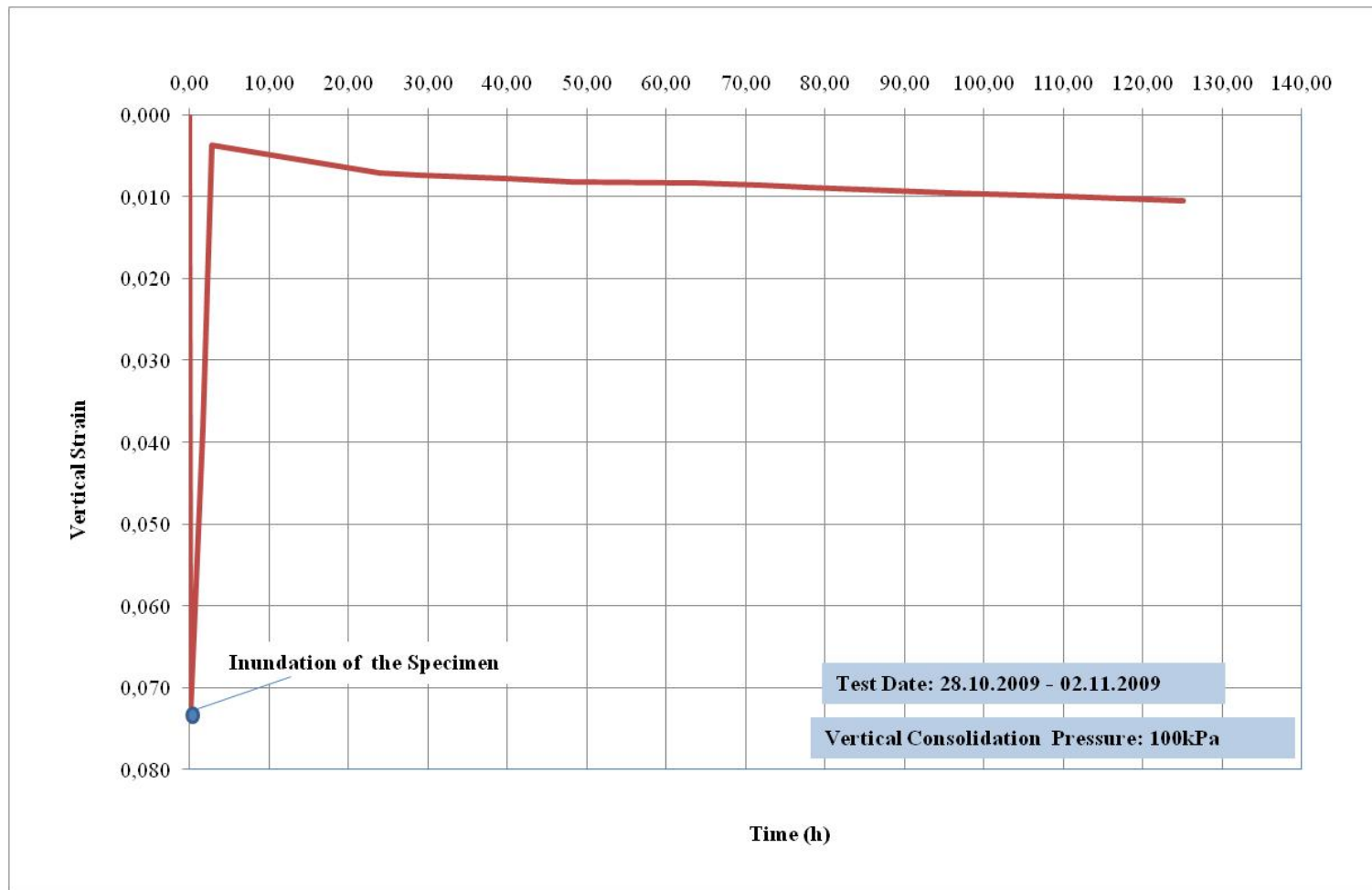
Figure C9: Vertical Strain – Time Graph Test No: 28; (28.10.2009)

TEST NO: 29	
Test Start:	
Date:	03.11.2009
Time:	14:00
Test Duration:	51,00 hours
Test End:	
Date:	05.11.2009
Time:	17:00
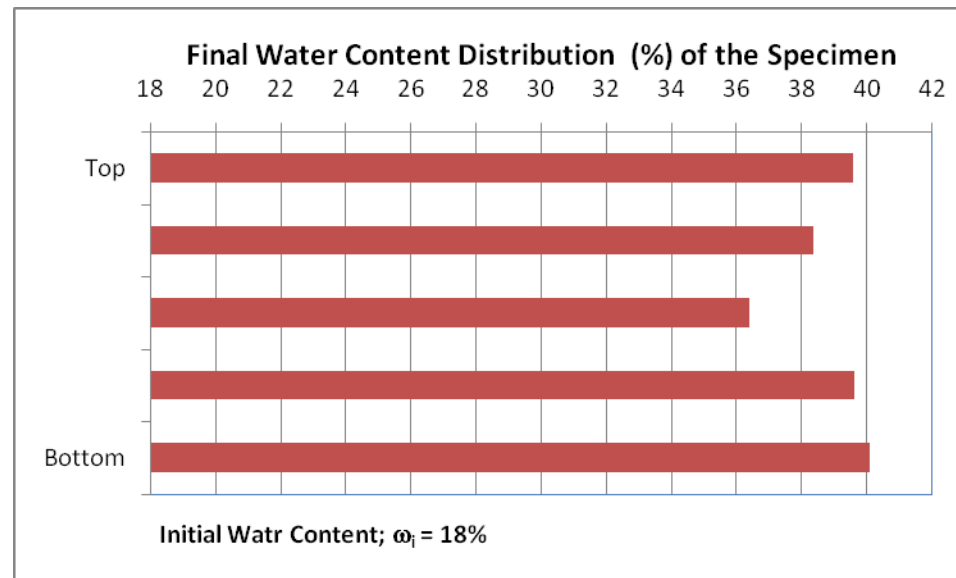
Figure C10: Initial and Final Water Contents Test No: 29; (03.11.2009)
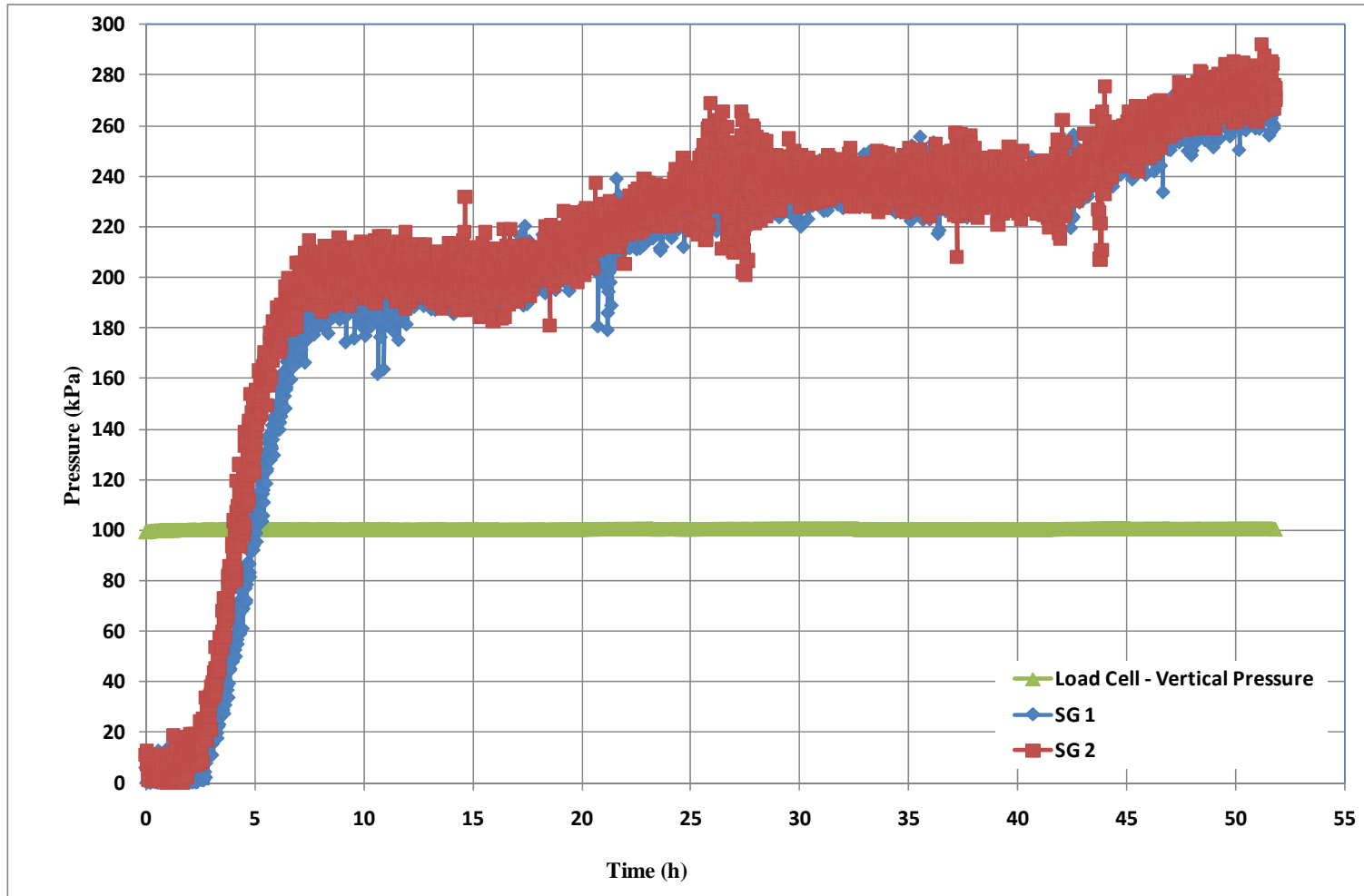
Figure C11: Pressure – Time Graph Test No: 29; (03.11.2009)
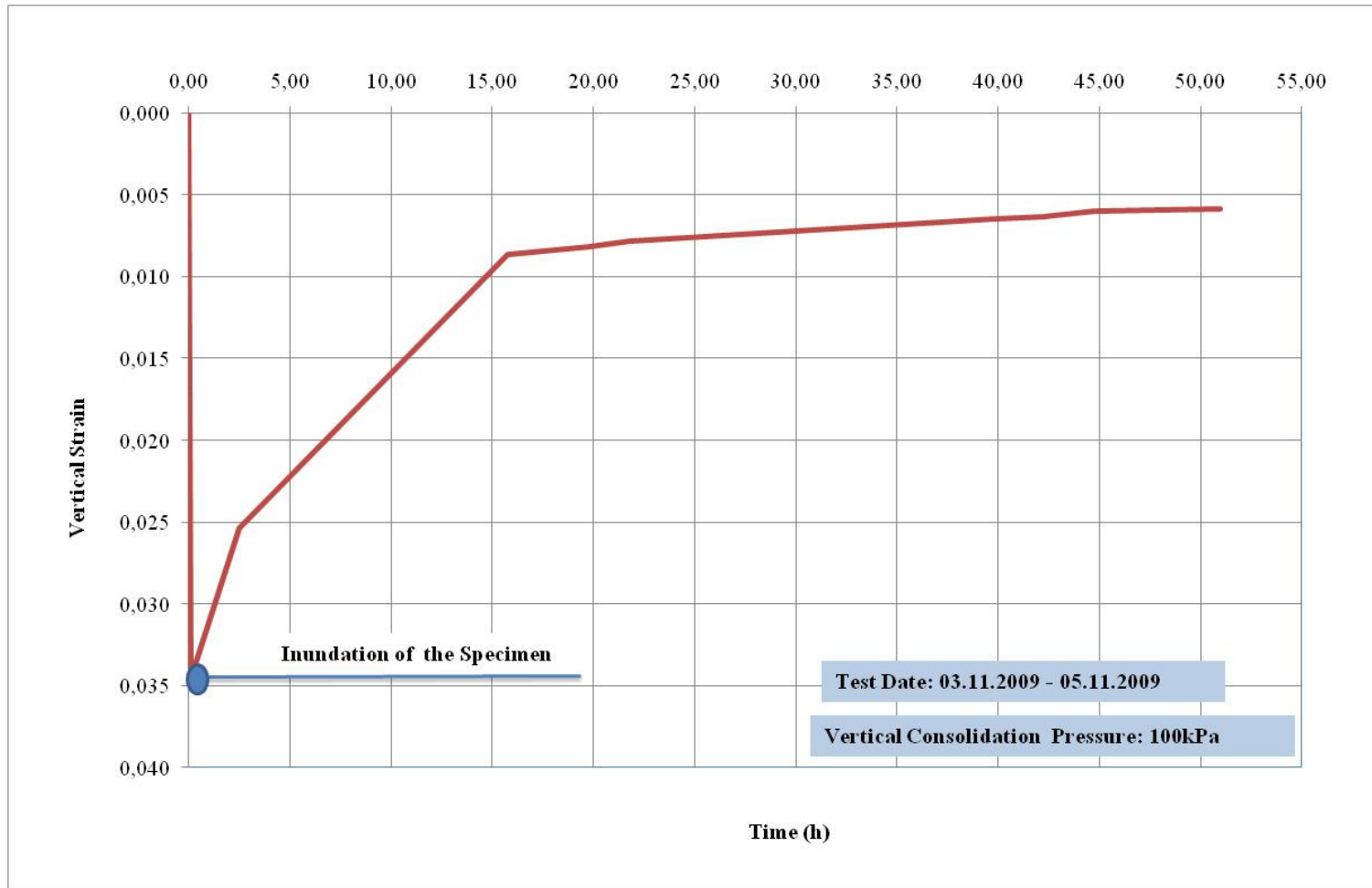
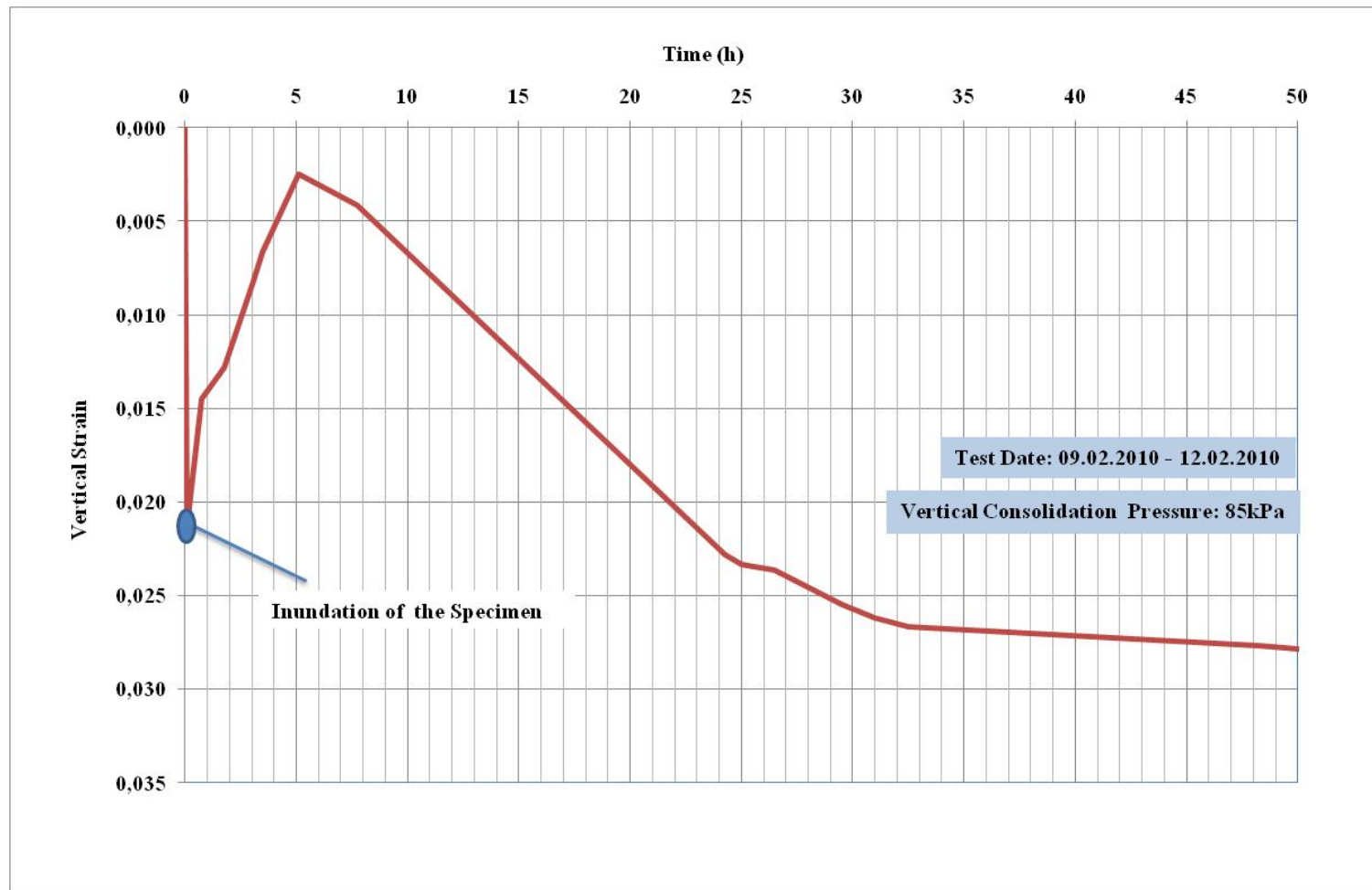**Figure C12:** Vertical Strain – Time Graph Test No: 29; (03.11.2009)

TEST NO: 32	
Test Start:	
Date:	04.12.2009
Time:	13:00
Test Duration:	67 hours
Test End:	
Date:	06.12.2009
Time:	08:00
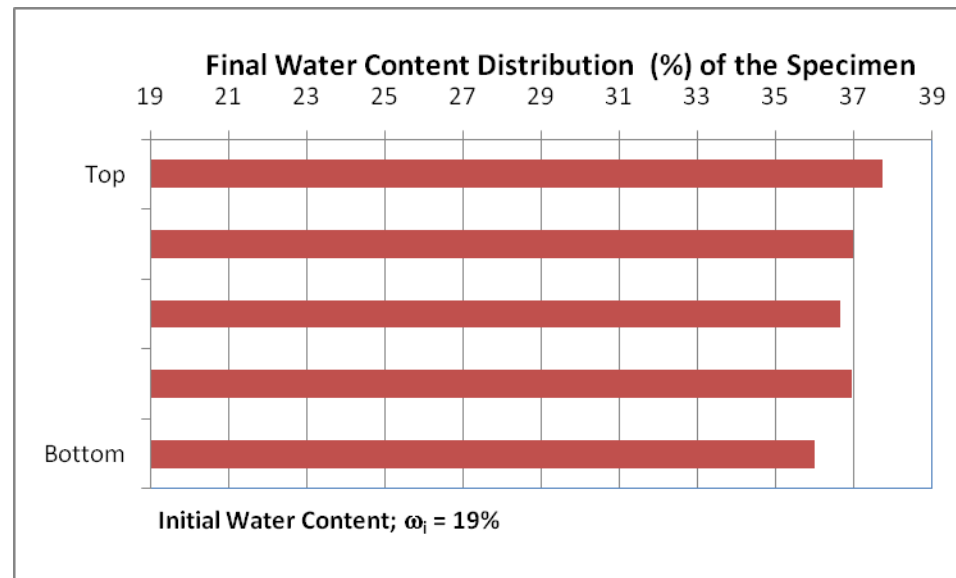
Figure C13: Initial and Final Water Contents Test No: 32; (04.12.2009)
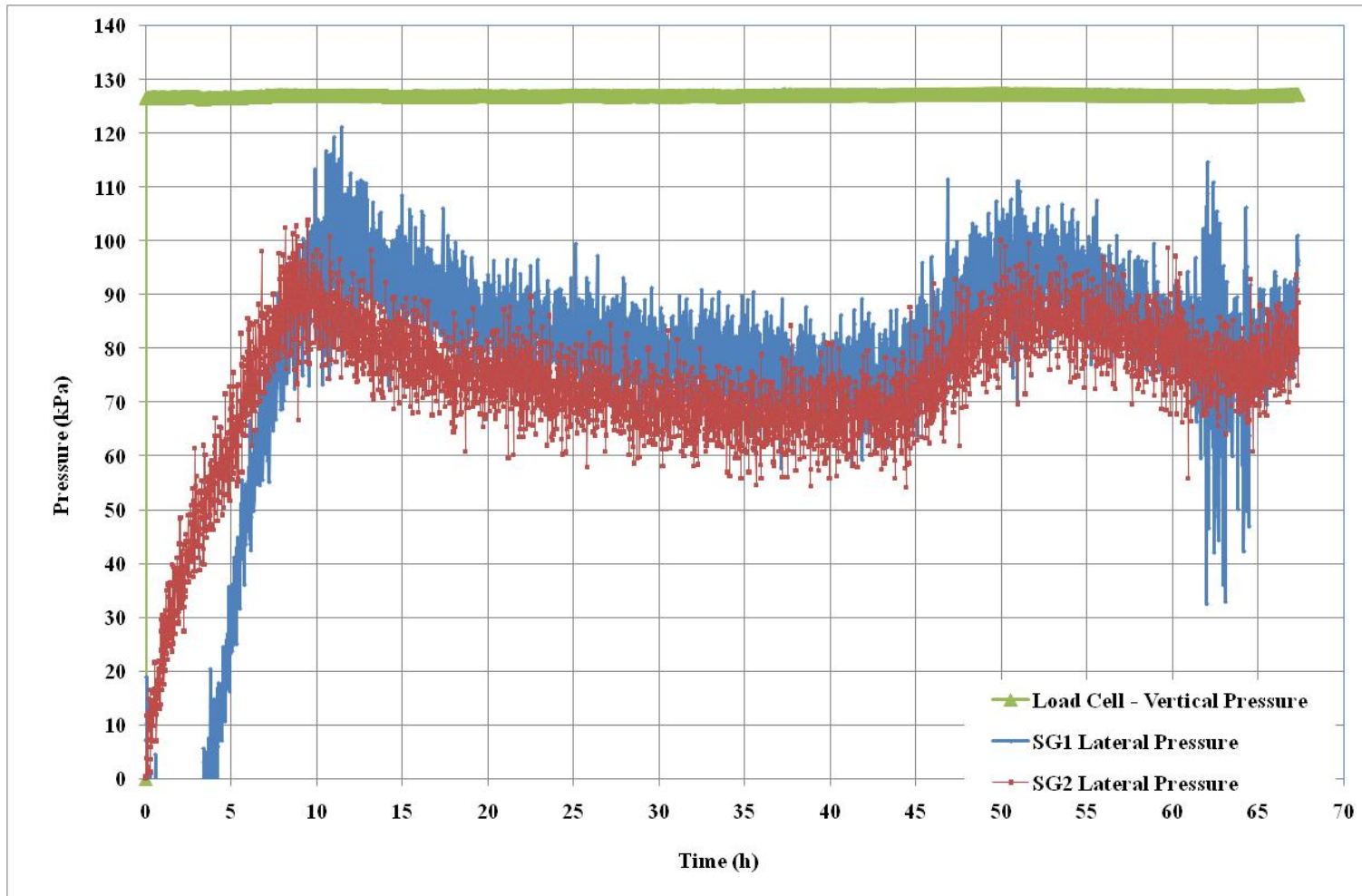
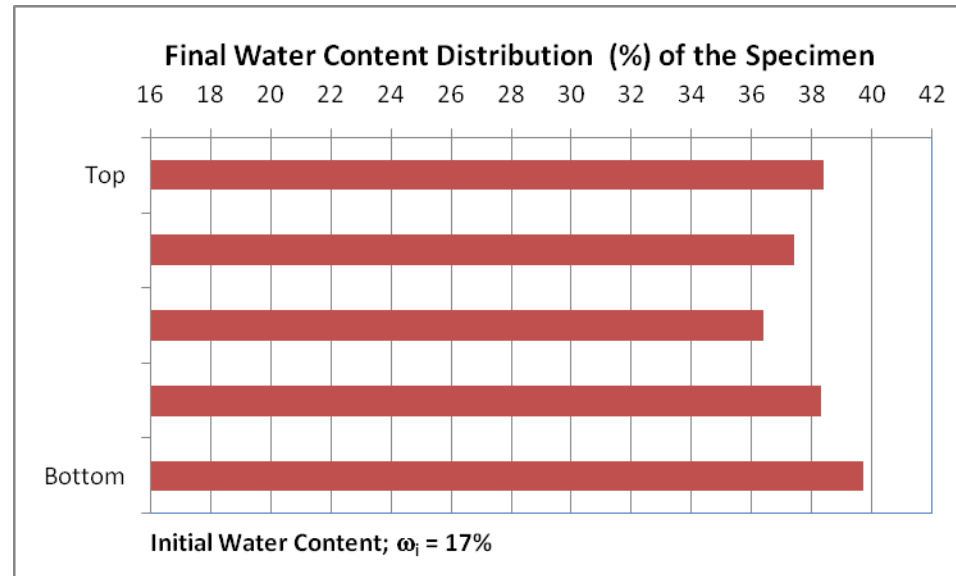**Figure C14:** Pressure – Time Graph Test No: 32; (04.12.2009)
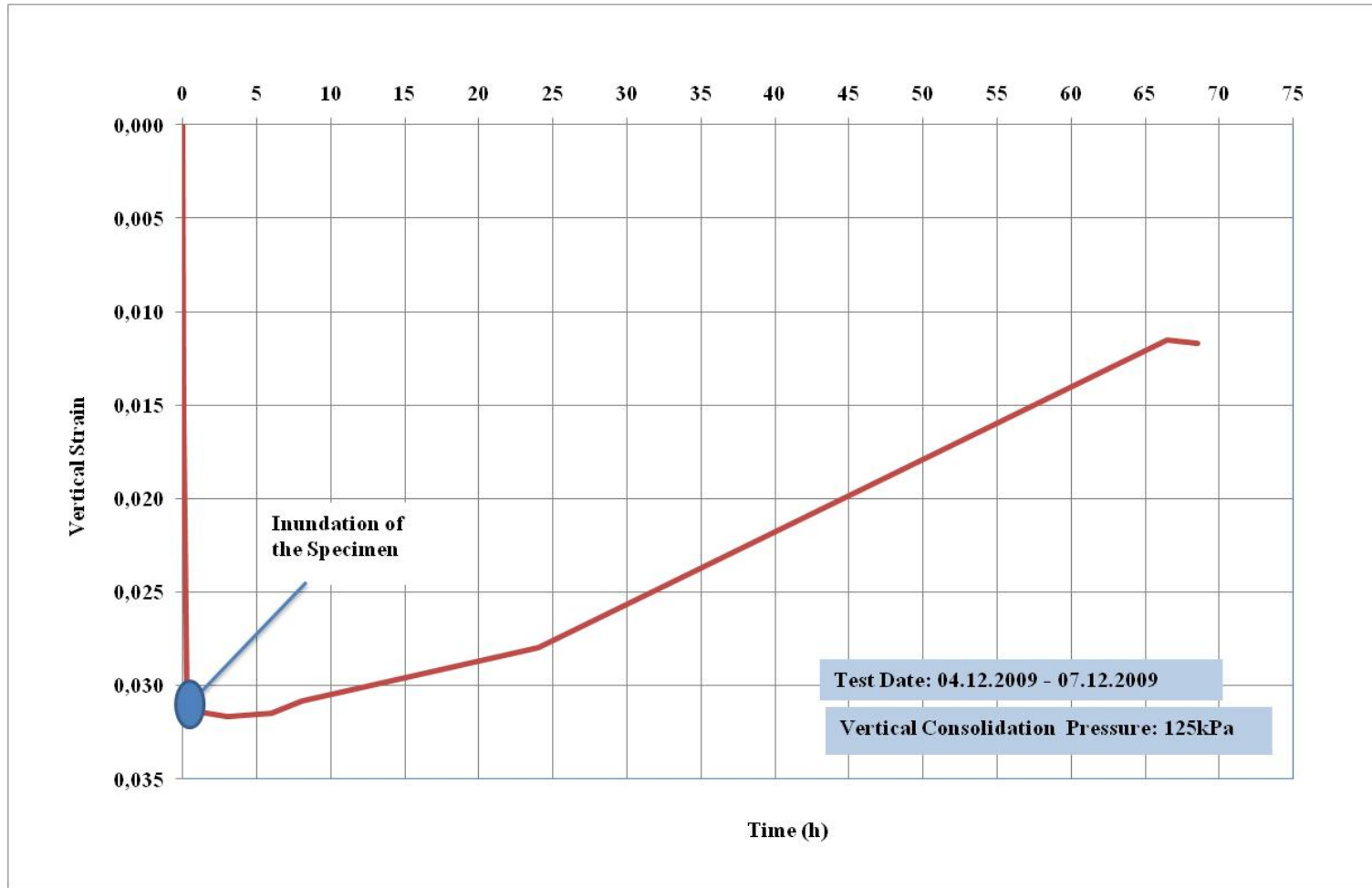
Figure C15: Vertical Strain – Time Graph Test No: 32; (04.12.2009)

TEST NO: 33	
Test Start:	
Date:	08.12.2009
Time:	09:30
Test Duration:	96 hours
Test End:	
Date:	12.12.2009
Time:	09:30

Figure C16: Initial and Final Water Contents Test No: 33; (08.12.2009)
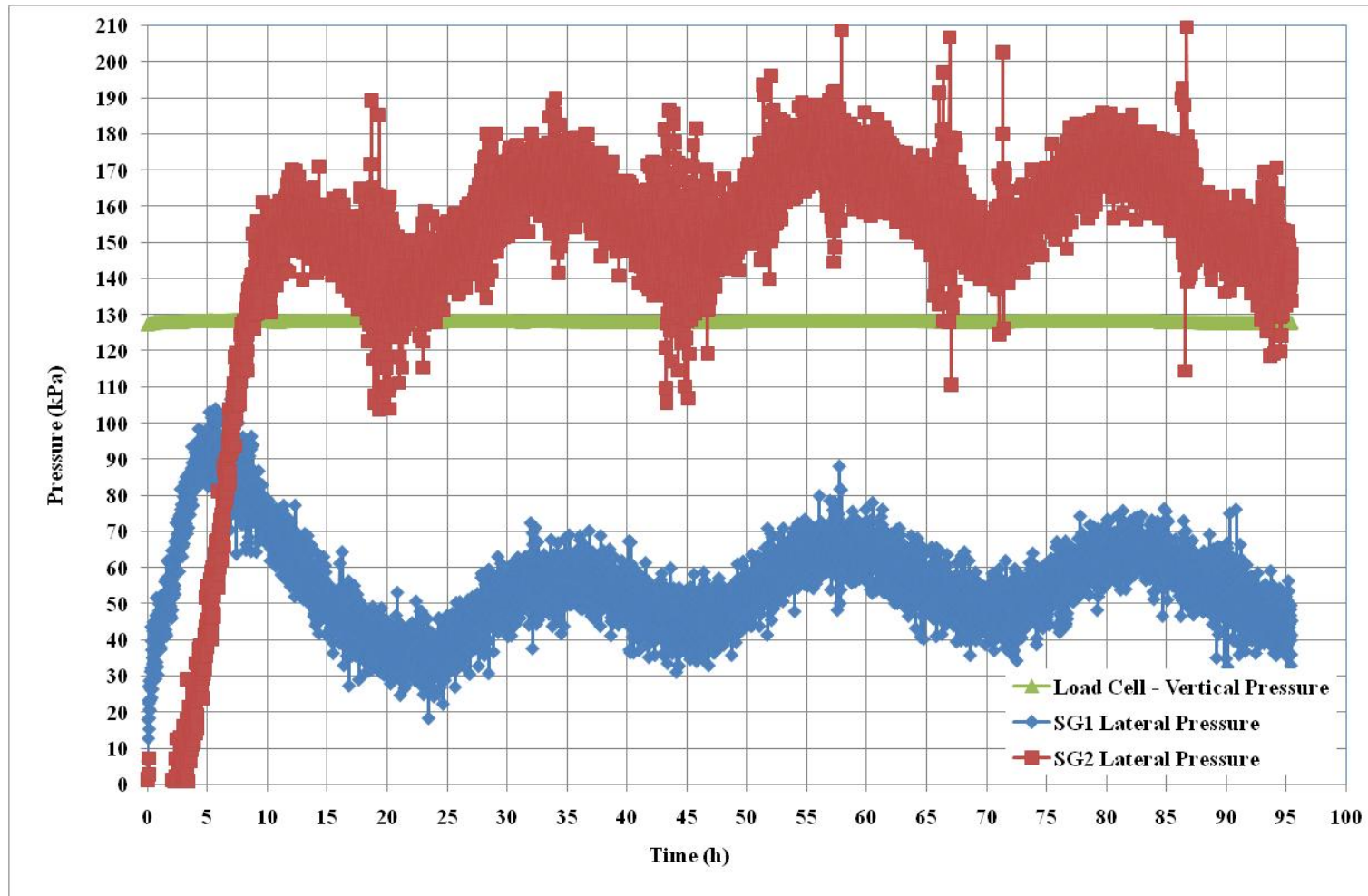
Figure C17: Pressure – Time Graph Test No: 33; (08.12.2009)
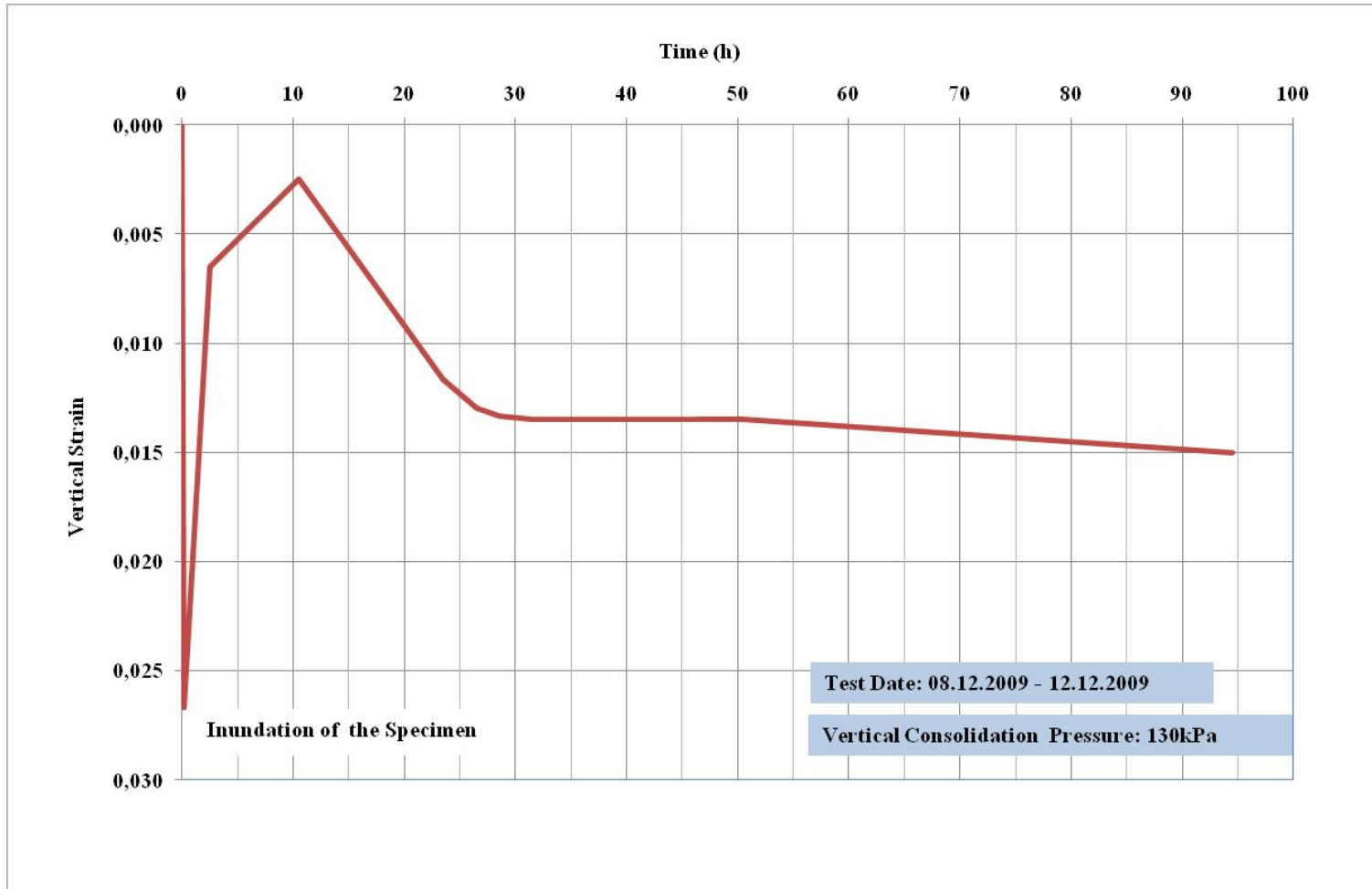
Figure C18: Vertical Strain – Time Graph Test No: 33; (08.12.2009)

TEST NO: 34	
Test Start:	
Date:	12.12.2009
Time:	11:45
Test Duration:	70,00 hours
Test End:	
Date:	15.12.2009
Time:	09:45
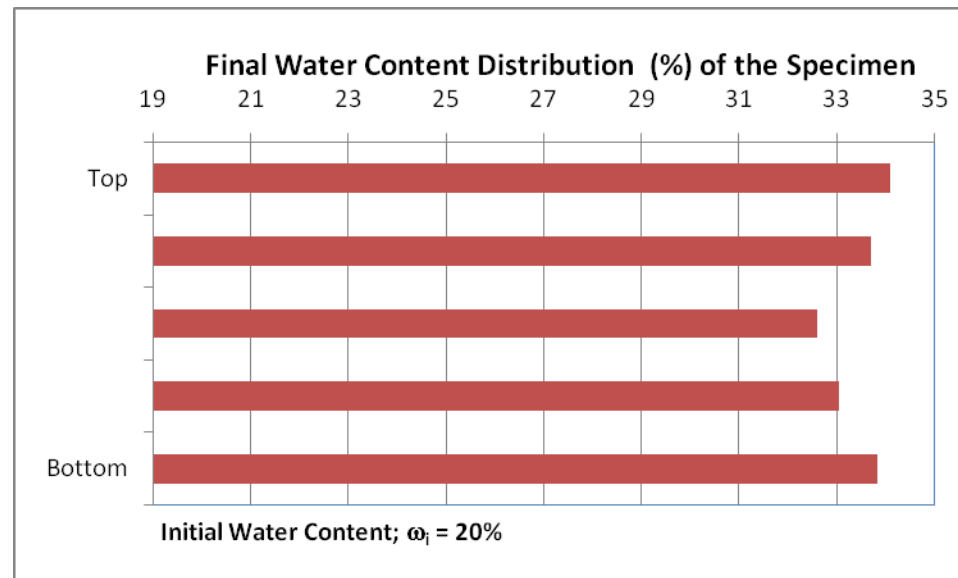
Figure C19: Initial and Final Water Contents Test No: 34; (12.12.2009)
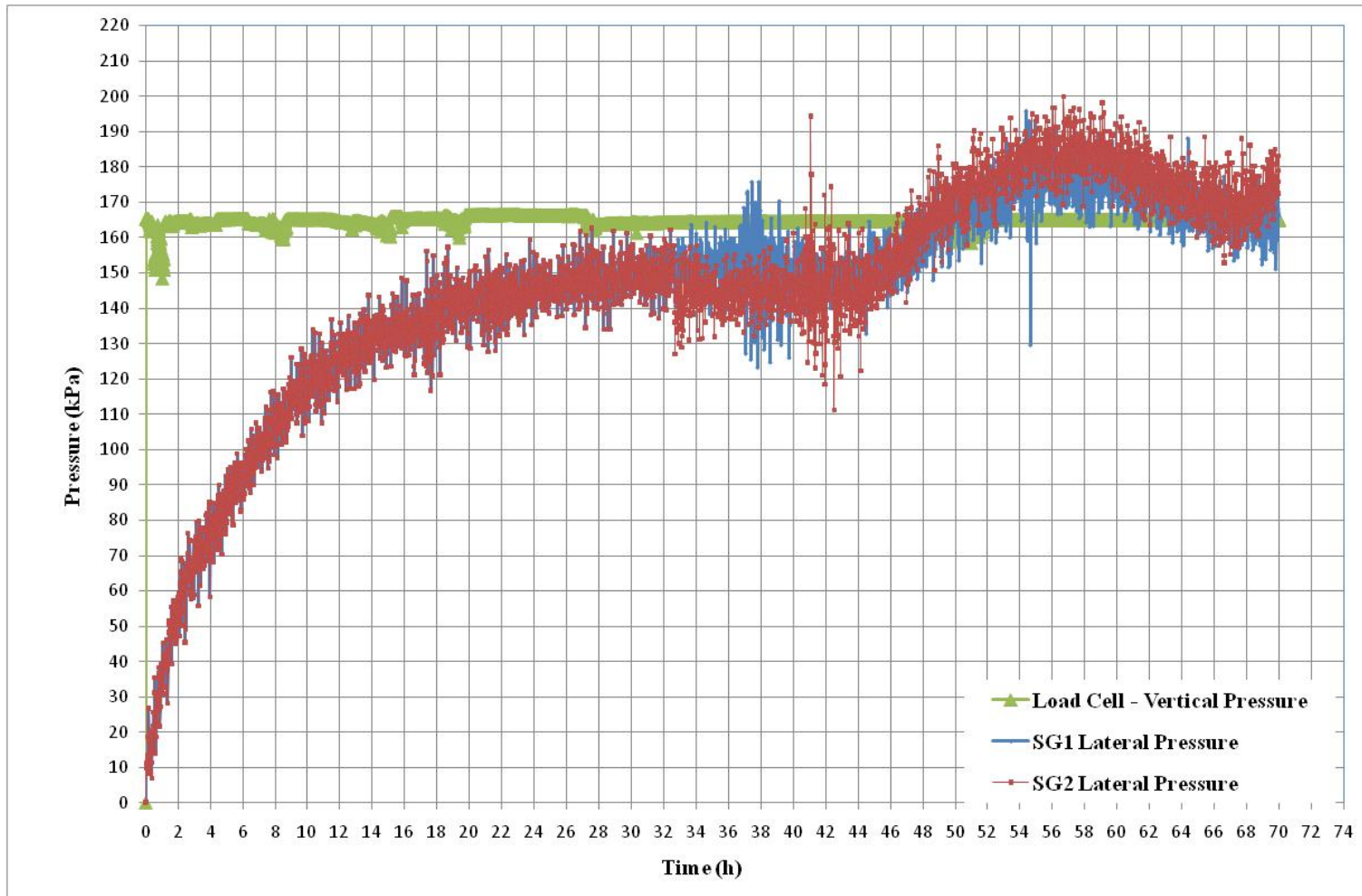
Figure C20: Pressure – Time Graph Test No: 34; (12.12.2009)
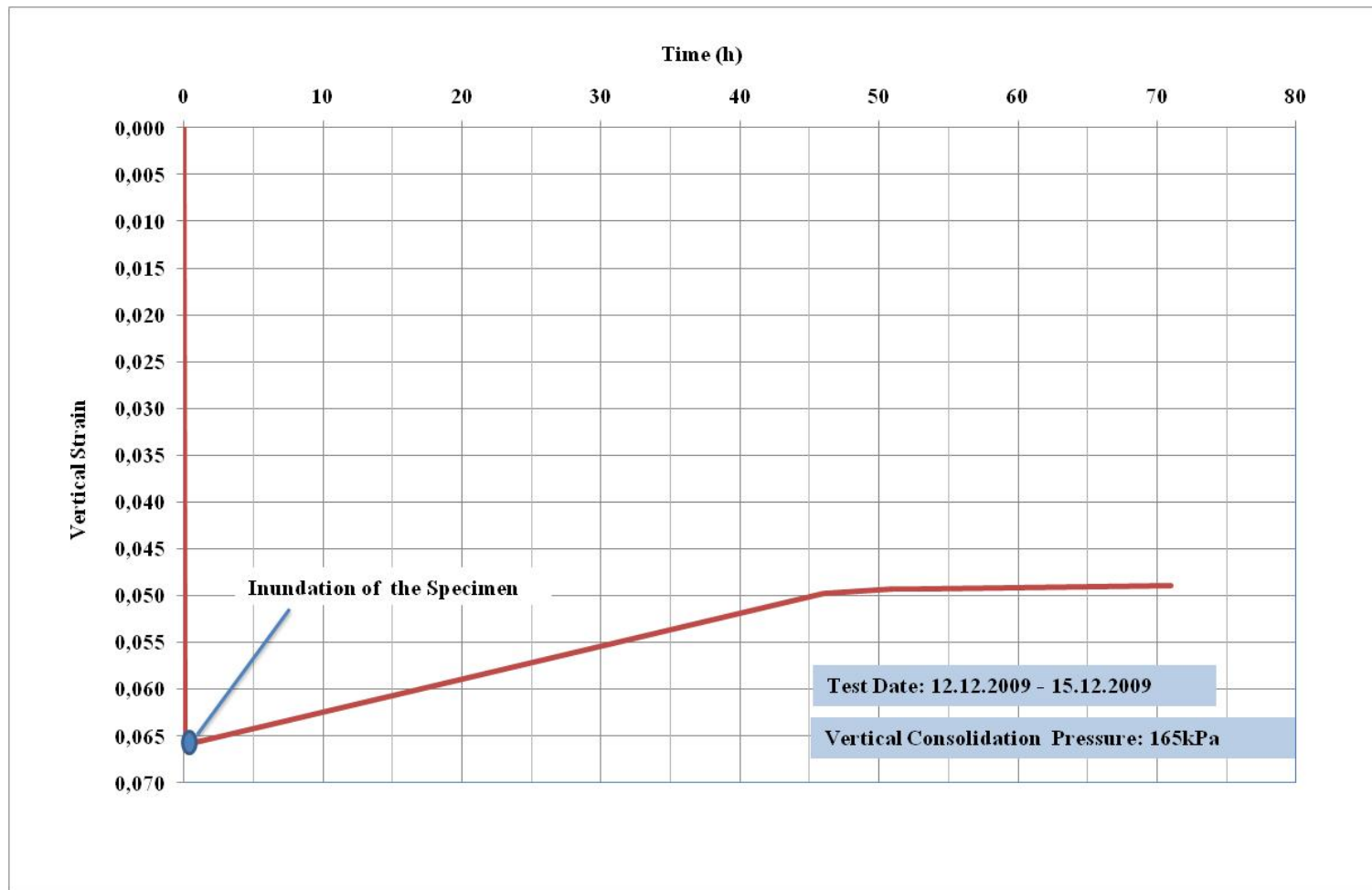
Figure C21: Vertical Strain – Time Graph Test No: 34; (12.12.2009)

TEST NO: 37	
Test Start:	
Date:	29.12.2009
Time:	17:00
Test Duration:	45 hours
Test End:	
Date:	31.12.2009
Time:	12:00
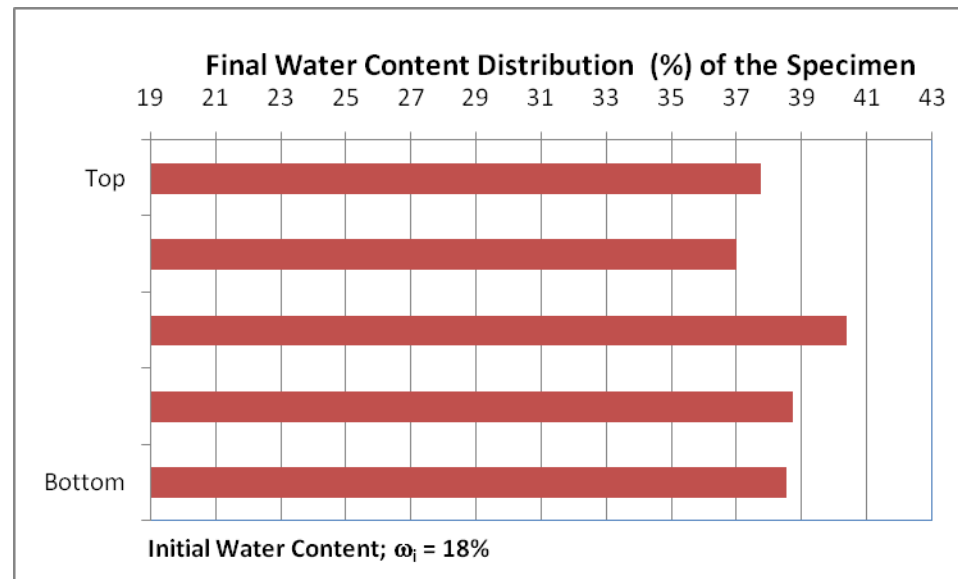
Figure C22: Initial and Final Water Contents Test No: 37; (29.12.2009)
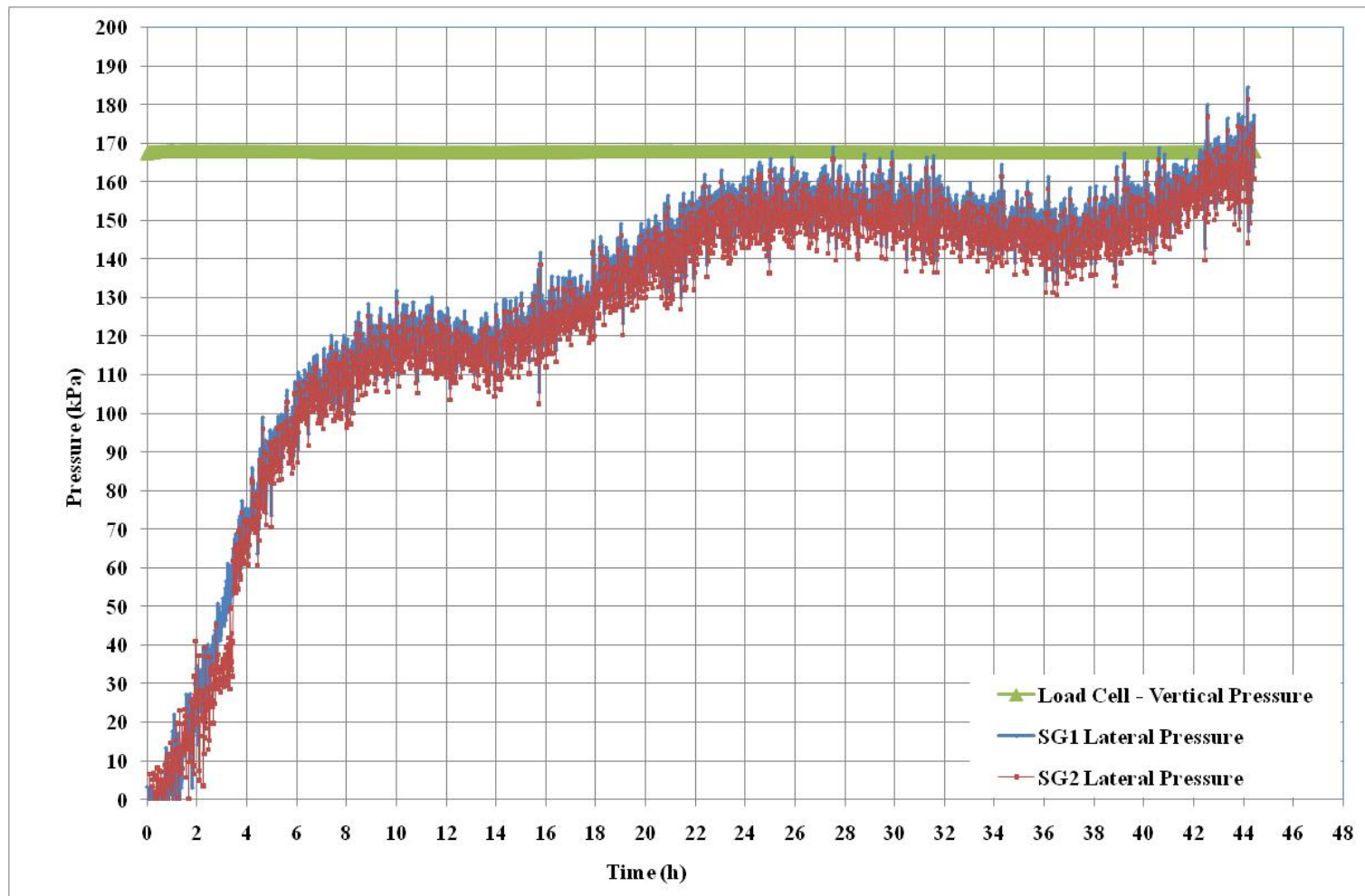
Figure C23: Pressure – Time Graph Test No: 37; (29.12.2009)
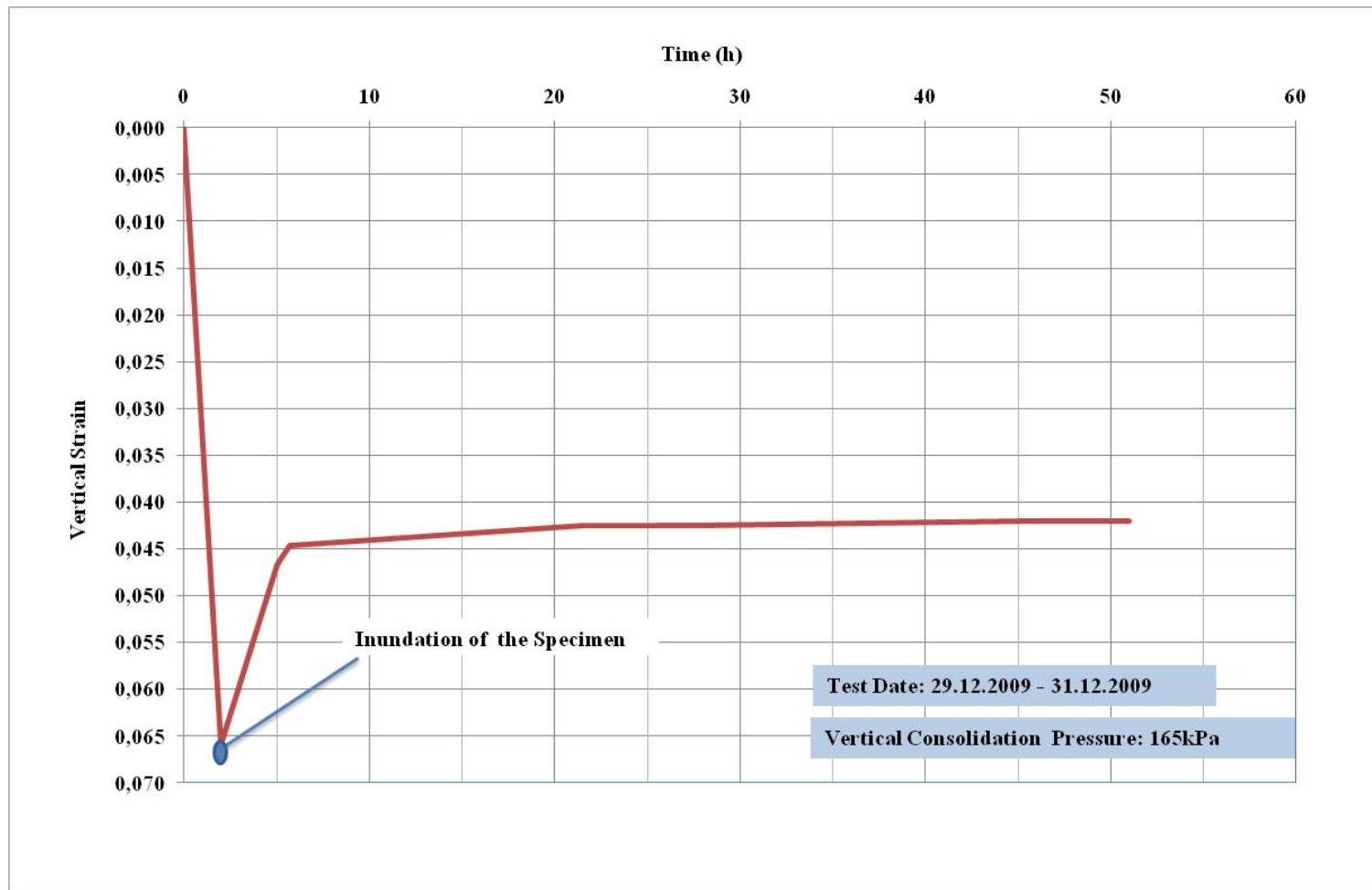
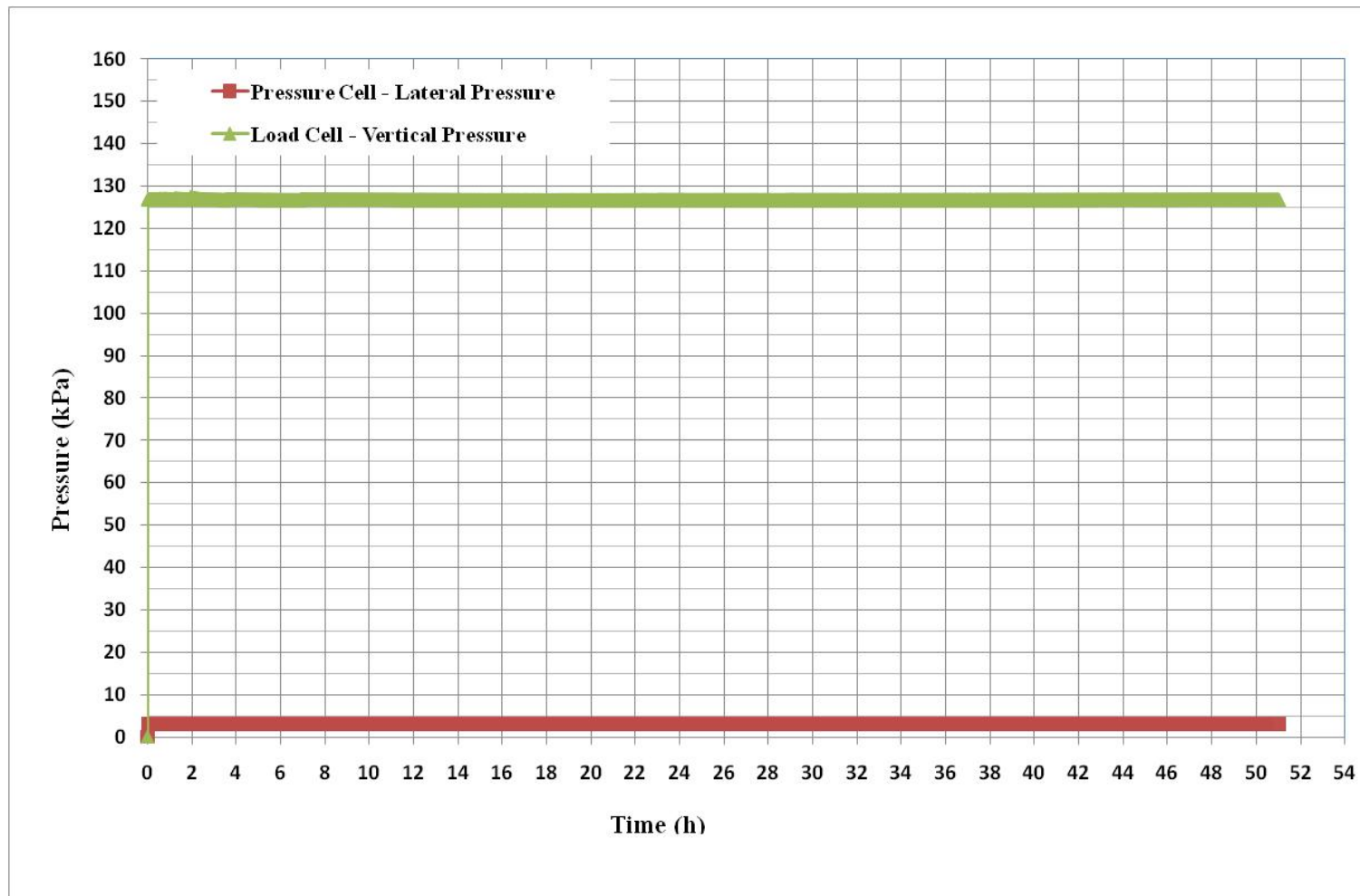**Figure C24:** Vertical Strain – Time Graph Test No: 37; (29.12.2009)

APPENDIX D

CONSTSANT VER. SURCHARGE–ZERO LATERAL STRAIN TESTS

TEST NO: 38	
Test Start:	
Date:	19.01.2010
Time:	10:00
Test Duration:	52 hours
Test End:	
Date:	21.01.2010
Time:	14:00
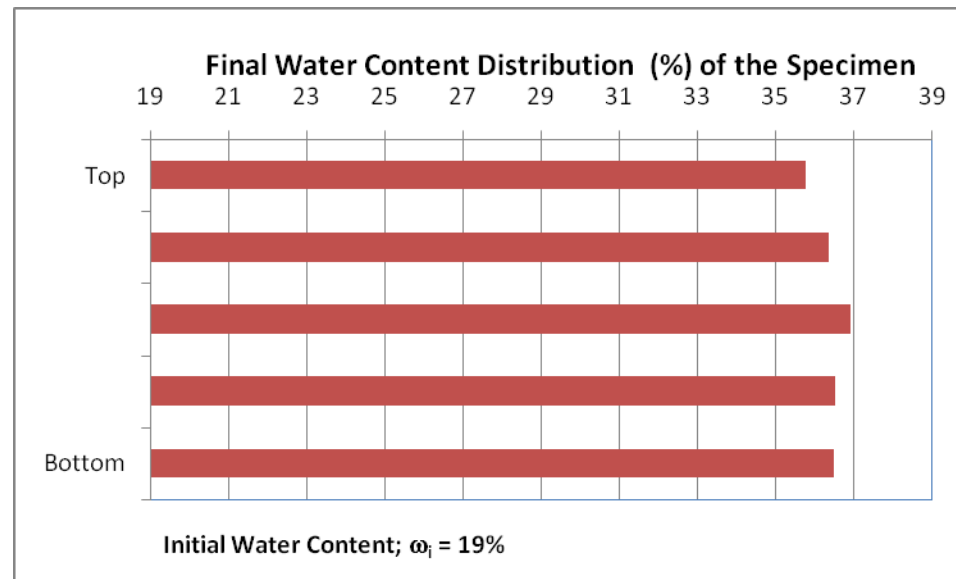
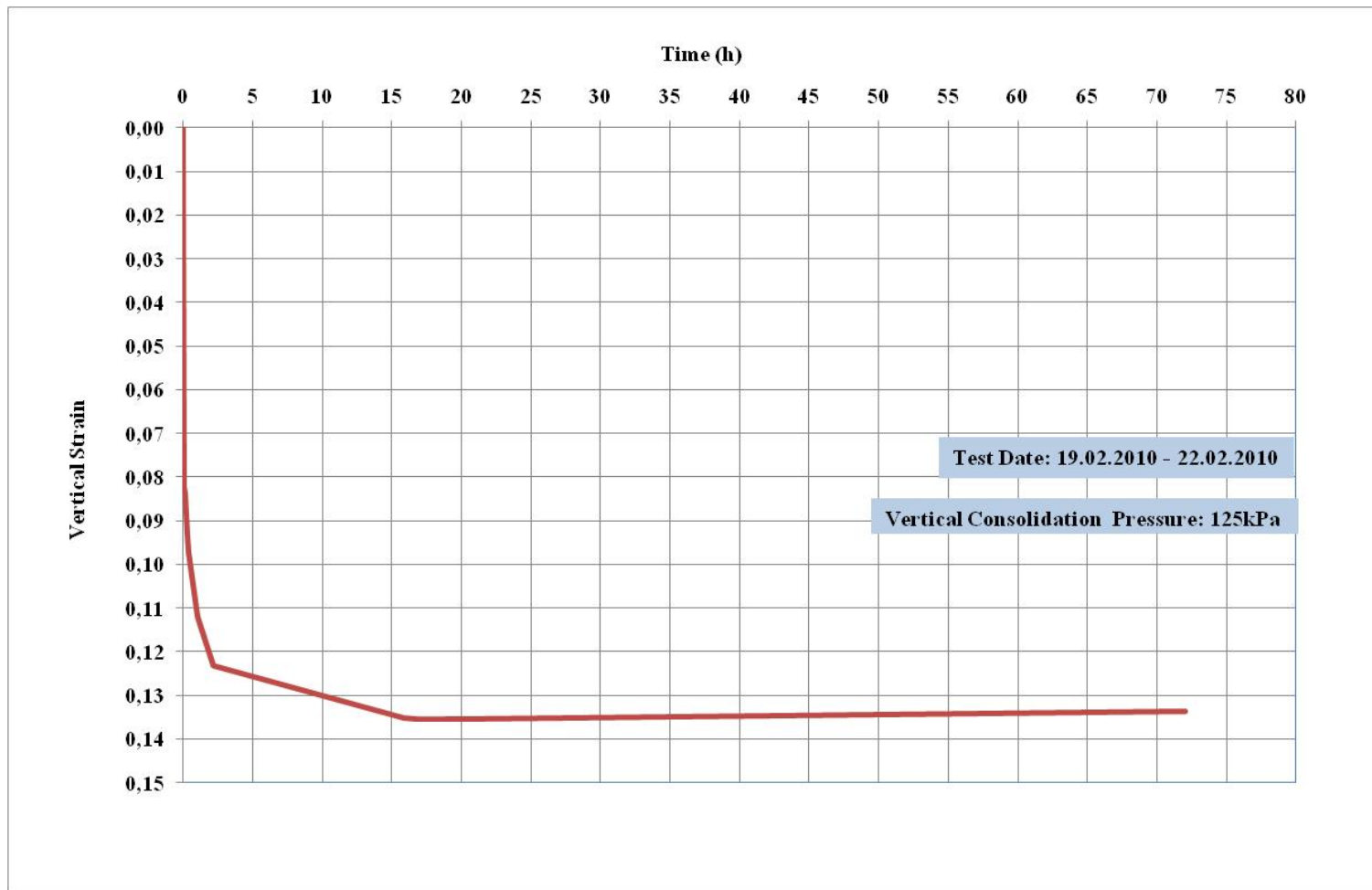**Figure D1:** Initial and Final Water Contents Test No: 38; (19.01.2010)
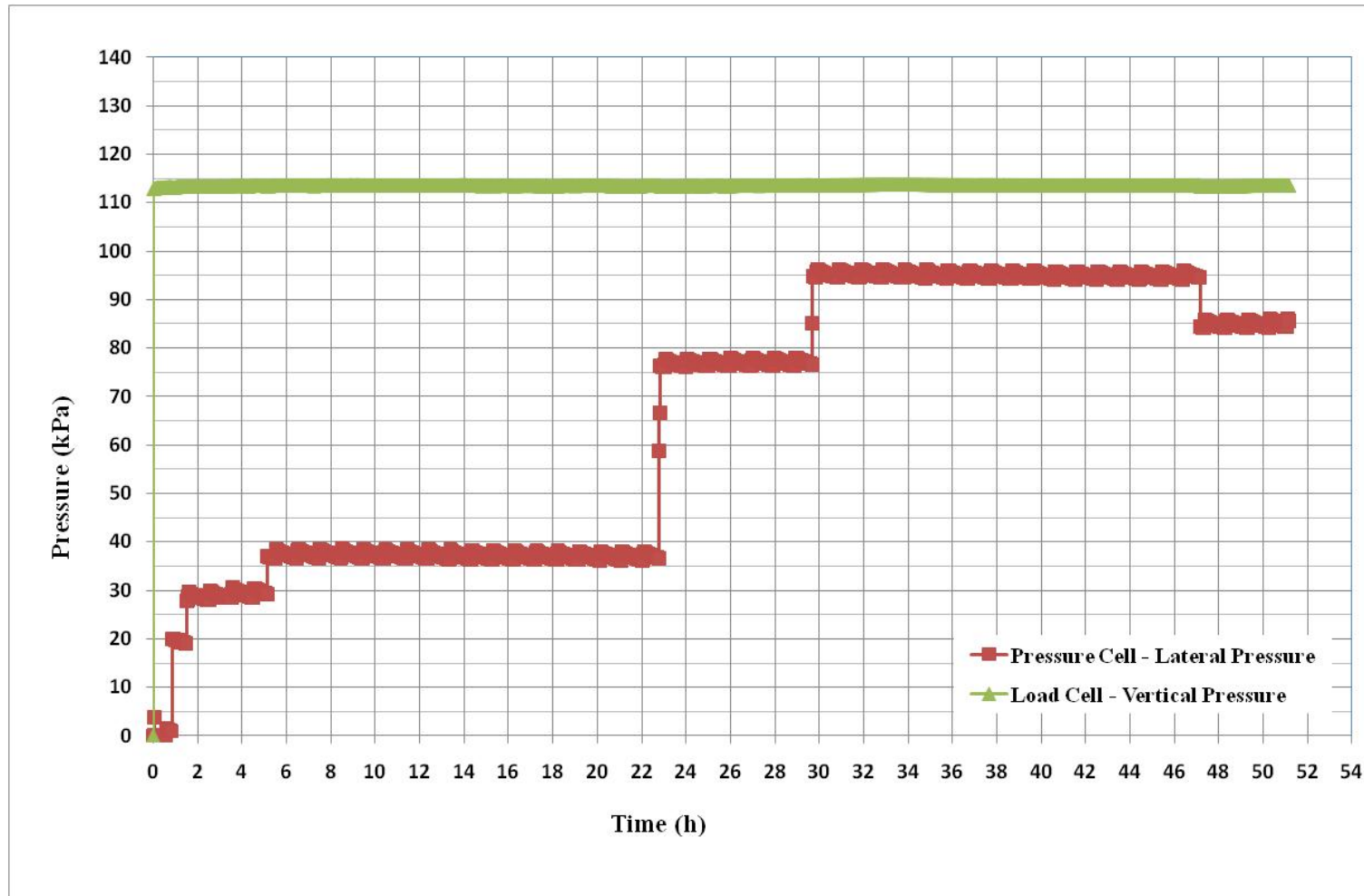
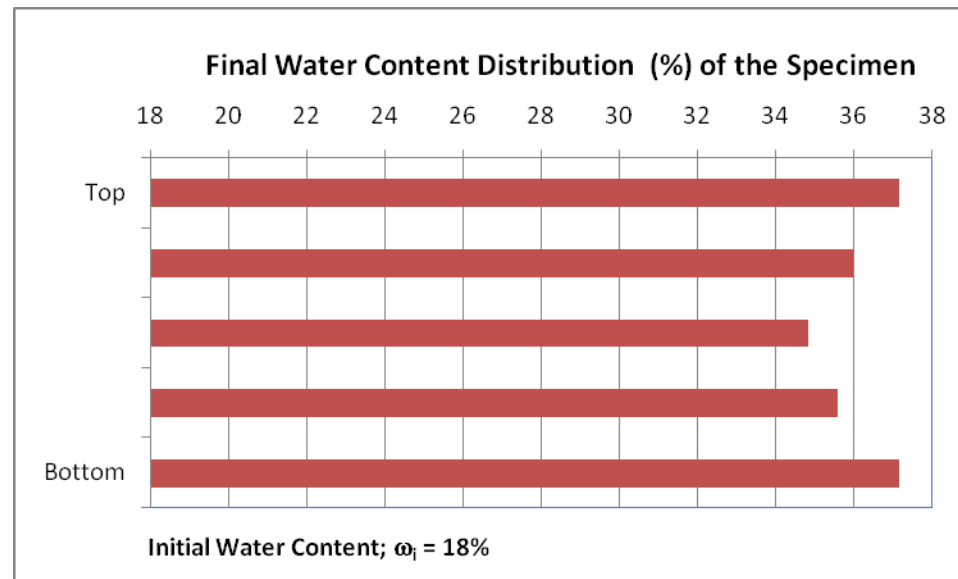**Figure D2:** Pressure – Time Graph Test No: 38; (19.01.2010)
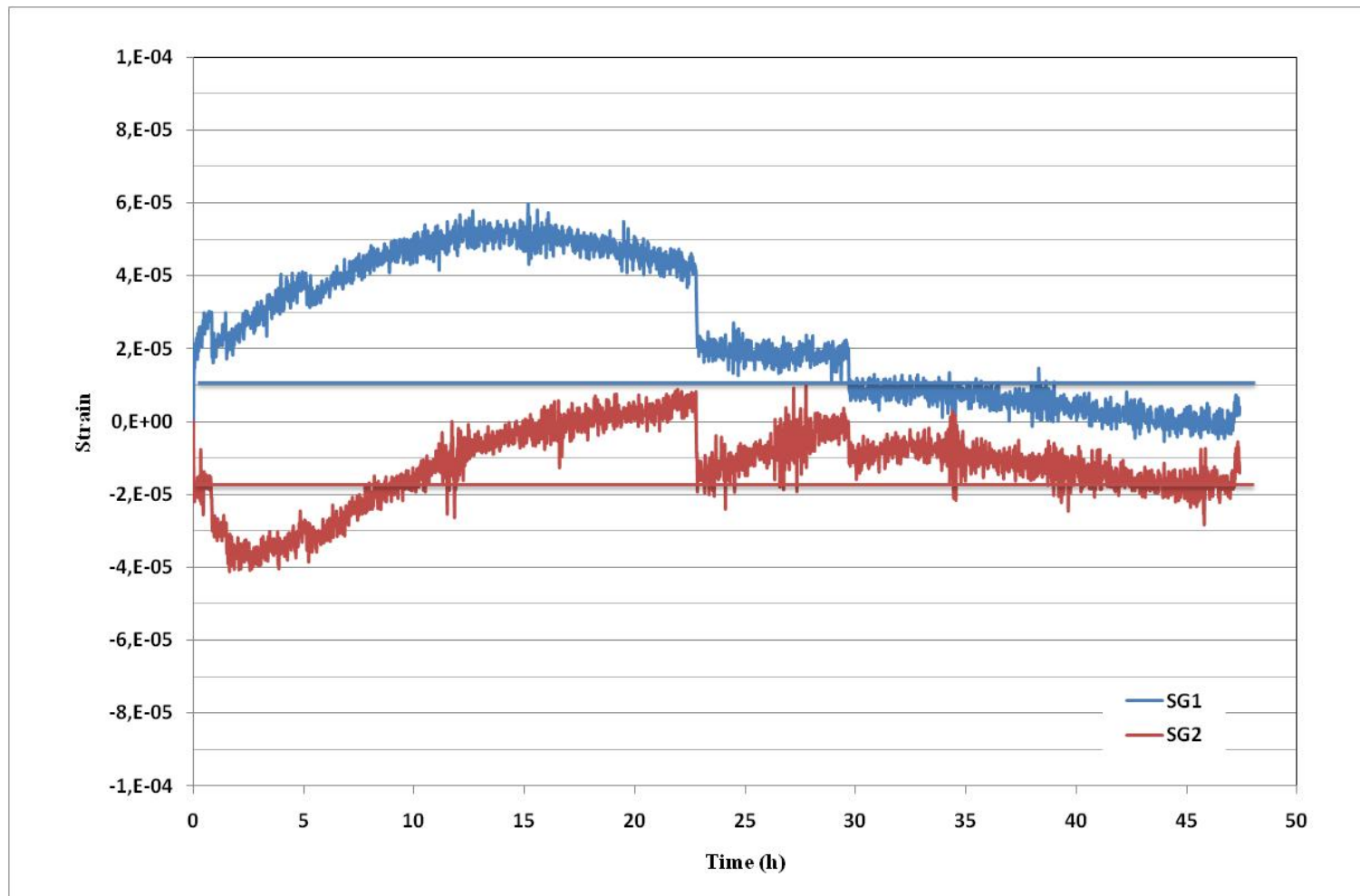
Figure D3: Lateral Strain – Time Graph Test No: 38; (19.01.2010)
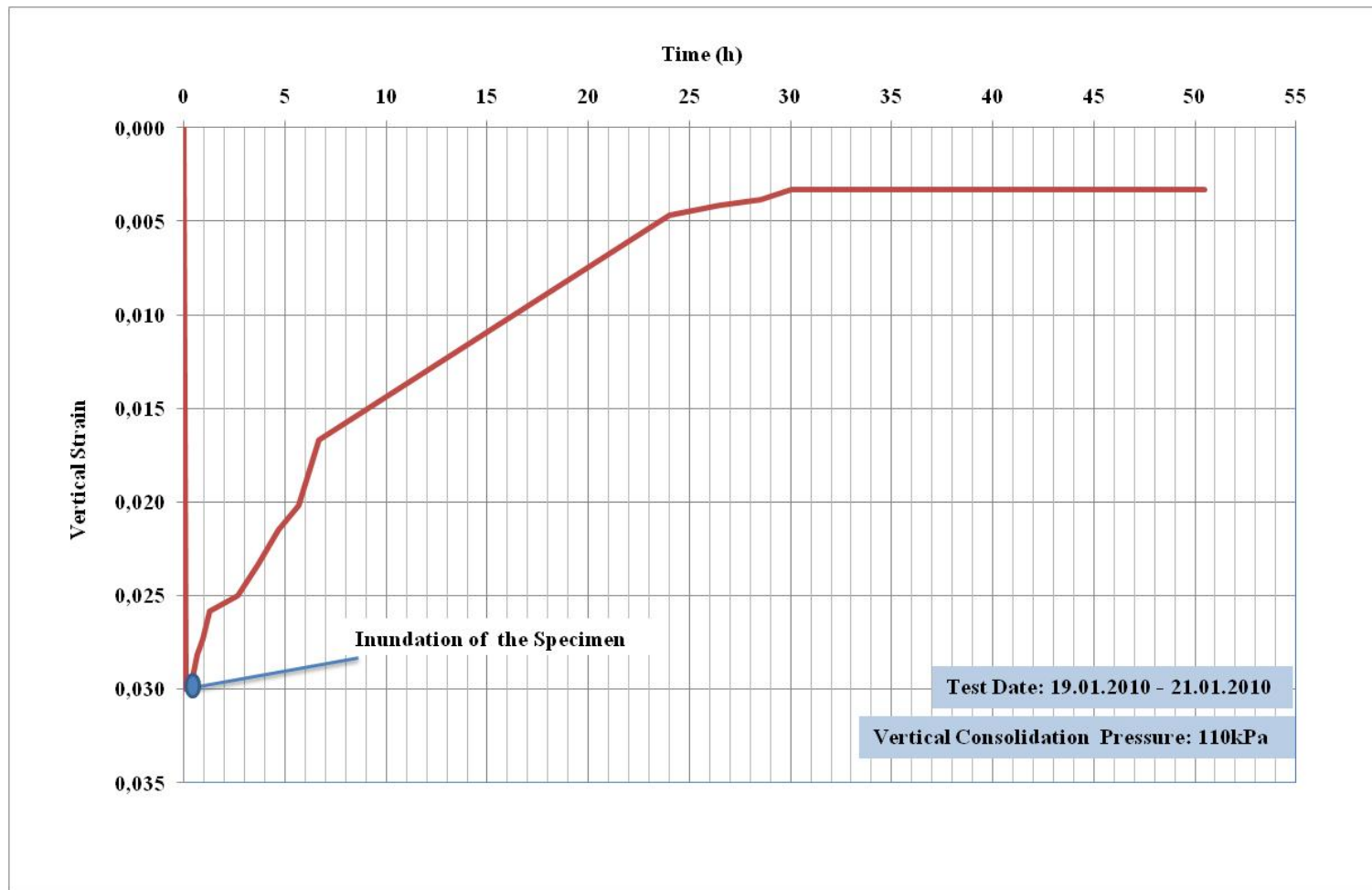
Figure D4: Vertical Strain – Time Graph Test No: 38; (19.01.2010)

TEST NO: 39	
Test Start:	
Date:	28.01.2010
Time:	10:45
Test Duration:	29 hours
Test End:	
Date:	29.01.2010
Time:	14:45
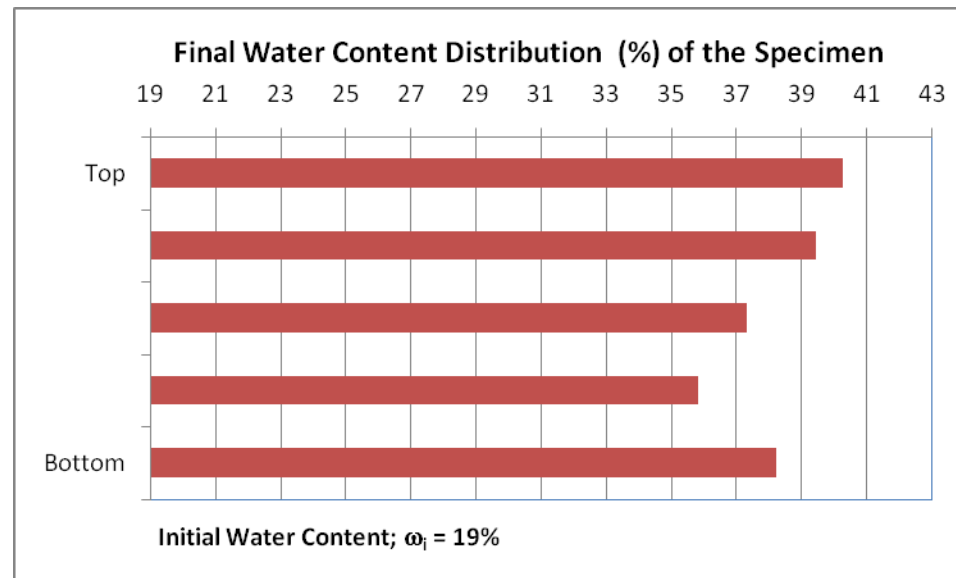
Figure D5: Initial and Final Water Contents Test No: 39; (28.01.2010)
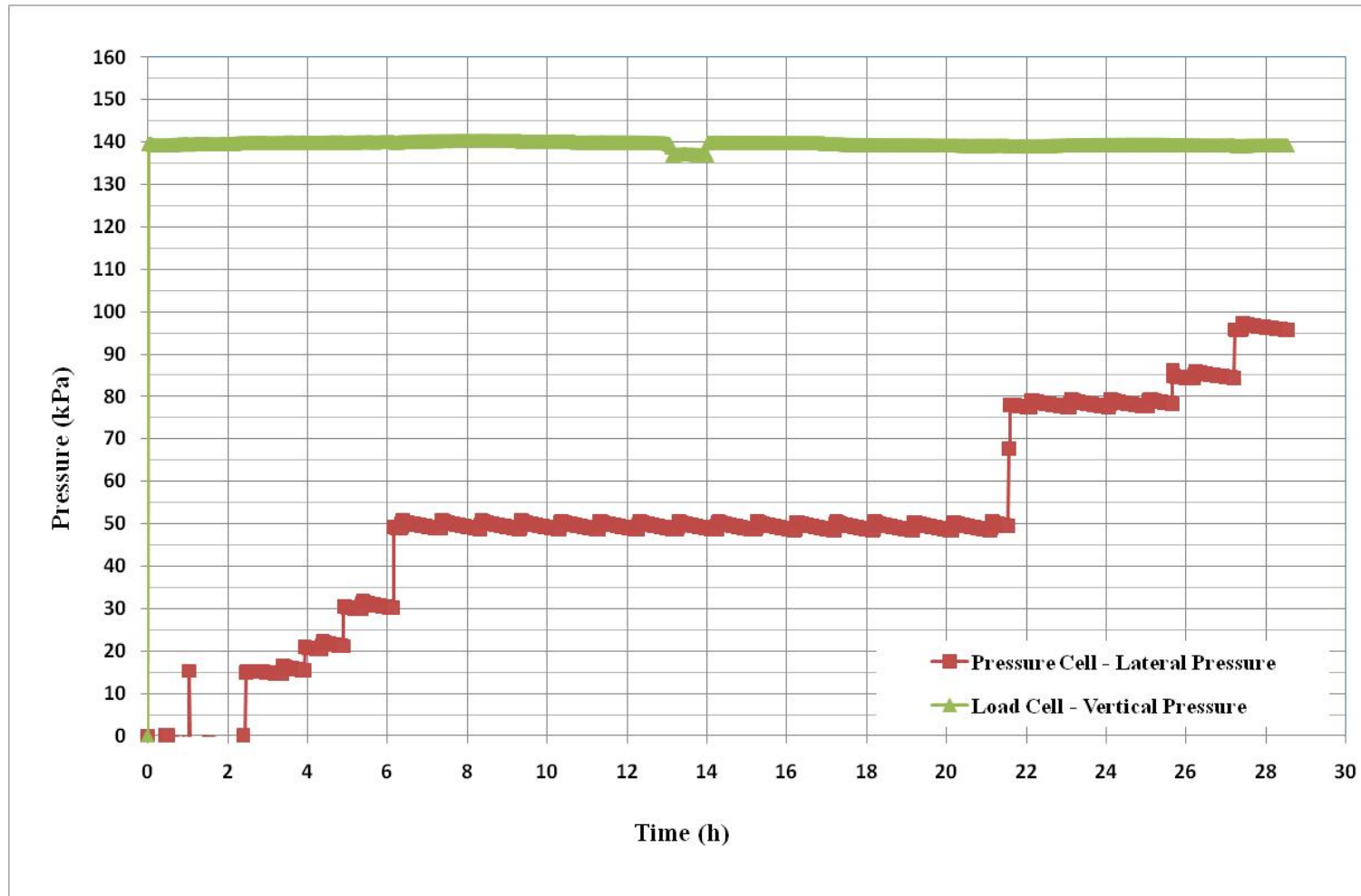
Figure D6: Pressure – Time Graph Test No: 39; (28.01.2010)
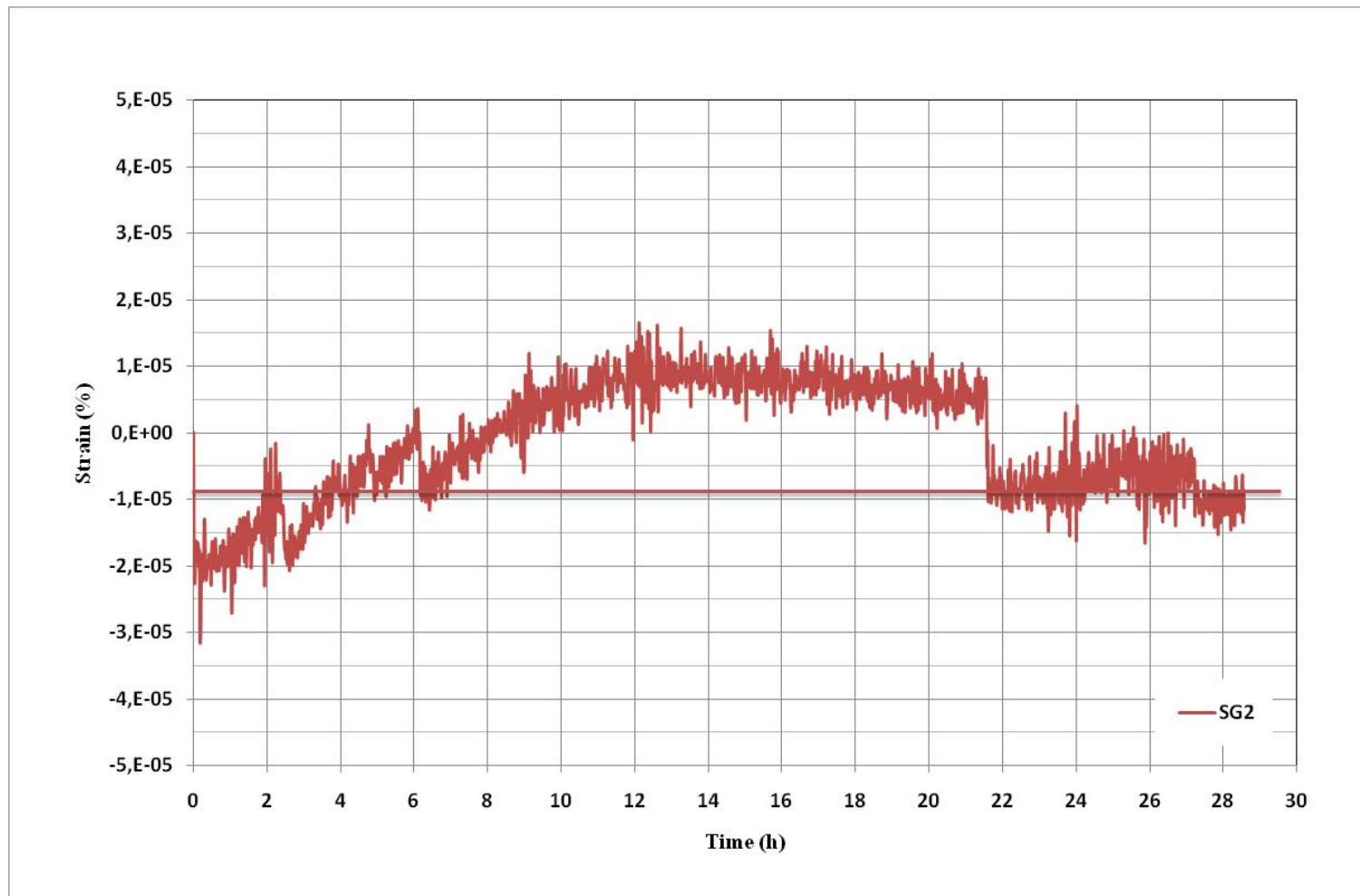
Figure D7: Lateral Strain – Time Graph Test No: 39; (28.01.2010)
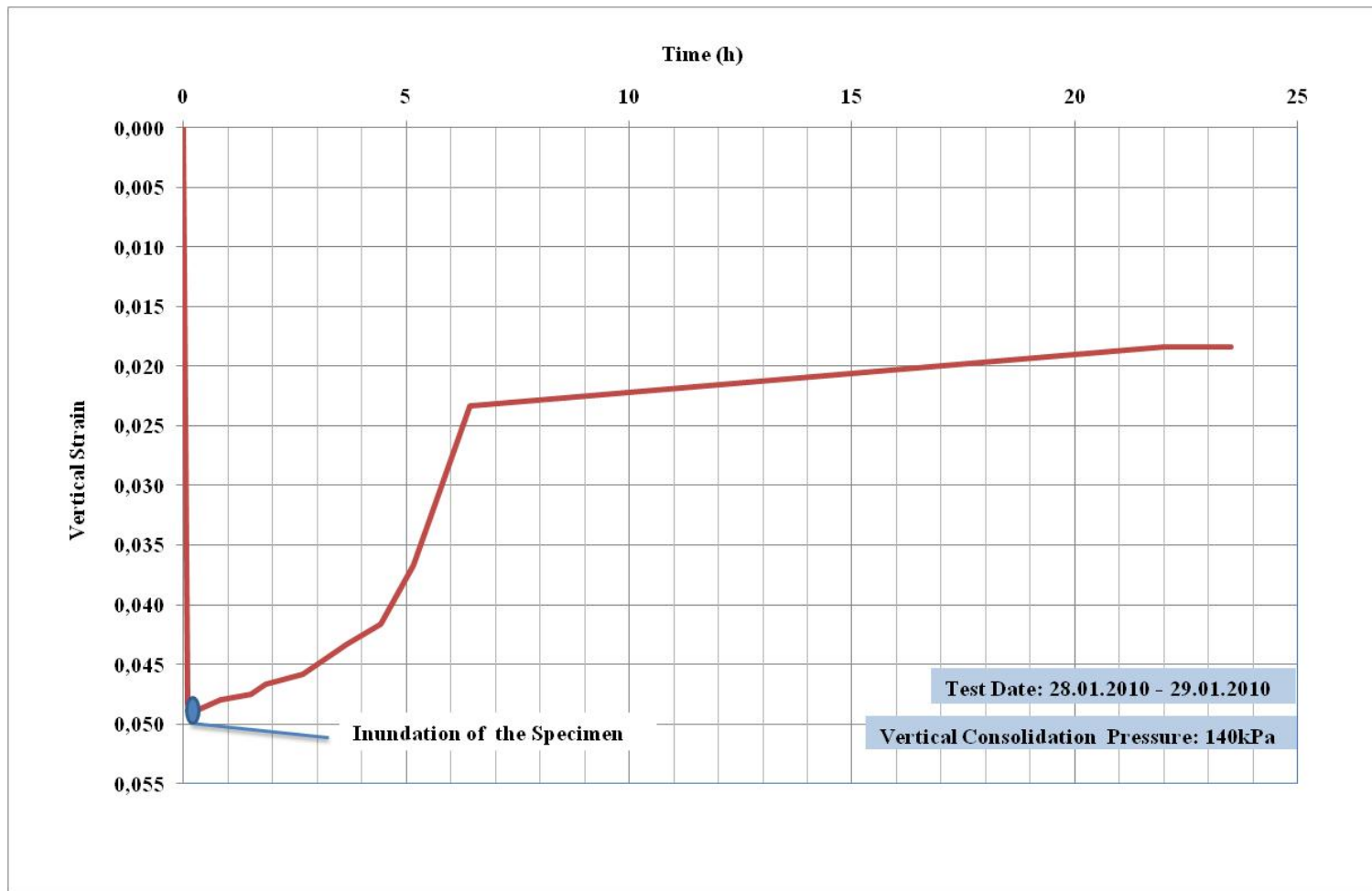
Figure D8: Vertical Strain – Time Graph Test No: 39; (28.01.2010)

TEST NO: 40	
Test Start:	
Date:	02.02.2010
Time:	10:00
Test Duration:	48 hours
Test End:	
Date:	04.02.2010
Time:	10:00
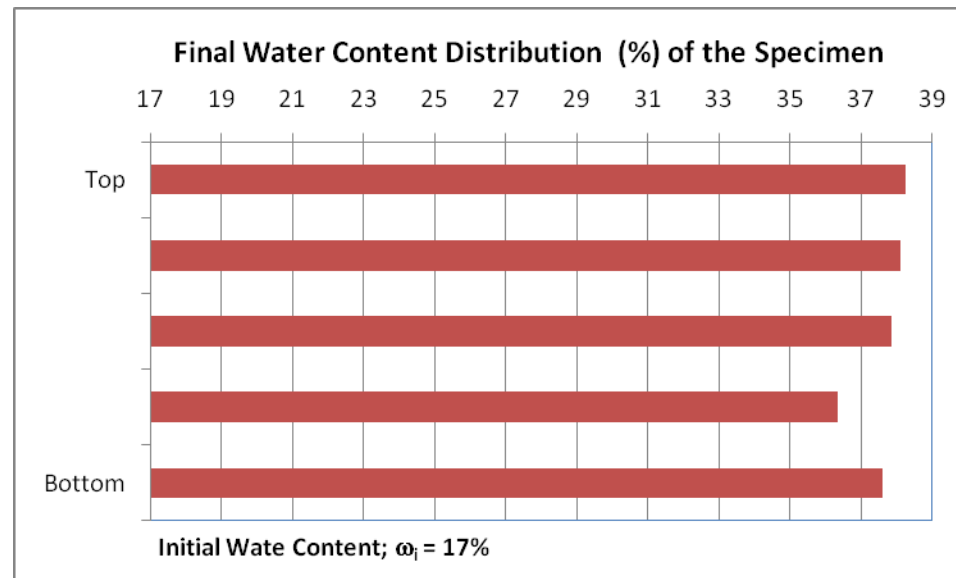
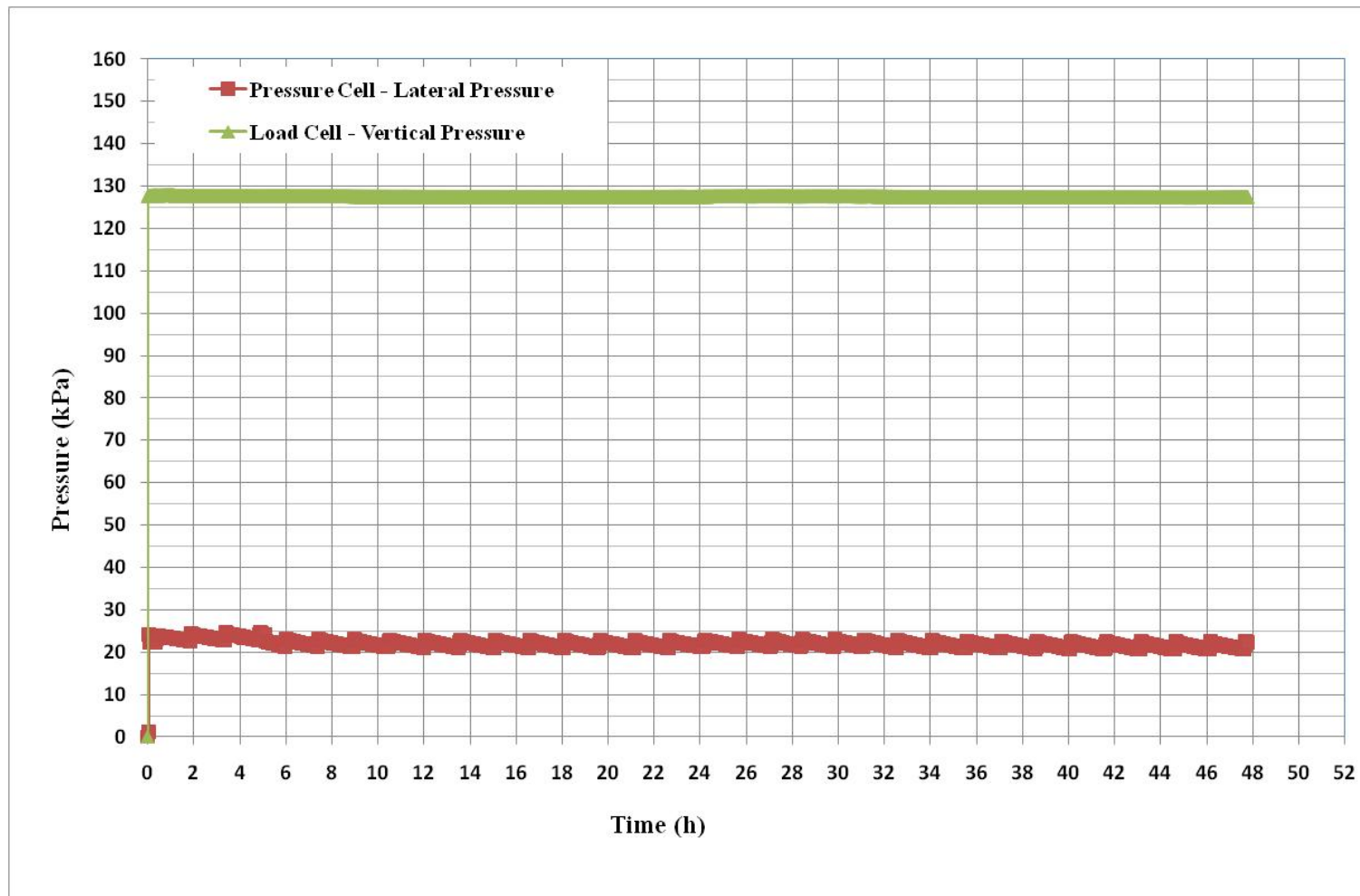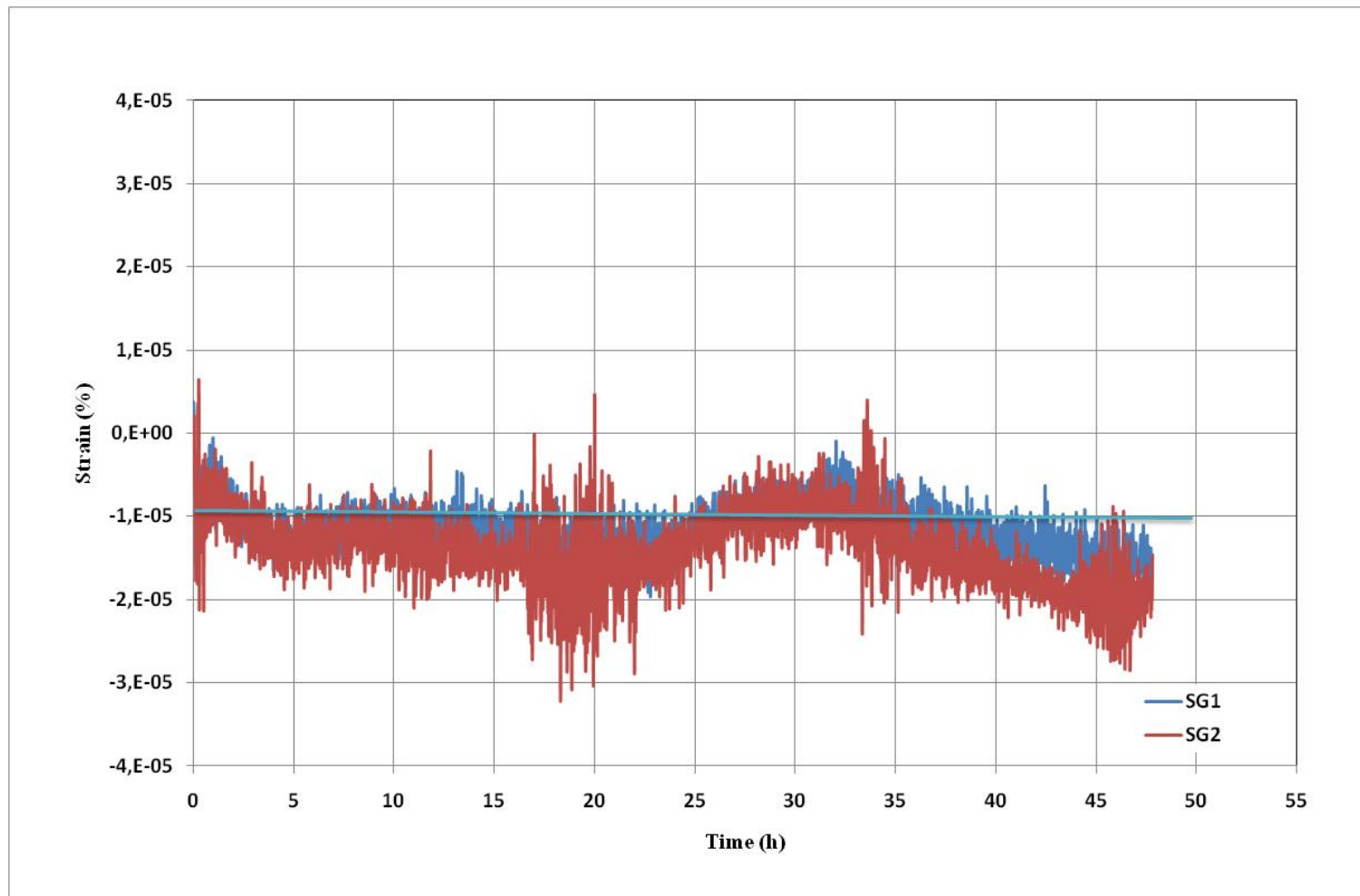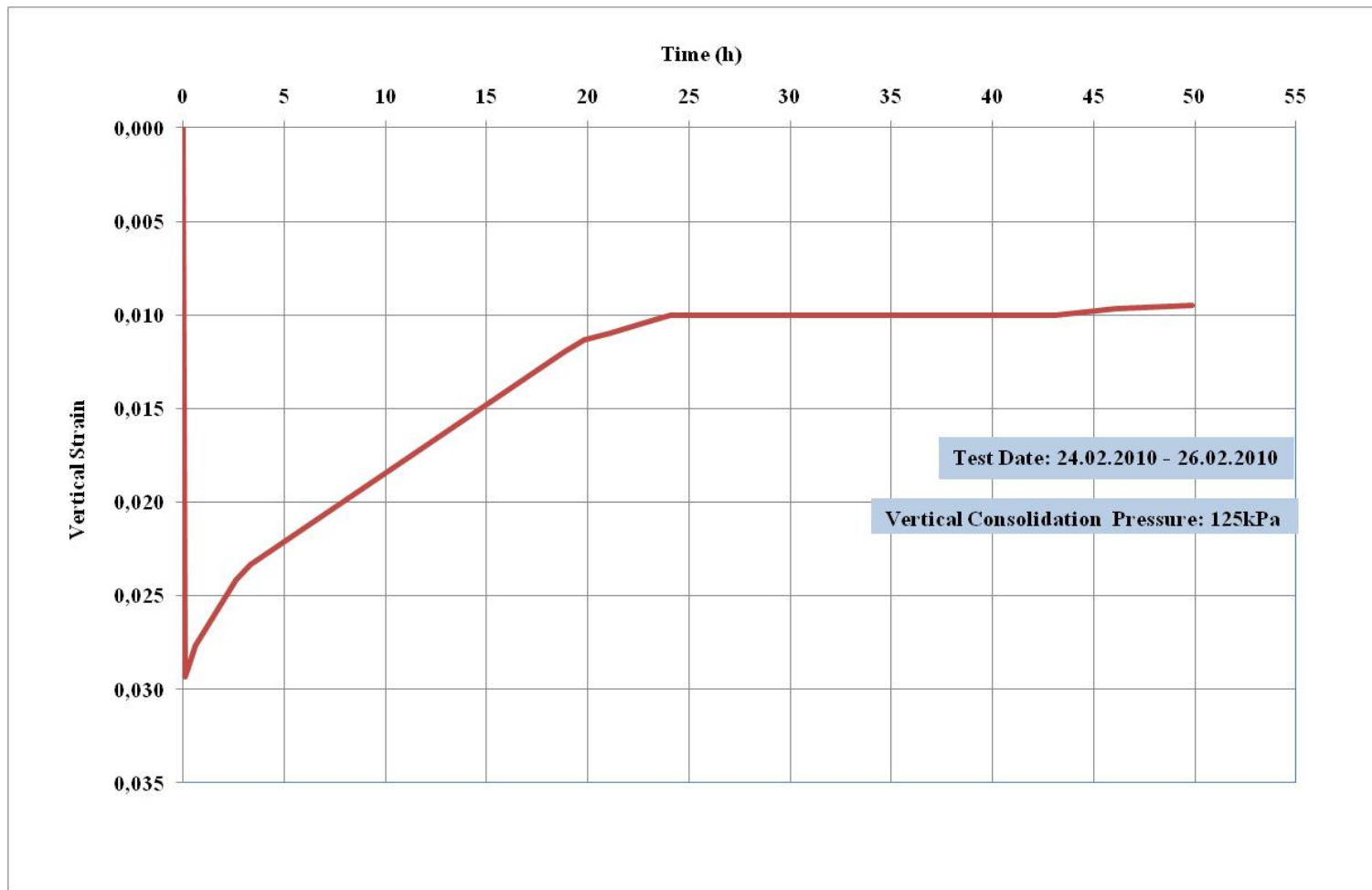**Figure D9:** Initial and Final Water Contents Test No: 40; (02.02.2010)
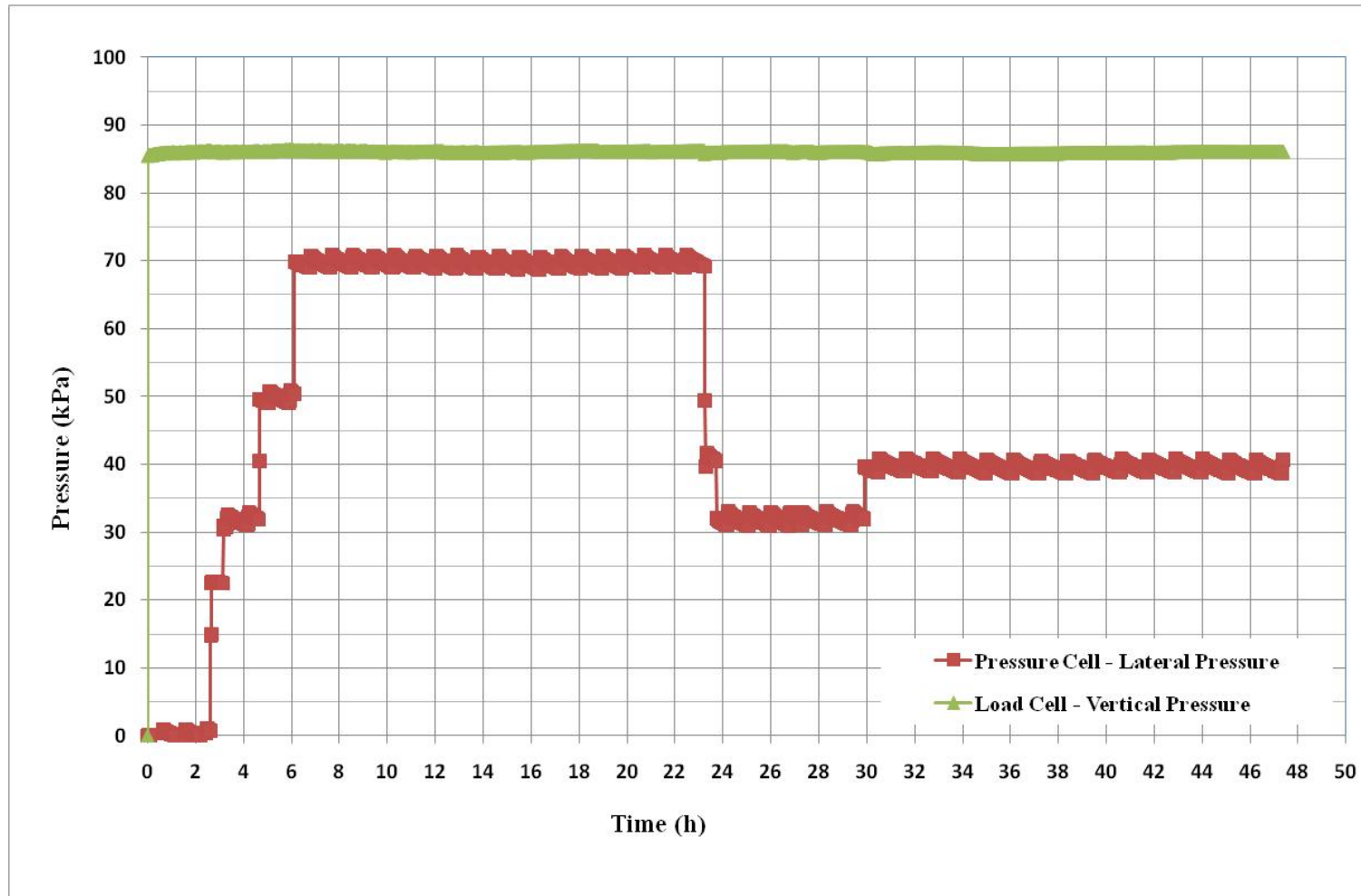
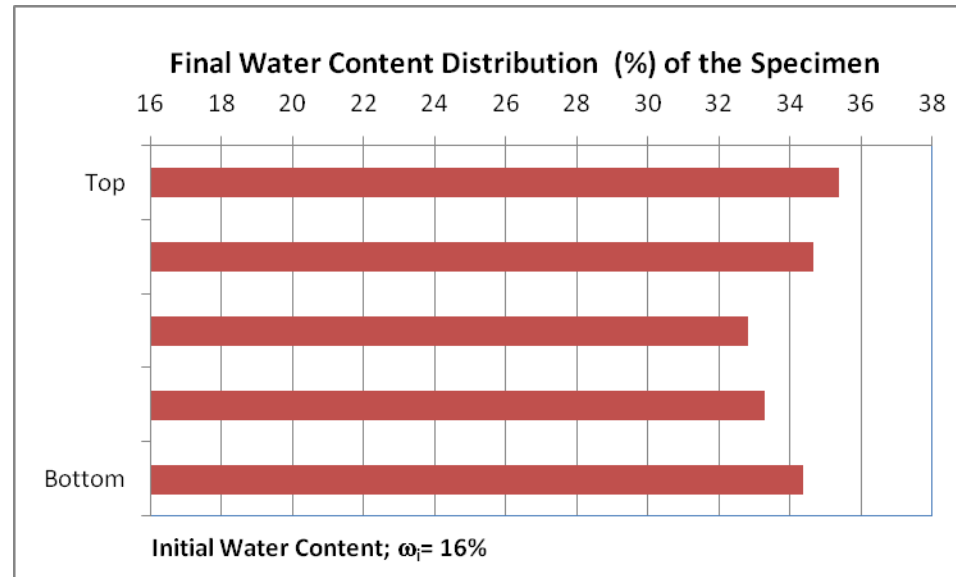**Figure D10:** Pressure – Time Graph Test No: 40; (02.02.2010)
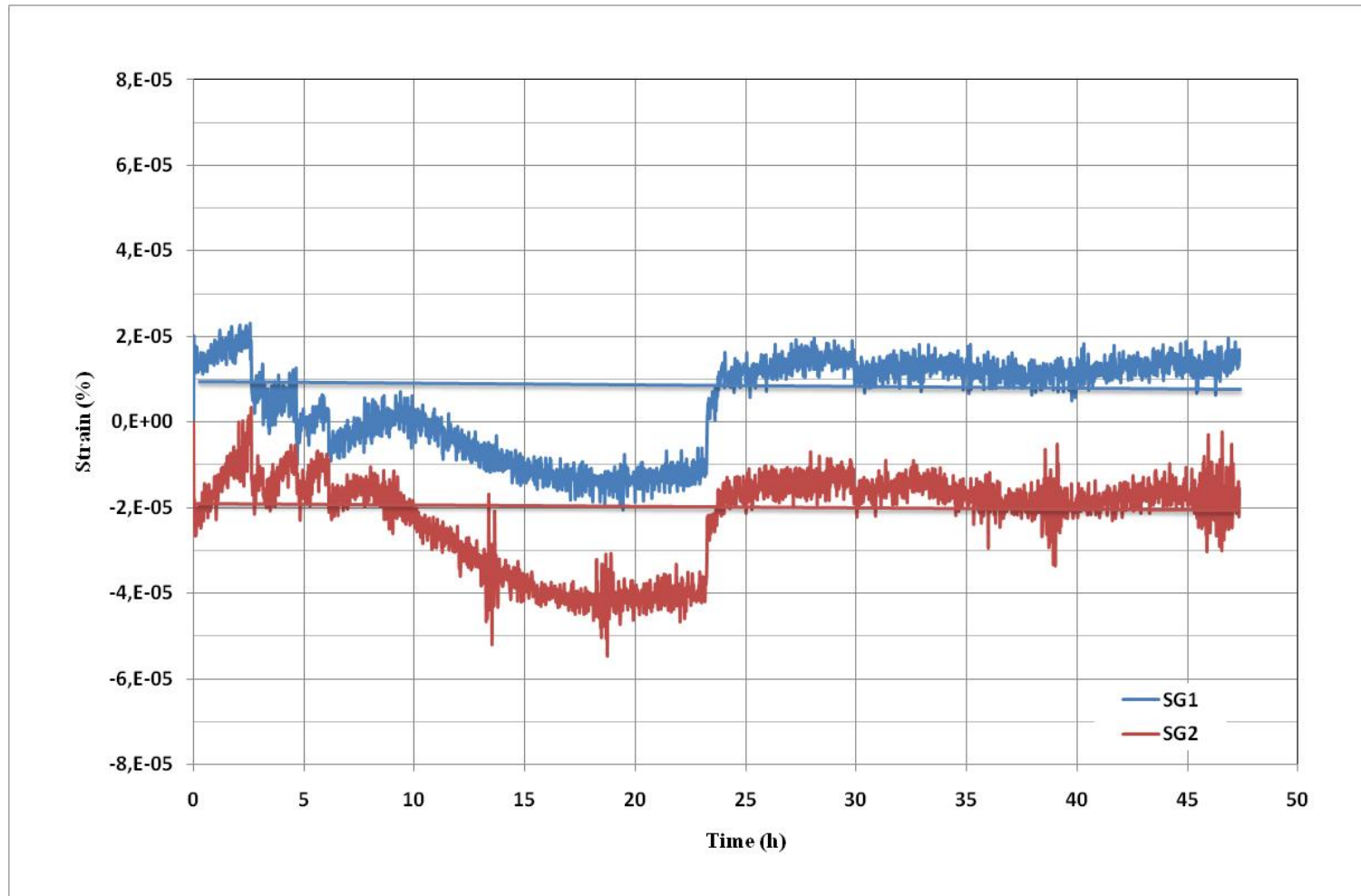
Figure D11: Lateral Strain – Time Graph Test No: 40; (02.02.2010)
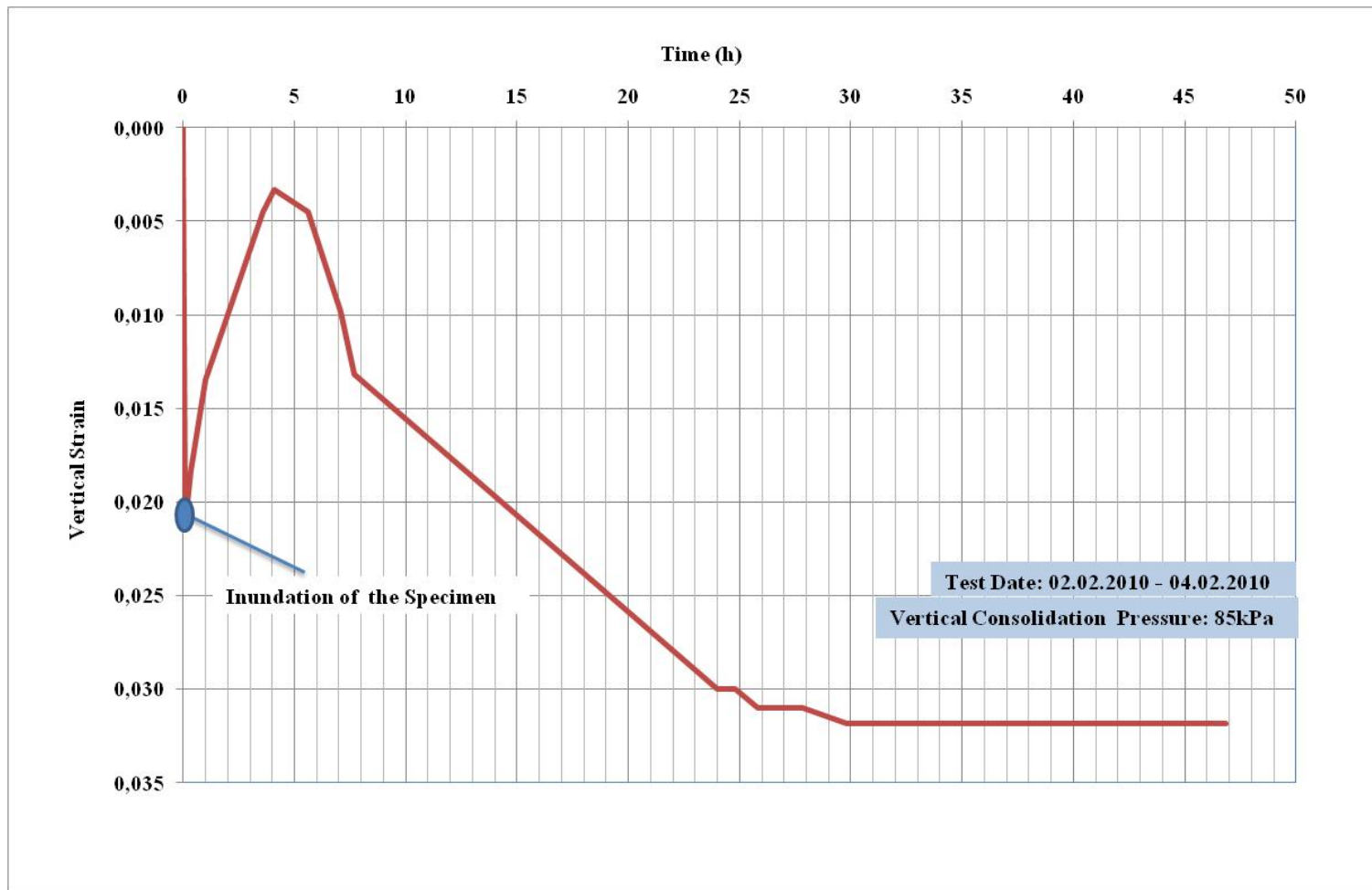
Figure D12: Vertical Strain – Time Graph Test No: 40; (02.02.2010)

TEST NO: 41	
Test Start:	
Date:	05.02.2010
Time:	08:00
Test Duration:	51 hours
Test End:	
Date:	07.02.2010
Time:	11:00
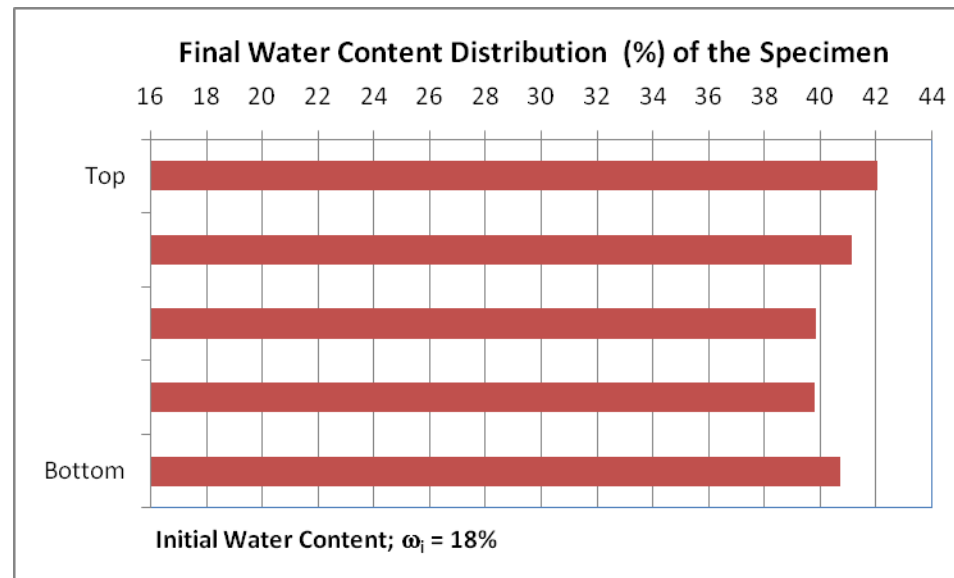
Figure D13: Initial and Final Water Contents Test No: 41; (05.02.2010)
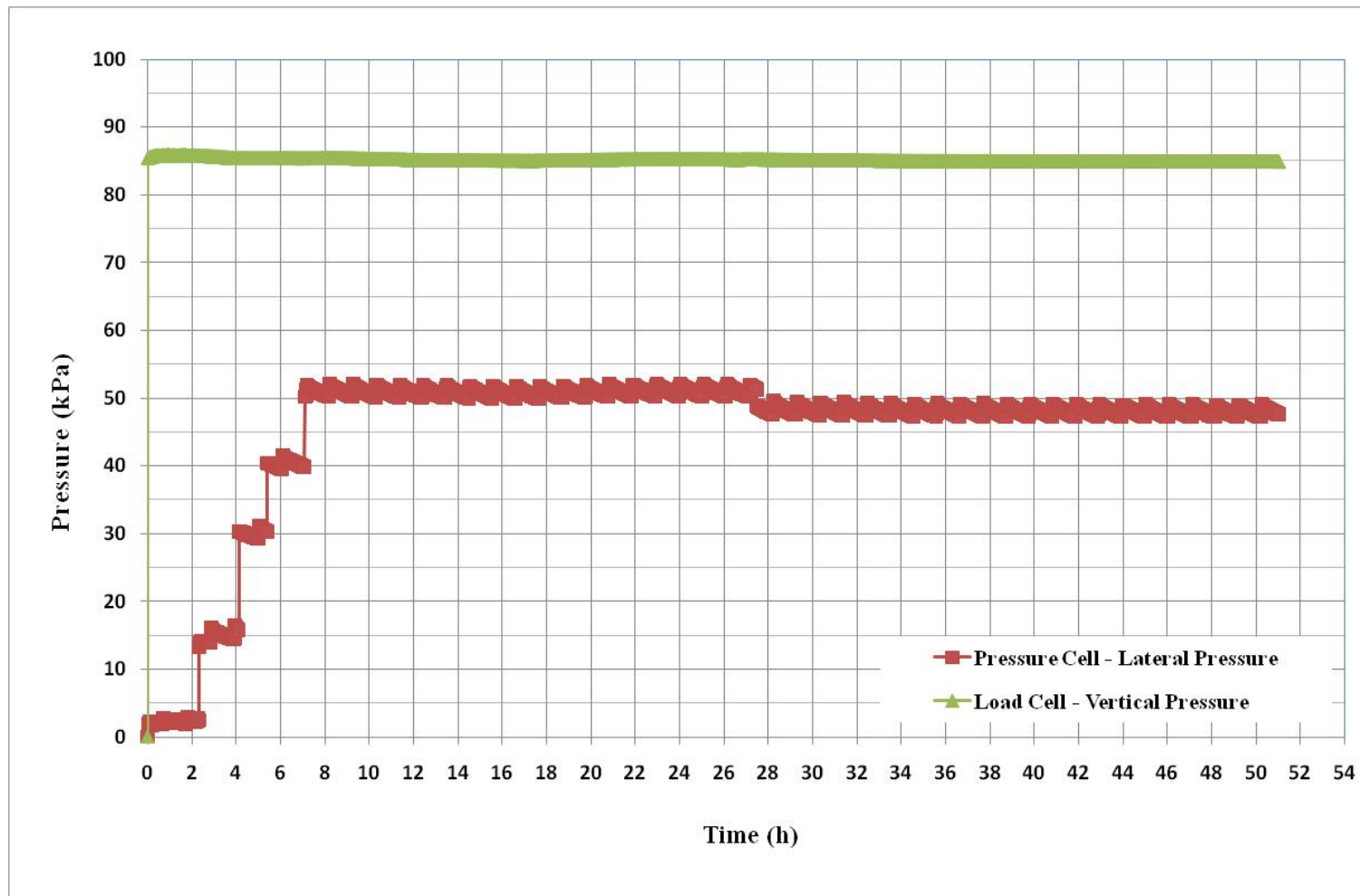
Figure D14: Pressure – Time Graph Test No: 41; (05.02.2010)
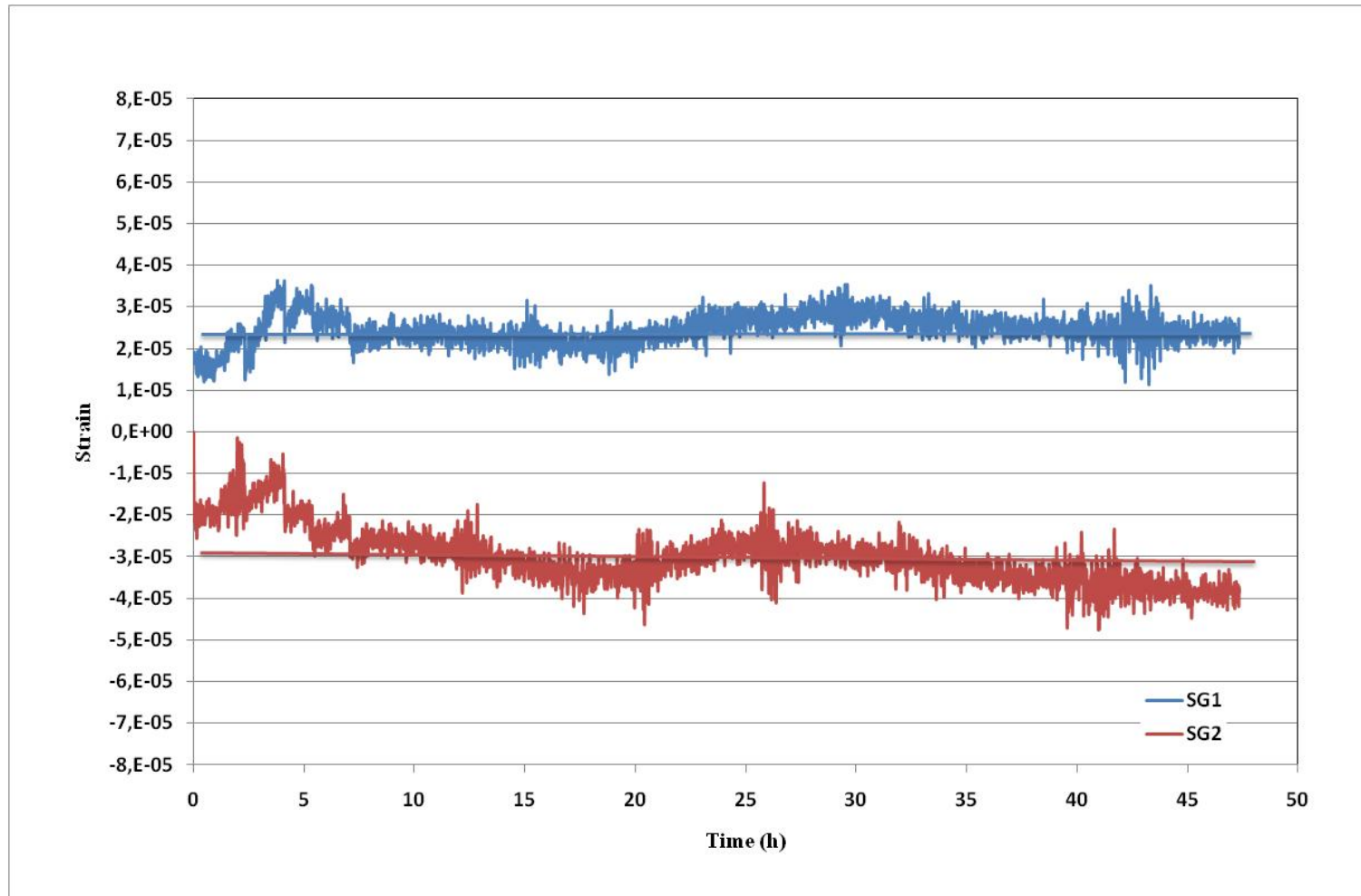
Figure D15: Lateral Strain – Time Graph Test No: 41; (05.02.2010)
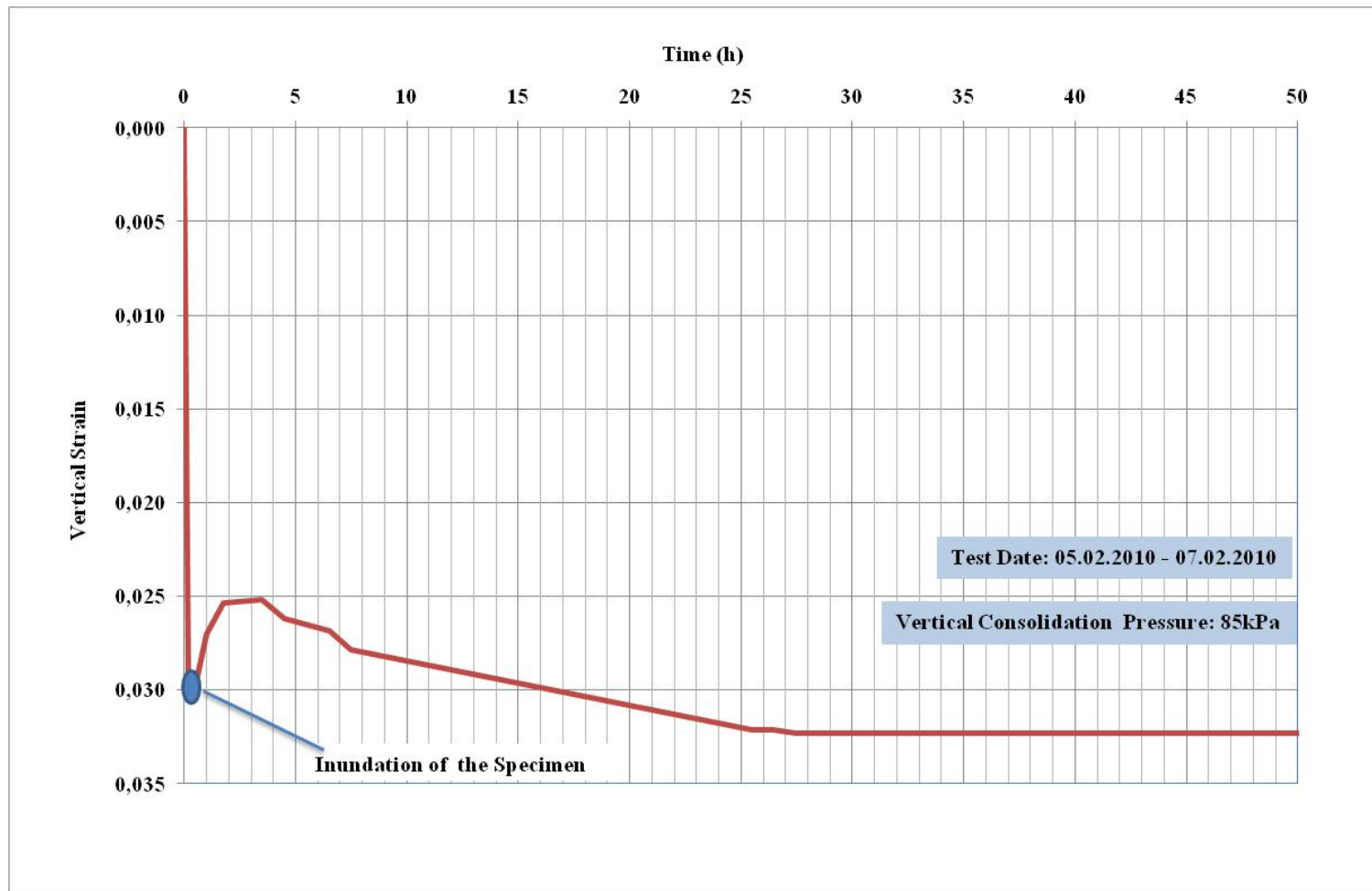
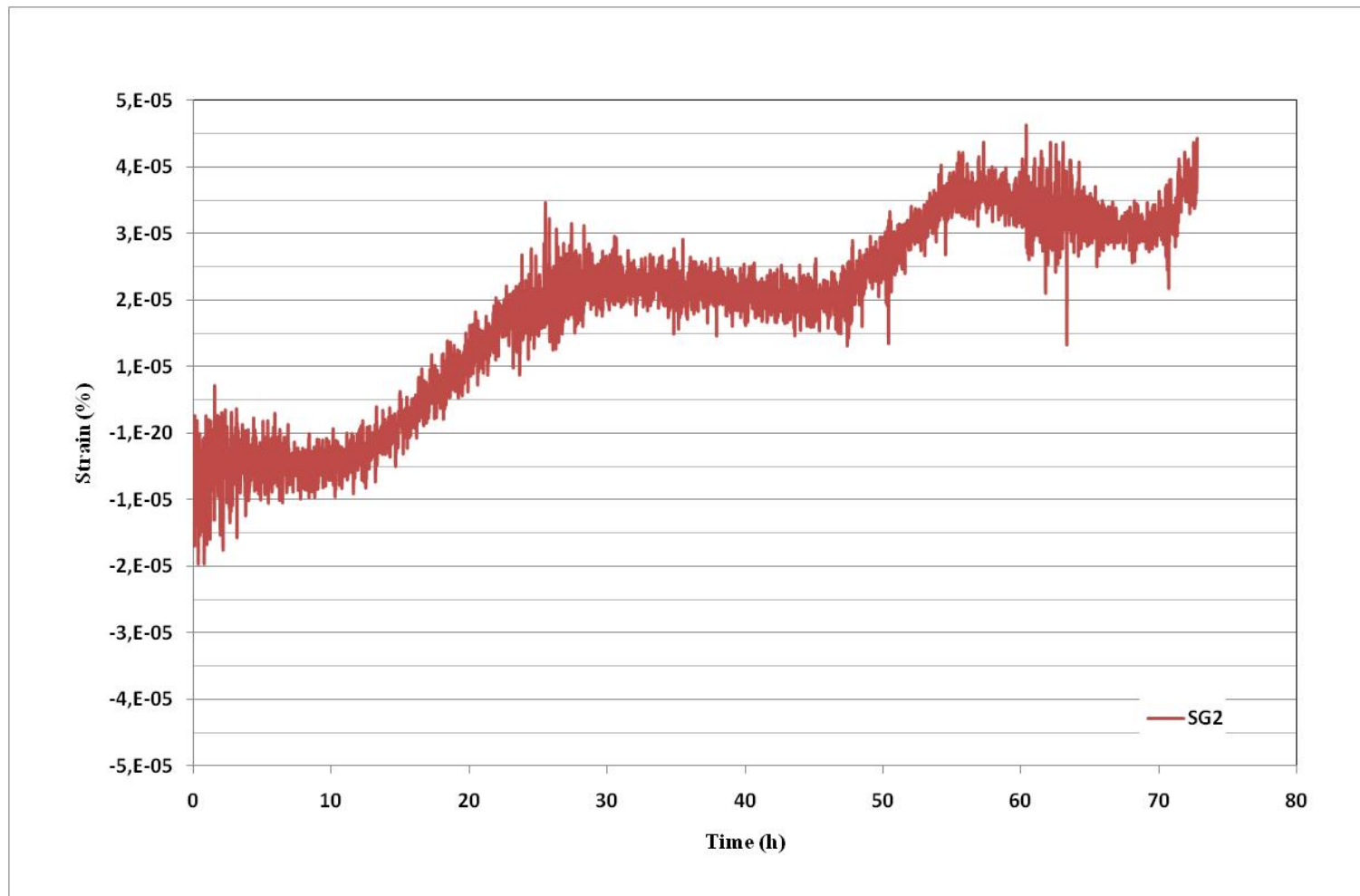**Figure D16:** Vertical Strain – Time Graph Test No: 41; (05.02.2010)

TEST NO: 42	
Test Start:	
Date:	09.02.2010
Time:	08:30
Test Duration:	48 hours
Test End:	
Date:	04.02.2010
Time:	08:30
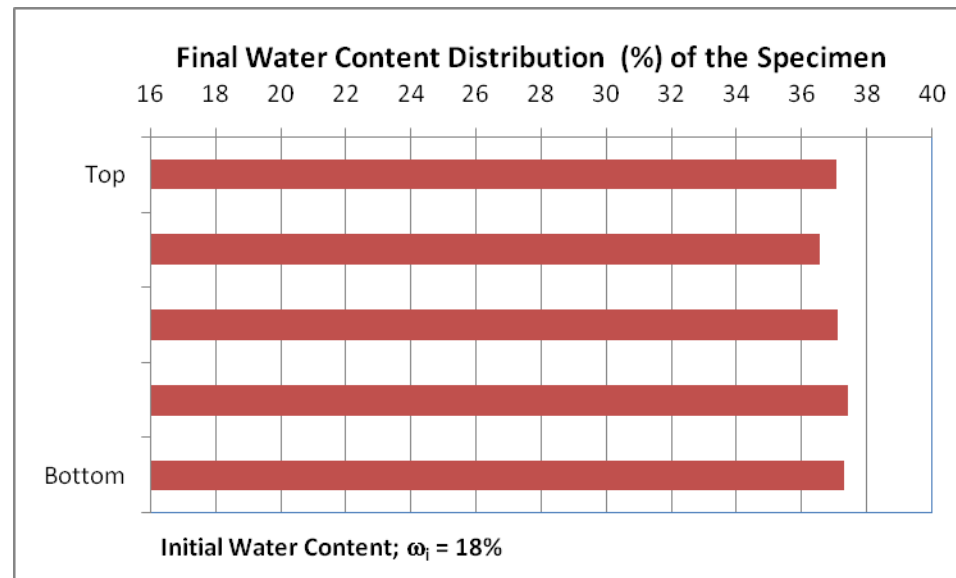
Figure D17: Initial and Final Water Contents Test No: 42; (09.02.2010)
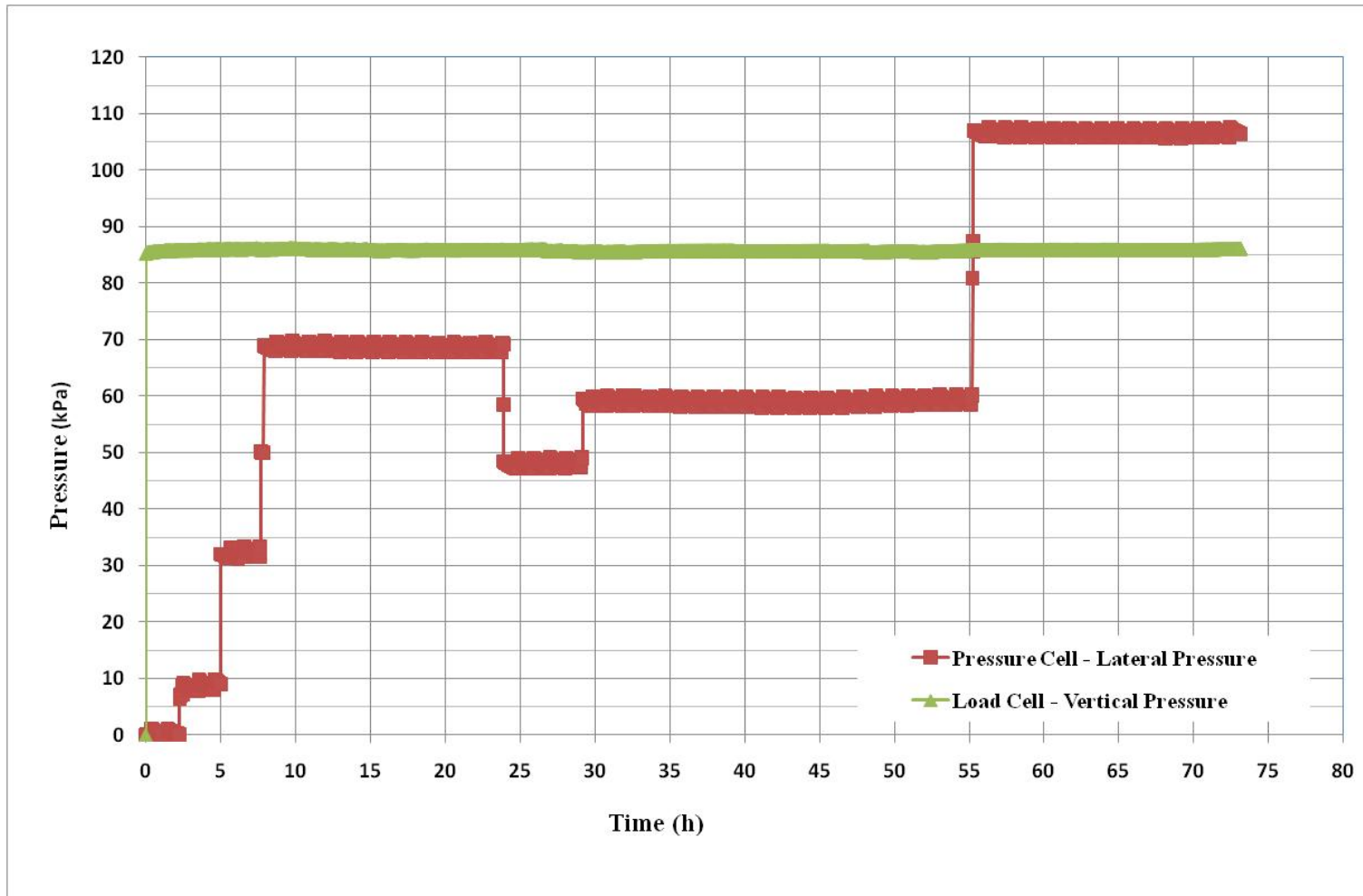
Figure D18: Pressure – Time Graph Test No: 42; (09.02.2010)
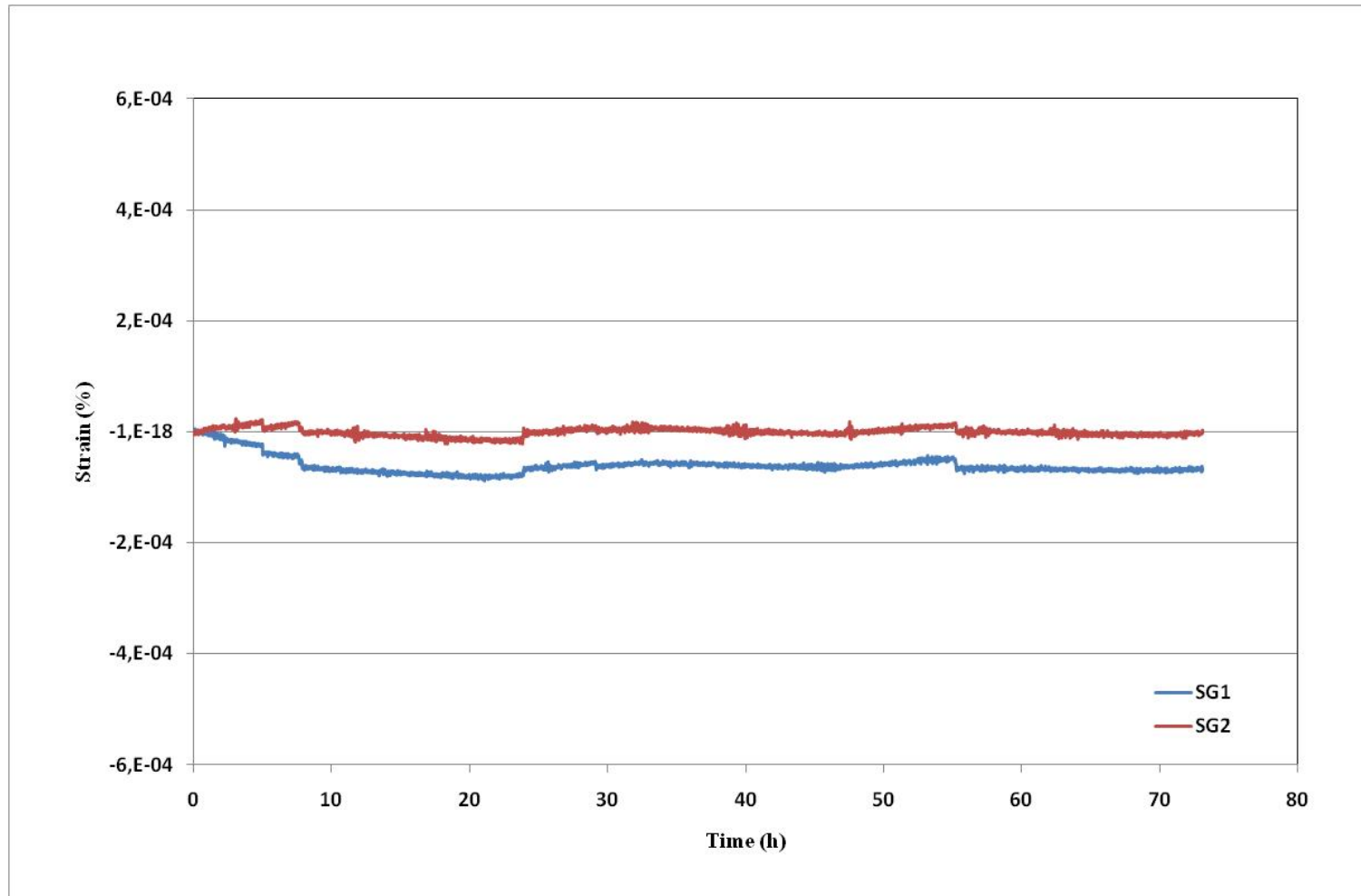
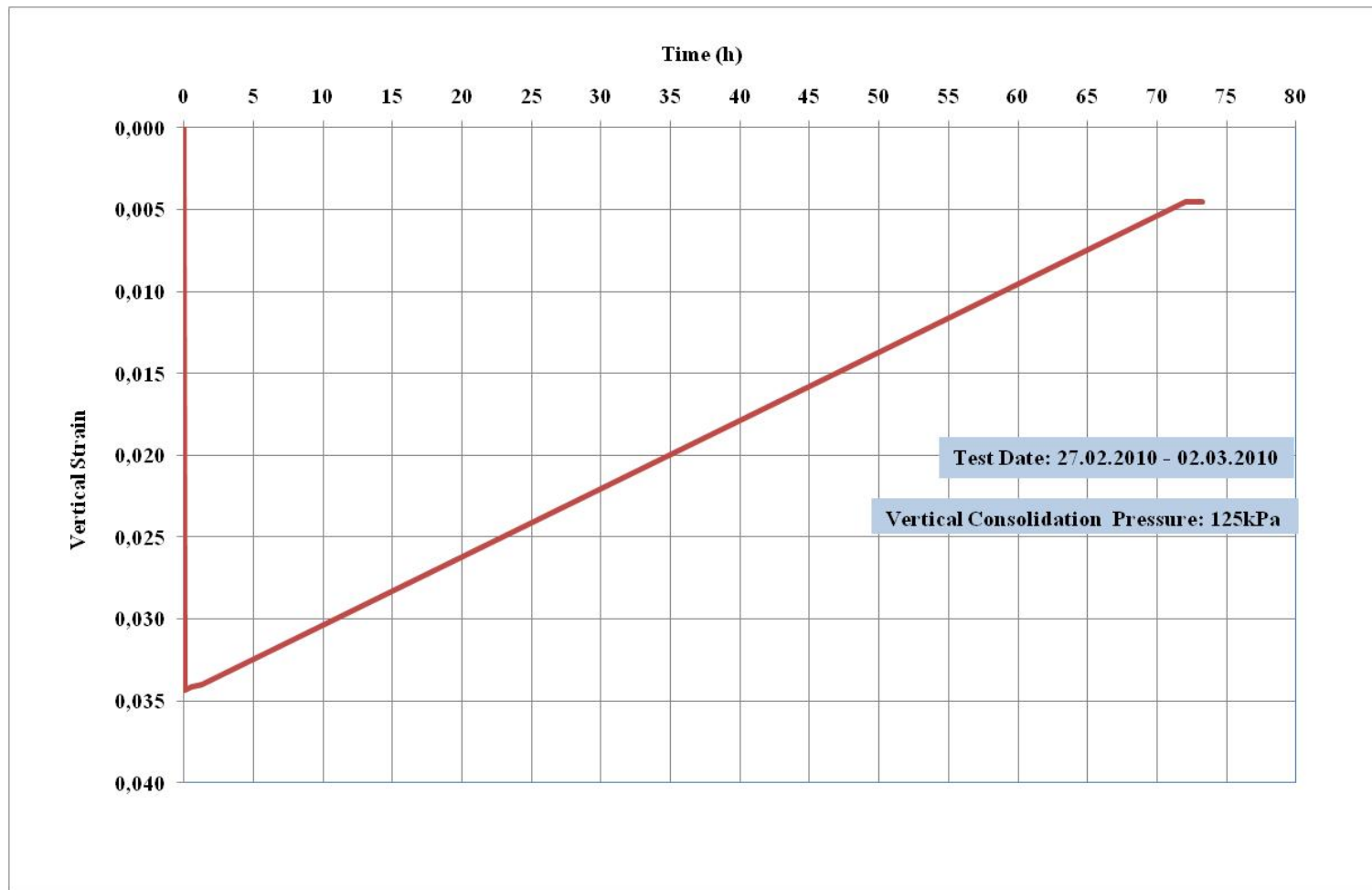**Figure D19:** Lateral Strain – Time Graph Test No: 42; (09.02.2010)

Figure D20: Vertical Strain – Time Graph Test No: 42; (09.02.2010)

TEST NO: 43	
Test Start:	
Date:	13.02.2010
Time:	09:00
Test Duration:	25 hours
Test End:	
Date:	14.02.2010
Time:	10:00

Figure D21: Initial and Final Water Contents Test No: 43; (13.02.2010)
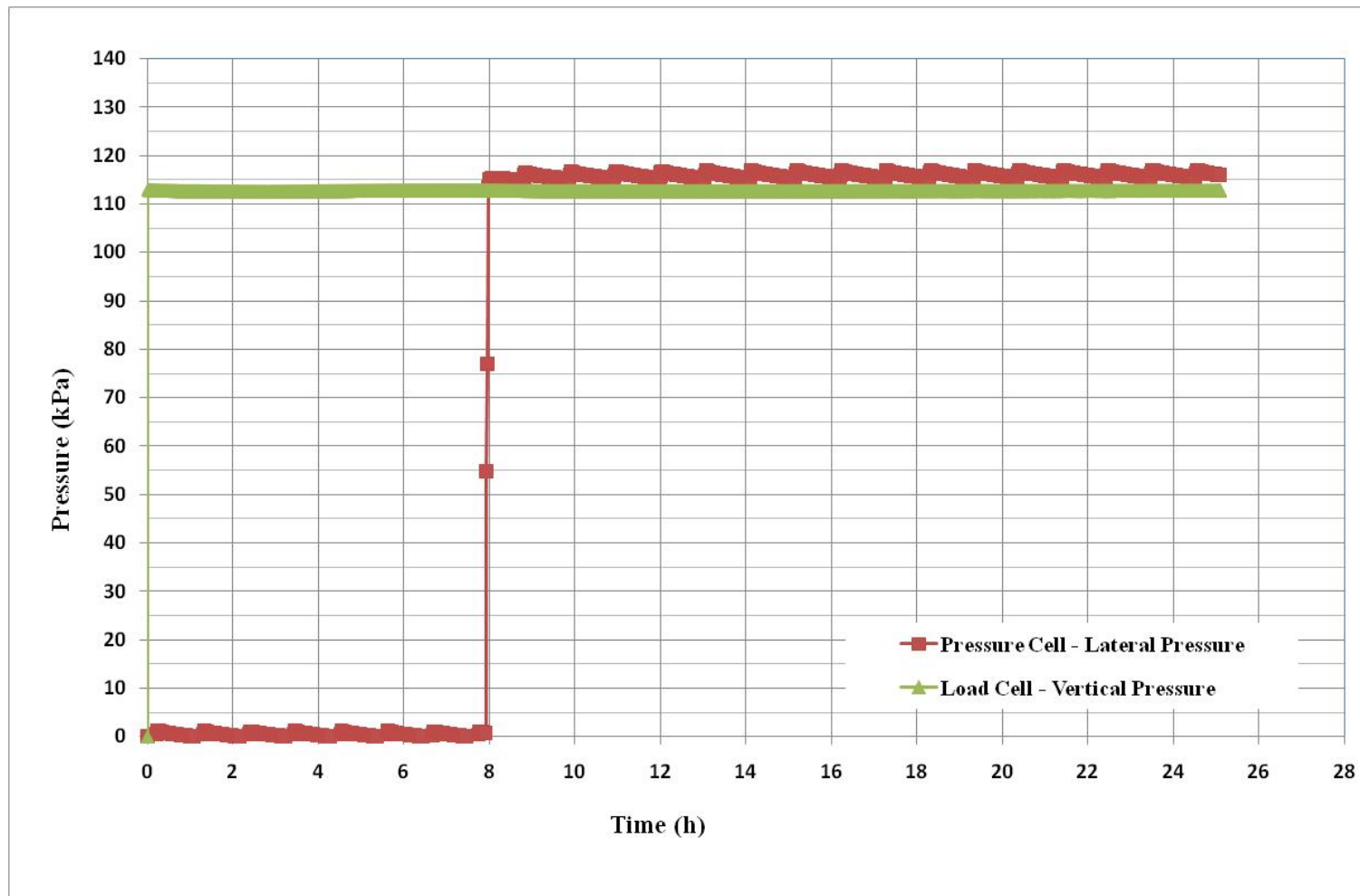
Figure D22: Pressure – Time Graph Test No: 43; (13.02.2010)
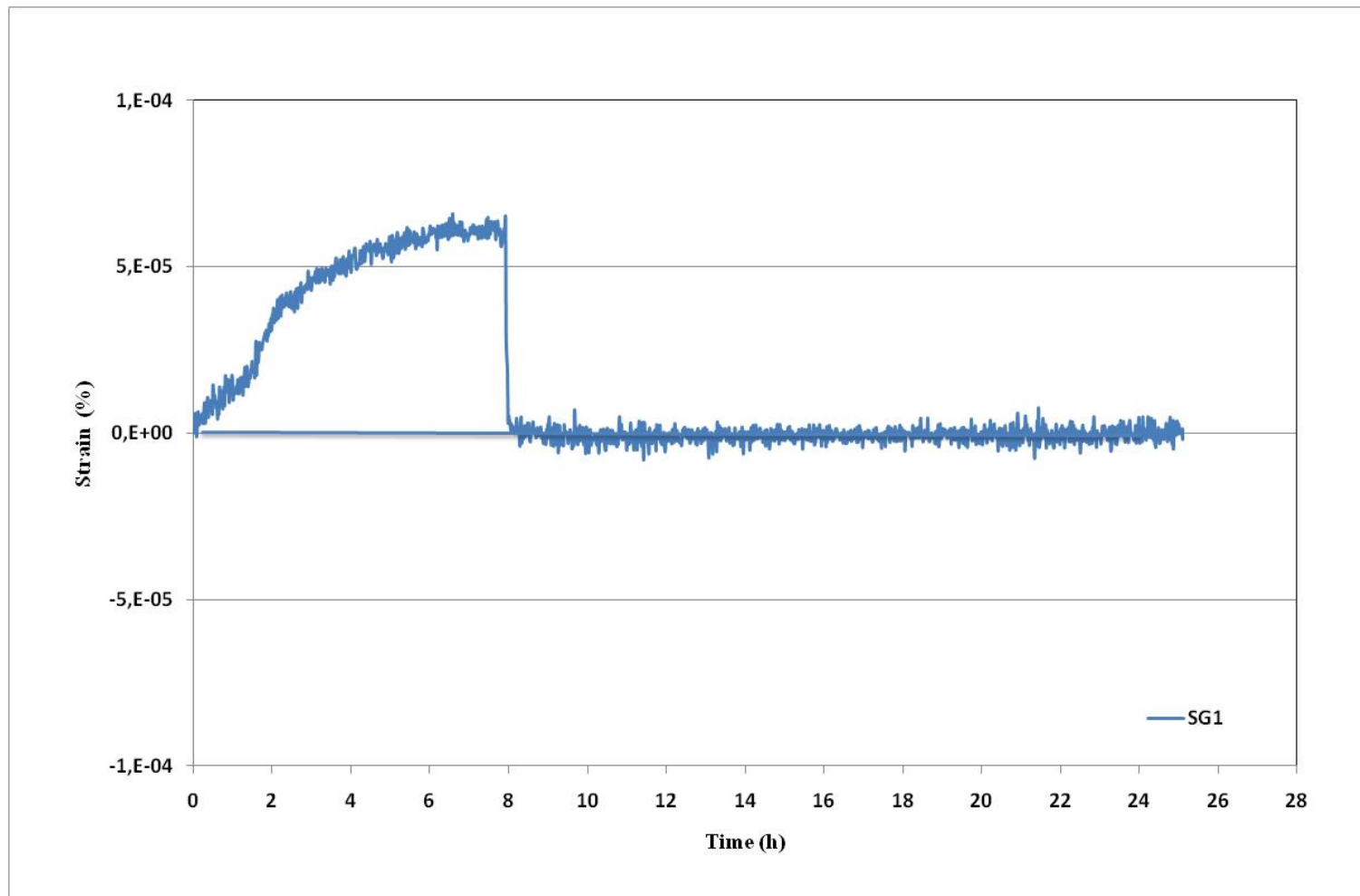
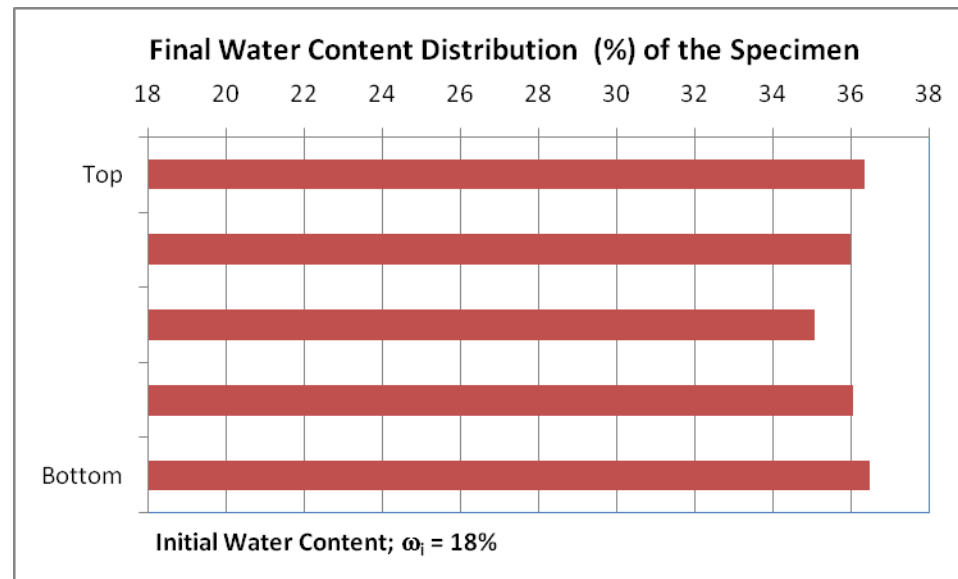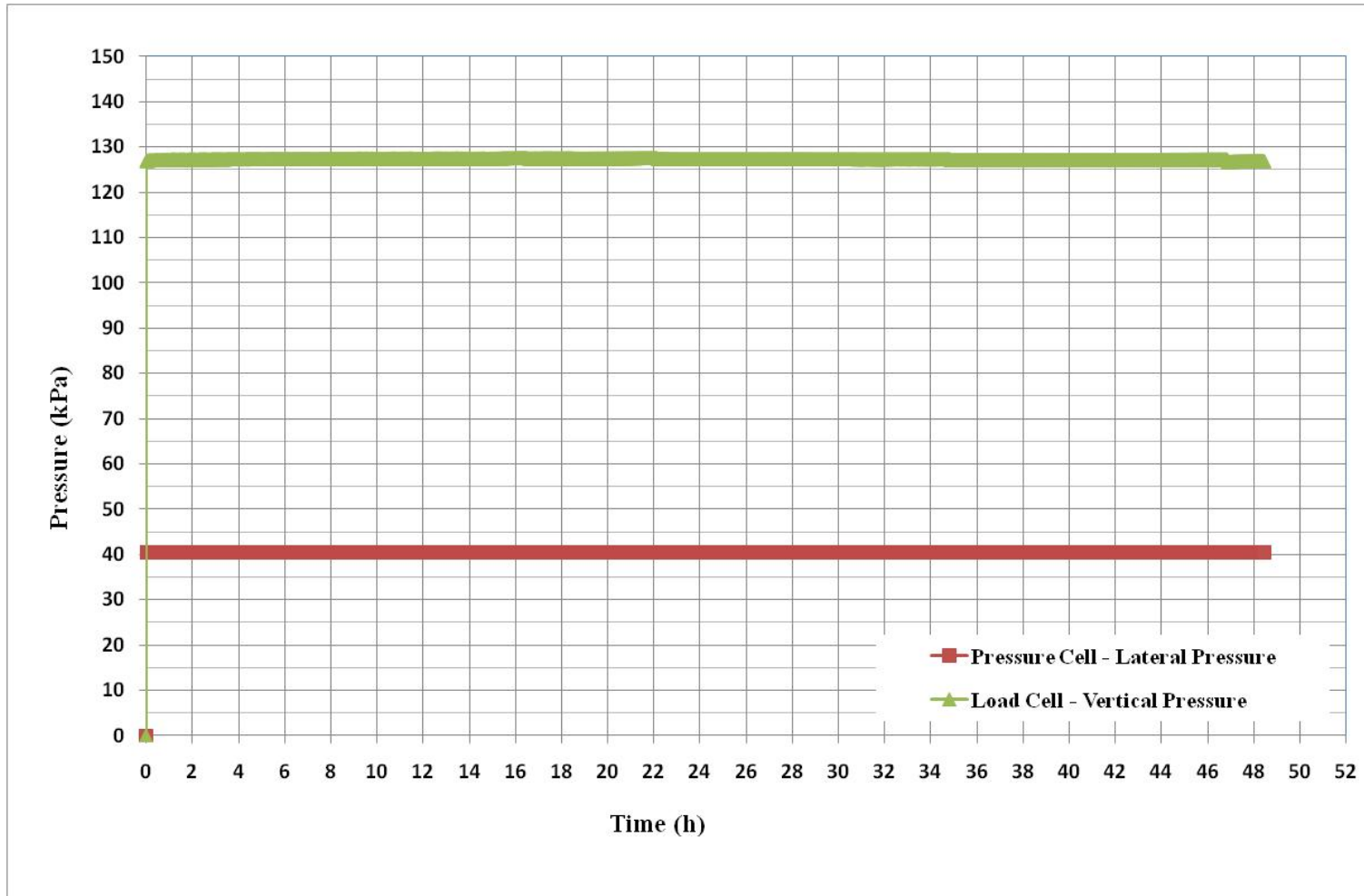**Figure D23:** Lateral Strain – Time Graph Test No: 43; (13.02.2010)
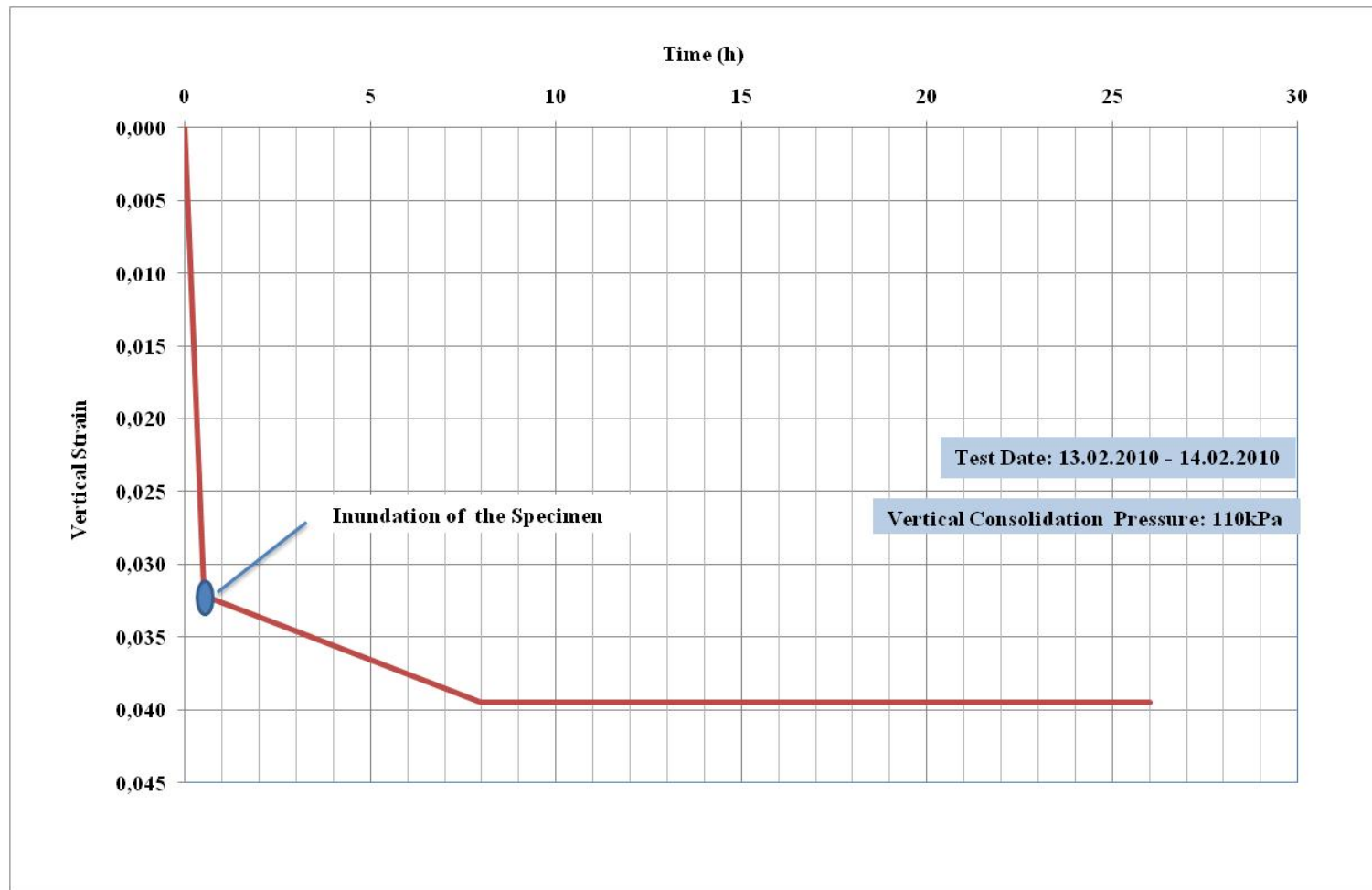
Figure D24: Vertical Strain – Time Graph Test No: 43; (13.02.2010)

APPENDIX E
LATERAL SWELLING PRESSURE DETERMINATION BASED ON THE
METHOD OF EQUILIBRIUM

(UNDER CONSTANT VERTICAL SURCHARGE)

TEST NO: 44	
Test Start:	
Date:	19.02.2010
Time:	15:00
Test Duration:	70 hours
Test End:	
Date:	22.02.2010
Time:	13:00
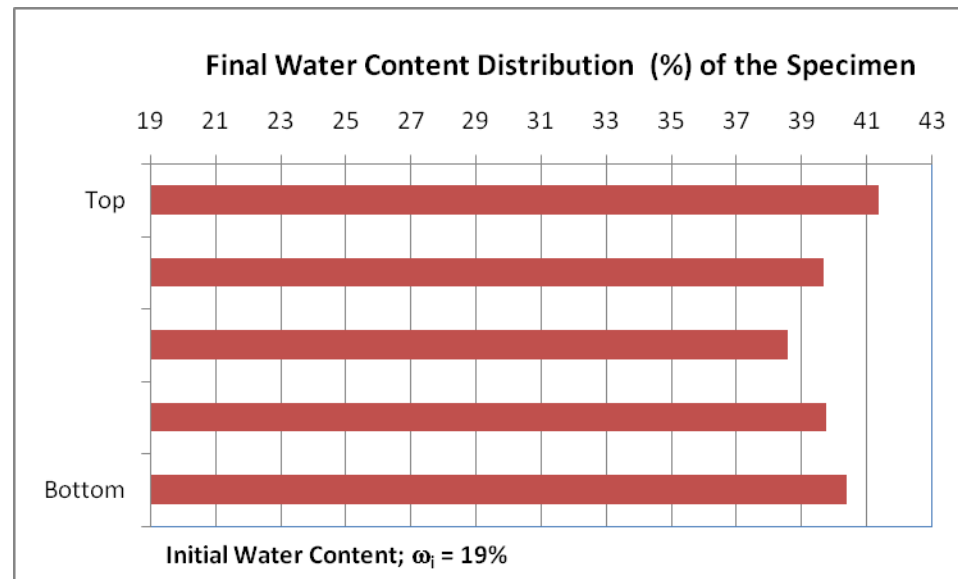
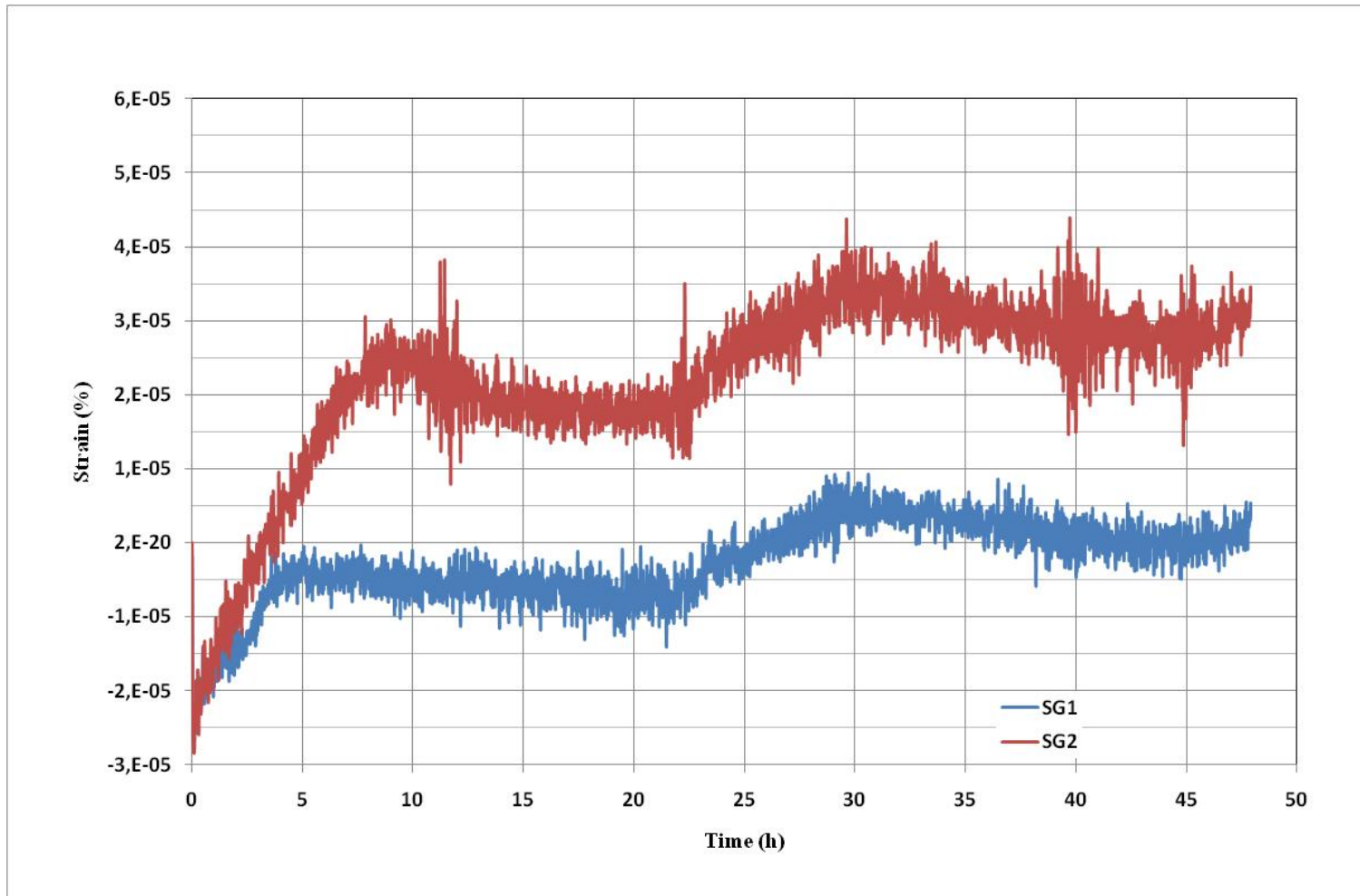**Figure E1:** Initial and Final Water Contents Test No: 44; (19.02.2010)

Figure E2: Pressure – Time Graph Test No: 44; (19.02.2010)
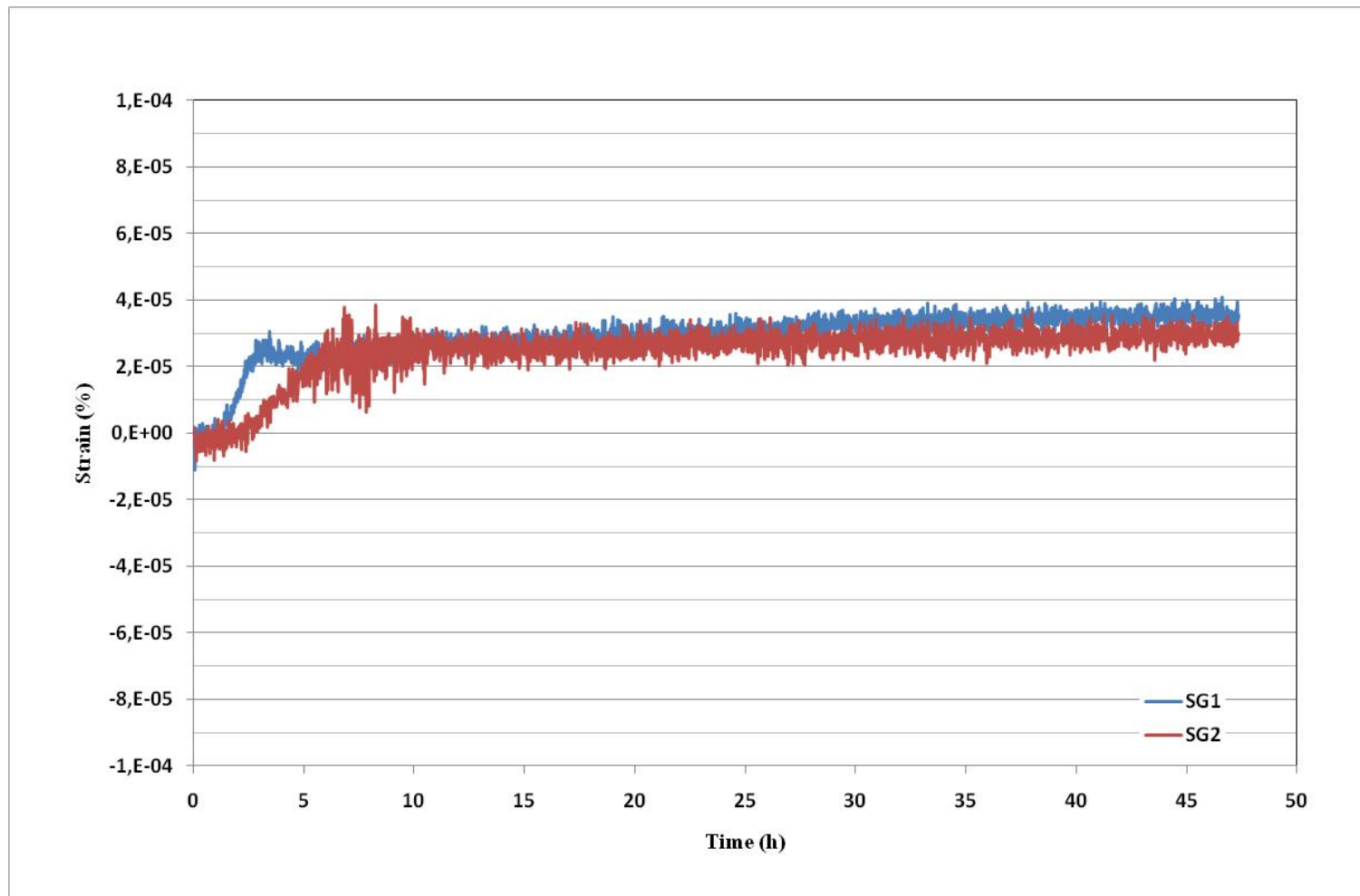
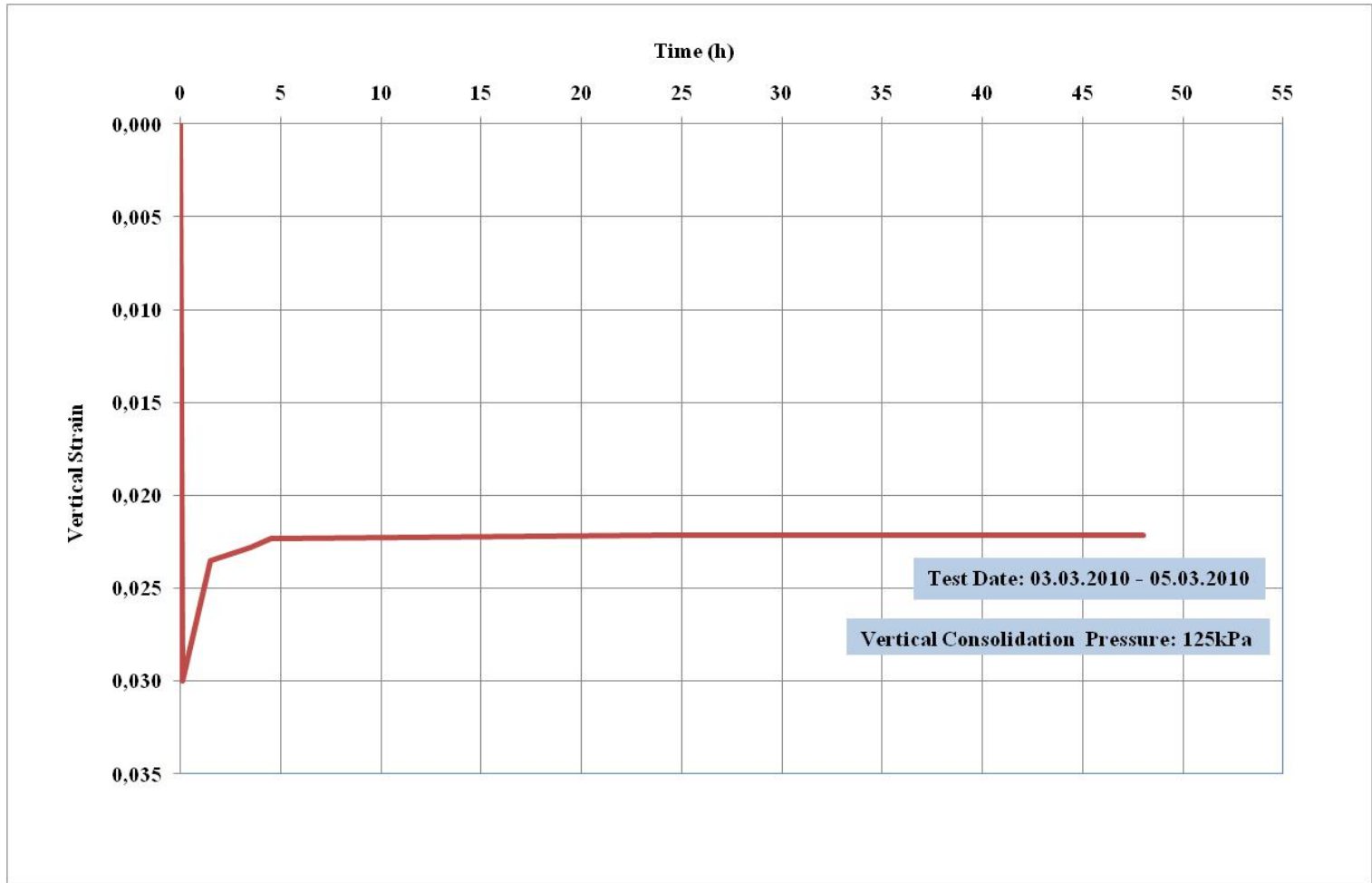**Figure E3:** Lateral Strain – Time Graph Test No: 44; (19.02.2010)

Figure E4: Vertical Strain – Time Graph Test No: 44; (19.02.2010)

TEST NO 45	
Test Start:	
Date:	24.02.2010
Time:	15:00
Test Duration:	48 hours
Test End:	
Date:	26.02.2010
Time:	15:00

Figure E5: Initial and Final Water Contents Test No: 45; (24.02.2010)

Figure E6: Pressure – Time Graph Test No: 45; (24.02.2010)

Figure E7: Lateral Strain – Time Graph Test No: 45; (24.02.2010)

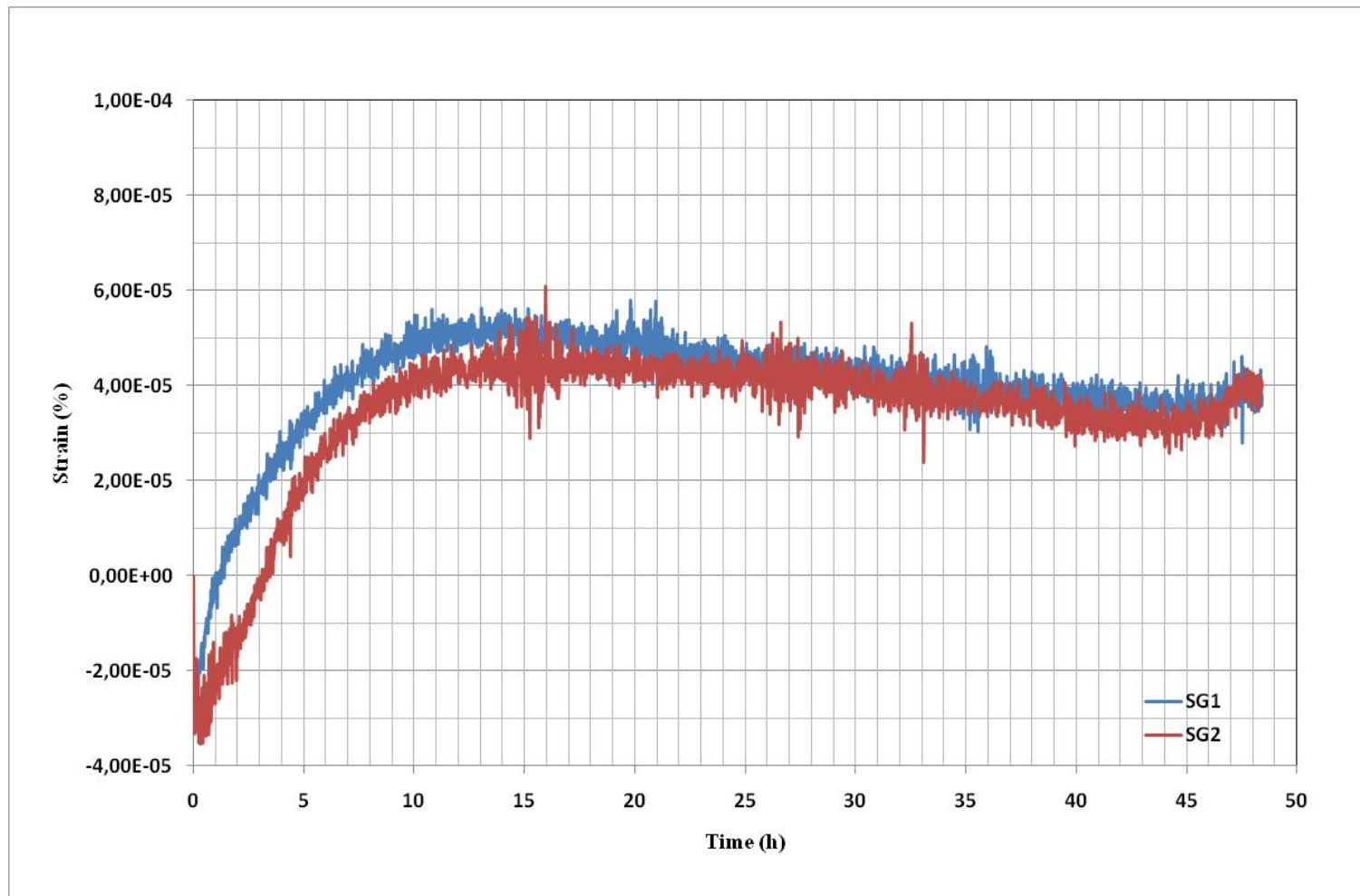**Figure E8:** Vertical Strain – Time Graph Test No: 45; (24.02.2010)

TEST NO: 46	
Test Start:	
Date:	27.02.2010
Time:	09:30
Test Duration:	72 hours
Test End:	
Date:	02.03.2010
Time:	09:30

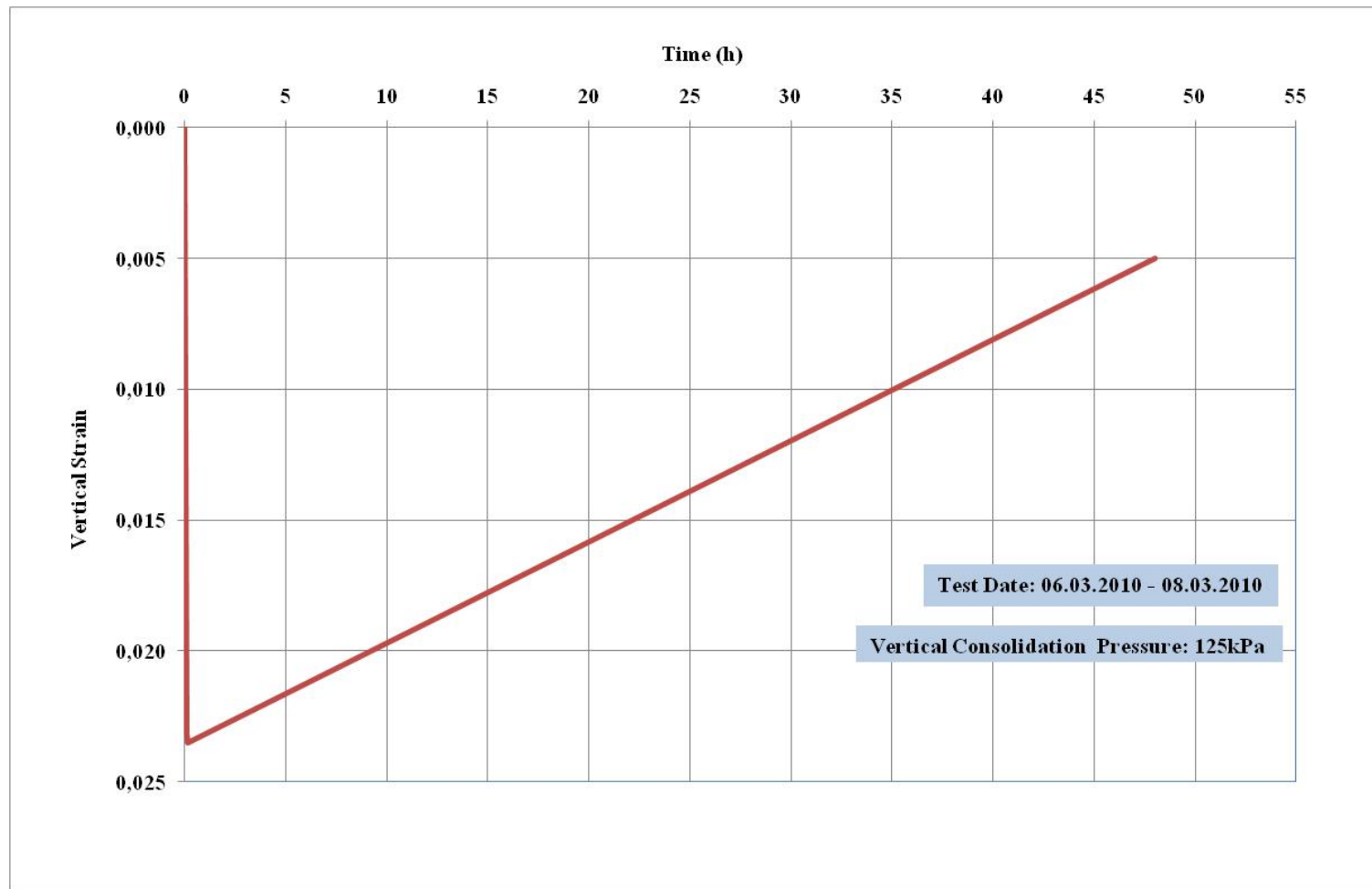**Figure E9:** Initial and Final Water Contents Test No: 46; (27.02.2010)
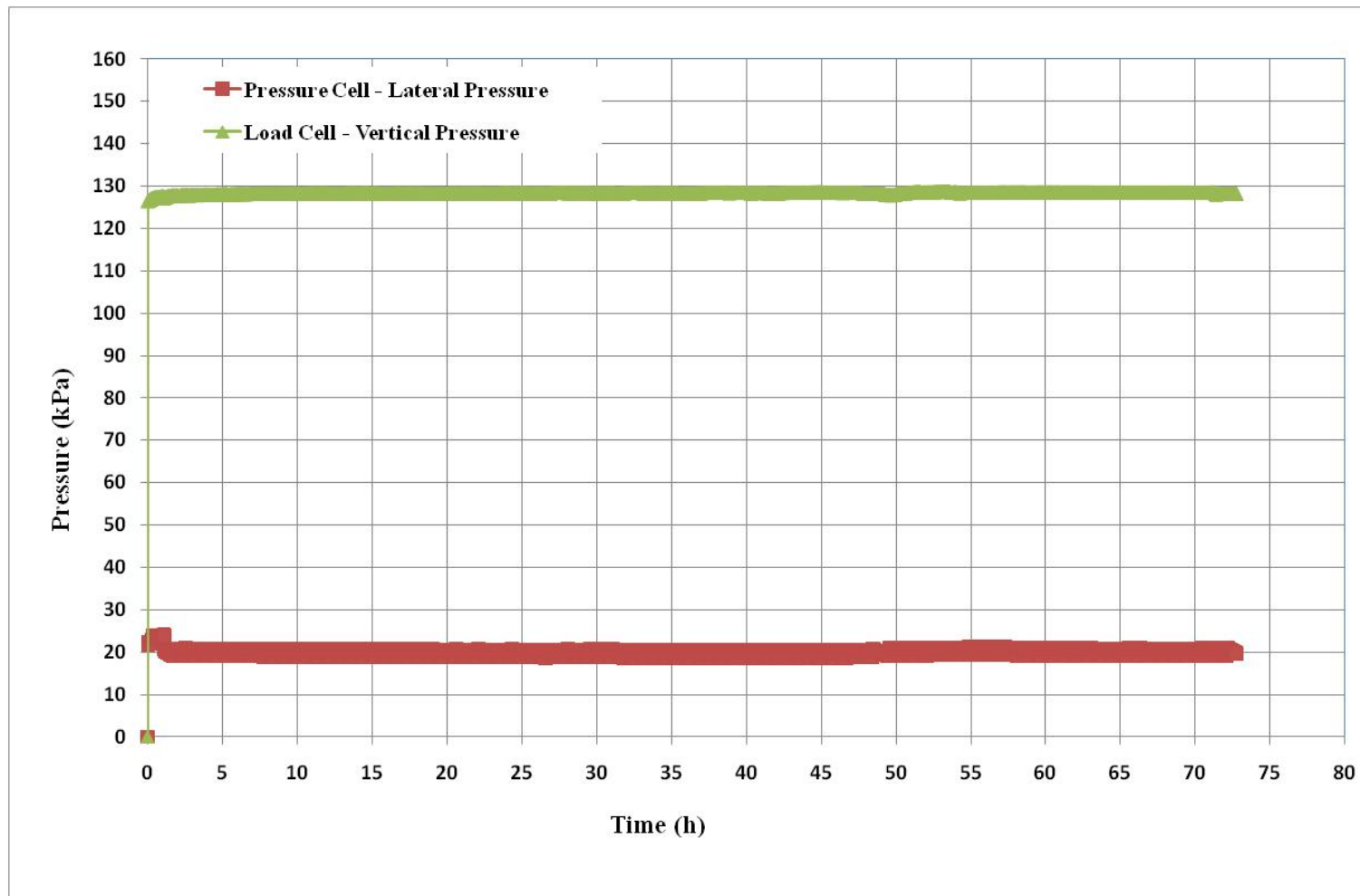
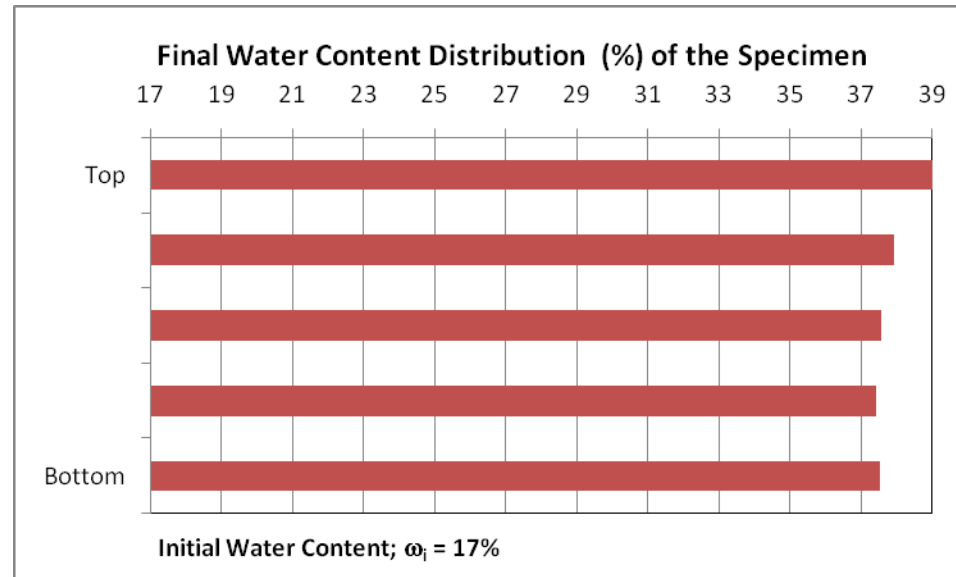**Figure E10:** Pressure – Time Graph Test No: 46; (27.02.2010)

Figure E11: Lateral Strain – Time Graph Test No: 46; (27.02.2010)

Figure E12: Vertical Strain – Time Graph Test No: 46; (27.02.2010)

TEST NO: 47	
Test Start:	
Date:	03.03.2010
Time:	11:30
Test Duration:	48 hours
Test End:	
Date:	05.03.2010
Time:	11:30

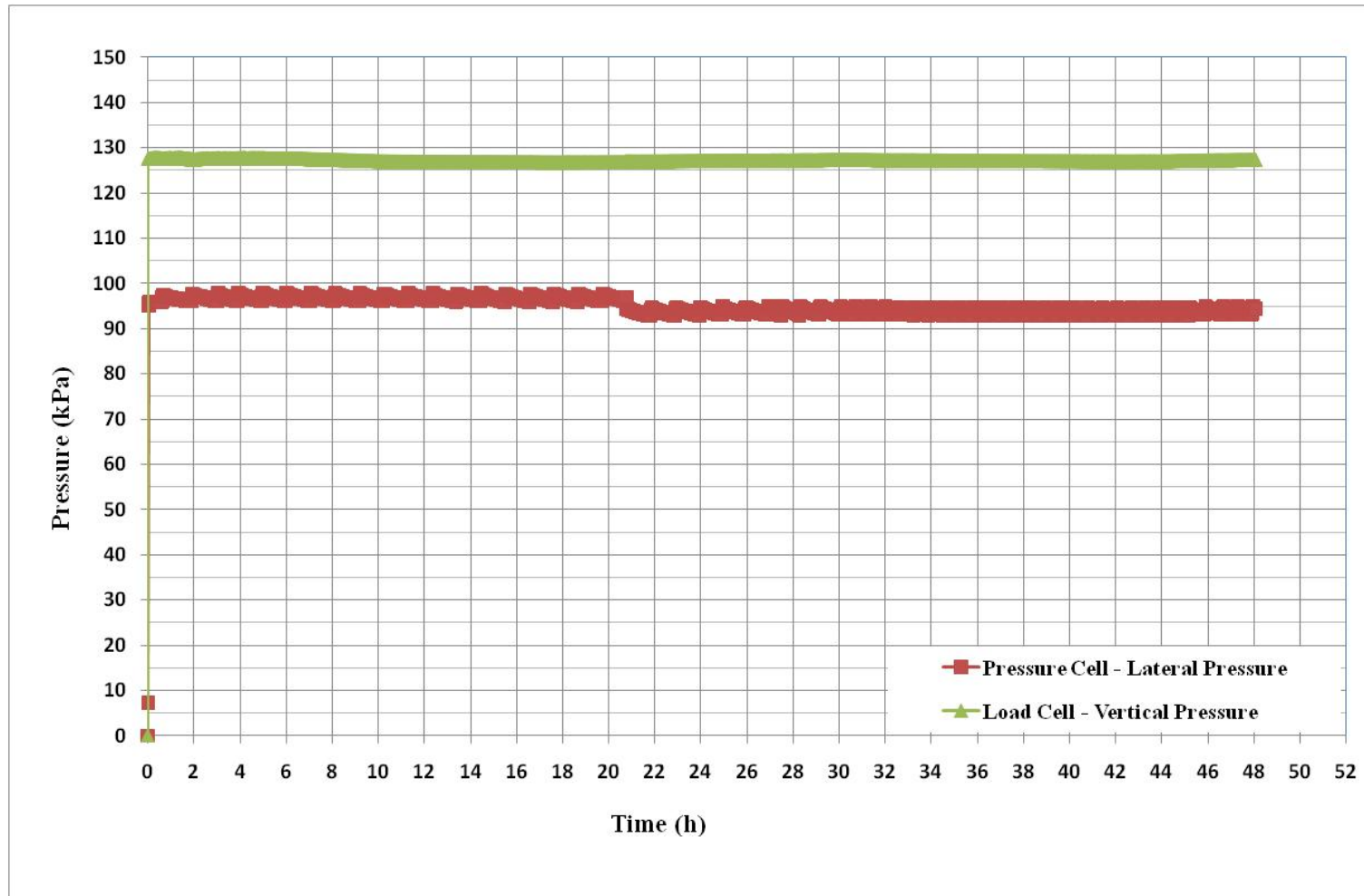**Figure E13:** Initial and Final Water Contents Test No: 47; (03.03.2010)

Figure E14: Pressure – Time Graph Test No: 47; (03.03.2010)

Figure E15: Lateral Strain – Time Graph Test No: 47; (03.03.2010)

Figure E16: Vertical Strain – Time Graph Test No: 47; (03.03.2010)

TEST NO: 48	
Test Start:	
Date:	06.03.2010
Time:	11:00
Test Duration:	48 hours
Test End:	
Date:	08.03.2010
Time:	11:00
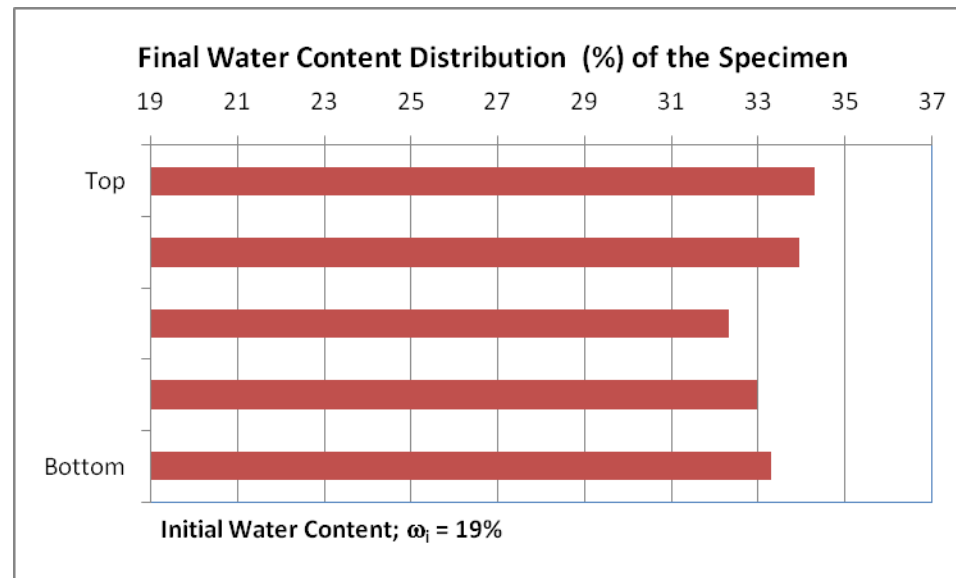
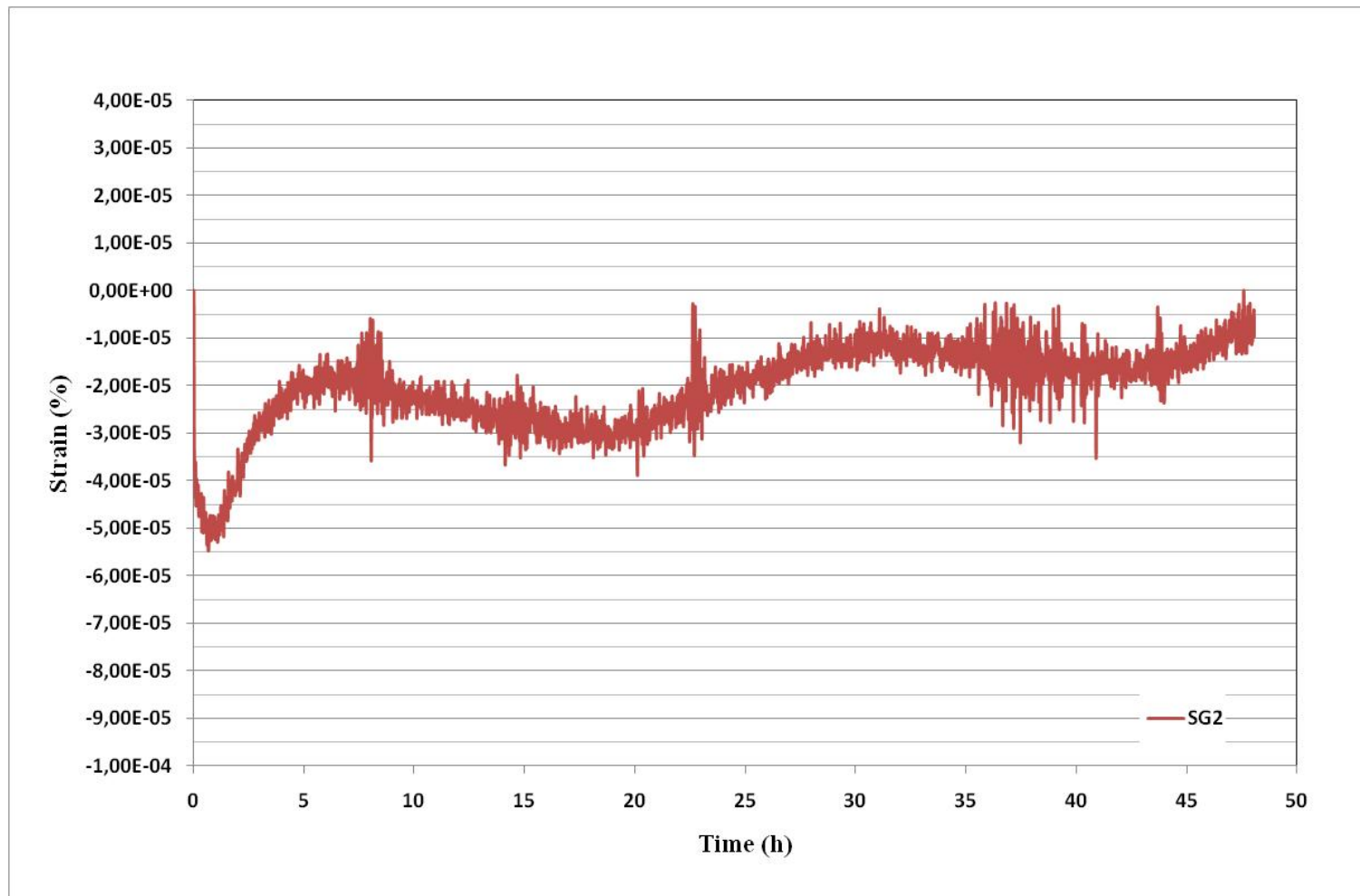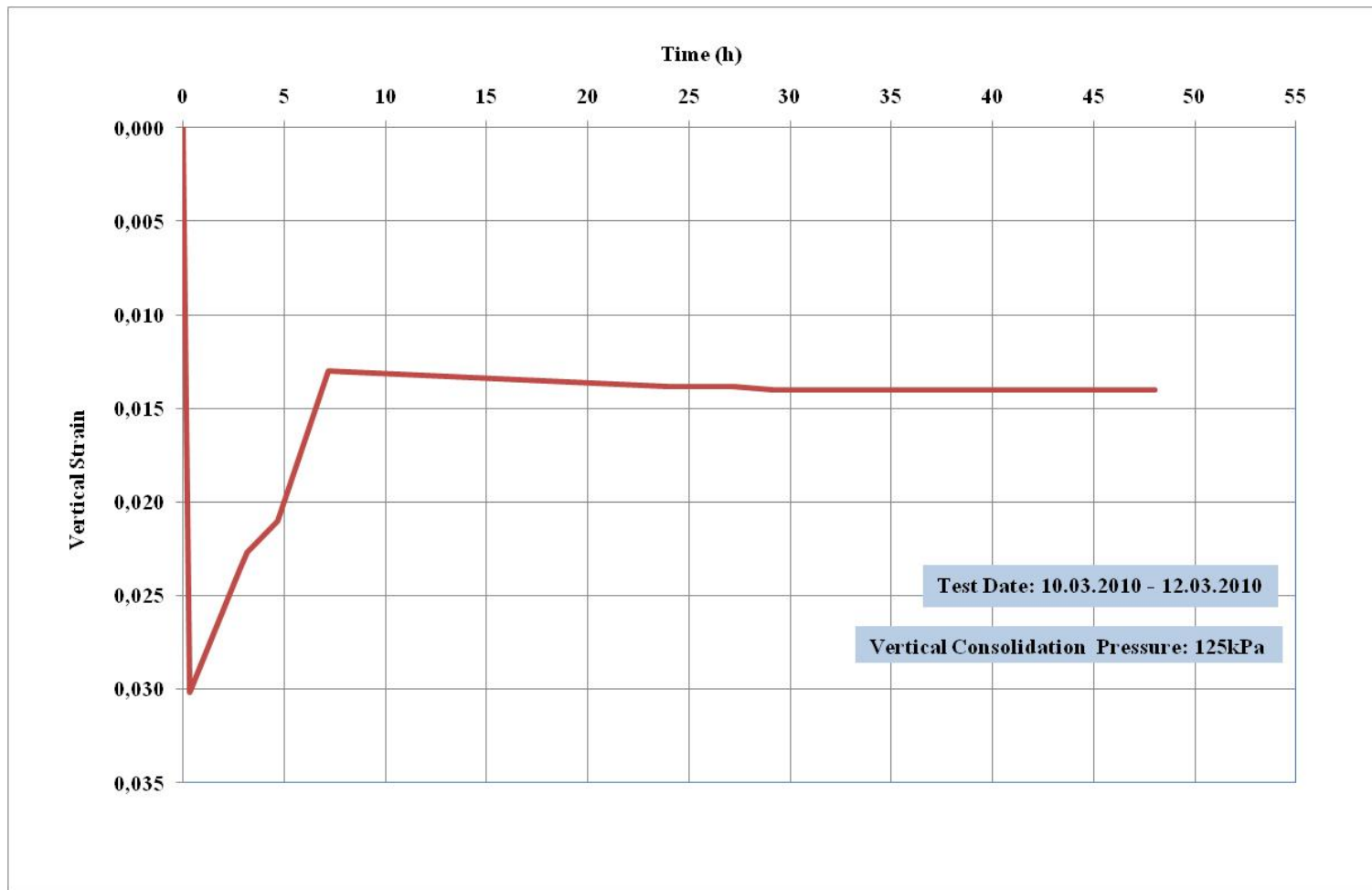**Figure E17:** Initial and Final Water Contents Test No: 48; (06.03.2010)
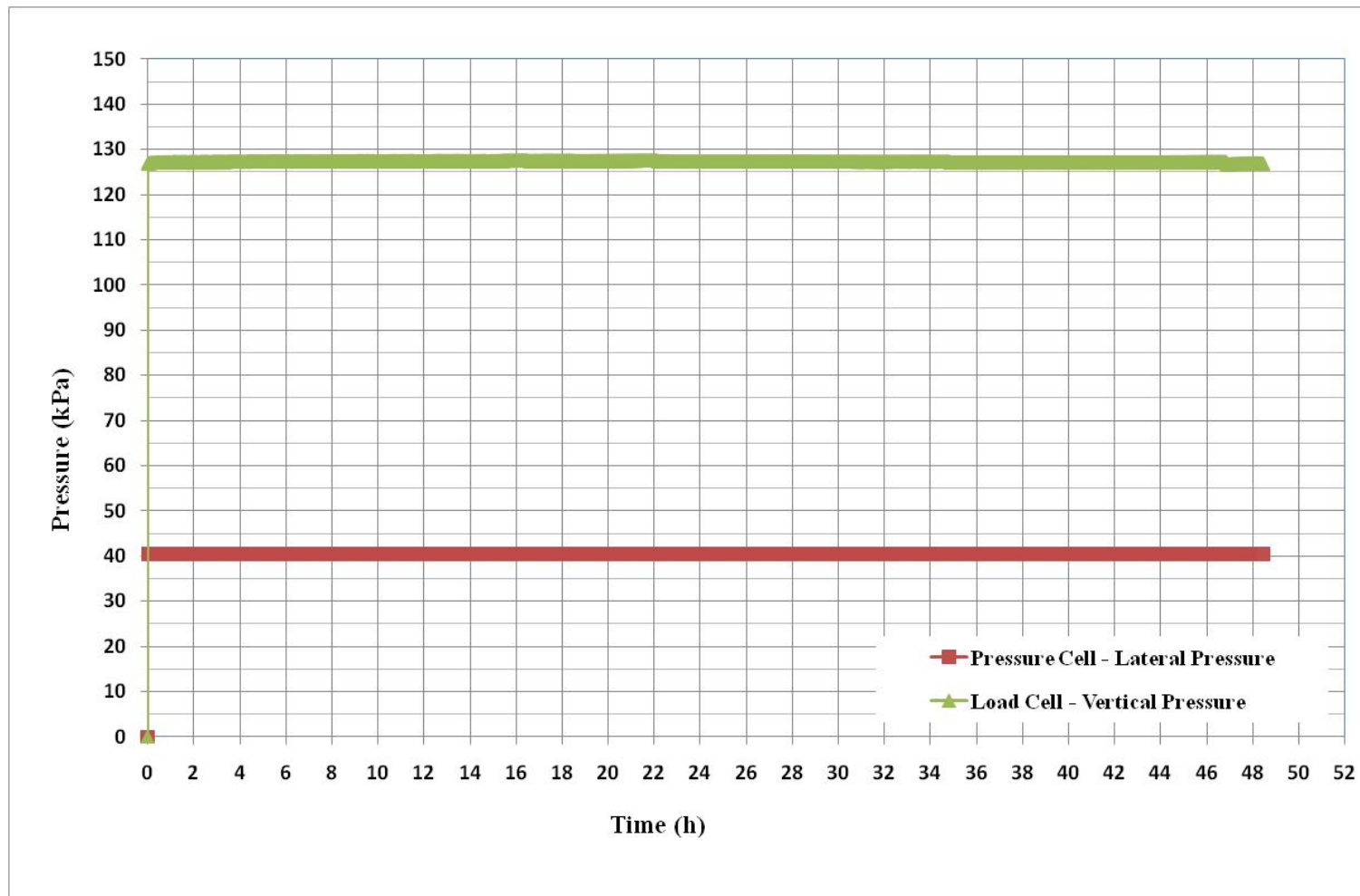
Figure E18: Pressure – Time Graph Test No: 48; (06.03.2010)

Figure E19: Lateral Strain – Time Graph Test No: 48; (06.03.2010)

Figure E20: Vertical Strain – Time Graph Test No: 48; (06.03.2010)

TEST NO: 49	
Test Start:	
Date:	10.03.2010
Time:	12:00
Test Duration:	48 hours
Test End:	
Date:	12.03.2010
Time:	12:00

Figure E21: Initial and Final Water Contents Test No: 49; (10.03.2010)
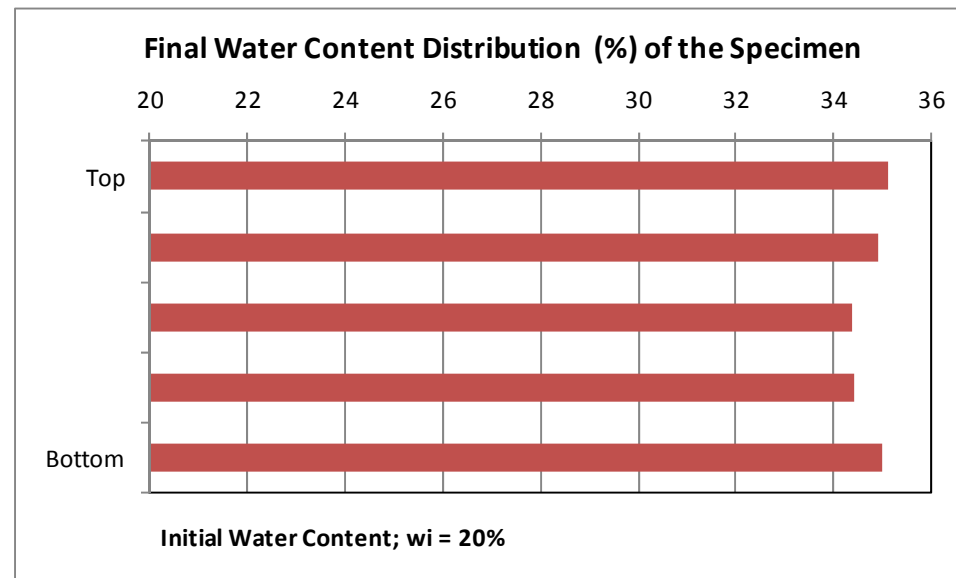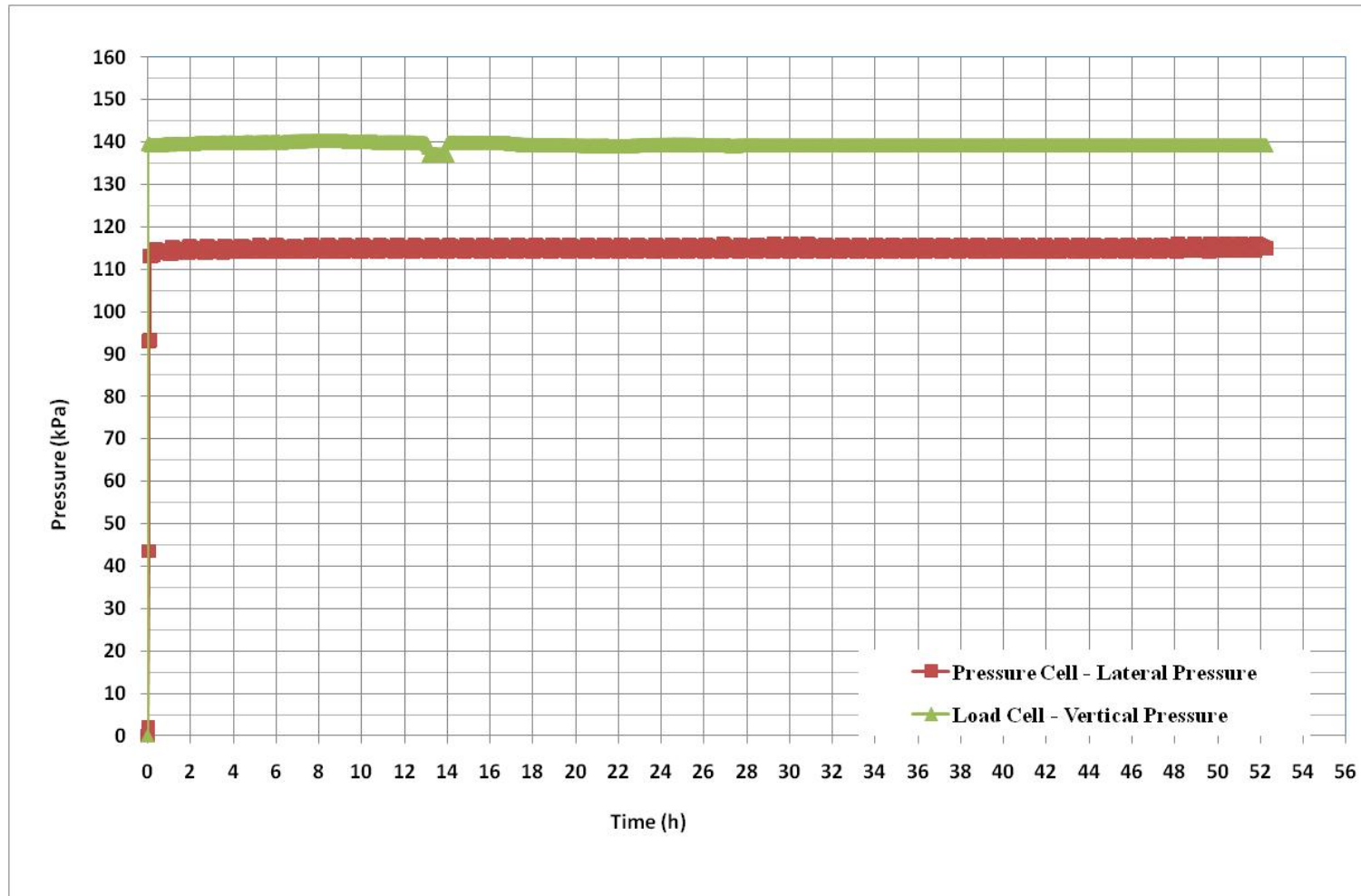
Figure E22: Pressure – Time Graph Test No: 49; (10.03.2010)

Figure E23: Lateral Strain – Time Graph Test No: 49; (10.03.2010)

Figure E24: Vertical Strain – Time Graph Test No: 49; (10.03.2010)

TEST NO: 50	
Test Start:	
Date:	1303.2010
Time:	1000
Test Duration:	52 hours
Test End:	
Date:	15.03.2010
Time:	14:00

Final Water Content Distribution (%) of the Specimen

Initial Water Content; wi = 20%

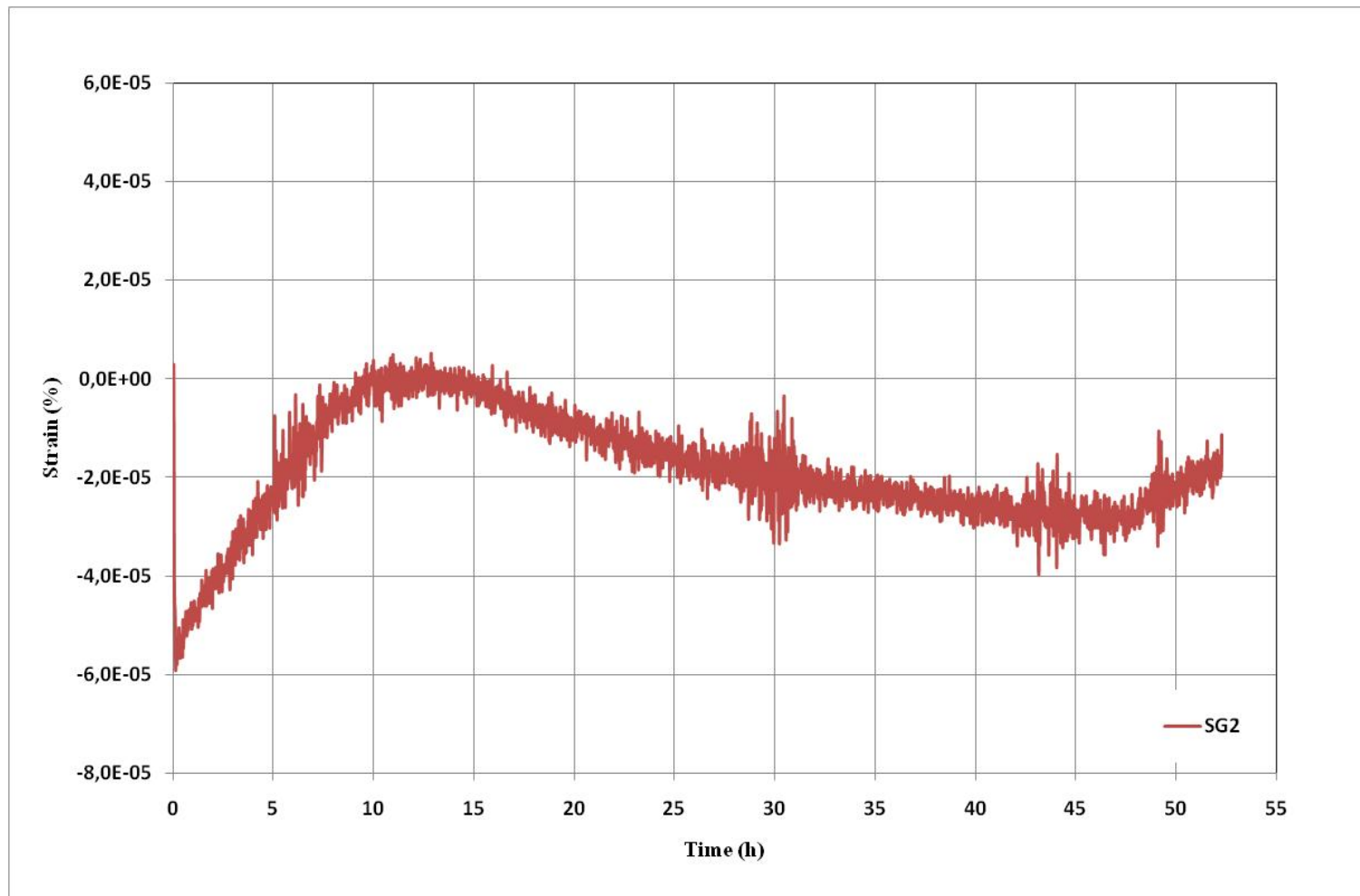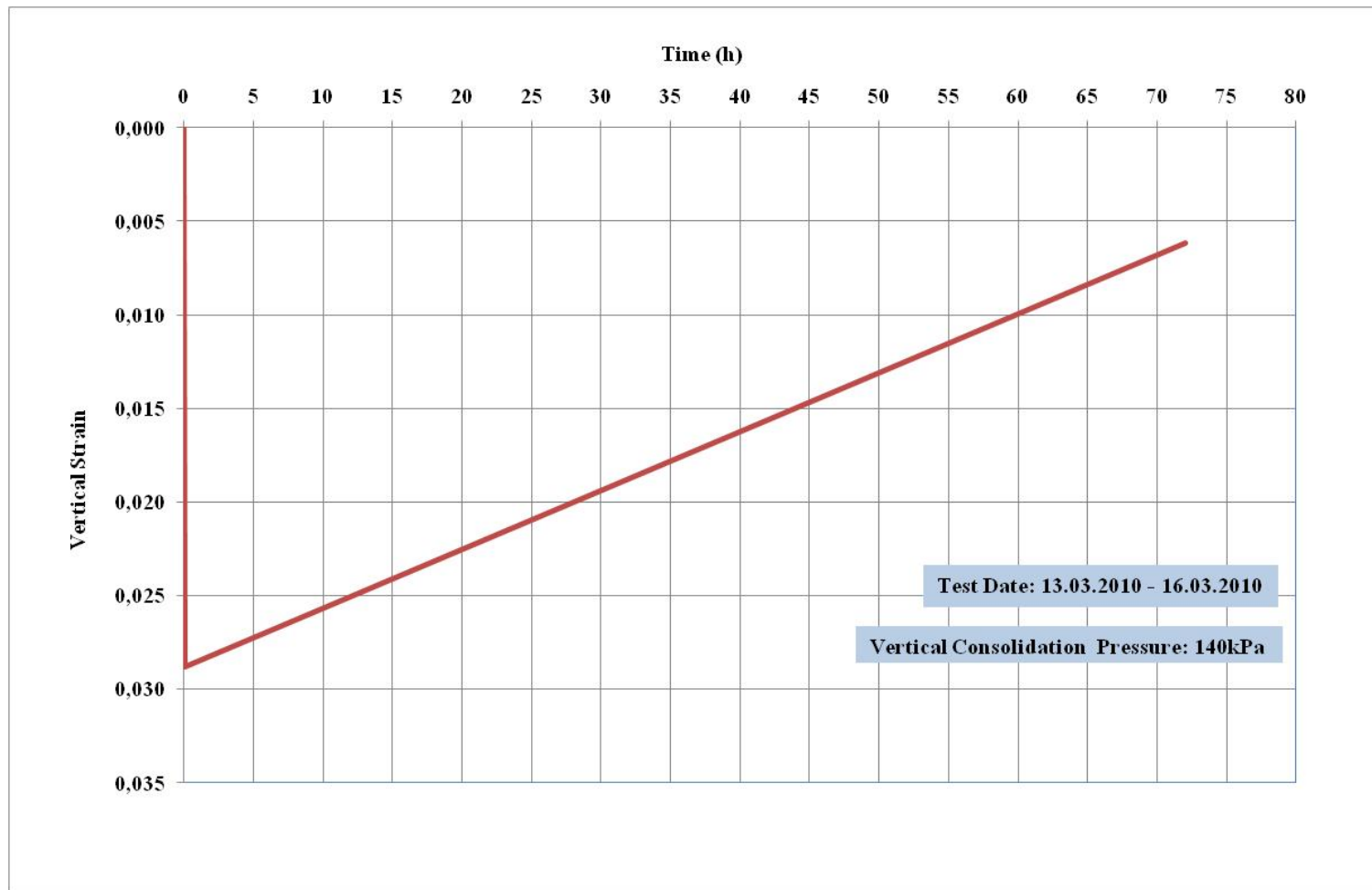**Figure E25:** Initial and Final Water Contents Test No: 50; (13.03.2010)

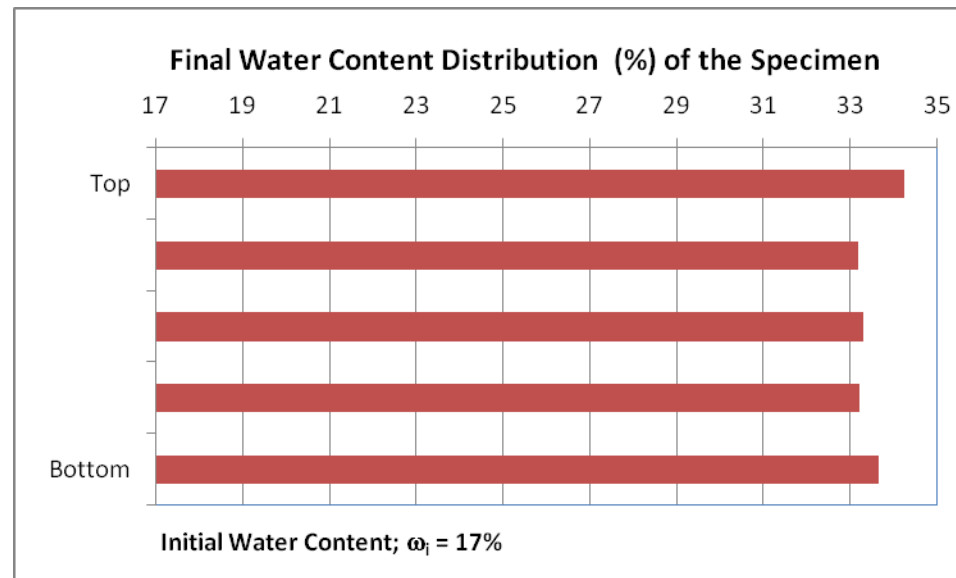**Figure E26:** Pressure – Time Graph Test No: 50; (13.03.2010)

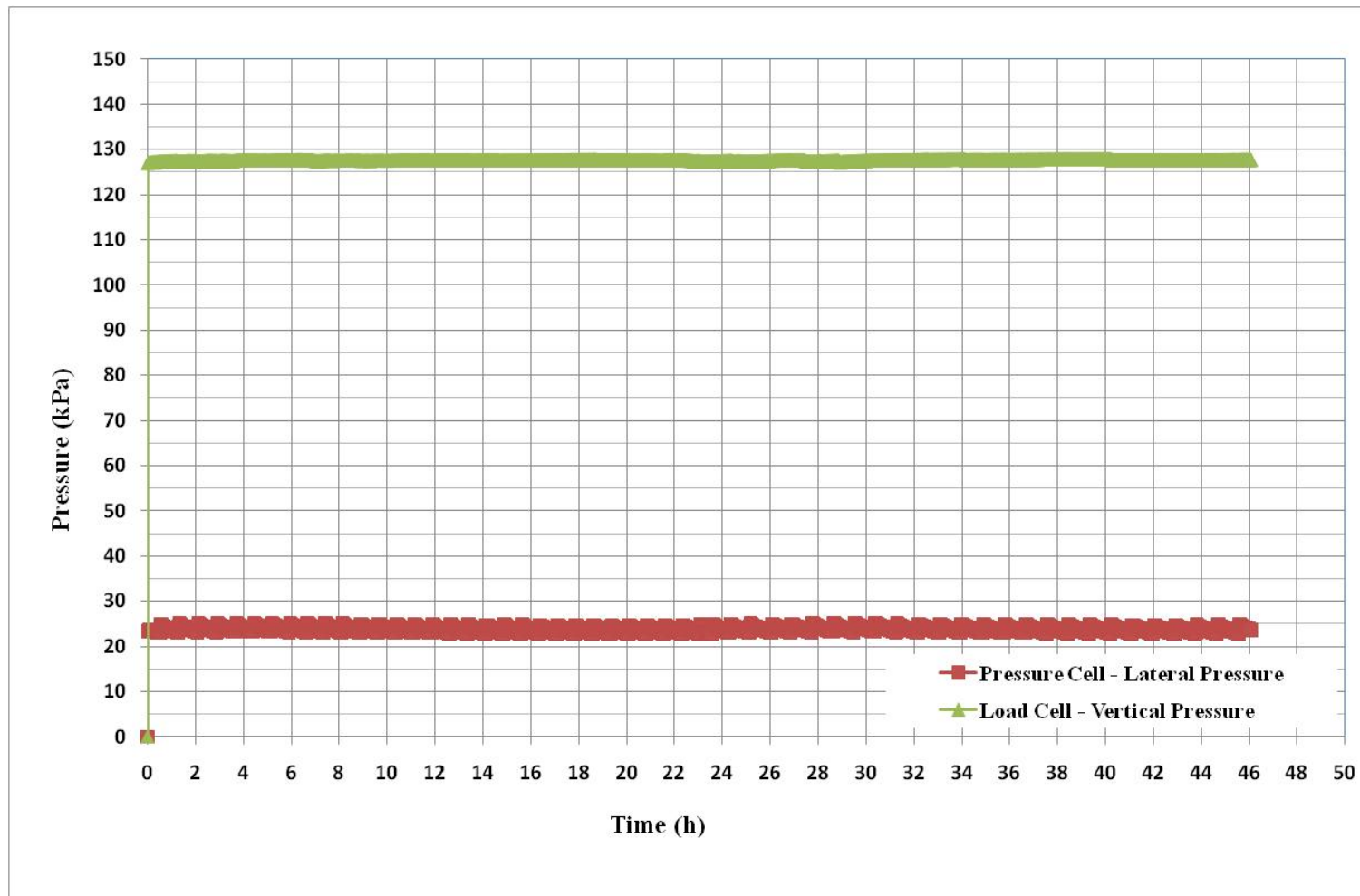**Figure E27:** Lateral Strain – Time Graph Test No: 50; (13.03.2010)

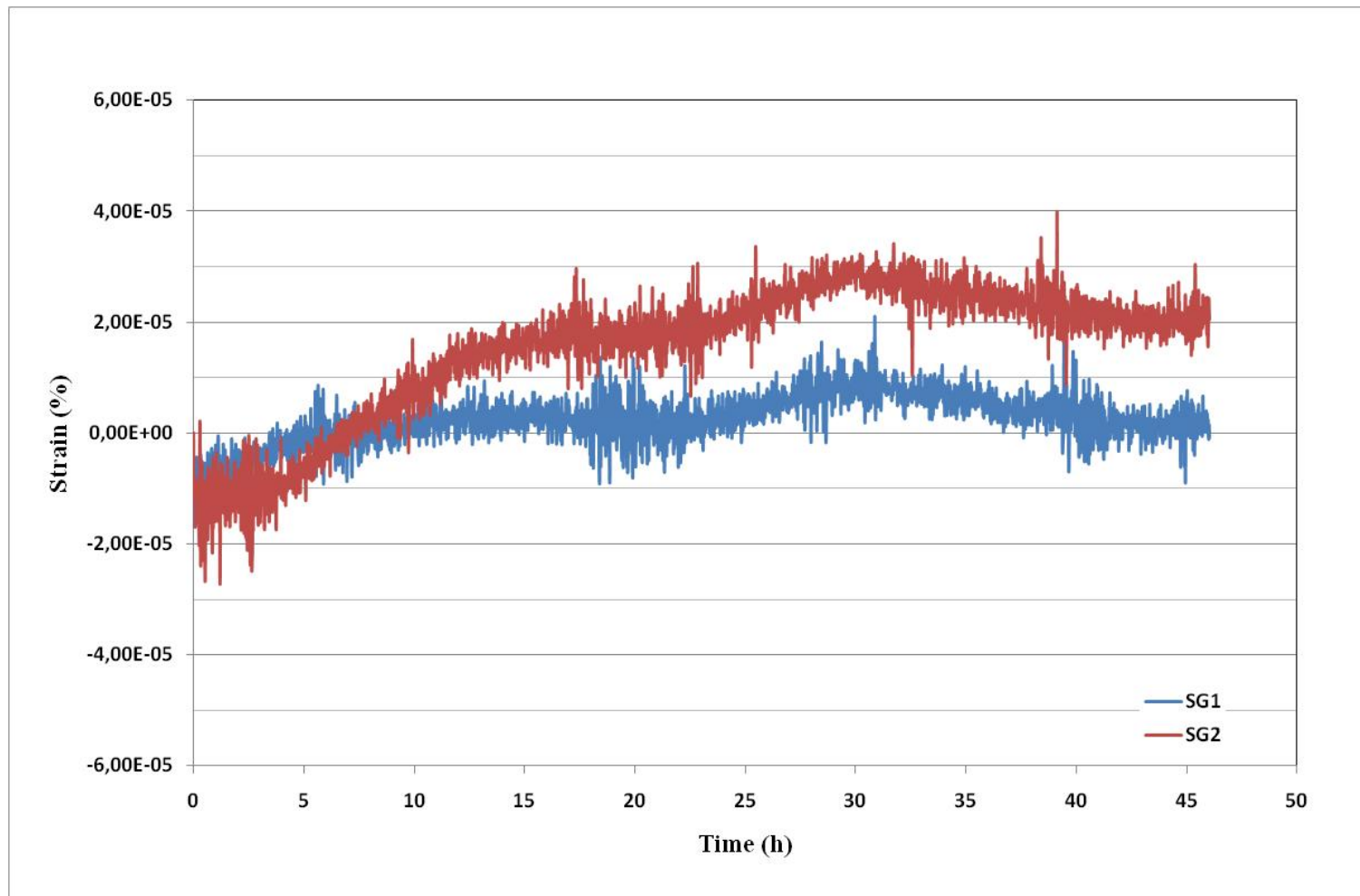**Figure E28:** Vertical Strain – Time Graph Test No: 50; (13.03.2010)

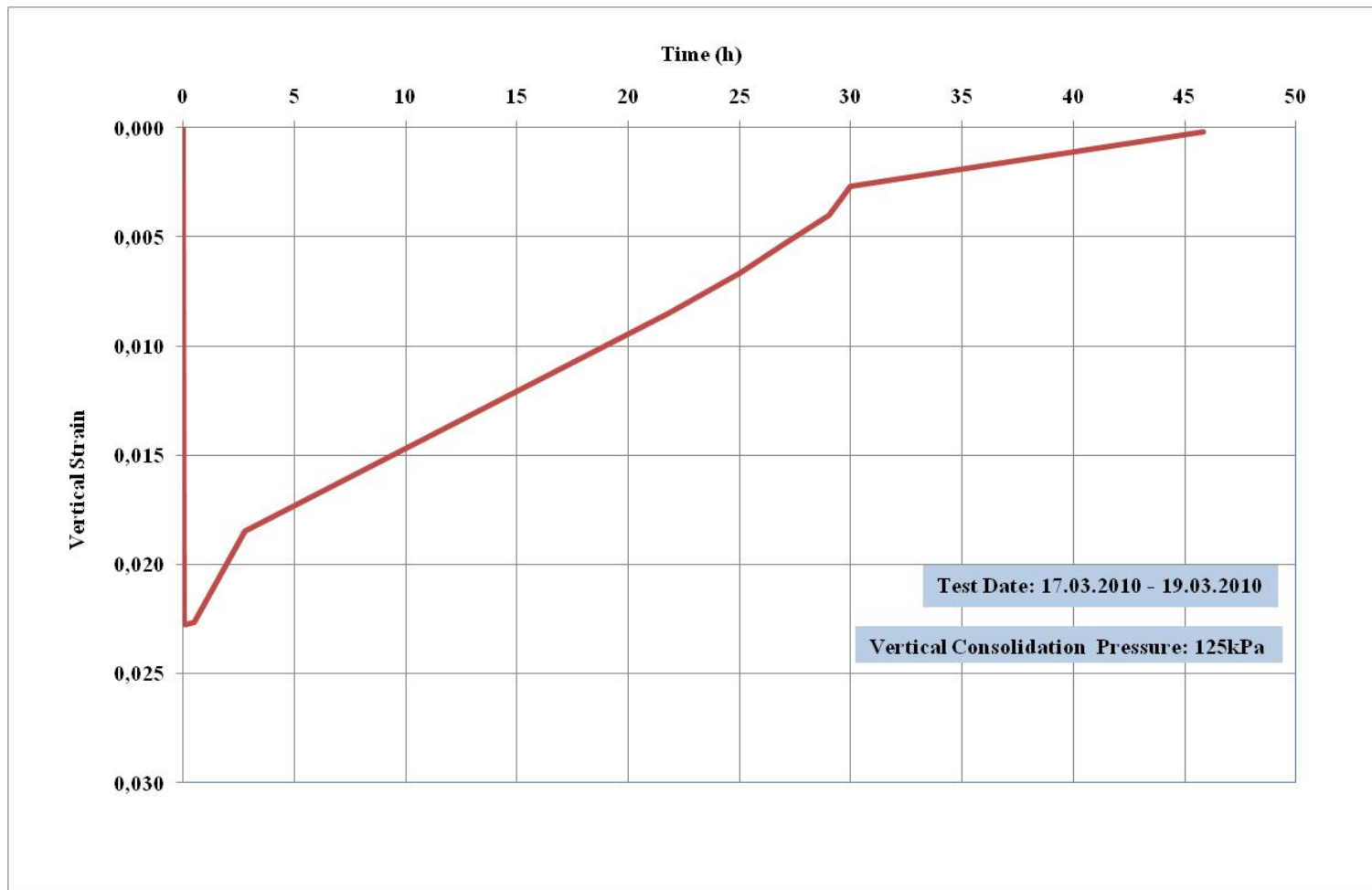| TEST NO: 51	
Test Start:	
Date:	17.03.2010
Time:	11:00
Test Duration:	46 hours
Test End:	
Date:	19.03.2010
Time:	09:00

Figure E29: Initial and Final Water Contents Test No: 51; (17.03.2010)

Figure E30: Pressure – Time Graph Test No: 51; (17.03.2010)

Figure E31: Lateral Strain – Time Graph Test No: 51; (17.03.2010)

Figure E31: Vertical Strain – Time Graph Test No: 51; (17.03.2010)

CURRICULUM VITAE

Candidate's full name:	**Hüsnü Korhan ÖZALP**
Place and date of birth:	**Ankara – 01/08/1979**
Permanent Address:	**Sedef Caddesi Ata 2-2 Blok D: 98**
	Ataşehir/İSTANBUL

Civil Engineering, BS.	Dokuz Eylul University	2001
Geotechnical Eng. MS.	Istanbul Technical University	2004
Geotechnical Eng. PhD.	Istanbul Technical University	2004-…

PUBLICATIONS

MSc Thesis

- **Özalp, H.K.**, 2004. "Soil Improvement With Jet Grouting Systems", *MSc Thesis*, ITU, Istanbul

Other Publications

- Saglamer, A., Yılmaz, E., Balık, E., **Özalp, H. K**, "Jet Grout Application under a Building Subjected to Differential Settlement, *Proc. of Int. Conference on Problematic Soils"*, Doğu Akdeniz Üniversitesi, Lefkoşe, KKTC, Mayıs 2005
- **Özalp, H.K**., "A Deep Excavation for the Construction of a Hotel Building in Istanbul", *Proc. of European Young Geotechnical Engineers Conference on Soil Mechanics and Geotechnical Engineering,* Zagreb, July 2006
- Saglamer, A., Balik, E., **Özalp, H.K.** and Aslay, Z., "A deep excavation for the construction of a hotel building in Istanbul", *Proc. of European Conference on Soil Mechanics and Geotechnical Engineering,* Madrid, September 2007
- Saglamer, A., Aslay, Z. and **Ozalp, H.K**., "Revitalization of a history: underpinning of Istanbul Silahtaraga Power Plant", *Proc. of European Conference on Soil Mechanics and Geotechnical Engineering,* Madrid, September 2007
- Sağlamer, A., **Özalp H.K.**, "Piled Foundations Of Zine El Abidine Ben Ali Airport In Tunisia", 2nd International Conference on New Developments in Soil Mechanics and Geotechnical Engineering, Nicosia, Northern Cyprus, 2009